Energy Technologies Area

WINDOW Technical Documentation

Charlie Curcija, Simon Vidanovic, Robert Hart, Jacob Jonsson, Rebecca Powles, Robin Mitchell

Windows and Envelope Materials Group

Lawrence Berkeley National Laboratory

Berkeley, California 94720

Date: April 2018

DISCLAIMER

---

1. INTRODUCTION

This document presents the mathematical models for calculating the thermal and solar-optical performance of glazing systems and whole fenestration products in the Berkeley Lab WINDOW computer program, referred to as "WINDOW" in this document.

The glazing system thermal and solar-optical performance algorithms are incorporated into the TARCOG module (incorporated into WINDOW 7 as well as EnergyPlus 8.3 and later) and the WinCalc module (incorporated into EnergyPlus 8.8 and later and future versions of WINDOW 8). Both the TARCOG and WinCalc modules are also incorporated and used in EnergyPlus whole building energy simulation tool, with the WinCalc module being more recent and representing the future, fully portable window thermal and solar-optical calculation module, which will be interchangeably used in future WINDOW and EnergyPlus software tools. Algorithms include the calculation of glazing system thermal transmittance (U_g), solar transmittance ($Tsol_g$), visible transmittance (VT_g), solar heat gain coefficient ($SHGC_g$), condensation resistance (CR) and temperature distribution across the central portion of glazing system, according to the ISO 15099 and ISO/EN 10077 standards. Calculations and outputs include many more indices of performance, such as solar reflectances, visible reflectances, layer absorptances, UV transmittance, etc. All of these functions and outputs are accessible through either an API (see the public open source Github repository: https://github.com/LBNL-ETA/Windows-CalcEngine), or the WINDOW Graphic User Interface.

Algorithms for the thermal and solar-optical performance of glazing systems consider the glazing system as an array of layers and gaps, where some layers may be in direct contact with each other (i.e., laminates). In addition, these algorithms consider shading devices and treat them as planar layers with additional characteristics, such as air flow around or through them. Glazing gaps may be filled with pure gasses, gas mixtures or be evacuated (i.e., various levels of vacuum). Deflection of glazing gaps is also calculated as well as the effects of deflection on thermal performance.

Optical properties are calculated for both specular glazing layers and for scattering glazing and shading layers. Broad band optical properties, such as Tsol, Tvis, etc. are calculated from basic material spectral-optical data and the application of source spectra. Source spectra is supplied through standard file. Multi-layer optical calculations are performed spectrally and broad band results are calculated by the post-spectral integration.

Algorithms for calculating whole fenestration product thermal and solar-optical performance (*U, VT, SHGC*) are also included. Because a whole fenestration product is three dimensional, its indices of performance are calculated as area-weighted averages of one dimensional center of glazing performance numbers and two dimensional frame and edge of glazing performance numbers. These two dimensional calculations are done in the LBNL THERM software tool.

2. WHOLE FENESTRATION PRODUCT PERFORMANCE

2.1. Window U-value

The total U-value for the window is the area-weighted average of the component U-values:

$$U_{TOT} = \frac{\sum_i (U_{Fi} \cdot A_{Fi} + \sum_j U_{Ei,j} \cdot A_{Ei,j}) + \sum_j (U_{Cj} \cdot A_{Cj} + U_{Dj} \cdot A_{Dj} + U_{DEj} \cdot A_{DEj})}{A_{TOT}} \qquad [2\text{-}1]$$

For single or planar combination windows, A_{TOT} is the total window area. A_{TOT} is the product of the user input dimensions of the height and width of the window. For nonplanar combination windows, A_{TOT} is the projected area input by the user.

Figure 2.1 shows the different areas (also known as components) of the fenestration product.
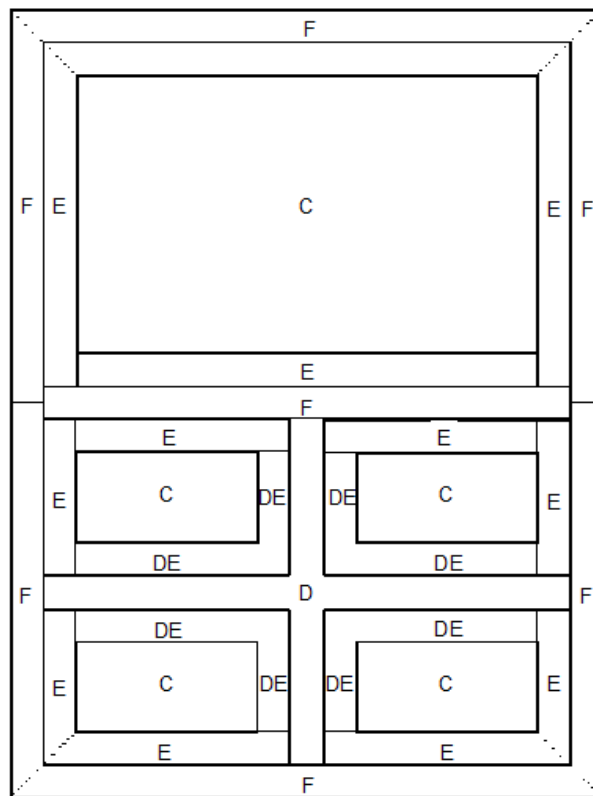
LEGEND
C   Center-of-glazing
E   Edge-of-glazing
F   Frame
D   Divider
DE   Edge-of-divider
Center-of-glazing, edge-of-glazing, divider, edge-of-divider and frame areas for a typical fenestration product. Edge-of-glazing and edge-of-divider areas are 63.5 mm (2.5 in.) wide. The sum of these component areas equals the total projected fenestration product area.

Figure 2-1. Schematic for whole product area-weighting

2.2. Window Solar Heat Gain Coefficient

The total Solar Heat Gain Coefficient is determined by an area weighted average of contributions from the transparent and the opaque elements in the window. The entire vision area is multiplied by the center-of-glass Solar Heat Gain Coefficient. Determination of the SHGC of opaque window components and the total SHGC is also discussed in this section.

2.2.1. Solar Heat Gain Coefficient of Opaque Window Components

In its most general form, the Solar Heat Gain Coefficient, SHGC, is a function of the solar transmittance, the solar absorptance(s) and the inward flowing fraction of thermal energy. The SHGC is calculated for each component of the window separately (components are shown in Figure 2-1 and takes the general form:

$$SHGC = T^{SOL} + A^{SOL} \cdot N \qquad [2\text{-}2]$$

Where T^{SOL} is the solar transmittance, A^{SOL} is the solar absorptance and N is the inward flowing fraction. For the opaque components of the window, such as frame elements and dividers, $T_{SOL} = 0$ and Equation [2-2] reduces to the product of the solar absorptance and the inward flowing fraction. The inward flowing fraction for the opaque components, N_{opq}, is the U-Value of the component, U_{opq}, divided by the external convective film coefficient, h_{cout}:

$$SHGC_{opq} = A_{opq}^{SOL} \cdot N_{opq} = \frac{A_{opq}^{SOL} \cdot U_{opq}}{h_{c,out}} \qquad [2\text{-}3]$$

where U_{opq} is the area weighted average of the U-values of the opaque elements of the window:

$$A_{opq}^{SOL} \cdot U_{opq} = \frac{\sum_i A_{Fi}^{SOL} \cdot U_{Fi} \cdot A_{Fi} + \sum_j A_{Dj}^{SOL} \cdot U_{Dj} \cdot A_{Dj}}{\sum_i A_{Fi} + \sum_j A_{Dj}} \qquad [2\text{-}4]$$

Where Fi stands for components of the frame (i.e., sill, head, jamb, meeting rail) and Dj stands for divider components.

The solar absorptances A_F^{SOL} and A_D^{SOL}, are found in the FRAME LIBRARY and the DIVIDER LIBRARY.

2.2.2. Total Solar Heat Gain Coefficient

All the transparent regions, center-of-glass, edge-of-glass, and divider edge, have the same SHGC. Once the SHGC of the opaque elements is determined the total Solar Heat Gain Coefficient is calculated as the area weighted average of the SHGC through the transparent and the opaque portions of the window:

$$SHGC_{TOT} = \frac{\sum_j (SHGC_{Cj} \cdot A_{VISj} + SHGC_{Dj} \cdot A_{Dj}) + \sum_i SHGC_{Fi} \cdot A_{Fi}}{A_{TOT}} \qquad [2\text{-}5]$$

Where, Visj stands for visible area of window glazing panes. This includes COG and EOG regions of glazing.

2.2.3. Window Visible Transmittance

The visible transmittance of the window is obtained by multiplying the center-of-glass transmittance by the ratio of the vision area to the total area:

$$T_{VIS} = \frac{\sum\limits_{j} T_{VIS\,j} \cdot A_{VIS\,j}}{A_{TOT}}$$

[2-6]

2.3. Combination Windows

WINDOW program does not model combination windows, but they can be calculated in other tools, such as Excel spreadsheet. The total properties of combination windows are calculated by multiplying the total window properties of each window making up the combination by their respective areas. These weighted properties are then summed and divided by the projected area of the combination window. The combination window calculation allows the user to design nonplanar windows, such as greenhouse windows. In the case of nonplanar windows the user inputs a value for the projected area of the total combination window. The projected area is defined as the rough opening less the installation clearances. This area may be different than the sum of the areas of the windows that make up the combination.

3. CALCULATION OF WINDOW COMPONENT AREAS

WINDOW calculates five possible component areas: frame, divider, center-of-glass, edge-of-glass and divider edge, as shown in the figure below. The calculation procedure for each of these components is considered separately. The vision area is defined in this document, to include all other components of the window except the frame.
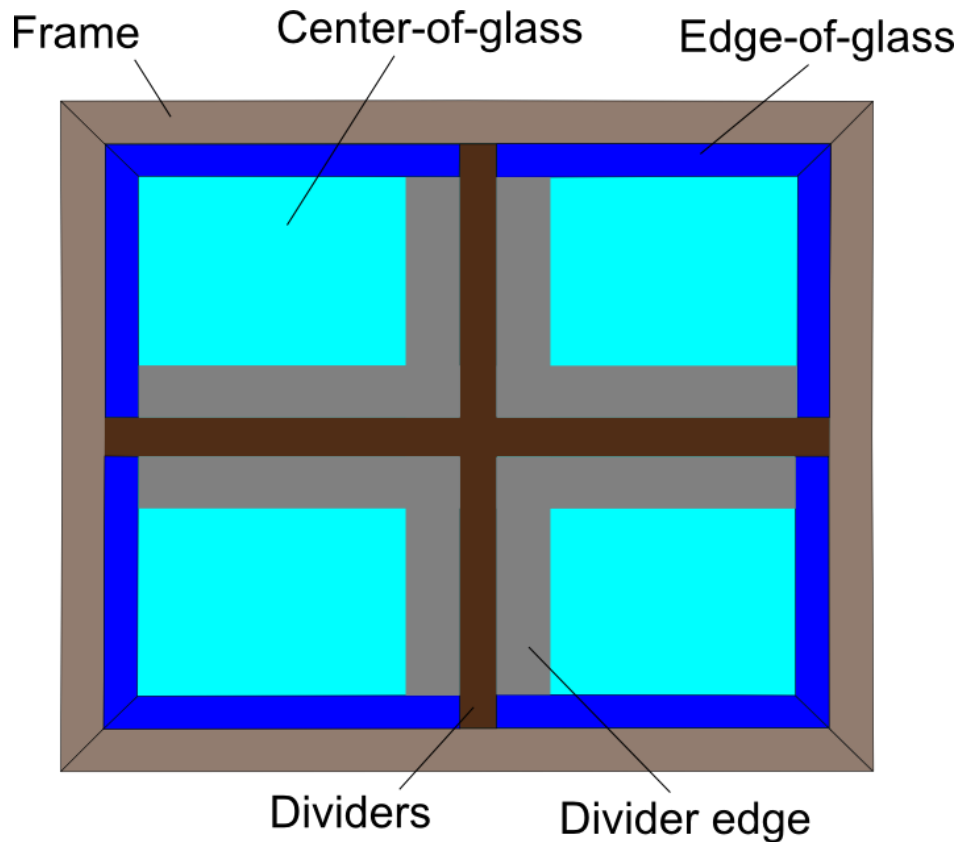
Figure 3-1. Window component areas

WINDOW allows the user to specify the properties of the individual components that make up a total frame. The user selected operator type (such as fixed, vertical slider, horizontal slider) determines which components (head, jamb, sill and meeting rail) are required to define a window. The following sections describe calculations for windows with one and two glazing systems. WINDOW calculates the frame areas based on mitered corners, as they are shown in the figures below.

3.1. Calculation of Vision Area

The vision area includes all the components of the window except for the frame elements. The dimensions of the vision area are determined by subtracting the Projected Frame Dimensions, W_i, from the total window dimensions. The vision area, $A_{vis,j}$, is defined for the jth glazing systems in the window:

$$A_{VIS,j} = V_j \cdot H_j$$
[3-1]

Where V_j is the vertical dimension and H_j is the horizontal dimension of the vision area of the jth glazing system. For a window with one glazing system (Figure 3-2), $j = 1$. The vertical and horizontal dimensions of the vision area, V_1 and H_1, are defined:

$$V_1 = V_{TOT} - W_1 - W_3$$
[3-2]

$$H_1 = H_{TOT} - W_2 - W_4$$
[3-3]

For a horizontal slider type window (Figure 3-3), $j = 1$ and 2. The horizontal dimensions of the vision area, H_1 and H_2, are specified by the user on the main screen and the vertical dimensions are defined:

$$V_1 = V_{TOT} - W_2 - W_4$$
[3-4]

$$V_2 = V_{TOT} - W_5 - W_7$$
[3-5]

The dimensions of the vision areas of a vertical slider type window are analogous to those of a horizontal slider type window with the horizontal and vertical orientations exchanged.

3.2. Windows with One Glazing System

The frame elements of windows with one glazing system are trapezoidal. Equations [3-6] - [3-9] are used to calculate the areas of frame elements in a window with only one glazing system.

$$AF_1 = W_1 \cdot (H_1 + 0.5 \cdot (W_2 + W_4)) \qquad\qquad [3\text{-}6]$$

$$AF_2 = W_2 \cdot (V_1 + 0.5 \cdot (W_1 + W_3)) \qquad\qquad [3\text{-}7]$$

$$AF_3 = W_3 \cdot (H_1 + 0.5 \cdot (W_2 + W_4)) \qquad\qquad [3\text{-}8]$$

$$AF_4 = W_4 \cdot (V_1 + 0.5 \cdot (W_1 + W_3)) \qquad\qquad [3\text{-}9]$$
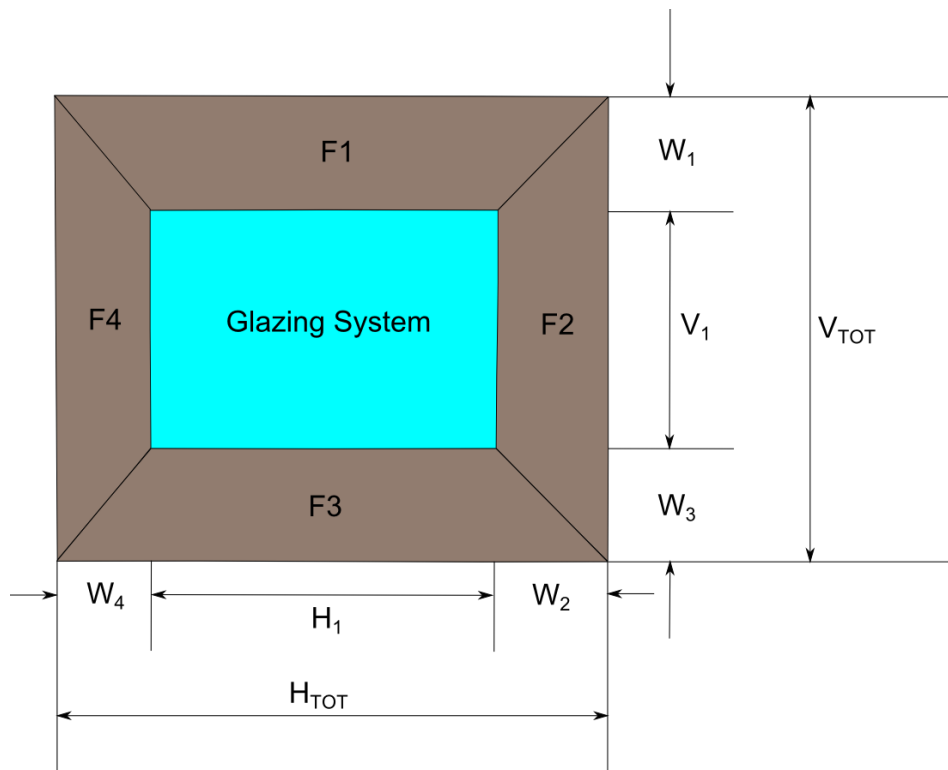
Figure 3-2. Schematic of a window with one glazing system

3.3. Windows with Two Glazing Systems

Windows with two glazing systems have the added complication of a mullion or meeting rail. The meeting rail is artificially divided in half for calculation purposes. The left half is associated with Glazing System 1 and the right half is associated with Glazing System 2. The meeting rail in a Vertical Slider is treated in an analogous manner. Equations [3-10] - [3-16] are used to calculate the areas of the various frame elements found in windows with two glazing systems.

$$AF_1 = W_1 \cdot (V_1 + 0.5 \cdot (W_2 + W_4)) \qquad \text{[3-10]}$$

$$AF_2 = W_2 \cdot (H_1 + 0.5 \cdot (W_1 + W_3)) \qquad \text{[3-11]}$$

$$AF_3 = 0.5 \cdot W_3 \cdot (V_1 + V_2) \qquad \text{[3-12]}$$

$$AF_4 = W_4 \cdot (H_1 + 0.5 \cdot (W_1 + W_3)) \qquad \text{[3-13]}$$

$$AF_5 = W_5 \cdot (H_2 + 0.5 \cdot (W_3 + W_6)) \qquad \text{[3-14]}$$

$$AF_6 = W_6 \cdot (V_2 + 0.5 \cdot (W_5 + W_7)) \qquad \text{[3-15]}$$

$$AF_7 = W_7 \cdot (H_2 + 0.5 \cdot (W_3 + W_6)) \qquad \text{[3-16]}$$
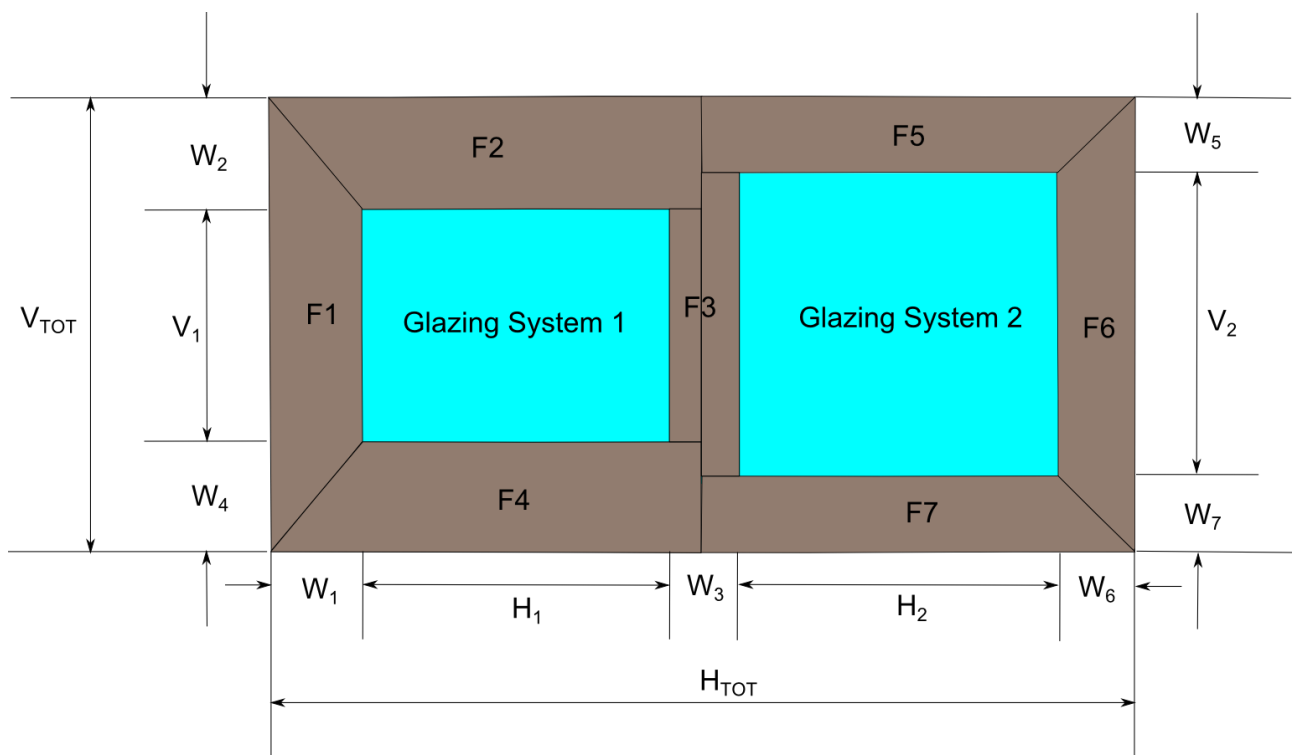
Figure 3-3. Schematic of window types with two glazing systems

3.4. Calculation of Divider Area

A typical window with a system of dividers is shown below. The Projected Divider Dimension, W_{Dj}, is the same for all dividers in a glazing system. The total divider area is the sum of the horizontal divider area plus the vertical divider area, minus the area of overlap. The divider area for the jth glazing system is the product of the divider width, W_D; the dimension of the vision area; and the number of dividers, N.

$$A_{Dj} = W_{Dj} \cdot H_j \cdot N_{Hj} + W_{Dj} \cdot V_j \cdot N_{Vj} - W_{Dj}^2 \cdot N_{Hj} \cdot N_{Vj} \qquad [3\text{-}17]$$
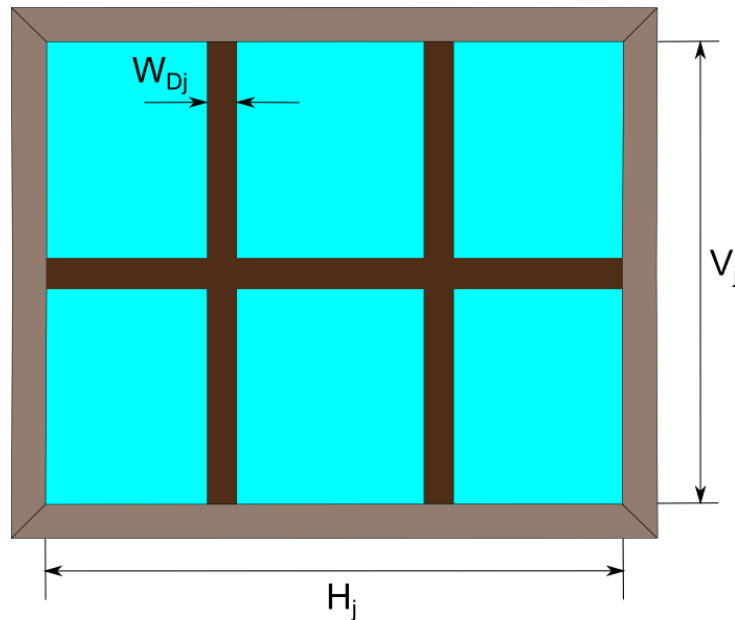
Figure 3-4. In this example, N_H, the number of horizontal dividers, equals 1, and N_V, the number of vertical dividers, equals 2

3.5. Calculation of Edge-of-Glass Area

The edge-of-glass is the region of two-dimensional heat transfer, as opposed to the one-dimensional heat transfer in the center-of-glass region. The edge-of-glass extends from the frame sightline and has a width, W_E, of 63.55 mm. The thermal behavior of the edge region is strongly affected by the spacer and frame construction. A separate edge area and edge-of-glass U-value is calculated for each frame element. Equations [3-18] and [3-19] are used to calculate the edge areas, $A_{Ei,j}$, adjacent to i^{th} frame element for the jth glazing system.

For horizontal frame elements:

$$A_{Ei,j} = W_E \cdot (H_j - W_E - N_{Vj} \cdot W_{Dj})$$
[3-18]

For vertical frame elements:

$$A_{Ei,j} = W_E \cdot (V_j - W_E - N_{Hj} \cdot W_{Dj})$$
[3-19]
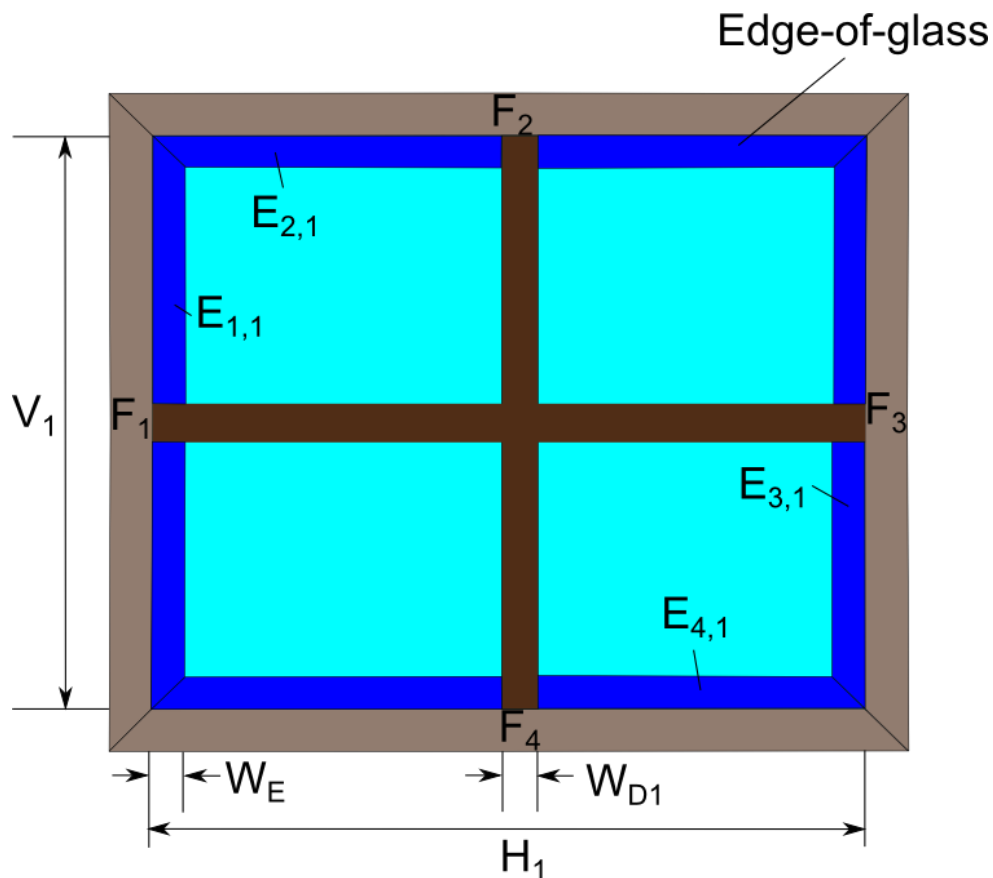
Figure 3-5. The edge-of-glass area

3.6. Calculation of Divider Edge Area

The presence of dividers within an insulated glass unit can create a region of two-dimensional heat transfer in the glass near the dividers. This region is referred to as the divider edge area. The width of the divider edge (W_{DE}) is the same as the width of the edge-of-glass, 63.55 mm. The divider edge area is shown in the figure below. It extends a width of W_{DE} on either side of the divider, but does not extend into the area defined as the edge-of-glass area. The divider edge area for the jth glazing system is calculated as follows:

$$A_{DEj} = 2 \cdot W_E \cdot [N_{Hj} \cdot (H_j - 2 \cdot W_E) + N_{Vj} \cdot (V_j - 2 \cdot W_E)]$$
$$- N_{Hj} \cdot N_{Vj} \cdot (4 \cdot W_{DE}^2 + 4 \cdot W_E \cdot W_{Dj})$$

[3-20]
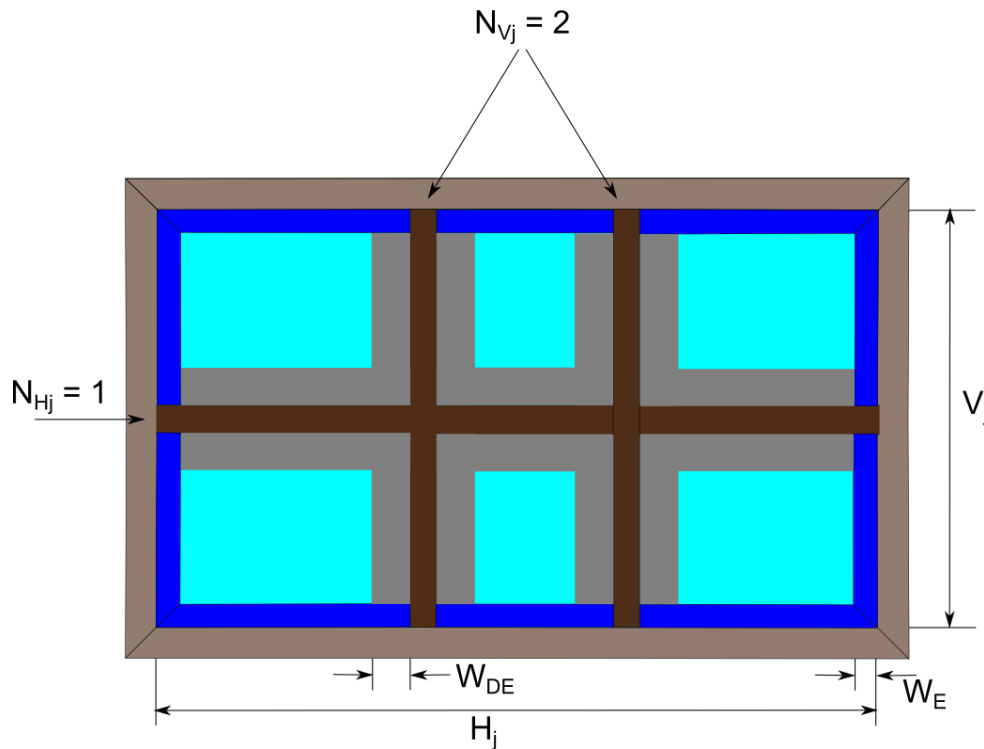
Figure 3-6. The divider edge area

3.7. Calculation of the Center-of-Glass Area

The center-of-glass area of the jth glazing system, is calculated by subtracting the total edge-of-glass area, the divider area and the divider edge area for each glazing system from the vision area (see Equation [3-1]):

$$A_{Cj} = A_{VISj} - A_{Dj} - A_{DEj} - \sum_{i=1}^{M} A_{Ei,j}$$

[3-21]

Where M is the number of different frame elements that make up the total frame.

4. GLAZING LAYER DESCRIPTION

4.1. Layer

Layers, being constitutive part of glazing systems, are defined with a list of geometrical and thermo-physical properties. The geometric properties are width (W), height (H) and thickness (t).
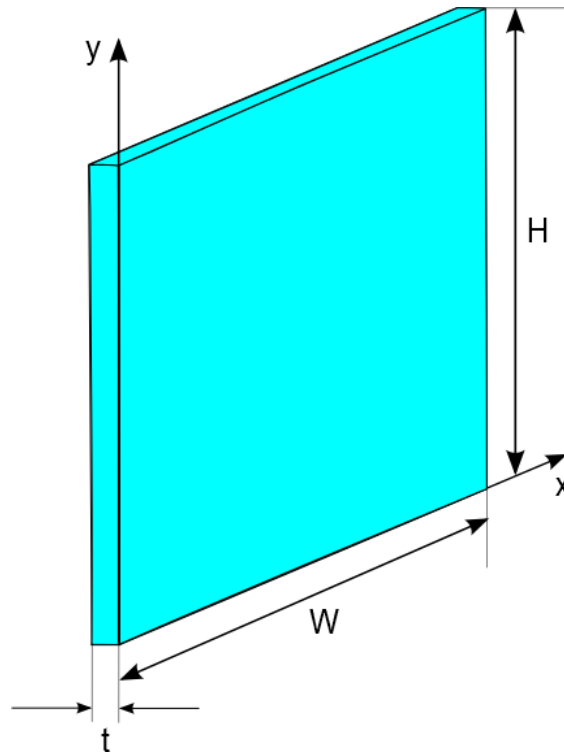
Figure 4-1. Geometry of a Layer

The geometry (shown in Figure 4-1), completely describes the specular planar layer (e.g., glass, suspended film, etc.). On the other hand, a layer can represent a shading device, which has several additional geometrical parameters (see Figure 4-2).
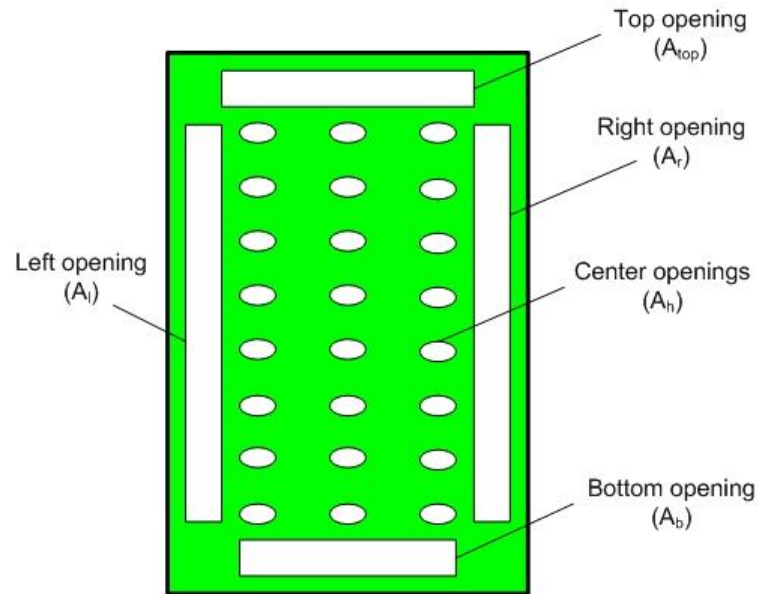
Figure 4-2. Geometry of a Generalized Shading Layer

The thermo-physical properties of a layer, which are important for the calculation of the thermal and solar-optical properties of a glazing system are:

- Emissivity of both glazing surfaces

- Transmittance as a function of wavelength

- Reflectance, back and front, as a function of wavelength

- Thermal conductivity

The energy balance of a glazing layer, or the entire glazing system, is determined by the transmitted, reflected and absorbed energy, which can be calculated by the application of the conservation of energy principle. Figure 4-3, shows this energy balance:
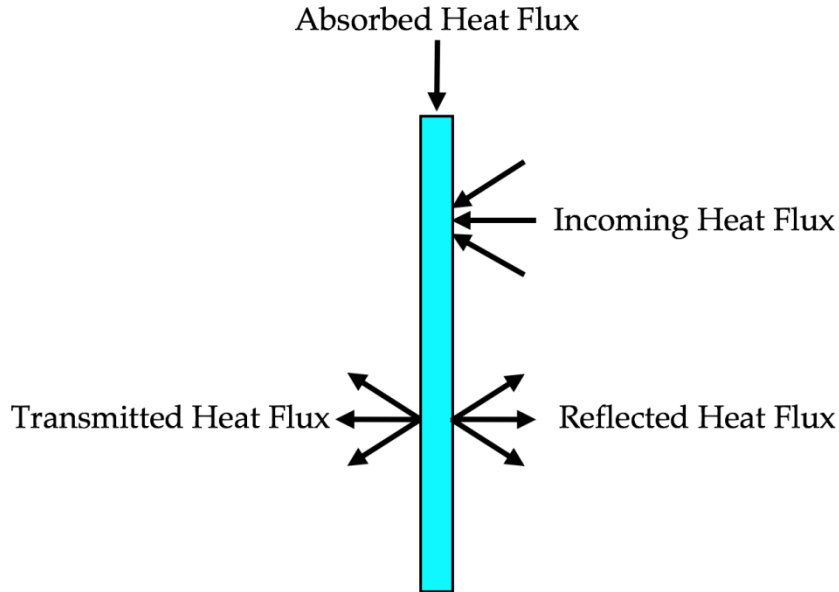
Figure 4-3. Energy Balance of a Single Monolithic Glazing Layer

Laminate type layers are represented by several solid layers in contact with each other (i.e., no gas in between), as shown in Figure 4-4. Models for laminate type layers can be used to model typical laminated glass, consisting of PVB interlayer(s) sandwiched between glass panes, or for the modeling of low-e coatings, or other very thin layers deposited on glass. This model can also be used to simulate spandrel panels, where several solid layers may be in direct contact.
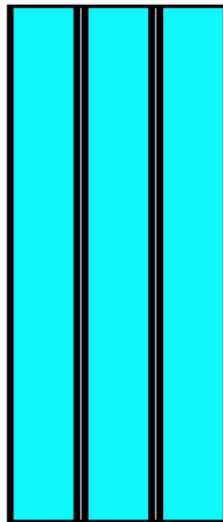
Figure 4-4. Laminate Layer

4.2. Glazing Gaps

A glazing gap can contain pure gas or a gas mixture. A glazing gap may also be evacuated (i.e., vacuum). A glazing system may have one or more glazing gaps. Figure 4-5, shows a single gap in a double-glazed system. Figure 4-6, shows four glass layers separated by three glazing gaps.
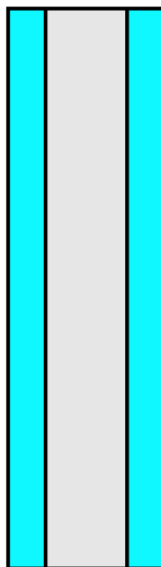
Figure 4-5. Glazing Gap (Gas Fill) Between Two Layers

- Gasses that are filled in glazing gaps have the following thermo-physical properties:
  - o Thermal conductivity [W/(m·K)]
  - o Dynamic viscosity [g/(m·s)]
  - o Density [kg/m³]
  - o Specific heat [J/(g·K)]
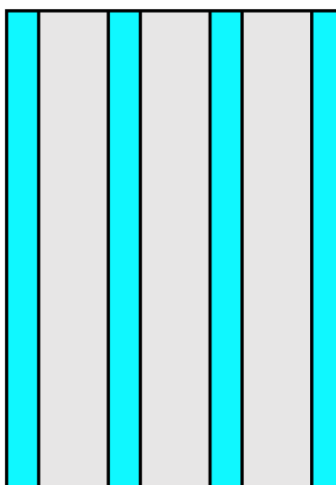
Figure 4-6. Glazing System Consisting of Specular Layers

4.3. Shading Devices

Shading devices are modeled similarly to solid glazing layers, with the exception that the model accounts for potential airflow pathways, such as side gaps, top and bottom gaps, and air flow through the shading device

(porosity). Figure 4-7, shows a triple glazed system (three glass layers) and one shading layer, and Figure 4-8, shows a room side shading layer.
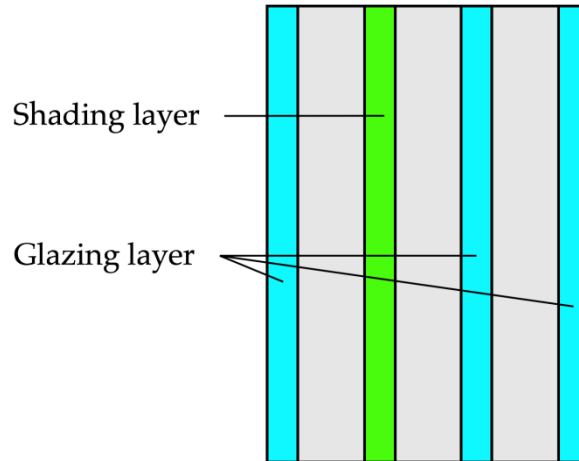
Figure 4-7. Glazing System Consisting of three Glazing Layers and one Shading Layer
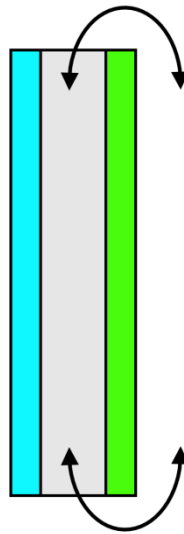
Figure 4-8. Shading Layer on Indoor (Room) Side

The current implementation of the thermal model for glazing systems allows for a large number of specular layers (1000), but only one shading layer.

In glazing systems without shading layers, there is no cross-flow from one glazing gap to another or from a glazing gap to the outdoor or indoor environment. However, when there is a shading layer present, gas can flow between gaps or between the glazing gap and indoor and outdoor environment (see Figure 4-9). This is referred to as a ventilated gap.
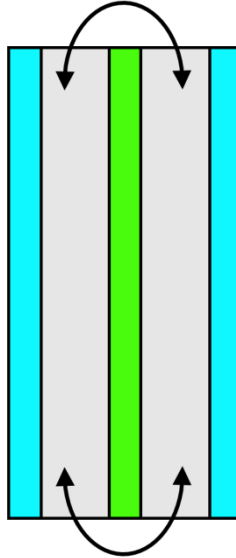
Figure 4-9. Two Gaps Connected

There can be two different types of flow in the case of ventilated gaps, a) *natural convection*, which is temperature driven due to the differences in density of the gas (i.e., buoyancy); and b) *forced convection*, caused by some external force, such as a fan or wind.

5. GLAZING SYSTEM THERMAL PERFORMANCE: ISO 15099

ISO 15099 is a detailed calculational standard, which is used in North America to predict the thermal and optical performance of windows. In this document, the procedures for calculating center of glazing performance are presented (i.e., areas of glazing where heat transfer can be assumed to be one-dimensional). Separate documents are dedicated to 2-D and 3-D heat transfer for the edge of glazing and frame, and for combining these various componnets into the overall window heat transfer and optical performance.

5.1. Glazing Systems Consisting of Monolithic Layers

The calculation of glazing system thermal properties is based on a comprehensive heat transfer model, with analysis of coupled conductive, convective and radiative heat transfer. Radiative heat exchange between glazing layers, as well as conductive heat transfer within each layer, can be described using first principles calculation. Convection heat transfer is modeled using heat transfer correlations, which are based on experimental measurements and numerical modeling of selected heat transfer cases (e.g., natural convection over a flat plate, natural convection in a rectangular enclosure, forced convection over a flat plate, etc.).

5.1.1. Definitions

Before the presentation of the algorithms and mathematical models, the following definitions are necessary.

Orientation of the glazing system: the outdoor (exterior) environment is always located on the left, while the indoor (interior) side is always located on the right side of the glazing system (see Figure 5-1)

Layer and gap numbering is done from left to right (see Figure 5-2)

Each layer has a front and back surface, labeled "f" and "b" (see Figure 5-3)

Glazing system properties also have a front and back side (see Figure 5-4)
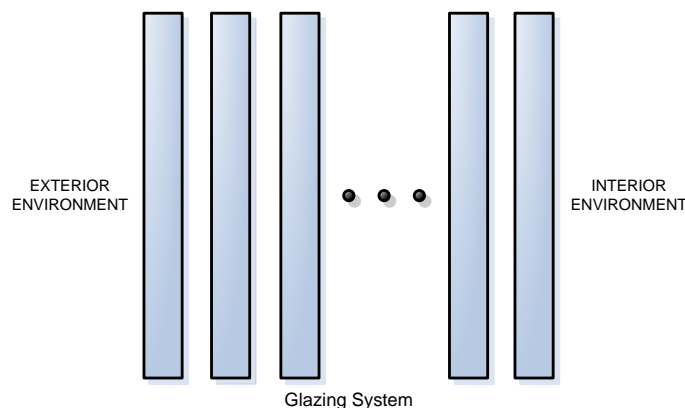
Figure 5-1. Orientation of the Glazing System with Respect to Outdoor (Exterior) and Indoor (Interior) Environment
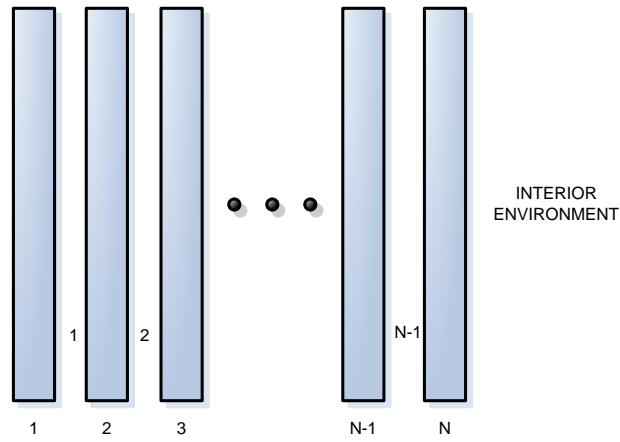
Figure 5-2. Layer and Gap Numbering
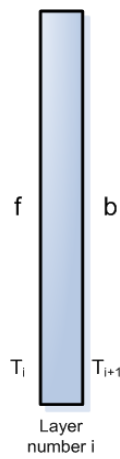
Figure 5-3. Layer Number i
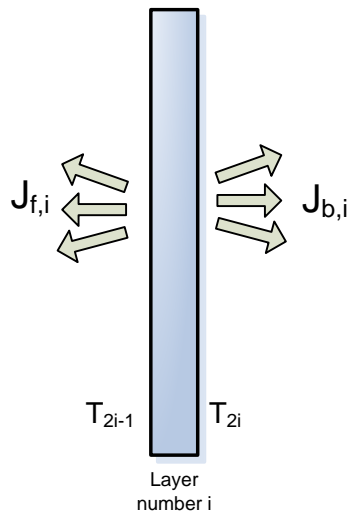
Figure 5-4. Temperatures and Energy Balance Notation

5.1.2. Heat transfer calculations

Figure 5-5 shows the glazing system, consisting of *n* layers, that is subjected to the set of standard boundary conditions. Each glazing layer is described with three longwave infra-red (IR) optical properties: the front and back surface emissivities, $\varepsilon_{f,i}$ and $\varepsilon_{b,i}$, and the transmittance τ_i.
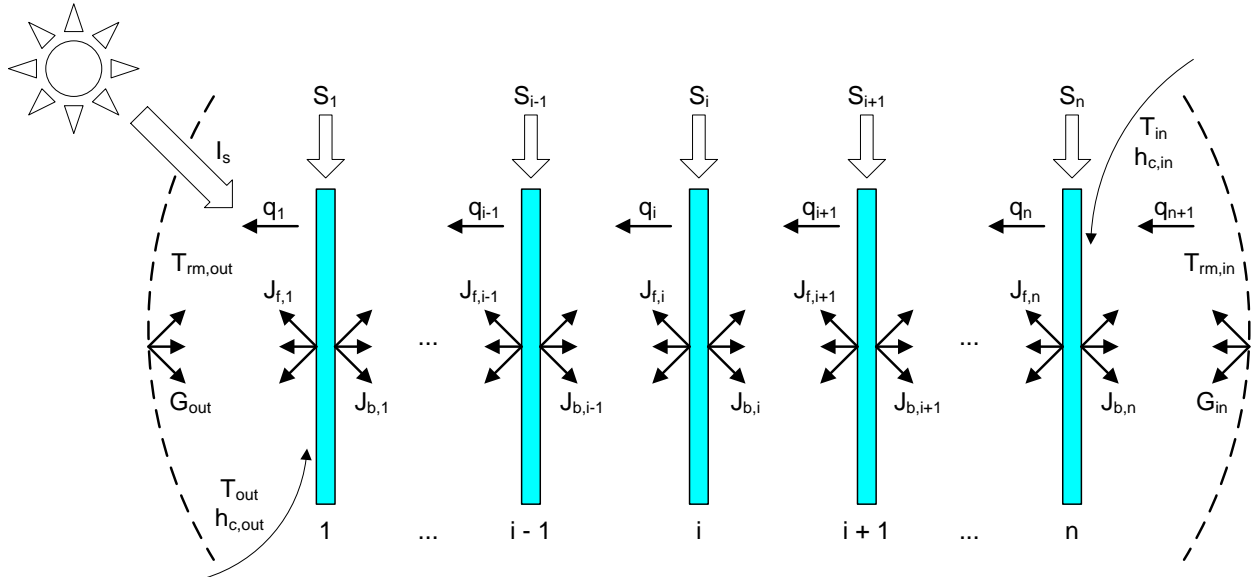
Figure 5-5. Numbering System, Boundary Conditions and Energy Balance for N-Layer Glazing System

5.1.2.1. Energy Balance

For each layer in the glazing system, shown in Figure 5-5, the energy balance is set up, and the values of four variables are sought. These are the temperatures of the outdoor and indoor facing surfaces, $T_{f,i}$ and $T_{b,i}$, plus the radiant heat fluxes leaving the front and back facing surfaces (i.e. the radiosities), $J_{f,i}$ and $J_{b,i}$. In terms of these variables the heat flux across the *i*th gap (i.e. q_i) is:

$$q_i = h_{c,i}[T_{f,i} - T_{b,i-1}] + J_{f,i} - J_{b,i-1}$$

[5-1]

Similarly, the heat flux across (*i*+1)th gap is determined as:

$$q_{i+1} = h_{c,i+1}[T_{f,i+1} - T_{b,i}] + J_{f,i+1} - J_{b,i}$$

[5-2]

Heat transfer through a solid layer:

$$q_{gl} = \frac{k_{g,i}}{t_{g,i}} \cdot (T_{b,i} - T_{f,i})$$

[5-3]

where,

$k_{g,i}$ = layer conductivity

$t_{g,i}$ = layer thickness

The solution (i.e. temperatures at each glazing surface and corresponding radiant fluxes) is generated by applying the following four equations at each layer:

$$q_i = S_i + q_{i+1} \tag{5-4}$$

$$J_{f,i} = \varepsilon_{f,i} \sigma T_{f,i}^4 + \tau_i J_{f,i+1} + \rho_{f,i} J_{b,i-1} \tag{5-5}$$

$$J_{b,i} = \varepsilon_{b,i} \sigma T_{b,i}^4 + \tau_i J_{b,i-1} + \rho_{b,i} J_{f,i+1} \tag{5-6}$$

$$T_{b,i} - T_{f,i} = \frac{t_{g,i}}{2k_{g,i}} \left[2q_{i+1} + S_i \right] \tag{5-7}$$

Equation [5-4] describes an energy balance imposed at the surfaces of the ith glazing layer. Equations [5-5] and [5-6] define the radiosities at the ith glazing, where $\rho_{f,i} = 1 - \varepsilon_{f,i} - \tau_i$ and $\rho_{b,i} = 1 - \varepsilon_{b,i} - \tau_i$, while the temperature difference across the ith glazing layer is given by equation [5-7].

In all, 4n (n – number of glazing layers) equations can be written for the glazing system.

These equations needs to be solved for front and back radiosities (Jf,i and Jb,i) and front and back temperatures (Tf,i and Tb,i). Unknown variables for ith layer within the glazing system can be presented in vector form:

$$\begin{bmatrix} T_{f,i} \\ T_{b,i} \\ J_{f,i} \\ J_{b,i} \end{bmatrix} \tag{5-8}$$

While equations [5-4] to [5-7] are valid for a layer in between, they need slight modifications for layers next to exterior and interior environments.

Outdoor layer

$$q_1 = h_{c,out} \cdot (T_{f,1} - T_{out}) + J_{f,1} + G_{out} \tag{5-9}$$

$$J_{f,1} = \varepsilon_{f,1} \cdot \sigma \cdot T_{f,1}^4 + \tau_{b,1} \cdot J_{f,2} + \rho_{f,1} \cdot G_{out} \tag{5-10}$$

$$J_{b,1} = \varepsilon_{b,1} \cdot \sigma \cdot T_{b,1}^4 + \tau_{f,1} \cdot G_{out} + \rho_{b,1} \cdot J_{f,2} \tag{5-11}$$

Indoor layer

$$q_{n+1} = h_{c,in} \cdot (T_{in} - T_{b,n}) + G_{in} - J_{b,n} \tag{5-12}$$

$$J_{f,n} = \varepsilon_{f,n} \cdot \sigma \cdot T_{f,n}^4 + \tau_{b,n} \cdot G_{in} + \rho_{f,n} \cdot J_{b,n-1} \tag{5-13}$$

$$J_{b,n} = \varepsilon_{b,n} \cdot \sigma \cdot T_{b,n}^4 + \tau_{f,n} \cdot J_{b,n-1} + \rho_{b,n} \cdot G_{in}$$

The equations contain terms in temperature ($T_{f,i}, T_{b,i}$) and black emissive power ($E_{bf,i} = \sigma T_{f,i}^4$, $E_{bb,i} = \sigma T_{b,i}^4$) and, hence, are nonlinear. They would become linear only if solved in terms of black emissive power instead of temperature (Note: The system of equations is still non-linear due to the fourth power of temperature in radiation terms and 1/3rd and 1/4th power of temperature in natural convection terms and therefore needs to be solved iteratively), These equations are linearized by splitting the above terms into two parts $\sigma T_{f,i}^3$ and

$T_{f,i}$. The first term is carried from the previous iteration, while the second term is the current iteration unknown, thus linearizing equations. This process produces accurate results only if the unknown variable does not change significantly between the two final iterations. Therefore, it is necessary to define two new quantities:

convection heat transfer coefficient based on emissive power

$$\hat{h}_i = h_{c,i} \frac{T_{f,i} - T_{b,i-1}}{E_{bf,i} - E_{bb,i-1}}$$

[5-14]

conduction heat transfer coefficient based on emissive power

$$\hat{h}_i^{gl} = \frac{k_{gl,i}}{t_{gl,i}} \cdot \frac{T_{b,i} - T_{f,i}}{E_{bb,i} - E_{bf,i}}$$

[5-15]

The application of black emissive power terms (i.e. $E_{bf,i}$ and $E_{bb,i}$) and heat transfer coefficients based on the emissive power (i.e. $\hat{h}_i$ and $\hat{h}_i^{gl}$) gives the following relations for heat fluxes across gas spaces:

$$q_i = \hat{h}_i [E_{bf,i} - E_{bb,i-1}] + J_{f,i} - J_{b,i-1}$$

[5-16]

$$q_{i+1} = \hat{h}_{,i+1}[E_{bf,i+1} - E_{bb,i}] + J_{f,i+1} - J_{b,i}$$

[5-17]

The basic energy balance equations [5-4] – [5-7] are transformed into the following system:

$$q_i = S_i + q_{i+1}$$

[5-18]

$$J_{f,i} = \varepsilon_{f,i} E_{bf,i} + \tau_i J_{f,i+1} + \rho_{f,i} J_{b,i-1}$$

[5-19]

$$J_{b,i} = \varepsilon_{b,i} E_{bb,i} + \tau_i J_{b,i-1} + \rho_{b,i} J_{f,i+1}$$

[5-20]

$$\hat{h}_i^{gl}[E_{bb,i} - E_{bf,i}] = 0.5 S_i + \hat{h}_{i+1}[E_{bf,i+1} - E_{bb,i}] + J_{f,i+1} - J_{b,i}$$

[5-21]

This system of 4n non-linear equations can be solved using an iterative solution algorithm that is comprised of following steps:

Calculation of initial glazing layer temperatures

Calculation of heat transfer coefficients based on temperatures defined in previous step

Solution of the system of linear equations and definition of new sets of temperatures at each glazing layer

Convergence checking (comparison of new sets of temperatures to old sets)

If each temperature in the new set is not equal to the corresponding temperature in the old set within a defined tolerance, the new sets are used to replace the old sets and the calculation proceeds to the second step.

This calculation procedure is described in more detail in Section 5.1.2.4.

5.1.2.2. Initial Temperature Distribution

Initial glazing layer temperatures are calculated assuming a constant temperature gradient across the window. Thus, the temperature at each glazing layer surface can be determined by the following equation:

$$T_i = T_{out} + x_i \frac{T_{in} - T_{out}}{t_{gs}}$$
[5-22]

Where:

x_i = distance between i[th] glazing layer and outdoor environment

t_{gs} = thickness of whole glazing system

5.1.2.3. Boundary Conditions

5.1.2.3.1. Outdoor Heat Transfer Coefficients

O*utdoor radiation heat transfer coefficient* ($h_{r,out}$) is calculated using following two relations:

$$h_{r,out} = 4\sigma\varepsilon_{f,1}\left(\frac{T_{rm,out} + T_{f,1}}{2}\right)^3$$
[5-23]

$$h_{r,out} = \frac{G_{out} - R_{f,1}}{T_{rm,out} - T_{f,1}}$$
[5-24]

where,

$\varepsilon_{f,1}$ = emissivity of the front surface of the first glazing layer

$T_{f,i}$ = temperature of the front surface of the first glazing layer

$R_{f,i}$ = radiative flux leaving the front surface of the first glazing layer

In the first iteration, $h_{r,out}$ is calculated using equation [5-23], but in the second and all later iterations (if necessary), equation [5-24] is used.

O*utdoor convection heat transfer coefficient* ($h_{c,out}$) depends on the method for defining the outdoor combined heat transfer coefficient (h_{out}).

If the value of h_{out}, which incorporates the effects of both convective and radiative heat transfer, is prescribed, the outdoor convection heat transfer coefficient is calculated as:

$$h_{c,out} = h_{out} - h_{r,out}$$
[5-25]

Otherwise, the calculation of $h_{c,out}$ is based on the known value for outdoor wind speed:

$$h_{c,out} = 4 + 4w_s$$
[5-26]

Where:

w_s = outdoor wind speed near glass surface,

Combined outdoor surface heat transfer coefficient (h_{out}) is:

$$h_{out} = h_{c,out} + h_{r,out}$$
<div align="right">[5-27]</div>

When the outdoor convection heat transfer coefficient ($h_{c,out}$) is determined, the corresponding *outdoor heat transfer coefficient based on emissive power* can defined as:

$$\hat{h}^{out} = h_{c,out} \frac{T_{f,1} - T_{amb}}{E_{bf,1} - G_{out}}$$
<div align="right">[5-28]</div>

Where:

$E_{bf,1}$ = emissive power of the front surface of the first glazing layer

T_{amb} = outdoor environment temperature, given as:

$$T_{amb} = \frac{h_{c,out} T_{out} + h_{r,out} T_{rm,out}}{h_{c,out} + h_{r,out}}$$
<div align="right">[5-29]</div>

5.1.2.3.2. Indoor Heat Transfer Coefficients

Indoor radiation heat transfer coefficient ($h_{r,in}$) is calculated using different relations for the first and for all other iterations. In the first iteration, the calculation is performed according to equation [5-30], while equation [5-31] gives the relation used in all other iterations.

$$h_{r,in} = 4\sigma\varepsilon_{b,n}\left(\frac{T_{rm,in} + T_{f,n}}{2}\right)^3$$
<div align="right">[5-30]</div>

$$h_{r,out} = \frac{G_{in} - R_{b,n}}{T_{rm,in} - T_{b,n}}$$
<div align="right">[5-31]</div>

Where:

$\varepsilon_{b,n}$ = emissivity of the back surface of the nth glazing layer

$T_{b,n}$ = temperature of the back surface of the nth glazing layer

$R_{b,n}$ = radiative flux leaving the back surface of the nth glazing layer

Indoor convection heat transfer coefficient ($h_{c,in}$) can be determined in two ways, depending on the method for the calculation of indoor combined heat transfer coefficient (h_{in}).

When the value of h_{in} is prescribed, the indoor convection heat transfer coefficient is calculated as:

$$h_{c,in} = h_{in} - h_{r,in}$$
<div align="right">[5-32]</div>

Otherwise, natural convection is assumed to be on the indoor side of fenestration system, and $h_{c,in}$ can be determined as:

$$h_{c,in} = N_u \frac{k}{H}$$

[5-33]

Where:

N_u = Nusselt number

k = thermal conductivity of air

H = height of the fenestration system

The Nusselt number is a function of the Rayleigh number, based on the height of the fenestration system, and the tilt angle. Dependence on the window tilt angle is given through the following set of equations, and each of them corresponds to one particular range of tilt angle:

Window inclined from 0° to 15° $(0^o \le \theta < 15^o)$

$$N_u = 0.13 Ra_H^{1/3}$$

[5-34]

Window inclined from 15° to 90° $(15^o \le \theta \le 90^o)$

$$Ra_C = 2.5 \cdot 10^5 \left(\frac{e^{0.72 \cdot \theta}}{\sin \theta} \right)^{1/5} \; ; \theta \text{ in degrees}$$

[5-35]

$$N_u = 0.56 \cdot (Ra_H \sin \theta)^{1/4} \; ; \; Ra_H \le Ra_C$$

[5-36]

$$N_u = 0.13 \cdot (Ra_H^{1/3} - Ra_C^{1/3}) + 0.56 \cdot (Ra_C \sin \theta)^{1/4} \; ; \; Ra_H > Ra_C$$

[5-37]

Window inclined from 90° to 179° $(90^o < \theta \le 179^o)$

$$N_u = 0.56 \cdot (Ra_H \sin \theta)^{1/4} \; ; \; 10^5 \le Ra_H \sin \theta < 10^{11}$$

[5-38]

Window inclined from 179° to 180° $(179^o < \theta \le 180^o)$

$$N_u = 0.58 Ra_H^{1/5} \; ; \; Ra_H \le 10^{11}$$

[5-39]

Where:

Ra_H = Rayleigh number based on the height of the fenestration system, defined as:

$$Ra_H = \frac{\rho^2 H^3 g C_p (T_{in} - T_{b,n})}{T_{mf} \mu k}$$

[5-40]

Air properties (i.e. density, specific heat, viscosity and thermal conductivity) are evaluated at the mean film temperature:

$$T_{mf} = T_{in} + \frac{1}{4} \left(T_{b,n} - T_{in} \right)$$

[5-41]

Indoor combined surface heat transfer coefficient is determined as:

$$h_{in} = h_{c,in} + h_{r,in}$$

[5-42]

After determination of the indoor convection heat transfer coefficient ($h_{c,in}$), the corresponding *indoor heat transfer coefficient based on emissive power* can be found as:

$$h_{hat}^{in} = h_{c,in} \frac{T_{room} - T_{b,n}}{G_{out} - E_{bb,n}}$$

[5-43]

Where:

$E_{bb,n}$ = emissive power of the back surface of the nth glazing layer

T_{room} = indoor environment temperature, given as:

$$T_{room} = \frac{h_{c,in} T_{in} + h_{r,in} T_{rm,in}}{h_{c,in} + h_{r,in}}$$

[5-44]

5.1.2.3.3. Glazing Cavity Heat Transfer

The glazing cavity convective heat transfer coefficient is determined using following relation:

$$h_{c,i} = N_{u,i} \frac{k_{g,i}}{d_{g,i}}$$

[5-45]

Where:

$N_{u,i}$ = Nusselt number

$k_{g,i}$ = thermal conductivity of the fill gas in the cavity

$d_{g,i}$ = thickness of the glazing cavity

The Nusselt number, calculated using correlations based on experimental measurements of heat transfer across inclined air layers, is a function of the Rayleigh number, the cavity aspect ratio and the glazing system tilt angle.

The Rayleigh number can be expressed as (omitting the "i" and "g" subscripts for convenience):

$$R_a = \frac{\rho^2 d^3 g C_p (T_{f,i} - T_{b,i-1})}{T_m \mu k}$$

[5-46]

All gas fill properties (i.e. density, specific heat, viscosity and thermal conductivity) are evaluated at mean gas fill temperature, defined as:

$$T_m = \frac{T_{f,i} + T_{b,i-1}}{2}$$

[5-47]

The aspect ratio of the glazing cavity is:

$$A_{g,i} = \frac{H}{d_{g,i}}$$

[5-48]

Where:

H = distance between the top and bottom of glazing cavity, usually the same as the height of the window view area

The correlation between the Nusselt number and glazing system tilt angle is given in following equations for different tilt angle ranges:

Windows inclined from 0° to 60° $(0^o \leq \theta < 60^o)$

$$N_{u,i} = 1 + 1.44 \left(1 - \frac{1708}{R_a \cos\theta}\right)^{\bullet} \left[1 - \frac{1708 \sin^{1.6}(1.8 \cdot \theta)}{R_a \cos\theta}\right] + \left[\left(\frac{R_a \cos\theta}{5830}\right)^{1/3} - 1\right]^{\bullet}, R_a < 10^5 \text{ and } A_{g,i} > 20 \qquad [5\text{-}49]$$

$$(X)^{\bullet} = \frac{X + |X|}{2} \qquad [5\text{-}50]$$

Windows inclined at 60° $(\theta = 60^o)$

$$N_{u,i} = (N_{u1}, N_{u2})_{max} \qquad [5\text{-}51]$$

$$N_{u1} = \left[1 + \left(\frac{0.0936 R_a^{0.314}}{1+G}\right)^7\right]^{1/7} \qquad [5\text{-}52]$$

$$N_{u2} = \left(0.104 + \frac{0.175}{A_{g,i}}\right) R_a^{0.283} \qquad [5\text{-}53]$$

$$G = \frac{0.5}{\left[1 + \left(\frac{R_a}{3160}\right)^{20.6}\right]^{0.1}} \qquad [5\text{-}54]$$

Windows inclined from 60° to 90° $(60^o < \theta < 90^o)$

In this case, the Nusselt number is calculated using straight-line interpolation between the results of equations [5-51] and [5-55].These equations are valid in the ranges of $10^2 < R_a < 2 \cdot 10^7$ and $5 < A_{g,i} < 100$.

Windows inclined at 90° $(\theta = 90^o)$

$$N_{u,i} = (N_{u1}, N_{u2})_{max} \qquad [5\text{-}55]$$

where,

$$N_{u1} = 0.0673838 R_a^{1/3} \; ; \; 5 \cdot 10^4 < R_a \qquad [5\text{-}56]$$

$$N_{u1} = 0.028154 R_a^{0.4134} \quad ; \quad 10^4 < R_a \leq 5 \cdot 10^4 \tag{5-57}$$

$$N_{u1} = 1 + 1.7596678 \cdot 10^{-10} R_a^{2.2984755} \quad ; \quad R_a \leq 10^4 \tag{5-58}$$

$$N_{u2} = 0.242 \cdot \left(\frac{R_a}{A_{g,i}} \right)^{0.272} \tag{5-59}$$

Windows inclined from 90° to 180° $(90^o < \theta < 180^o)$

$$N_{u,i} = 1 + (N_{uv} - 1)\sin\theta \tag{5-60}$$

Where:

N_{uv} = Nusselt number for a vertical cavity, given by equation [5-55]

When the convective heat transfer coefficient is found, the corresponding coefficient based on emissive power can be calculated, as described in equation [5-61]:

$$h_{hat,i} = h_{c,i} \frac{T_{f,i} - T_{b,i-1}}{E_{bf,i} - E_{bb,i-1}} \tag{5-61}$$

Where:

$E_{bb,i-1}, E_{bf,i}$ = emissive powers of glazing surfaces surrounding the glazing cavity

5.1.2.3.4. Thermo-physical Properties of Gases

The density of individual gasses is calculated using the perfect gas law, while the other properties are determined as a linear function of mean temperature – T_m. The properties of gas mixtures are determined as per the following procedure:
Density

$$\rho = \frac{P\hat{M}_{mix}}{\Re T_m} \tag{5-62}$$

where,

P = normal pressure (101325 Pa)

M_{mix} = molecular mass of the gas mixture, given in equation [5-63]

$\Re$ = universal gas constant (8314.41 J/kmol)

T_m = mean gas mixture temperature, defined as per [5-47]

Molecular Mass

$$\hat{M}_{mix} = \sum_{i=1}^{v} x_i \hat{M}_i \qquad \text{[5-63]}$$

where,

x_i = mole fraction of the ith gas component in a mixture of v gases

Specific Heat

$$C_{pmix} = \frac{\hat{C}_{pmix}}{\hat{M}_{mix}} \qquad \text{[5-64]}$$

Where:

$$\hat{C}_{pmix} = \sum_{i=1}^{v} x_i \hat{C}_{p,i} \qquad \text{[5-65]}$$

and, the molar specific heat of the ith gas is:

$$\hat{C}_{p,i} = C_{p,i} \hat{M}_i \qquad \text{[5-66]}$$

Dynamic Viscosity

$$\mu_{mix} = \sum_{i=1}^{v} \frac{\mu_i}{\left\{ 1 + \sum_{\substack{j=1 \\ j \neq i}}^{v} \varphi^{\mu}_{i,j} \dfrac{x_j}{x_i} \right\}} \qquad \text{[5-67]}$$

Where:

$$\varphi^{\mu}_{i,j} = \frac{\left[1 + \left(\mu_i / \mu_j \right)^{1/2} \left(\hat{M}_j / \hat{M}_i \right)^{1/4} \right]^2}{2\sqrt{2} \left[1 + \left(\hat{M}_i / \hat{M}_j \right) \right]^{1/2}} \qquad \text{[5-68]}$$

Thermal Conductivity

$$\lambda_{mix} = \lambda'_{mix} + \lambda''_{mix} \qquad \text{[5-69]}$$

Where:

λ' = monatomic thermal conductivity

λ'' = accounts for additional energy moved by the diffusional transport of indoor energy in polyatomic gases.

$$\lambda'_{mix} = \sum_{i=1}^{\upsilon} \frac{\lambda'_i}{\left\{ 1 + \sum_{\substack{j=1 \\ j \neq i}}^{\upsilon} \psi_{i,j} \frac{x_j}{x_i} \right\}}$$

[5-70]

$$\psi_{i,j} = \frac{\left[1 + \left(\lambda'_i / \lambda'_j \right)^{1/2} \left(\hat{M}_i / \hat{M}_j \right)^{1/4} \right]^2}{2\sqrt{2} \left[1 + \left(\hat{M}_i / \hat{M}_j \right) \right]^{1/2}} \cdot \left[1 + 2{,}41 \frac{\left(\hat{M}_i - \hat{M}_j \right)\left(\hat{M}_i - 0{,}142\hat{M}_j \right)}{\left(\hat{M}_i + \hat{M}_j \right)^2} \right]$$

[5-71]

$$\lambda''_{mix} = \sum_{i=1}^{\upsilon} \frac{\lambda''_i}{\left\{ 1 + \sum_{\substack{j=1 \\ j \neq i}}^{\upsilon} \varphi^{\lambda}_{i,j} \frac{x_j}{x_i} \right\}}$$

[5-72]

where the expression for $\phi_{i,j}$ is given as:

$$\varphi^{\lambda}_{i,j} = \frac{\left[1 + \left(\lambda'_i / \lambda'_j \right)^{1/2} \left(\hat{M}_i / \hat{M}_j \right)^{1/4} \right]^2}{2\sqrt{2} \left[1 + \left(\hat{M}_i / \hat{M}_j \right) \right]^{1/2}}$$

[5-73]

To find λ_{mix}, it is necessary to:

calculate λ'_i

$$\lambda'_i = \frac{15}{4} \frac{\mathfrak{R}}{\hat{M}_i} \mu_i$$

[5-74]

calculate λ''_i

$$\lambda''_i = \lambda_i - \lambda'_i$$

[5-75]

λ_i – conductivity of the ith fill gas component

use λ'_i to calculate λ'_{mix}

use λ''_i to calculate λ''_{mix}

determine λ_{mix} as per equation [5-69]

5.1.2.3.5. Interaction with the Environment

The effect of boundary conditions imposed by the environment on the glazing system is given by:

Temperatures
Outdoor and indoor temperatures are defined as:

$$T_{b,0} = T_{out} \qquad\qquad \text{[5-76]}$$

$$T_{f,n+1} = T_{in} \qquad\qquad \text{[5-77]}$$

Where:

T_{out} = outdoor air temperature

T_{in} = indoor air temperature

Long Wave Irradiance
Outdoor irradiance is set as:

$$J_{b,0} = G_{out} = \sigma T_{rm,out}^4 \qquad\qquad \text{[5-78]}$$

where,

$T_{rm,out}$ = outdoor mean radiant temperature, calculated as:

$$T_{rm,out} = \left\{ \frac{[F_{gd} + (1 - f_{clr})F_{sky}]\sigma T_{out}^4 + f_{clr}F_{sky}J_{sky}}{\sigma} \right\}^{1/4} \qquad\qquad \text{[5-79]}$$

f_{clr} = fraction of the sky that is clear

J_{sky} = radiosity of the clear sky, defined as:

$$J_{sky} = 5.31 \cdot 10^{-13} T_{out}^6 \qquad\qquad \text{[5-80]}$$

F_{sky} = view factor from the outdoor surfaces of the fenestration system to the sky, defined as:

$$F_{sky} = \frac{1 + \cos\theta}{2} \qquad\qquad \text{[5-81]}$$

θ = glazing system tilt angle measured from horizontal

F_{gd} = view factor from the outdoor surfaces of the fenestration system to the ground, defined as:

$$F_{gd} = 1 - F_{sky} \qquad\qquad \text{[5-82]}$$

Indoor irradiance is:

$$J_{f,n+1} = G_{in} = \sigma T_{rm,in}^4 \qquad\qquad\qquad\qquad\qquad [5\text{-}83]$$

where,

$T_{rm,in}$ = indoor mean radiant temperature

The indoor mean radiant temperature is usually assumed to be equal to the indoor air temperature, thus indoor irradiance becomes:

$$G_{in} = \sigma T_{in}^4 \qquad\qquad\qquad\qquad\qquad\qquad [5\text{-}84]$$

Convection
Convection at the outdoor and indoor glazing surfaces is defined as:

$$h_{c,1} = h_{c,out} \qquad\qquad\qquad\qquad\qquad\qquad [5\text{-}85]$$

$$h_{c,n+1} = h_{c,in} \qquad\qquad\qquad\qquad\qquad\qquad [5\text{-}86]$$

where,

$h_{c,out}$ = outdoor convective heat transfer coefficient

$h_{c,in}$ = indoor convective heat transfer coefficient

5.1.2.4. Solution of the System of Non-Linear Equations

The system of basic energy balance equations for each glazing layer, expressed in terms of black emissive power in equations [5-18] – [5-21], is solved as follows.

Using equations [5-16] – [5-21], which describe heat fluxes across gas spaces and glass layers, as well as boundary conditions in Section 5.1.2.3., the following system of non-linear equations is obtained:

$$J_{f,1} + \hat{h}^{out} E_{bf,1} + \hat{h}_{,2} E_{bb,1} + J_{b,1} - J_{f,2} - \hat{h}_{,2} E_{bf,2} = S_1 + G_{out} + \hat{h}^{out} G_{out} \qquad [5\text{-}87]$$

$$-J_{f,1} + \varepsilon_{f,1} E_{bf,1} + \tau_1 J_{f,2} = -\rho_{f,1} G_{out} \qquad\qquad\qquad [5\text{-}88]$$

$$\varepsilon_{b,1} E_{bb,1} - J_{b,1} + \rho_{b,1} J_{f,2} = -\tau_1 G_{out} \qquad\qquad\qquad [5\text{-}89]$$

$$\hat{h}_1^{gl} E_{bf,1} + (\hat{h}_1^{gl} + \hat{h}_2) E_{bb,1} + J_{b,1} - J_{f,2} - \hat{h}_2 E_{bf,2} = 0.5 S_1 \qquad [5\text{-}90]$$

…

$$-\hat{h}_{,i} E_{bb,i-1} - J_{b,i-1} + J_{f,i} + \hat{h}_{,i} E_{bf,i} + \hat{h}_{,i+1} E_{bb,i} + J_{b,i} - J_{f,i+1} - \hat{h}_{,i+1} E_{bf,i+1} = S_i \qquad [5\text{-}91]$$

$$\rho_{f,i} J_{b,i-1} - J_{f,i} + \varepsilon_{f,i} E_{bf,i} + \tau_i J_{f,i+1} = 0 \qquad\qquad\qquad [5\text{-}92]$$

$$\tau_i J_{b,i-1} + \varepsilon_{b,i} E_{bb,i} - J_{b,i} + \rho_{b,i} J_{f,i+1} = 0 \qquad \qquad \textit{[5-93]}$$

$$\hat{h}_i^{gl} E_{bf,i} + (\hat{h}_i^{gl} + \hat{h}_{i+1}) E_{bb,i} + J_{b,i} - J_{f,i+1} - \hat{h}_{i+1} E_{bf,i+1} = 0.5 S_i \qquad \qquad \textit{[5-94]}$$

…

$$-\hat{h}_n E_{bb,n-1} - J_{b,n-1} + J_{f,n} + \hat{h}_n E_{bf,n} + \hat{h}^{in} E_{bb,n} + J_{b,n} = S_n + G_{in} + \hat{h}^{in} G_{in} \qquad \qquad \textit{[5-95]}$$

$$\rho_{f,n} J_{b,n-1} - J_{f,n} + \varepsilon_{f,n} E_{bf,n} = -\tau_n G_{in} \qquad \qquad \textit{[5-96]}$$

$$\tau_n J_{b,n-1} + \varepsilon_{b,n} E_{bb,n} - J_{b,n} = -\rho_{b,n} G_{in} \qquad \qquad \textit{[5-97]}$$

$$\hat{h}_n^{gl} E_{bf,n} + (\hat{h}_n^{gl} + \hat{h}^{in}) E_{bb,n} + J_{b,n} = 0.5 S_n + G_{in} + \hat{h}^{in} G_{in} \qquad \qquad \textit{[5-98]}$$

The equations [5-87] – [5-98] can be set in a matrix form [A] [X] = [B] for the whole glazing system.

Elements of matrix A are long wave optical properties of each layer (i.e. front and back surface emissivities), as well as heat transfer coefficients, based on emissive power, calculated in a previous step.

$$[A] = \begin{bmatrix}
1 & \hat{h}^{out} & \hat{h}_2 & 1 & \dots & 0 & 0 & 0 & 0 & \dots & 0 & 0 & 0 & 0 \\
-1 & \varepsilon_{f,1} & 0 & 0 & \dots & 0 & 0 & 0 & 0 & \dots & 0 & 0 & 0 & 0 \\
0 & 0 & \varepsilon_{b,1} & -1 & \dots & 0 & 0 & 0 & 0 & \dots & 0 & 0 & 0 & 0 \\
0 & -\hat{h}_1^{gl} & \hat{h}_1^{gl} + \hat{h}_2 & 1 & \dots & 0 & 0 & 0 & 0 & \dots & 0 & 0 & 0 & 0 \\
\dots & \dots & \dots & \dots & \dots & \dots & \dots & \dots & \dots & \dots & \dots & \dots & \dots & \dots \\
0 & 0 & 0 & 0 & \dots & 1 & \hat{h}_i & \hat{h}_{i+1} & 1 & \dots & 0 & 0 & 0 & 0 \\
0 & 0 & 0 & 0 & \dots & -1 & \varepsilon_{f,i} & 0 & 0 & \dots & 0 & 0 & 0 & 0 \\
0 & 0 & 0 & 0 & \dots & 0 & 0 & \varepsilon_{b,i} & -1 & \dots & 0 & 0 & 0 & 0 \\
0 & 0 & 0 & 0 & \dots & 0 & -\hat{h}_i^{gl} & \hat{h}_i^{gl} + \hat{h}_{i+1} & 1 & \dots & 0 & 0 & 0 & 0 \\
\dots & \dots & \dots & \dots & \dots & \dots & \dots & \dots & \dots & \dots & \dots & \dots & \dots & \dots \\
0 & 0 & 0 & 0 & \dots & 0 & 0 & 0 & 0 & \dots & 1 & \hat{h}_n & \hat{h}^{in} & 1 \\
0 & 0 & 0 & 0 & \dots & 0 & 0 & 0 & 0 & \dots & -1 & \varepsilon_{f,n} & 0 & 0 \\
0 & 0 & 0 & 0 & \dots & 0 & 0 & 0 & 0 & \dots & 0 & 0 & \varepsilon_{b,n} & -1 \\
0 & 0 & 0 & 0 & \dots & 0 & 0 & 0 & 0 & \dots & 0 & -\hat{h}_n^{gl} & \hat{h}_n^{gl} + \hat{h}^{in} & 1
\end{bmatrix}$$

The column vector X consists of variables that are sought for each glazing layer (i.e. radiosities and black emissive powers).

Finally, the column vector B contains terms of absorbed solar fluxes in each glazing layer; terms of radiative energy from the outdoor and indoor environment that irradiates the glazing system surfaces, as well as

portions of the outdoor and indoor radiative energy that are reflected from 1st and nth layer and transmitted through them.

$$[X] = \begin{bmatrix} J_{f,1} \\ E_{bf,1} \\ E_{bb,1} \\ J_{b,1} \\ \dots \\ J_{f,i} \\ E_{bf,i} \\ E_{bb,i} \\ J_{b,i} \\ \dots \\ J_{f,n} \\ E_{bf,n} \\ E_{bb,n} \\ J_{b,n} \end{bmatrix} \qquad [B] = \begin{bmatrix} S_1 + G_{out} + \hat{h}^{out} G_{out} \\ -\rho_{f,1} G_{out} \\ -\tau_1 G_{out} \\ 0.5 S_1 \\ \dots \\ S_i \\ 0 \\ 0 \\ 0.5 S_i \\ \dots \\ S_n + G_{in} + \hat{h}^{in} G_{in} \\ -\tau_n G_{in} \\ -\rho_{b,n} G_{in} \\ 0.5 S_n + G_{in} + \hat{h}^{in} G_{in} \end{bmatrix}$$

The solution method consists of decomposition of the matrix A, and solving matrix equation [A] [X] = [B], where [A] is decomposed matrix.

That way, sets of black emissive power (i.e. $E_{bf,i}$ and $E_{bb,i}$) are found and new sets of temperatures can be determined as:

$$T_{f,i} = \left(\frac{E_{bf,i}}{\sigma} \right)^{1/4} \qquad \text{and} \qquad T_{b,i} = \left(\frac{E_{bb,i}}{\sigma} \right)^{1/4} \qquad\qquad [5\text{-}99]$$

Where:

$$\sigma = 5.6697 \cdot 10^{-8} \frac{W}{m^2 K^4} - \text{Stefan} - \text{Boltzmann's constant}$$

5.1.2.5. Convergence Checking

When the new sets of front and back layer surface temperatures are determined, they are compared to the old sets. If each member of the new set is not equal to the corresponding member of the old set within the prescribed tolerance (default is 10-8 K), the new set is used to replace the old set and the solution algorithm proceeds to the second step (i.e. calculation of heat transfer coefficients).

5.1.3. Calculation of U–factor

The calculation of U – factor is based on heat flux through the glazing system for the specified environmental conditions, which is determined as per section 5.1.2, but without incident solar radiation (i.e. $I_s = 0$). It means that the fluxes of absorbed solar radiation in each glazing layer, are set to zero in the corresponding energy balance equations (i.e. $S_i = 0$).

U-factor is determined as the reciprocal of the total glazing system thermal resistance – R_{tot}.

$$U = \frac{1}{R_{tot}}$$

[5-100]

The total thermal resistance of a glazing system can be calculated by summing the thermal resistance on the outdoor side of the glazing system, the individual thermal resistance values of the glazing layers and glazing cavities, and the thermal resistance on the indoor side of the glazing system:

$$R_{tot} = R_{out} + \sum_{i=1}^{n} R_{gl,i} + \sum_{i=1}^{n} R_{gap,i} + R_{in}$$

[5-101]

The thermal resistance on the outdoor side of the glazing system – R_{out}, can be described by the following equation:

$$R_{out} = \frac{T_{f,1} - T_{amb}}{h_{c,out}(T_{f,1} - T_{out}) + J_{f,1} - G_{out}}$$

[5-102]

The thermal resistance of the glazing layer – $R_{gl,i}$, is:

$$R_{gl,i} = \frac{t_{gl,i}}{k_{gl,i}}$$

[5-103]

The thermal resistance of the glazing cavity – $R_{gap,i}$, is given as:

$$R_{gap,i} = \frac{T_{f,i} - T_{b,i-1}}{h_{c,i}(T_{f,i} - T_{b,i-1}) + J_{f,i} - J_{b,i-1}}$$

[5-104]

Finally, the thermal resistance on the indoor side of the glazing system – R_{in}, is:

$$R_{in} = \frac{T_{room} - T_{b,n}}{h_{c,in}(T_{room} - T_{b,n}) + G_{in} - J_{b,n}}$$

[5-105]

5.1.4. Calculation of solar heat gain coefficient

Opposite to the calculation of thermal transmittance (U–factor), calculation of solar heat gain coefficient (SHGC) incorporates all the effects of the incident solar radiation.

The solar heat gain coefficient (SHGC) is determined by the difference between the heat fluxes into the indoor environment with and without incident solar radiation, where the both fluxes are found as per the procedure given in section 5.1.2

$$SHGC = T_{sol} + \frac{q_{in(Is=0)} - q_{in}}{I_s}$$

[5-106]

where,

T_{sol} = total solar transmittance of the glazing system (–)

$q_{in(Is=0)}$ = heat flux into the indoor environment without incident solar radiation (W/m²)

q_{in} = heat flux into the indoor environment with incident solar radiation (W/m²)

I_s = incident solar radiation (W/m²)

5.2. Glazing Systems with Laminated Layers

For a glazing system incorporating laminated layers, the algorithm for calculation of thermal properties is very similar to the glazing systems consisting of monolithic layers, given in section 5.1. Laminated layers are modeled as monolithic layers subdivided into the arbitrary number of slices that have no gap in-between them. A system of linear equations, from which layer surface temperatures and radiant fluxes (i.e. radiosities) are determined, is given here.

5.2.1. Energy balance equations for laminated layers
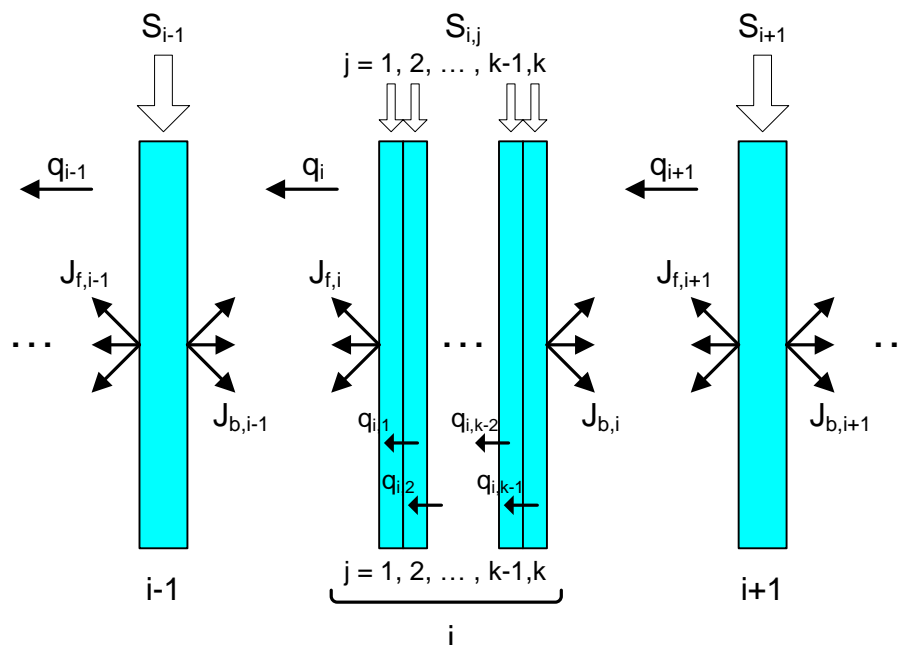
Figure 5-6. Numbering System and Energy Balance for Laminated Glazing Layers in the Glazing System

In the case of a laminated layer, shown in Figure 5-6, the basic energy balance equations [5-4] – [5-7] are modified by applying the following relations to the unexposed surfaces of the layer slices:

$$T_{b,ij} = T_{f,ij+1}$$

<div align="right">[5-107]</div>

$$J_{b,ij} = J_{f,ij+1}$$

<div align="right">[5-108]</div>

Where:

$j = 1,\ldots,k$ = number of slices in the laminated layer.

In that way, the following energy balance equations are set for the slices of the laminated glazing layer:

SLICE 1

$$q_i = S_{i,1} + q_{i,1}$$

<div align="right">[5-109]</div>

$$J_{f,i} = \varepsilon_{f,i}\sigma T_{f,i}^4 + \tau_i J_{f,i+1} + \rho_{f,i} J_{b,i-1}$$

<div align="right">[5-110]</div>

$$T_{b,i1} - T_{f,i} = \frac{t_{sl,i1}}{2k_{sl,i1}}(2q_{i,1} + S_{i,1})$$

<div align="right">[5-111]</div>

SLICE 2

$$q_{i,1} = S_{i,2} + q_{i,2}$$

<div align="right">[5-112]</div>

$$T_{f,i2} = T_{b,i1}$$

<div align="right">[5-113]</div>

$$T_{b,i2} - T_{f,i2} = \frac{t_{sl,i2}}{2k_{sl,i2}}(2q_{i,2} + S_{i,2})$$

<div align="right">[5-114]</div>

…

SLICE k-1

$$q_{i,k-2} = S_{i,k-1} + q_{i,k-1}$$

<div align="right">[5-115]</div>

$$T_{f,ik-1} = T_{b,ik-2}$$

<div align="right">[5-116]</div>

$$T_{b,ik-1} - T_{f,ik-1} = \frac{t_{sl,ik-1}}{2k_{sl,ik-1}}(2q_{i,k-1} + S_{i,k-1})$$

<div align="right">[5-117]</div>

SLICE k

$$q_{i,k-1} = S_{i,k} + q_{i+1} \qquad\qquad\qquad \text{[5-118]}$$

$$T_{f,ik} = T_{b,ik-1} \qquad\qquad\qquad \text{[5-119]}$$

$$J_{b,i} = \varepsilon_{b,i} \sigma T_{b,i}^4 + \tau_i J_{b,i-1} + \rho_{b,i} J_{f,i+1} \qquad\qquad\qquad \text{[5-120]}$$

$$T_{b,i} - T_{f,ik} = \frac{t_{sl,ik}}{2k_{sl,ik}}(2q_{i+1} + S_{i,k}) \qquad\qquad\qquad \text{[5-121]}$$

From equations [5-109], [5-112], [5-115] and [5-118], which describe energy balances imposed at the surfaces of the laminated layer slices, the energy balance relation for the whole laminated layer can be derived as:

$$q_i = \sum_{j=1}^{k} S_{i,j} + q_{i+1} \qquad\qquad\qquad \text{[5-122]}$$

At the same time, equations [5-111], [5-114], [5-117] and [5-121], which define the temperature difference across the laminated layer slices (this is a variation of equation [5-7] for monolithic layers), in conjunction with equations [5-113], [5-116] and [5-119], which define the temperature at the unexposed surfaces of the layer slices, give the modified relation for the temperature difference across the whole laminated layer. If we use the 1st and 2nd slice of a laminated layer as an example, the temperature difference equation becomes:

$$T_{b,i1} - T_{f,i} = \frac{t_{sl,i1}}{2k_{sl,i1}}(2q_{i,1} + S_{i,1}) \qquad\qquad\qquad \text{[5-123]}$$

$$T_{b,i2} - T_{f,i2} = \frac{t_{sl,i2}}{2k_{sl,i2}}(2q_{i,2} + S_{i,2}) \qquad\qquad\qquad \text{[5-124]}$$

Since the temperature of adjacent surfaces of the 1st and 2nd slice is equal (i.e. $T_{b,i1} = T_{f,i2}$), as per the assumption given in equation [5-107], the following relation can be derived from equations [5-123] and [5-124]:

$$T_{b,i2} - T_{f,i} = \frac{t_{sl,i1}}{2k_{sl,i1}}(2q_{i,1} + S_{i,1}) + \frac{t_{sl,i2}}{2k_{sl,i2}}(2q_{i,2} + S_{i,2}) \qquad\qquad\qquad \text{[5-125]}$$

Application of the same methodology to all other slices gives the relation for temperature difference across the whole laminated layer:

$$T_{b,i} - T_{f,i} = \frac{t_{sl,i1}}{2k_{sl,i1}}(2q_{i,1} + S_{i,1}) + \frac{t_{sl,i2}}{2k_{sl,i2}}(2q_{i,2} + S_{i,2}) + ... + \frac{t_{sl,ik-1}}{2k_{sl,ik-1}}(2q_{i,k-1} + S_{i,k-1}) + \frac{t_{sl,ik}}{2k_{sl,ik}}(2q_{i+1} + S_{i,k}) \text{ [5-126]}$$

From equations [5-109], [5-112], [5-115] and [5-118] it is obvious that heat fluxes entering the back surface of each slice (i.e. $q_{i,1}, q_{i,2}, ..., q_{i,k-2}, q_{i,k-1}$) can be expressed in terms of fluxes of solar energy absorbed in the previous slices – $S_{i,2}, ..., S_{i,k-1}, S_{i,k}$ (going toward outdoor environment), and heat flux entering the back surface of laminated layer (i.e. q_{i+1}):

$$q_{i,j} = \sum_{p=j+1}^{k} S_{i,p} + q_{i+1}$$

[5-127]

After using relation [5-127] for fluxes $q_{i,1}$, $q_{i,2}$, …, $q_{i,k-2}$, $q_{i,k-1}$ and some rearrangements, the equation [5-126] becomes:

$$T_{b,i} - T_{f,i} = \sum_{j=1}^{k} \frac{t_{sl,ij}}{2k_{sl,ij}} S_{i,j} + \sum_{j=1}^{k-1} \left(\frac{t_{sl,ij}}{k_{sl,ij}} \sum_{p=j+1}^{k} S_{i,p} \right) + q_{i+1} \sum_{j=1}^{k} \frac{t_{sl,ij}}{k_{sl,ij}}$$

[5-128]

or,

$$T_{b,i} - T_{f,i} = A + Bq_{i+1}$$

[5-129]

where the terms A and B are given as:

$$A = \sum_{j=1}^{k} \left(\frac{t_{sl,ij}}{2k_{sl,ij}} S_{i,j} \right) + \sum_{j=1}^{k-1} \left(\frac{t_{sl,ij}}{2k_{sl,ij}} \sum_{p=j+1}^{k} S_{i,p} \right)$$

[5-130]

$$B = \sum_{j=1}^{k} \frac{t_{sl,ij}}{2k_{sl,ij}}$$

[5-131]

Using equations [5-122] and [5-129], the system of basic energy balance equations [5-4] – [5-7] can be transformed into the following system for laminated layers:

$$q_i = \sum_{j=1}^{k} S_{i,j} + q_{i+1}$$

[5-132]

$$J_{f,i} = \varepsilon_{f,i} \sigma T_{f,i}^4 + \tau_i J_{f,i+1} + \rho_{f,i} J_{b,i-1}$$

[5-133]

$$J_{b,i} = \varepsilon_{b,i} \sigma T_{b,i}^4 + \tau_i J_{b,i-1} + \rho_{b,i} J_{f,i+1}$$

[5-134]

$$T_{b,i} - T_{f,i} = A + Bq_{i+1}$$

[5-135]

Using the same notation (e.g., A and B), the temperature difference terms for monolithic layers can be expressed as:

$$A = \frac{t_{gl,i}}{2k_{gl,i}} S_i$$

[5-136]

$$B = \frac{t_{gl,i}}{k_{gl,i}}$$

[5-137]

As in the case of glazing systems consisting of monolithic layers, this system of energy balance equations for laminated layers would become linear only if solved in terms of black emissive power instead of temperature. Note that the system of equations is still non-linear due to the fourth power of temperature in the radiation terms and $1/3^{rd}$ and $1/4^{th}$ power of temperature in the natural convection terms and therefore needs to be solved iteratively, but the appearance of equations for single iteration is linear and for given temperature field allows solution of linear system of equations.

Considering that the differences between glazing systems with laminated layers and glazing systems consisted of monolithic layers are reflected only in equations related to conductive heat transfer through the glazing layers, the new relationship for the conduction heat transfer coefficient based on emissive power, is introduced and shown in equation [5-138].

$$\hat{h}_i^{lgl} = \frac{1}{B} \cdot \frac{T_{b,i} - T_{f,i}}{E_{bb,i} - E_{bf,i}}$$

[5-138]

The expression for the convection heat transfer coefficient based on emissive power, given in equation [5-14] remains the same here.

5.2.2. System of equations for glazing systems incorporating laminated layers

Using the method described at the beginning of section 5.1.2.1. along with relations [5-132] – [5-135] and [5-138] for laminated layers, the following system of equations is obtained for the glazing system, which incorporates laminated layers:

$$J_{f,1} + \hat{h}^{out}E_{bf,1} + \hat{h}_{,2}E_{bb,1} + J_{b,1} - J_{f,2} - \hat{h}_{,2}E_{bf,2} = S_1 + G_{out} + \hat{h}^{out}G_{out}$$

[5-139]

$$-J_{f,1} + \varepsilon_{f,1}E_{bf,1} + \tau_1 J_{f,2} = -\rho_{f,1}G_{out}$$

[5-140]

$$\varepsilon_{b,1}E_{bb,1} - J_{b,1} + \rho_{b,1}J_{f,2} = -\tau_1 G_{out}$$

[5-141]

$$\hat{h}_1^{gl}E_{bf,1} + (\hat{h}_1^{gl} + \ddot{h}_2)E_{bb,1} + J_{b,1} - J_{f,2} - \hat{h}_{,2}E_{bf,2} = 0.5S_1$$

[5-142]

…

$$-\hat{h}_iE_{bb,i-1} - J_{b,i-1} + J_{f,i} + \hat{h}_iE_{bf,i} + \hat{h}_{i+1}E_{bb,i} + J_{b,i} - J_{f,i+1} - \hat{h}_{i+1}E_{bf,i+1} = \sum_{j=1}^{k} S_{i,j}$$

[5-143]

$$\rho_{f,i}J_{b,i-1} - J_{f,i} + \varepsilon_{f,i}E_{bf,i} + \tau_i J_{f,i+1} = 0$$

[5-144]

$$\tau_i J_{b,i-1} + \varepsilon_{b,i} E_{bb,i} - J_{b,i} + \rho_{b,i} J_{f,i+1} = 0 \qquad \textit{[5-145]}$$

$$\hat{h}_i^{\lg l} E_{bf,i} + (\hat{h}_i^{\lg l} + \hat{h}_{i+1}) E_{bb,i} + J_{b,i} - J_{f,i+1} - \hat{h}_{i+1} E_{bf,i+1} = \frac{A}{B} \qquad \textit{[5-146]}$$

…

$$-\hat{h}_n E_{bb,n-1} - J_{b,n-1} + J_{f,n} + \hat{h}_n E_{bf,n} + \hat{h}^{in} E_{bb,n} + J_{b,n} = S_n + G_{in} + \hat{h}^{in} G_{in} \qquad \textit{[5-147]}$$

$$\rho_{f,n} J_{b,n-1} - J_{f,n} + \varepsilon_{f,n} E_{bf,n} = -\tau_n G_{in} \qquad \textit{[5-148]}$$

$$\tau_n J_{b,n-1} + \varepsilon_{b,n} E_{bb,n} - J_{b,n} = -\rho_{b,n} G_{in} \qquad \textit{[5-149]}$$

$$\hat{h}_n^{gl} E_{bf,n} + (\hat{h}_n^{gl} + \hat{h}^{in}) E_{bb,n} + J_{b,n} = 0.5 S_n + G_{in} + \hat{h}^{in} G_{in} \qquad \textit{[5-150]}$$

Similarly to the standard glazing systems, equations [5-139] – [5-150] are set in a matrix form [A] [X] = [B] for the whole glazing system, consisting of laminated layers.

$$[A] = \begin{bmatrix}
1 & \hat{h}^{out} & \hat{h}_2 & 1 & \ldots & 0 & 0 & 0 & 0 & \ldots & 0 & 0 & 0 & 0 \\
-1 & \varepsilon_{f,1} & 0 & 0 & \ldots & 0 & 0 & 0 & 0 & \ldots & 0 & 0 & 0 & 0 \\
0 & 0 & \varepsilon_{b,1} & -1 & \ldots & 0 & 0 & 0 & 0 & \ldots & 0 & 0 & 0 & 0 \\
0 & -\hat{h}_1^{gl} & \hat{h}_1^{gl} + \hat{h}_2 & 1 & \ldots & 0 & 0 & 0 & 0 & \ldots & 0 & 0 & 0 & 0 \\
\ldots & \ldots & \ldots & \ldots & \ldots & \ldots & \ldots & \ldots & \ldots & \ldots & \ldots & \ldots & \ldots & \ldots \\
0 & 0 & 0 & 0 & \ldots & 1 & \hat{h}_i & \hat{h}_{i+1} & 1 & \ldots & 0 & 0 & 0 & 0 \\
0 & 0 & 0 & 0 & \ldots & -1 & \varepsilon_{f,i} & 0 & 0 & \ldots & 0 & 0 & 0 & 0 \\
0 & 0 & 0 & 0 & \ldots & 0 & 0 & \varepsilon_{b,i} & -1 & \ldots & 0 & 0 & 0 & 0 \\
0 & 0 & 0 & 0 & \ldots & 0 & -\hat{h}_i^{\lg l} & \hat{h}_i^{\lg l} + \hat{h}_{i+1} & 1 & \ldots & 0 & 0 & 0 & 0 \\
\ldots & \ldots & \ldots & \ldots & \ldots & \ldots & \ldots & \ldots & \ldots & \ldots & \ldots & \ldots & \ldots & \ldots \\
0 & 0 & 0 & 0 & \ldots & 0 & 0 & 0 & 0 & \ldots & 1 & \hat{h}_n & \hat{h}^{in} & 1 \\
0 & 0 & 0 & 0 & \ldots & 0 & 0 & 0 & 0 & \ldots & -1 & \varepsilon_{f,n} & 0 & 0 \\
0 & 0 & 0 & 0 & \ldots & 0 & 0 & 0 & 0 & \ldots & 0 & 0 & \varepsilon_{b,n} & -1 \\
0 & 0 & 0 & 0 & \ldots & 0 & 0 & 0 & 0 & \ldots & 0 & -\hat{h}_n^{gl} & \hat{h}_n^{gl} + \hat{h}^{in} & 1
\end{bmatrix}$$

$$[X] = \begin{bmatrix} J_{f,1} \\ E_{bf,1} \\ E_{bb,1} \\ J_{b,1} \\ \dots \\ J_{f,i} \\ E_{bf,i} \\ E_{bb,i} \\ J_{b,i} \\ \dots \\ J_{f,n} \\ E_{bf,n} \\ E_{bb,n} \\ J_{b,n} \end{bmatrix} \qquad [B] = \begin{bmatrix} S_1 + G_{out} + \hat{h}^{out} G_{out} \\ -\rho_{f,1} G_{out} \\ -\tau_1 G_{out} \\ 0.5 S_1 \\ \dots \\ \sum S_{i,j} \\ 0 \\ 0 \\ A/B \\ \dots \\ S_n + G_{in} + \hat{h}^{in} G_{in} \\ -\tau_n G_{in} \\ -\rho_{b,n} G_{in} \\ 0.5 S_n + G_{in} + \hat{h}^{in} G_{in} \end{bmatrix}$$

5.2.3. Determination of glazing surface temperatures

The matrix equation [A] [X] = [B] is solved in the same manner as in the previous case (i.e. glazing systems consisting of monolithic layers), and sets of black emissive power (i.e. $E_{bf,i}$ and $E_{bb,i}$) and radiant fluxes (i.e. $J_{f,i}$ and $J_{b,i}$) for exposed glazing surfaces are determined. Then, new sets of temperatures of exposed glazing surfaces (i.e. $T_{f,i}$ and $T_{b,i}$) are found, as described by equation [5-99], and convergence checking (i.e. comparison between the new and old sets of glazing surface temperatures) is performed. After that, the old set is replaced by the new set, and the iterative algorithm is repeated until the prescribed tolerance is satisfied.

When the final temperatures of the exposed glazing surfaces are found, the rest of the solution (i.e. temperatures of unexposed surfaces of layer slices) is calculated using the following procedure:

Calculate the heat flux leaving the front facing surface of the laminated layer (i.e. q_i) using equation [5-1].

Calculate the temperature of the back surface of the first slice (i.e. $T_{bi,1}$) using the following relation, derived from equations [5-109] and [5-111]:

$$T_{b,i1} = T_{f,i} + \frac{t_{sl,i1}}{2 k_{sl,i1}} (2 q_i - S_{i,1}) \qquad\qquad [5\text{-}151]$$

Calculate, in sequential manner, the remaining temperatures of the unexposed surfaces of layer slices using similar relations, obtained from the equations that describe energy balances imposed at the surfaces of the laminated layer slices (i.e. [5-112], [5-115] and [5-118]), equations that define temperature difference across the laminated layer slices (i.e. [5-114], [5-117] and [5-121]) and equations that define temperature at the adjacent unexposed surfaces of the layer slices (i.e. [5-113], [5-116] and [5-119]).

5.2.4. Calculation of U–factor and SHGC for laminated layers

The U–factor of glazing systems with laminated layers is calculated using basically the same procedure as in previous case (i.e. glazing systems with monolithic layers).

It is determined as the reciprocal of the total glazing system thermal resistance – R_{tot}, and the R_{tot} is found by summing the thermal resistance on the outdoor side of the glazing system, the thermal resistances of the glazing layers and glazing cavities, and the thermal resistance on the indoor side of the glazing system.

The values of thermal resistance on the glazing system outdoor side, the thermal resistance of glazing cavities and the thermal resistance on the glazing system indoor side are determined as per equations [5-102], [5-104] and [5-105], respectively. The only difference from the previous case is reflected in the thermal resistance of the laminated layer, which can be found by summing the individual thermal resistances of layer slices:

$$R_{\lg l,i} = \sum_{j=1}^{k} \frac{t_{sl,ij}}{k_{gl,ij}}$$
[5-152]

Regarding the solar heat gain coefficient (SHGC), the calculation is performed in the same manner as for glazing systems with monolithic layers using the equation [5-106].

6. GLAZING SYSTEM THERMAL PERFORMANCE: ISO/EN 10077

ISO/EN 10077-1 algorithms are substantially simplified over the ISO 15099 algorithms. These algorithms are used in new product standards in EU and associated countries. This standard relies on additional standards ISO 10292/EN673 (specular glazing layers) and EN 13663 (shading devices).

6.1. Specular Glazing Layers (EN673/ISO10292)

6.1.1. Definition of Outdoor and Indoor Heat Transfer Coefficients

The value of **outdoor heat transfer coefficient** (i.e. h_e) depends on the wind speed near the glazing system and other climate factors, as well as on the outdoor glazing surface emissivity. The EN 673 standard does not consider coated outdoor glazing surfaces, which emissivities are lower than 0.840, and the value of h_e is standardized to:

$$h_e = 23 \; \frac{W}{m^2 K} \qquad\qquad [6\text{-}1]$$

At the same time, the **indoor heat transfer coefficient** (i.e. h_i) is defined by following equation:

$$h_i = h_{r,i} + h_{c,i} \qquad\qquad [6\text{-}2]$$

where,

$h_{r,i}$ = radiation conductance

$h_{c,i}$ = convection conductance

The radiation conductance of uncoated indoor glazing surfaces is set to 4.4 W/m²K, while for the coated ones it is given as:

$$h_{r,i} = \frac{4.4\varepsilon_i}{0.840} \qquad\qquad [6\text{-}3]$$

where,

ε_i = emissivity of coated indoor glazing surface

Finally, free convection is assumed to be on the indoor side of the glazing system, so the value of convection conductance (i.e. $h_{c,i}$) is:

$$h_{c,i} = 3.6 \ \frac{W}{m^2 K} \qquad\qquad\qquad\qquad\qquad\qquad\qquad\qquad \textit{[6-4]}$$

6.2. Glazing Cavity Thermal Conductance

The thermal conductance of glazing cavity can be determined by summing the convective and radiative components. The convection component is defined in terms of the gas conductance (i.e. $h_{gs,i}$), while the radiation conductance of glazing cavity (i.e. $h_{rs,i}$) determines the radiative component.

$$h_{s,i} = h_{rs,i} + h_{gs,i} \qquad\qquad\qquad\qquad\qquad\qquad\qquad\qquad \textit{[6-5]}$$

6.2.1. Gas Conductance

The gas conductance of the glazing cavity can be determined according to the following relation:

$$h_{gs,i} = N_{u,i} \frac{\lambda_i}{s_i} \qquad\qquad\qquad\qquad\qquad\qquad\qquad\qquad \textit{[6-6]}$$

where,

$N_{u,i}$ = Nusselt number

λ_i = thermal conductivity of the fill gas in the glazing cavity

s_i = width of the glazing cavity

Nusselt number, which is a function of Grashof number, Prandtl number and glazing system inclination (i.e. tilt angle), is calculated as:

$$N_{u,i} = A(G_r \cdot P_r)^n \qquad\qquad\qquad\qquad\qquad\qquad\qquad\qquad \textit{[6-7]}$$

where,

A = constant

G_r = Grashof number

P_r = Prandtl number

n = exponent

If the calculated value of the Nusselt number is less than 1, it is set to the bounding value of 1.

The Nusselt number dependence on the glazing system tilt angle is given through the following relations for the constant A and exponent n:

- Glazing system inclined at 0° $(\theta = 0^o)$

$$A = 0.16 \ ; \ n = 0.28 \qquad\qquad\qquad\qquad\qquad\qquad\qquad\qquad \textit{[6-8]}$$

- Glazing system inclined at 45° $(\theta = 45^o)$

$$A = 0.10 \; ; \; n = 0.31 \hspace{4cm} [6\text{-}9]$$

- Glazing system inclined at 90° $(\theta = 90^o)$

$$A = 0.035 \; ; \; n = 0.38 \hspace{4cm} [6\text{-}10]$$

The Grashof and Prandtl numbers can be expressed as:

$$G_r = \frac{9.81 \cdot s_i^3 \cdot \Delta T_i \cdot \rho_i^2}{T_{m,i} \cdot \mu_i^2} \hspace{3cm} [6\text{-}11]$$

$$P_r = \frac{\mu_i \cdot c_i}{\lambda_i} \hspace{4cm} [6\text{-}12]$$

where,

ρ_i = density of the gas space

μ_i = dynamic viscosity of the gas space

c_i = specific heat capacity of the gas space

$T_{m,i}$ = mean temperature of the gas space, set to 283 K for all glazing cavities

ΔT_i = temperature difference between glass surfaces bounding the gas space

Gas fill properties (i.e. density, thermal conductivity, viscosity and specific heat capacity) are evaluated at the mean temperature of the gas space ($T_{m,i}$). The density is determined using the perfect gas law, while the other properties of individual gasses, used in sealed glazing units, are determined as a linear function of temperature. The properties of gas mixtures can be calculated as a function of corresponding properties of the individual constituents.

$$P = \sum_{i=1}^{k} P_i F_i \hspace{4cm} [6\text{-}13]$$

where,

P = relevant property (density, thermal conductivity, viscosity or specific heat capacity)

P_i = corresponding property of the individual gas in the gas mixture

F_i = volume fraction of the individual gas in the gas mixture

For double glazing systems the temperature difference ΔT_i has fixed value of 15 K. For the glazing systems with more than one gas space, which require iterative solution algorithm, the temperature difference ΔT_i is determined using following relations for the first and for all other iterations.

$$\Delta T_i = \frac{15}{N}$$

[6-14]

where,

N = number of glazing cavities (i.e. gas spaces)

$$\Delta T_i = 15 \frac{1 / h_{s,i}}{\sum\limits_{i=1}^{N} 1 / h_{s,i}}$$

[6-15]

where,

$1/h_{s,i}$ = glazing cavity thermal resistance from the previous iteration

$\sum\limits_{i=1}^{N} 1 / h_{s,i}$ = overall thermal resistance of glazing cavities

In the first iteration, ΔT_i is calculated using equation [6-14], while in the second and all later iterations (if necessary), the equation [6-15] is used.

6.2.2. Radiation Conductance

The radiation conductance of the glazing cavity is defined as a function of mean temperature of the glazing cavity, as well as emissivities of the surfaces bounding the glazing cavity.

$$h_{rs,i} = 4\sigma \left(\frac{1}{\varepsilon_1} + \frac{1}{\varepsilon_2} - 1 \right)^{-1} T_{m,i}^{\;3}$$

[6-16]

where,

$\sigma = 5.6697 \cdot 10^{-8} \dfrac{W}{m^2 K^4}$ – Stefan – Boltzmann's constant

$T_{m,i}$ = mean temperature of the glazing cavity (gas space)

ε_1 and ε_2 = emissivities of the surfaces bounding the glazing cavity

6.3. Calculation of U–factor

When the final value of overall thermal resistance of glazing cavities ($\sum\limits_{i=1}^{N} 1 / h_{s,i}$) is found, the total thermal conductance (h_t) of the glazing system is calculated as:

$$h_t = \cfrac{1}{\sum\limits_{i=1}^{N} \cfrac{1}{h_{s,i}} + \sum\limits_{j=1}^{M} d_j r_j}$$

[6-17]

where,

$\sum\limits_{j=1}^{M} d_j r_j$ = overall thermal resistance of glazing layers

d_j = glazing layer thickness

r_j = glazing layer thermal resistance, which represents the reciprocal of thermal conductance – k_j

Then, the glazing system thermal transmittance (U–factor) is determined using the following relation:

$$U = \left(\frac{1}{h_e} + \frac{1}{h_t} + \frac{1}{h_i} \right)^{-1}$$

[6-18]

where,

h_e = outdoor heat transfer coefficient, defined as per section 6.1

h_i = indoor heat transfer coefficient, defined as per section 6.1

h_t = total glazing system thermal conductance

7. GLAZING SYSTEM OPTICAL PERFORMANCE

Calculations of optical properties covers overall normal, angular, and hemispherical properties for a multiple layer glazing system based on visible, solar, infrared and ultraviolet averaging. The calculation of the layer by layer solar absorptance is also discussed as is the angular variation of the Solar Heat Gain Coefficient (SHGC). The above mentioned properties are calculated for all glazing systems. These optical properties are the UV Transmittance, the Damage Weighted UV Transmittance, and the Color Calculations. The color results are based on calculations using both the transmittance and the front reflectance of the glazing system. These calculations include the determination of the Purity, the Dominant Wavelength and the CIE L*, a*, b* values.

WINDOW uses a multi-band spectral model. In order to utilize the multi-band model, spectral data for the glazing layer must be available. This spectral data includes values for the transmittance, and reflectance of the front and back surfaces. The properties are recorded as direct normal values. The values for the infrared transmittance and hemispherical emittance are either provided in the spectral data file or calculated by the program. The solar, visible, and infrared optical properties are normalized weighted averages. Each of these averages is based on a different weighting function and wavelength range. The averages are calculated using a numerical integration. The method used to calculate the optical properties of single glazing layers is the same as is used with glazing systems made up of multiple layers. The method for determining the overall spectral transmittance and reflectances of multiple layer glazing systems is discussed in "Chapter 7.6. Determination of overall glazing system properties". For glazing systems with multiple layers, the optical properties for the total glazing system are calculated at each wavelength, and these values are integrated to obtain the various averages.

7.1. Calculation of average optical properties

The spectral average of property P of type 'x' is calculated according to:

$$P_x = \frac{\int_a^b \Phi_x(\lambda) \cdot P(\lambda) \cdot \Gamma_x(\lambda) \cdot d\lambda}{\int_a^b \Phi_x(\lambda) \cdot \Gamma_x(\lambda) \cdot d\lambda} \qquad \textit{[7-1]}$$

where P is the property to be averaged, Φ_x is a weighting function representing the relative intensity of source radiation for average type 'x' and Γ_x is a weighting function representing the detector response for average type 'x'. The integration is carried out between the wavelengths *a* and *b*.

In practice, P, Φ_x and Γ_x are often measured or tabulated at discrete wavelengths, so that the expression above must be evaluated numerically over a set of N discrete wavelengths $\lambda_1, \lambda_2 ... \lambda_{N-1}, \lambda_N$.

However, P, Φ_x and Γ_x may be measured or tabulated at different wavelengths, so there are two steps in calculating the spectral average:

- • Interpolate P, Φ_x and Γ_x onto a common wavelength set

- • Evaluate the integrals numerically, calculate the average

There are several methods for performing each step, and the combination of methods chosen will influence the final calculation.

7.1.1. Integration onto common wavelength set

P, Φ_x and Γ_x may be measured or tabulated at different wavelengths, and must be reduced to a single wavelength set in order to perform the summation. A common wavelength set is chosen, then P, Φ_x and Γ_x are interpolated onto that wavelength set. There are three usual choices for the wavelength set:

- the set of wavelengths that the data (P) has been measured or tabulated at

- the set of wavelengths that the source (Φ_x) has been measured or tabulated at

- the 'Complete Wavelength Set' consisting of a sorted set of the wavelengths that has been measured at combined with all the wavelengths that   and   have been measured or tabulated at with duplicates removed.

Other choices for the wavelength set are possible.

The interpolation of each data set onto the common wavelength set is generally performed using linear interpolation, but other methods may be chosen. In addition to the method of interpolation, the treatment of the end-points of data sets can affect the calculation.

For the numerical integration to be accurate, it is important to preserve the spectral features of the source, detector and measured data when they are interpolated onto the common wavelength set with the chosen interpolation method. Using the data or source wavelength sets generally leads to small errors in the average that depend on the spectral features of the spectra being interpolated. Using the CWS method ensures that error due to interpolation does not depend on the spectral features of the interpolated spectra.

7.2. Summation/Integration methods

7.2.1. Limits of integration

The limits of the integration/summation are generally dictated by the lowest and highest wavelength in the common wavelength set chosen, but can have other values. If they have other values, and particularly if they do not coincide with wavelengths for which tabulated weighting function values are available, special methods may be needed to incorporate the endpoints into the calculation.

7.2.2. Rectangular
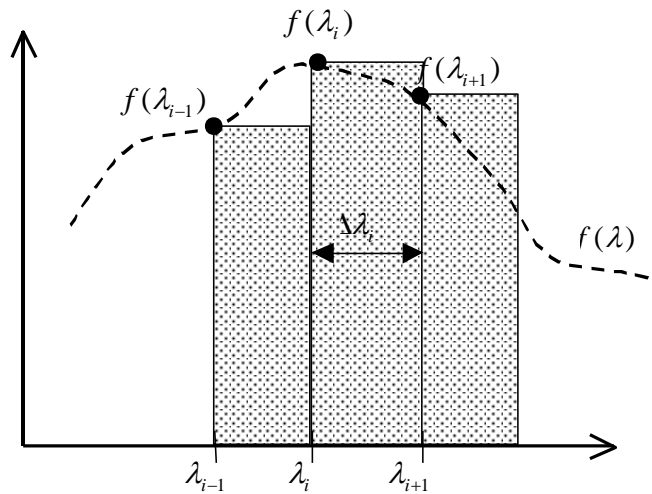
Figure 7-1. Rectangular integration of a function f(λ)

Approximates the integral (area under f) by a sum of the area of N-1 rectangles of width $\Delta\lambda_i$, height $f(\lambda_i)$.

Assumption: that the function is well represented in the interval $\Delta\lambda_i$ by its value at the start of the interval.

$$\Delta\lambda_i = \lambda_{i+1} - \lambda_i \qquad\qquad\qquad [7\text{-}2]$$

in this case the function is integrated between the first and last wavelengths in the common wavelength set, $a = \lambda_1$ and $b = \lambda_N$.

$$\int_a^b f(\lambda).d\lambda \approx \sum_{i=1}^{N-1} f(\lambda_i)\Delta\lambda_i \qquad\qquad\qquad [7\text{-}3]$$

7.2.3. Rectangular centroid
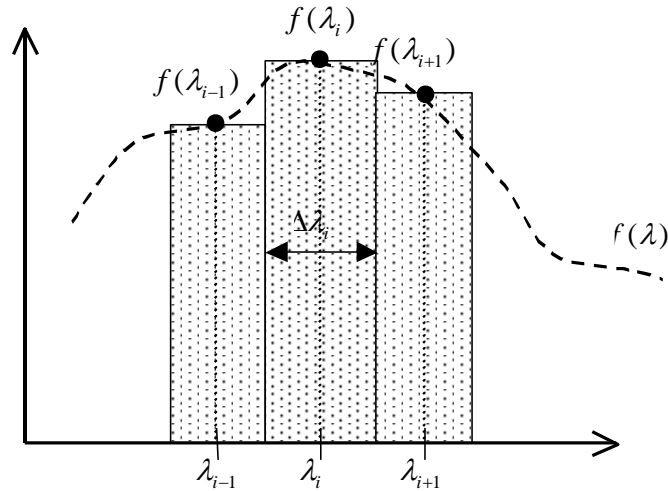
Figure 7-2. Rectangular centroid integration of a function f(λ)

Approximates the integral (area under f) by a sum of the area of N rectangles of width $\Delta\lambda_i$, height $f(\lambda_i)$

.

Assumption: that the function is well represented in the interval $\Delta\lambda_i$ by its value at the center of the interval

$$\Delta\lambda_i = \frac{\lambda_{i+1} - \lambda_{i-1}}{2} \qquad\qquad [7\text{-}4]$$

in this case $\Delta\lambda_1 = \lambda_2 - \lambda_1$, $\Delta\lambda_N = \lambda_N - \lambda_{N-1}$

The function is not integrated between the first and last points in the common wavelength set, but between $a = \lambda_1 - \frac{1}{2}\Delta\lambda_1$ and $b = \lambda_N - \frac{1}{2}\Delta\lambda_N$

$$\int_a^b f(\lambda).d\lambda \approx \sum_{i=1}^{N} f(\lambda_i)\Delta\lambda_i \qquad\qquad [7\text{-}5]$$

7.2.4. Trapezoidal
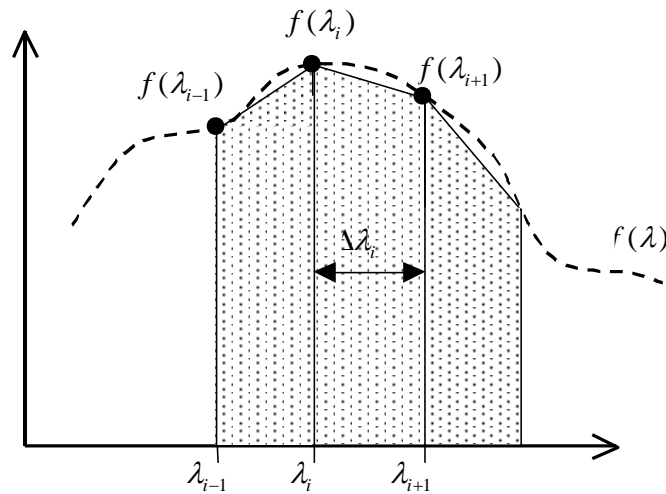
Figure 7-3. Trapezoidal integration of a function f(λ)

Also Trapezium. Approximates the integral (area under f) by a sum of the area of N-1 trapezoids.

Assumption: that the function is accurately represented by a linear variation between tabulated points.

$$\int_a^b f(\lambda).d\lambda \approx \sum_{i=1}^{N-1} \frac{f(\lambda_i) + f(\lambda_{i+1})}{2} \Delta\lambda_i \qquad\qquad [7\text{-}6]$$

where $\Delta\lambda_i = \lambda_{i+1} - \lambda_i$.

The function is integrated between the first and last points in the common wavelength set, $a = \lambda_1$, $b = \lambda_N$

7.2.5. 'Extended' trapezoidal methods

There are two alternative methods described in the literature for dealing with cases where the specified limits of integration lie outside the range of tabulated wavelengths -- they add 'end pieces' to the main sum in order to approximate the contribution of the function beyond the tabulated data. Generally these forms should only be used where the limits of integration extend significantly beyond the range of data available:

$$\int_0^\infty f(\lambda).d\lambda \approx \int_0^a f(\lambda).d\lambda + \int_a^b f(\lambda).d\lambda + \int_b^\infty f(\lambda).d\lambda \qquad\qquad [7\text{-}7]$$

The tabulated data extends from *a* to *b*, where $a = \lambda_1$, $b = \lambda_N$ and the integral between *a* and *b* is evaluated according to the trapezoidal rule above.

The contribution to the integral of the function above and below the ends of the tabulated wavelengths is approximated by adding two small 'end pieces'.

7.2.5.1. Trapezoidal 'A'
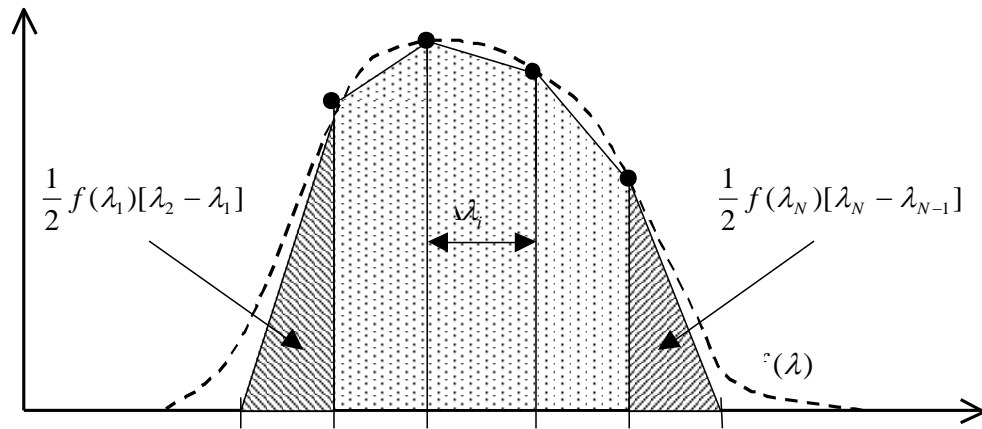
Figure 7-4. Trapezoidal 'A' integration of a function f(λ) that extends outside the limits a - b

The end pieces are:

$$\int_0^a f(\lambda).d\lambda \approx \frac{1}{2}f(\lambda_1)[\lambda_2 - \lambda_1] \text{ and } \int_b^\infty f(\lambda).d\lambda \approx \frac{1}{2}f(\lambda_N)[\lambda_N - \lambda_{N-1}] \ .$$

Making the complete integral:

$$\int_0^\infty f(\lambda).d\lambda \approx \frac{1}{2}f(\lambda_1)[\lambda_1 - \lambda_2] +$$
$$\frac{1}{2}\sum_{i=1}^{N-1}[f(\lambda_i) + f(\lambda_{i+1})][\lambda_{i+1} - \lambda_i] + \frac{1}{2}f(\lambda_N)[\lambda_{N-1} - \lambda_N]$$

[7-8]

7.2.5.2. Trapezoidal 'B'
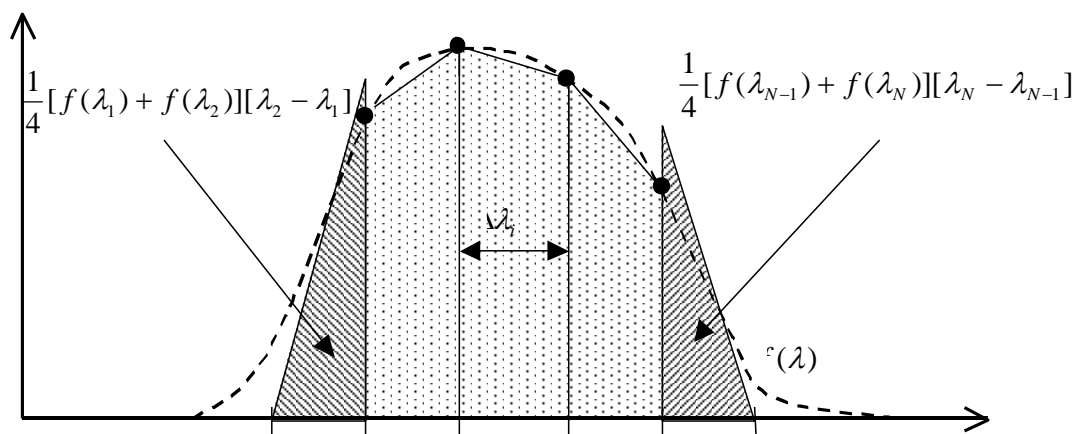
Figure 7-5. Trapezoidal 'B' integration of a function f(λ) that extends outside the limits a – b

The end pieces are:

$$\int_0^a f(\lambda).d\lambda \approx \frac{1}{4}[f(\lambda_1) + f(\lambda_2)][\lambda_2 - \lambda_1] \text{ and } \int_b^\infty f(\lambda).d\lambda \approx \frac{1}{4}[f(\lambda_{N-1}) + f(\lambda_N)][\lambda_N - \lambda_{N-1}].$$

Making the complete integral:

$$\int_0^\infty f(\lambda).d\lambda \approx \frac{1}{4}[f(\lambda_1) + f(\lambda_2)][\lambda_2 - \lambda_1] +$$
$$\frac{1}{2}\sum_{i=1}^{N-1}[f(\lambda_i) + f(\lambda_{i+1})][\lambda_{i+1} - \lambda_i] + \frac{1}{4}[f(\lambda_{N-1}) + f(\lambda_N)][\lambda_N - \lambda_{N-1}]$$

[7-9]

7.3. Tabulated source and detector weighting functions

7.3.1. Un-normalized tables

Un-normalized tables contain the value of the spectral weighting function at a number of wavelengths. The wavelength set for the table is often chosen to preserve features of the spectral weighting function.

7.3.2. Pre-weighted tables

Pre-weighted tables contain the pre-calculated product of one or both of the spectral weighting functions and the wavelength interval for a set of wavelengths:

$$S_x(\lambda_i) = \Phi_x(\lambda_i)\Delta\lambda_i$$

[7-10]

or

$$S_x(\lambda_i) = \Phi_x(\lambda_i)\Gamma_x(\lambda_i)\Delta\lambda_i$$

[7-11]

These tables are designed to be used by first interpolating the measured data onto the table wavelengths, then taking the sum of the product of the measured data and the weighting function for each wavelength in the table. The sum is then divided by a normalization constant, which is generally taken to be equivalent to the sum of the weighting function values in the table, but may have another value, K:

$$P_x = \frac{\sum_{i=1}^N S_x(\lambda_i)P(\lambda_i)}{\sum_{i=1}^N S_x(\lambda_i)}$$

[7-12]

or

$$P_x = \frac{1}{K}\sum_{i=1}^N S_x(\lambda_i)P(\lambda_i)$$

[7-13]

If the normalized table is presented for the first time, a detailed account of its derivation from a standard un-normalized table should be provided. This should include at least the convention for determining the wavelength interval, the method of interpolation used if the wavelength set is different from the un-normalized table on which it is based, and the value of any normalization constant. It should be sufficient to re-derive the table values from their original source.

7.3.3. Select ordinates tables

Selected ordinates tables are derived by selecting M wavelength intervals such that exactly $1/M$ of the total area under the spectral weighting function is found in each wavelength interval. This allows the weighting function to be factored out of the sum, so that the summation is only performed on the measured values.

These tables, which consist only of wavelengths, are designed to be used by first interpolating the measured data onto the table wavelengths, then taking the sum of the measured data values at the selected ordinates wavelengths. Finally the sum is divided by the number of wavelengths in the table, M.

$$P_x = \frac{1}{M} \sum_{i=1}^{M} P(\lambda_i)$$
$$\qquad\qquad\qquad\qquad\qquad\qquad\qquad\qquad\qquad\qquad\qquad\qquad\text{[7-14]}$$

7.4. Analytic source and detector weighting functions

There are some special source and detector spectral weighting functions which have analytic forms. Two common examples of these are the Planck blackbody spectral radiant intensity and the Krochmann UV relative damage function. Assuming they do not have singularities in the region of interest, analytic functions can be evaluated on any wavelength set, but care must be taken to ensure that the function can be treated accurately by the selected interpolation and numerical integration method using the wavelength set chosen.

7.5. Specifying a spectral averaging method

Incomplete or ambiguous specifications of spectral averaging methods leave room for the subjective interpretation of a given method when it is implemented by different people. This leads to different 'interpretations' yielding different calculated averages which may claim to be based on the same original specification. To ensure that a written description of a spectral averaging method contains all the information needed to exactly duplicate the method described, it should include:

1. the source of the common wavelength set

2. the limits of integration

3. how the endpoints of data sets that do not coincide with the limits of the common wavelength set are treated during interpolation

4. the method of interpolation

5. the method of numerical integration, including any special treatment of regions outside the range of tabulated wavelengths.

6. the source and detector spectra, including the derivation of any tabulated data and the meaning of the wavelength interval used in any tabulated data.

7.6. Determination of overall glazing system properties

The basic overall properties, transmittance, reflectance and absorptance, calculated for a glazing system are shown in following figure:
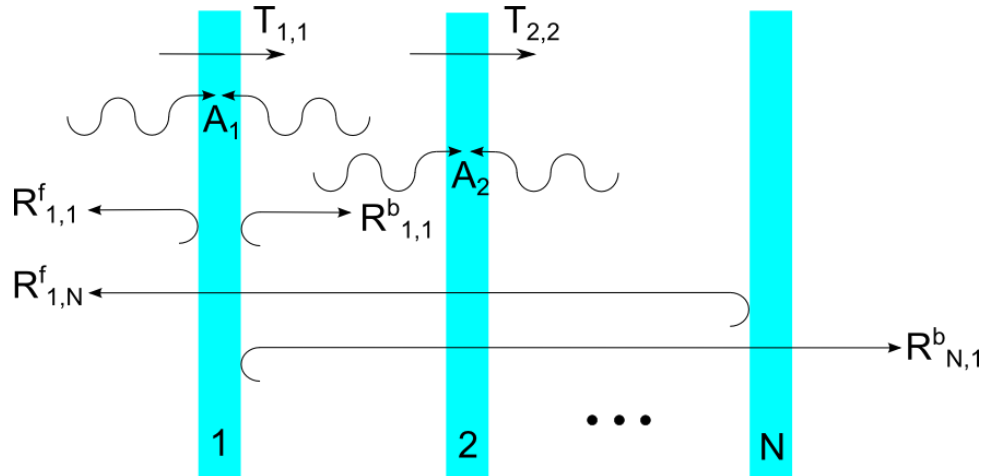
Figure 7-6: Schematic of transmission, reflection, and absorption of solar radiation within a multiple layer glazing system.

WINDOW calculates optical properties of total glazing systems in one of three ways depending on the availability of spectral data. A single band model is used if none of the glazing layers included in the glazing system have attached spectral data files. A multi-band model is used if all of the glazing layers included in the glazing system have attached spectral files. If some of the glazing layers have spectral data files and some do not then the program uses a combination of the multi-band and the single band models. In the combination model the program creates a pseudo-spectral data file for layers without spectral data files by assigning the average value of a property to every wavelength in the spectrum; a multi-band model on the entire assembly is then used.

7.6.1. Overall transmittance and reflectance

The overall transmittance and reflectances of the glazing system are determined using iterative equations which take into account the multiple internal reflections within the glazing system. The equations are written with a spectral dependency but are equally valid for single band models.

$$T_{i,j}(\lambda) = \frac{T_{i,j-1}(\lambda) \cdot T_{j,j}(\lambda)}{1 - R_{j,j}^f(\lambda) \cdot R_{j-1,i}^b(\lambda)} \qquad [7\text{-}15]$$

$$R_{i,j}^f(\lambda) = R_{i,j-1}^f(\lambda) + \frac{T_{i,j-1}^2(\lambda) \cdot R_{j,j}^f(\lambda)}{1 - R_{j,j}^f(\lambda) \cdot R_{j-1,i}^b(\lambda)} \qquad [7\text{-}16]$$

$$R_{j,i}^b(\lambda) = R_{i,j-1}^b(\lambda) + \frac{T_{j,j}^2(\lambda) \cdot R_{j-1,i}^b(\lambda)}{1 - R_{j,j}^f(\lambda) \cdot R_{j-1,i}^b(\lambda)} \qquad [7\text{-}17]$$

When the subscripts are equal the property referred to is the property of the single glazing layer. The iterative procedure is carried out until the transmittance and reflectances of the entire glazing system has been determined. This is equivalent to the case where i = 1 and j = N, where N is the number of glazing layers in the glazing system. Once the overall transmittance and reflectances have been calculated the angular dependence and hemispherical values of the properties can be determined. Finally the solar and visible averages can be performed as for a single glazing layer.

7.6.2. Calculation of absorption of each layer

The absorption of each layer is calculated using iterative equations, Equations [7-18] - [7-20] similar to those used to calculate the transmittance and the reflectances.

$$A_j(\lambda) = \frac{T_{1,j-1}(\lambda) \cdot A_j^f(\lambda)}{1 - R_{j,N}^f(\lambda) \cdot R_{j-1,1}^b(\lambda)} + \frac{T_{1,j}(\lambda) \cdot R_{j+1,N}^f(\lambda) \cdot A_j^b(\lambda)}{1 - R_{j,1}^b(\lambda) \cdot R_{j+1,N}^f(\lambda)}$$ *[7-18]*

$$A_j^f(\lambda) = 1 - T_{j,j}(\lambda) - R_{j,j}^f(\lambda)$$ *[7-19]*

$$A_j^b(\lambda) = 1 - T_{j,j}(\lambda) - R_{j,j}^b(\lambda)$$ *[7-20]*

The subscript **j** refers to the glazing layer. Layer 1 is the outermost layer and layer N is the inner most layer. The solar averaged value of the absorptance is determined using the methods outlined in "*7.6.2. Calculation of absorption of each layer*". Once the value for the layer is calculated the angular dependence is determined using the methods presented in "*7.7. Calculation of angular properties*" and the hemispherical values are determined using the method presented in "*7.8. Calculation of hemispherical properties*". The angular dependence of the Solar Heat Gain Coefficient is determined by using the angular values for the solar transmittance and absorbtance.

7.7. Calculation of angular properties

Many window applications require knowledge of the optical properties of glazings with incident radiation at off-normal incidence. Currently it is standard practice to measure optical properties at normal incidence. Most commercial spectroradiometers are constructed so that the light beam shines directly on the detector. This is a convenient configuration for transmittance measurements at normal incidence. Simply rotating the sample to obtain transmittance at off-normal incidence may offset the beam sufficiently to affect the measurement accuracy. In reflection, the beam will be directed away from the detector entirely. Furthermore, at oblique incidence, multiple reflections in the sample are separated into separate beams which must be properly collected. Accessories are available to measure both transmittance and reflectance at oblique angles, but they are not well integrated with the design of the base instrument. Instruments designed so that the detector and sample can move, in order to better measure angle-dependent optical properties, are call gonioradiometers. Existing gonioradiometers have deficiencies that make them unsuitable for routine measurements on glazing materials. Thus WINDOW includes a calculation scheme for determining the angular dependence of the glazing system optical properties. This calculation scheme is based on first principles for uncoated glass. For coated glass products the calculation procedure is less exact. The calculation of angular dependence of optical properties of coated glass in one of the areas slated for future improvement.

7.7.1. Angular properties of uncoated glass

WINDOW uses a method based on first principles for determining the angular dependence of the optical properties for uncoated glass. The algorithm used is described in a paper by Furler [1991]. A summary of the method is included here for completeness. The following discussion indicates a spectral dependence with a subscript λ. WINDOW uses the same method for uncoated glass whether or not spectral data is available. If there is no spectral data the angular dependence is calculated based on the single values for the transmittance and reflectance in the visible and solar range. In the visible range an average wavelength of 0.575 µm is used in the calculations. In the solar range an average wavelength of 0.898 µm is used.

The spectral data included in WINDOW contains the spectral transmittance, T_λ and the spectral reflectance, R_λ. For uncoated glass the front and back surfaces have the same reflectance. These values are obtained from spectroradiometer measurements. The transmittance and the reflectance are related to the transmissivity and the reflectivity through the following relations:

$$T_\lambda(\phi) = \frac{\tau_\lambda(\phi)^2 \cdot e^{-\alpha_\lambda \cdot \frac{d}{\cos(\phi')}}}{1 - \rho_\lambda(\phi)^2 \cdot e^{-2\alpha_\lambda \cdot \frac{d}{\cos(\phi')}}}$$ [7-21]

and

$$R_\lambda(\phi) = \rho_\lambda(\phi) \cdot (1 + T_\lambda(\phi) \cdot e^{-\alpha_\lambda \frac{t}{\cos(\phi')}})$$ [7-22]

Where d is the sample thickness, Φ is the incident angle at which the property is being evaluated, the angle of incidence as it would be measured in the glass is denoted by Φ', and λ, is the wavelength at which the property is being evaluated. Also appearing in [7-21] and [7-22] are the spectral values of the reflectivity, ρ_λ, the transmissivity, τ_λ, and the absorption coefficient, α_λ; these properties are defined below.

The spectral reflectivity is calculated from Fresnels equations assuming unpolarized incident radiation:

$$\rho_\lambda(\phi) = \frac{1}{2}((\frac{n_\lambda \cdot \cos(\phi) - \cos(\phi')}{n_\lambda \cdot \cos(\phi) + \cos(\phi')})^2 + (\frac{n_\lambda \cdot \cos(\phi') - \cos(\phi)}{n_\lambda \cdot \cos(\phi') + \cos(\phi)})^2)$$ [7-23]

Where n_λ is the ratio of the spectral index of refraction of the glass to the index of refraction of air. The index of refraction of air is unity. The angle of incidence measured in air is denoted by Φ and the angle of incidence as it would be measured in the glass is denoted by Φ'.

The spectral transmissivity is calculated from the reflectivity:

$$\tau_\lambda(\phi) = 1 - \rho_\lambda(\phi)$$ [7-24]

And the spectral absorption coefficient is defined as:

$$\alpha_\lambda = \frac{4\pi k_\lambda}{\lambda}$$ [7-25]

Where k_λ is the dimensionless spectrally dependent extinction coefficient and λ, is the wavelength expressed in the same units as the sample thickness to allow for a nondimensional exponential in Equations [7-21] and [7-22].

In order to determine the angular dependency of the transmittance and the reflectance the program first solves for the index of refraction and the extinction coefficient defined in Equations [7-26] and [7-27]. The spectral index of refraction can be found by inverting a special form of Equation [7-23] evaluated at normal incidence.

$$n_\lambda = \frac{1 + \sqrt{\rho_\lambda(0)}}{1 - \sqrt{\rho_\lambda(0)}}$$ [7-26]

Using Equation [7-22] evaluated at normal incidence an expression for the spectral extinction coefficient is obtained.

$$k_\lambda = -\frac{\lambda}{4\pi t} \ln(\frac{R_\lambda(0) - \rho_\lambda(0)}{\rho_\lambda(0) \cdot T_\lambda(0)})$$ [7-27]

In order to solve Equations [7-26] and [7-27] the value for reflectivity at normal incidence must be known. This value is determined by combining Equations [7-21] and [7-22] to eliminate the exponential factor, resulting in the following expression:

$$\rho_\lambda(0) = \frac{\beta - \sqrt{\beta^2 - 4(2 - R_\lambda(0)) \cdot R_\lambda(0)}}{2(2 - R_\lambda(0))} \qquad\qquad [7\text{-}28]$$

where

$$\beta = T_\lambda(0)^2 - R_\lambda(0)^2 + 2R_\lambda(0) + 1 \qquad\qquad [7\text{-}29]$$

All the values necessary for evaluating Equations [7-28] and [7-29] are given in the spectral data file. The value for the reflectivity is back substituted into Equations [7-26] and [7-27]. The result from Equation [7-27] is used to calculate the absorption coefficient in Equation [7-25]. The index of refraction is used to calculate the reflectivity in Equation [7-23] which is then used to calculate the transmissivity in Equation [7-24]. The reflectivity, transmissivity and absorption coefficient are then back substituted into Equations [7-21] and [7-22] to obtain the angular values of the reflectance and the transmittance. The spectral data is measured on commercially available thicknesses of glass. For some wavelengths the measured transmittance is zero . These values will cause Equation [7-27] to be undefined. There is a safeguard in WINDOW that sets the extinction coefficient to zero if the transmittance is zero.

7.7.2. Angular properties for coated glass

Starting with properties measured at normal incidence, WINDOW uses a regression fit to calculate the angular dependence of optical properties of coated glass. If the transmittance is greater than 0.645 the coated glass is modeled assuming the angular dependence of clear glass, if the transmittance is less than or equal to 0.645 the coated glass is modeled assuming the angular dependence of bronze glass. The values for the angular functions for the transmittance and reflectance of both clear glass ($\overline{\tau}_{clr}$, $\overline{\rho}_{clr}$) and bronze glass ($\overline{\tau}_{bnz}$, $\overline{\rho}_{bnz}$) are determined from a fourth order polynomial regression.

$$\overline{\tau}(\phi) = \overline{\tau_0} + \overline{\tau_1} \cdot \cos(\phi) + \overline{\tau_2} \cdot \cos^2(\phi) + \overline{\tau_3} \cdot \cos^3(\phi) + \overline{\tau_4} \cdot \cos^4(\phi) \qquad\qquad [7\text{-}30]$$

and

$$\overline{\rho}(\phi) = \overline{\rho_0} + \overline{\rho_1} \cdot \cos(\phi) + \overline{\rho_2} \cdot \cos^2(\phi) + \overline{\rho_3} \cdot \cos^3(\phi) + \overline{\rho_4} \cdot \cos^4(\phi) - \overline{\tau}(\phi) \qquad\qquad [7\text{-}31]$$

Where Φ is the angle of incidence with normal incidence defined as Φ = 0.0. The coefficients for the polynomial can be found in the following table:

Table 7-1. *Coefficients for Clear and Bronze angular dependence regression formulas used for calculating the angular properties of coated glass*

	0	1	2	3	4
$\overline{\tau}_{clr}$	-0.0015	3.355	-3.840	1.460	0.0288
$\overline{\rho}_{clr}$	0.999	-0.563	2.043	-2.532	1.054
$\overline{\tau}_{bnz}$	-0.002	2.813	-2.341	-0.05725	0.599
$\overline{\rho}_{bnz}$	0.997	-1.868	6.513	-7.862	3.225

Once these factors are calculated they are applied to the normal transmittance and reflectances of the glass. This is done at each wavelength if spectral data is available or for a single value if no spectral data is attached.

The angular transmittances and reflectances are calculated using the following formulas:

For $\tau_\lambda > 0.645$:

$$\tau_\lambda(\phi) = \tau_\lambda \cdot \overline{\tau}_{clr}(\phi) \qquad\qquad\qquad [7\text{-}32]$$

$$\rho_\lambda(\phi) = \rho_\lambda \cdot (1 - \overline{\rho}_{clr}(\phi)) + \overline{\rho}_{clr}(\phi) \qquad\qquad\qquad [7\text{-}33]$$

For $\tau_\lambda \le 0.645$:

$$\tau_\lambda(\phi) = \tau_\lambda \cdot \overline{\tau}_{bnz}(\phi) \qquad\qquad\qquad [7\text{-}34]$$

$$\rho_\lambda(\phi) = \rho_\lambda \cdot (1 - \overline{\rho}_{bnz}(\phi)) + \overline{\rho}_{bnz}(\phi) \qquad\qquad\qquad [7\text{-}35]$$

7.8. Calculation of hemispherical properties

Once the angular values of the properties are known the hemispherical values are determined by a numerical integration using the following integral:

$$P_{hem} = 2 \cdot \int_{0^0}^{90^0} P(\phi) \cdot \cos(\phi) \cdot \sin(\phi) \cdot d\phi \qquad\qquad\qquad [7\text{-}36]$$

7.9. Ultraviolet transmitance

If each glazing layer in the glazing system has a spectral data file with a minimum values less than or equal to 0.30 microns then the Ultraviolet Transmittance averages are calculated. The UV Transmittance values are calculated using the same procedure as for the other optical properties.

7.10. Calculation of the color properties

WINDOW calculates the Dominant Wavelength, Purity and CIE L*, a*, b* values for glazing systems if each glazing layer has an attached spectral data file. The color calculations are based on the recommendations presented in ASTM E308 - 90. A more complete discussion of color properties can be found in ASTM E308 or

in the IES Lighting Handbook [Kaufman, 1984]. The calculation requires spectral data files and three additional files: CIE64T.DAT, CIE64C.DAT and ILLD65.DAT.

CIE64T.DAT contains the spectral tristimulus values (Color Matching Functions x10 , y10 , z10) for the CIE 1964 Supplementary Standard (10°) Observer. CIE64C.DAT contains the coordinates of the spectrum locus. ILLD65.DAT contains the spectral weighting function recommended for use when calculating color recognition for objects exposed to daylight, Illuminant 065.

The color properties are functions of the chromaticity coordinates of the glazing system. These coordinates are determined from the spectral values for transmittance and front reflectance for the glazing system, calculated using Equations [7-21] and [7-22]; and from the spectral distribution of the light source. The color values based on transmittance are of interest for color perception of an observer located inside a building. The color values based on reflectance are of interest for color perception of an observer located outside the building.

7.10.1. Calculation of the chromaticity coordinates

The chromaticity coordinates x, y and z are calculated using the following method.

Calculate the total tristimulus values X, Y and Z

$$X = \frac{\displaystyle\int_{0.38}^{0.78} P(\lambda) \cdot S(\lambda) \cdot \overline{x}_{10}(\lambda) \cdot d\lambda}{\displaystyle\int_{0.38}^{0.78} S(\lambda) \cdot \overline{y}_{10}(\lambda) \cdot d\lambda} \qquad [7\text{-}37]$$

$$Y = \frac{\displaystyle\int_{0.38}^{0.78} P(\lambda) \cdot S(\lambda) \cdot \overline{y}_{10}(\lambda) \cdot d\lambda}{\displaystyle\int_{0.38}^{0.78} S(\lambda) \cdot \overline{y}_{10}(\lambda) \cdot d\lambda} \qquad [7\text{-}38]$$

$$Z = \frac{\displaystyle\int_{0.38}^{0.78} P(\lambda) \cdot S(\lambda) \cdot \overline{z}_{10}(\lambda) \cdot d\lambda}{\displaystyle\int_{0.38}^{0.78} S(\lambda) \cdot \overline{y}_{10}(\lambda) \cdot d\lambda} \qquad [7\text{-}39]$$

Where P(λ) is the spectral value of the property under consideration either transmittance or reflectance and S(λ) is the value of the spectral distribution of the illuminant. The spectral weighting functions of the illuminant are given every 0.05 μm. If the spectral data for the glazing system is at different wavelengths, a linear interpolation is performed to estimate the value of the properties at the required wavelengths.

In WINDOW the exact integration has been replaced with a numerical integration based on the trapezoid rule. This provides a more accurate approximation to an exact integral than does the simple summation suggested in ASTM E308.

The chromacity coordinates are obtained by normalizing the tristimulus values

$$x = \frac{X}{X + Y + Z} \qquad [7\text{-}40]$$

$$y = \frac{Y}{X + Y + Z}$$

[7-41]

Once the chromacity coordinates of the sample are known the color property values can be calculated.

7.10.2. Calculation of the dominant wavelength and purity

The Dominant Wavelength and the Excitation Purity relate to the color appearance of the glazing system. These values are indications of where the chromaticity coordinates of the sample lie with respect to the chromaticity coordinates of the light source and to the spectrum locus. The Dominant Wavelength is defined as the point where a line passing through the chromaticity coordinates of the light source and the sample intersect the spectrum locus.

In order to determine the Dominant Wavelength of the sample, the chromaticity coordinates of the source (x_n, y_n) are needed. These values are calculated using Equations [7-37] - [7-41] with $P(\lambda)$ set equal to 1.0 for each wavelength. Once the chromaticity coordinates of the source and the glazing system are known, the dominant wavelength is calculated using the following method.

The angle of the line connecting the source and the glazing system is determined by taking the inverse tangent of the slope:

$$\psi = \tan^{-1}(\frac{y_n - y}{x_n - x})$$

[7-42]

The angle between the coordinates of the spectrum locus and the chromaticity coordinates for the source is then calculated. If the angle between the sample and the source is greater than the angle associated with 0.38 µm and less than the angle associated with 0.78 µm, the line intersects the purple line. In this case the complimentary wavelength is reported. For example a red sample would have a reported dominant wavelength of 0.5 µm which is in the green range.

WINDOW does a simple search until the angle between sample and source is bracketed by adjacent angles between the source and the pure color chromaticity curve. WINDOW calculates the point of intersection between the line connecting the source, sample and chromaticity curve and a straight line connecting the adjacent points of the curve. The dominant wavelength is determined using linear interpolation based on the distance between the point of intersection and the endpoints that intersect the chromaticity diagram at the bracketing points.

The Excitation Purity is the ratio of the distance between the source and the sample and the distance between the source and the point of intersection with the chromaticity curve.

7.10.3. Calculation of the CIE L*, a*, b* values

Window also calculates the CIE L*, a*, b* values. These values represent where the sample lies in the CIE uniform color space. The uniform color space is formed by the mutually perpendicular L* a* and b* axes. The a* axis has values from -150 which is pure green to 150 which is pure red. The b* axis has values from -150 which is pure blue to 150 which is pure yellow. The L* axis also passes through the zero intersection point and has values of zero which is black to 100 which is white. The L*, a*, b* coordinates are functions of the ratios X/X_n, Y/Y_n, and Z/Z_n.

$$a^* = 500 \cdot [f(X / X_n) - f(Y / Y_n)]$$

[7-43]

$$b^* = 200 \cdot [f(Y / Y_n) - f(Z / Z_n)]$$

[7-44]

For $Y / Y_n > 0.008856$:

$$L^* = 116 \cdot (\frac{Y}{Y_n})^{1/3} - 16 \qquad\qquad [7\text{-}45]$$

For $Y / Y_n \leq 0.008856$:

$$L^* = 903.3 \cdot (\frac{Y}{Y_n}) \qquad\qquad [7\text{-}46]$$

where:

$$f(R) = R^{\frac{1}{3}} \qquad R > 0.008856 \qquad\qquad [7\text{-}47]$$

and

$$f(R) = 7.787 \cdot R + \frac{16}{116} \quad R \leq 0.008856 \qquad\qquad [7\text{-}48]$$

8. GLAZING DEFLECTION

Deflection of an insulated glazing unit (IGU) can result in thermal performance degradation or improvement due to the reduction or increase of gap space width. Convection of the gas fill is affected by the changed gap space and due to modified convection pattern and shorter or longer thermal path at the center of the glazing unit can result in increased or decreased thermal performance. For the most part, the U-factor is affected as a direct result of changed thermal performance; however, solar heat gain through the window (SHGC) can also be affected because of the effect of the inward flowing fraction of absorbed solar radiation, which is affected by the thermal performance of the IGU.

Deflection in a sealed IGU is caused by the difference in gas pressure in the IGU gap vs. outdoor/indoor pressure. Indoor and outdoor pressure can be considered equal, since the indoor building environment is generally in good contact with the outdoor environment. We will call this pressure an atmospheric pressure, P_a. The difference between the atmospheric pressure and the gap pressure is due to several factors, listed here:

1. Difference in atmospheric pressure between the IGU fabrication location and the end use location

2. Difference in temperature during fabrication and the actual operating conditions for the glazing. It should be noted that the initial temperature can be higher than the ambient temperature during the fabrication process, due to elevated sealant temperatures, which can raise local temperatures within the IGU.

3. Unbalanced gas fill leakage through the sealants, resulting in lower gap pressure and inward deflection.

4. Wind or static load pressure

Effects 1 and 2 will be modeled using equations presented below, while effect 3 does not have a credible mathematical model. However, cumulative deflection, resulting from all three effects, can be measured in the field and its effect on thermal performance can be modeled by specifying center glazing deflection.

Wind or static load pressure effects on deflection is not included in this model at this time, but will be considered for future versions.

Recognizing that indoor and outdoor air pressure could be different, such as in a hot box test environment, future plans for the extension of the model will include an option to specify different values for indoor and outdoor pressure. Another future improvement to the model will include linking certain air gaps with the indoor or outdoor environment, meaning that the respective pressures in linked spaces will be equal.

The mathematical model described in detail here is based on the research work by Bernier and Bourret (1997) and Timoshenko and Woinowsky-Krieger (1959). Bernier and Bourret (1997) of the Ecole Polytechnique Montréal adopted the Timoshenko and Woinowsky-Krieger (1959) model for calculating flat plate deflection subjected to the differential pressure field (static), while their original contribution was to develop correlations for changes in thermal performance, based on IGU deflection at the center of glazing location. In addition to adopting the Bernier and Bourret (1997) model here, we have also developed a model for calculating the change in thermal performance of deflected units when this deflection is measured in the field. Therefore, the mathematical formulation presented here is divided into two sections; 1) calculation of the deflection and resulting thermal performance caused by pressure and temperature effects and 2) calculation of the thermal performance of the IGU when the deflection is measured.

8.1. Calculation of the Deflection and Resulting Thermal Performance

If coordinate system is set as shown in Figure 8-1 and Figure 8-2,
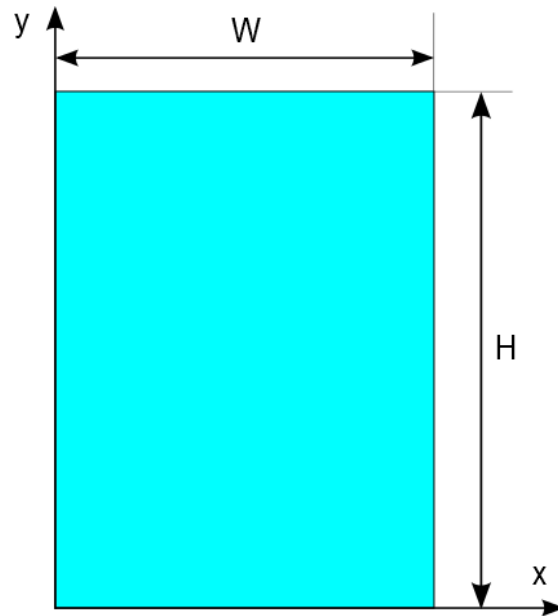
Figure 8-1. Deflection Coordinate System – 2D
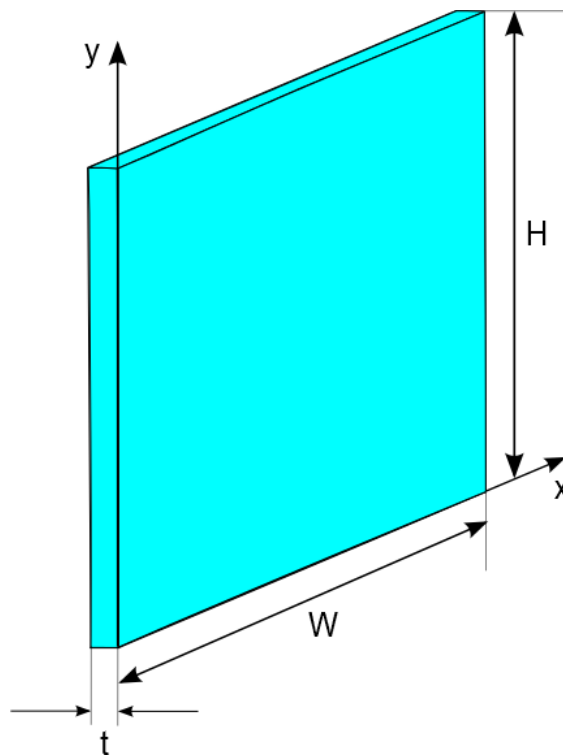
Figure 8-2. Deflection Coordinate System - 3D

it is possible to calculate the deflection distribution at each point of pane by using the following equation:

$$L_{D(i)}(x,y) = \frac{16 \cdot \Delta P_{(i)}}{\pi^6 \cdot D_{(i)}} \sum_{m=1,3,5\ldots}^{\infty} \sum_{n=1,3,5\ldots}^{\infty} \frac{\sin\frac{m\pi x}{W}\sin\frac{n\pi y}{H}}{mn\left(\left(\frac{m}{W}\right)^2 + \left(\frac{n}{H}\right)^2\right)^2} \qquad [8–1]$$

Where,

$$D_{(i)} = \frac{E \cdot t_{(i)}^3}{12 \cdot (1 - v^2)} \qquad [8–2]$$

Where,

E = Young's modulus (7.2×10^{10}) [Force per unit Area; SI: Pa, IP: psi]

t = thickness of glazing pane [Length; SI: m, IP: in.]

v = poison's ratio (0.22 for glass) [Non-Dimensional]

$\Delta P_i = P_{gap(i)}$ - $P_{gap(i-1)}$ (for i-th pane) [Force per unit Area; SI: Pa, IP: psi] $[8–3]$

$\Delta P_i = P_{gap(1)}$ - P_a (first pane) [Force per unit Area; SI: Pa, IP: psi] $[8–4]$

$\Delta P_i = P_a$ - $P_{gap(n-1)}$ (last pane) [Force per unit Area; SI: Pa, IP: psi] $[8–5]$

Where,

P_a = atmospheric pressure. [Force per unit Area; SI: Pa, IP: psi]

Air pressure above sea level can be calculated using the following formula:

$$p = 101325 \cdot \left(1 - 2.25577 \cdot 10^{-5} \cdot h\right)^{5.25588}$$

$$P_{gap(i)} = \frac{P_{ini}V_{ini(i)}T_{gap(i)}}{T_{ini}V_{gap(i)}} \qquad [8–6]$$

Where,

P_{ini} = Initial pressure. Applies to all gaps as a single value (input data - measured or otherwise) [Force per unit Area; SI: Pa, IP: psi]

T_{ini} = Initial temperature. Applies to all gaps as a single value (input data - measured or otherwise) [Degree Temperature; SI: K, IP: R]

$V_{ini(i)}$ = Initial volume for i-th gap. [Lentgh*Length*Length; SI: m^3, IP: in^3]

$$V_{ini(i)} = L_i \cdot W \cdot H \qquad [8–7]$$

Where,

L_i = non-deflected glazing gap width (for i-th gap) [Length; SI: m, IP: in.]

W = IGU width [Length; SI: m, IP: in.]

H = IGU height [Length; SI: m, IP: in.]

$T_{gap(i)}$ = temperature of the gap between two glass panes (calculated using center of glazing thermal calculation algorithm, as described in ISO 15099 (ISO 2003). This value is first calculated using the

non-deflected state and is recalculated after the resulting deflection is calculated. This process is repeated until the temperature at the next iteration does not differ by more than 0.1 °C

$V_{gap(i)}$ = volume of the IGU gap in deflected state [Lentgh*Length*Length; SI: m³, IP: in³]

$$V_{gap(i)} = V_{ini(i)} + W \cdot H \cdot \left(\overline{L_{D,\iota}} - \overline{L_{D,\iota+1}} \right) \qquad [8–8]$$

Where,

$\overline{L_{D,\iota}}$ is mean deflection value for i-th pane. [Length; SI: m, IP: in.]

The deflection of each pane can be positive or negative and is done solely to establish a reference. The current frame of reference is that positive deflection means that the pane is deflecting towards the left side, while negative deflection means that the pane is deflecting towards the right side (Figure 8-3). Whether the deflection is in the direction of reducing the gap width or increasing it, it will be the result of the pressure difference, as described in *[8–1]*. When the pressure in the glazing unit is higher than the surrounding environmental pressure, the deflection will be towards increasing the gap width (i.e., ballooning), while the opposite situation will result in decreasing the gap width (i.e., vacuuming)
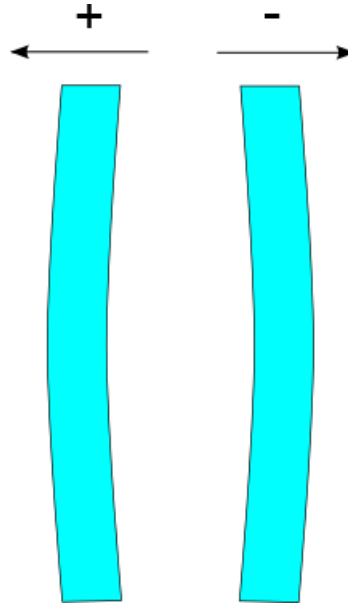
Figure 8-3. Deflection Direction Convention

An important part of calculating the deflection of the IGU is to determine the mean deflection value for each glazing pane. The mean deflection value is used to calculate the gap volume in the deflected state *[8–8]*. The mean deflection of the glazing pane can be calculated by integrating *[8–1]*:

$$\overline{L_{D(\iota)}} = \int_{x=0}^{W} \int_{y=0}^{H} \frac{16 \cdot \Delta P_{(i)}}{\pi^6 \cdot D_{(i)}} \sum_{m=1,3,5\ldots}^{\infty} \sum_{n=1,3,5\ldots}^{\infty} \frac{\sin \frac{m\pi x}{W} \sin \frac{n\pi y}{H}}{mn \left(\left(\frac{m}{W}\right)^2 + \left(\frac{n}{H}\right)^2 \right)^2} \qquad [8–9]$$

Which is identical with the following expression:

$$\overline{L_{D(i)}} = \frac{16 \cdot \Delta P_{(i)}}{\pi^6 \cdot D_{(i)}} \sum_{m=1,3,5\ldots}^{\infty} \sum_{n=1,3,5\ldots}^{\infty} \frac{\int_{x=0}^{W} \int_{y=0}^{H} sin\frac{m\pi x}{W} sin\frac{n\pi y}{H}}{mn \left(\left(\frac{m}{W}\right)^2 + \left(\frac{n}{H}\right)^2 \right)^2} \qquad [8-10]$$

and because integral of sin(x) is equal with –cos(x), above equation will become:

$$\overline{L_{D(i)}} = \frac{16 \cdot \Delta P_{(i)}}{\pi^6 \cdot D_{(i)}} \sum_{m=1,3,5\ldots}^{\infty} \sum_{n=1,3,5\ldots}^{\infty} \frac{(1 - cos(m\pi))(1 - cos(n\pi))}{mn \left(\left(\frac{m}{W}\right)^2 + \left(\frac{n}{H}\right)^2 \right)^2} \qquad [8-11]$$

Finally, because $cos(m\pi)$ and $cos(n\pi)$ values are always equal to -1 for the given range of m and n, the above equation will become:

$$\overline{L_{D(i)}} = \frac{16 \cdot \Delta P_{(i)}}{\pi^6 \cdot D_{(i)}} \sum_{m=1,3,5\ldots}^{\infty} \sum_{n=1,3,5\ldots}^{\infty} \frac{4}{m^2 n^2 \pi^2 \left(\left(\frac{m}{W}\right)^2 + \left(\frac{n}{H}\right)^2 \right)^2} \qquad [8-12]$$

After calculating the mean pane deflection, the following equation is used to calculate the mean gap width:

$$L_{r(i)} = L + \left(\overline{L_{D,(i)}} - \overline{L_{D,(i+1)}} \right) \qquad [8-13]$$

Where,

$L_{r(i)}$ = Mean gap "i" width after incorporating glazing deflection. This mean gap width is used to recalculate the thermal performance of the deflected IGU.

$\overline{L_{D,i}}$ = mean glazing deflection for each pane "i".

Calculation of the deflection at the center of glazing and mean glazing deflection for each pane is an iterative process, where the initial temperature distribution is calculated for the non-deflected state, then deflection is calculated based on this temperature distribution, a new temperature distribution is calculated for this deflected state, then temperatures from the previous iteration are compared to the current iteration and the process is repeated until the difference is no larger than 0.1 °C.

At the end of the calculations, the program will calculate and return the maximum deflection value for each pane (i.e., center of glazing deflection). If we label the maximum deflection of each pane as $L_{D(i),max}$, we can calculate this value by substituting $x=W/2$ and $y=H/2$ in equation *[8–1]* to determine the deflection at the center point. Therefore,

$$L_{D(i),max} = \frac{16 \cdot \Delta P_{(i)}}{\pi^6 \cdot D_{(i)}} \sum_{m=1,3,5\ldots}^{\infty} \sum_{n=1,3,5\ldots}^{\infty} \frac{sin\frac{m\pi}{2} sin\frac{n\pi}{2}}{mn \left(\left(\frac{m}{2}\right)^2 + \left(\frac{n}{2}\right)^2 \right)^2} \qquad [8-14]$$

For glazing systems with more than two glazing layers, meaning multiple gas filled gaps, the deflection will be calculated for each glazing pane assuming that the pressure in a gap is independent from each other and calculated separately, unless spaces are "linked" together (e.g., stretched film middle glazing that has hole for equalizing pressure).

8.1.1. Non-Linked Gaps in 3 or more glazing layer system:

The procedure shown above generally applies to glazing systems with 3 or more layers, with the exception that neighboring pressures are no longer P_a, but rather could be P_a on one side and P_{gap} on the other, or have P_{gap} on both sides, as shown in Figure 8-4 for gap "i". The center of glazing thermal calculation will determine the new temperature distribution, after deflection is calculated for each glazing and will be used to determine the new P_{gap}, as per the procedure above.

8.1.2. Linked Gaps in 3 or more glazing layer system:

When one or more gaps are linked together, their pressure is assumed to be identical (e.g., in a triple glazed IGU $P_{gap,1} = P_{gap,2}$.) This pressure is calculated from the temperatures of the bounding glazing for linked gaps (e.g., for triple glazing IGU, glazing 1 and 3) and using neighboring pressures outside of those bounding glazing (e.g., for triple glazed IGU, P_a on both sides).

Note: This feature is not implemented in the current version of WINDOW. It is considered for future enhancements to the program.
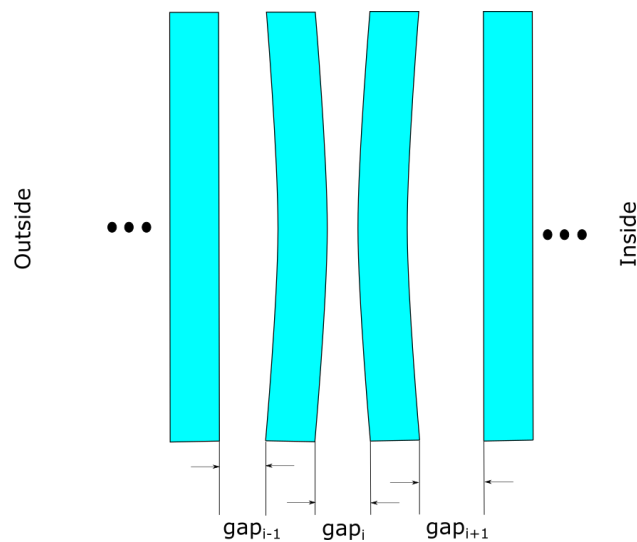
Figure 8-4. Sketch of deflection with non-linked gaps in 3 or more glazing layer system

8.1.3. Gap(s) Linked to Indoor or Outdoor Environment:

If one or more glazing gaps are linked to either the indoor or outdoor environment its pressure is fixed to P_a. In combination situations, such as two or more gaps linked together with one of them being linked to the indoor or outdoor environment, they will all have fixed pressure of P_a.

Note: This feature is not implemented in the current version of WINDOW. It is considered for future enhancements to the program.

8.2. Calculation of the Thermal Performance of the Deflected IGU

When deflection is measured, it is normally measured at the point of maximum deflection. Maximum deflection occurs at center of the IGU (at $W/2$ and $H/2$).

This measured value is typically the gap width at the point of maximum deflection, which we can label $L_{G(i)}$. For i-th measured gap the width is equal to:

$$L_{G(i)} = L_{(i)} + \left(L_{D(i),max} - L_{D(i+1),max} \right) \qquad\qquad [8\text{–}15]$$
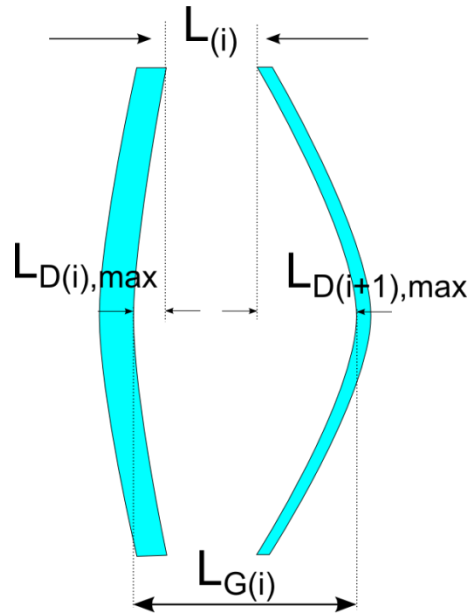
Figure 8-5. Sketch of the non-symetrically Deflected Glazing Panes

If we label the ratio of mean deflection and maximum deflection as $R_{(i)}$, then:

$$R_{(i)} = \frac{\overline{L_{D(i)}}}{L_{D(i),max}} = \frac{\sum_{m=1,3,5...}^{\infty}\sum_{n=1,3,5...}^{\infty} \dfrac{4}{m^2 n^2 \pi^2 \left(\left(\frac{m}{W}\right)^2 + \left(\frac{n}{H}\right)^2\right)^2}}{\sum_{m=1,3,5...}^{\infty}\sum_{n=1,3,5...}^{\infty} \dfrac{sin\frac{m\pi}{2} sin\frac{n\pi}{2}}{mn\left(\left(\frac{m}{2}\right)^2 + \left(\frac{n}{2}\right)^2\right)^2}} \qquad [8–16]$$

It is important to note that the ratios $(R_{(i)})$ for all gaps in the glazing system are equal.

$$R_{(1)} = R_{(2)} = ... = R_{(i)} = ... = R_{(n-1)} = R \qquad [8–17]$$

Replacing *[8–16]* and *[8–17]* into *[8–13]* the following equation is obtained:

$$L_{r(i)} = L_{(i)} + R(L_{D(i),max} - L_{D(i+1),max}) \qquad [8–18]$$

Combining *[8–18]* with *[8–15]* we get the following expression for the mean gap width:

$$L_{r(i)} = L_{(i)} + R(L_{G(i)} - L_{(i)}) \qquad [8–19]$$

The number of equations given in expression *[8–15]* is equal to n-1, where n is number of panes. Therefore, we need one more equation to complete the system of equations that would allow us to solve for all independent variables. To get the last equation we can rewrite *[8–14]* in slightly different manner:

$$L_{D(i),max} = \frac{\Delta P_{(i)}}{D_{(i)}} \cdot K \qquad [8–20]$$

Where coefficient K combines all constant terms, while $D_{(i)}$ is given by *[8–2]* and $\Delta P_{(i)}$ is calculated by *[8–3]*, *[8–4]* and *[8–5]*. Summing over all deflections, $L_{D(i),max}$ the following equation is obtained:

$$\sum_{i=1}^{n} \frac{D_{(i)}}{K} \cdot L_{D(i),max} = \sum_{i=1}^{n} \Delta P_{(i)} = 0 \qquad [8–21]$$

Note that sum of all $\Delta P_{(i)}$ is equal to zero since the outside pressure is equal to the inside. Therefore, the remaining equation that completes the set of equations is:

$$\sum_{i=1}^{n} D_{(i)} \cdot L_{D(i),max} = 0 \qquad [8–22]$$

8.2.1. Solving System of Equations

In order to the solve system of equations we will present *[8–15]* in slightly different manner:

$$0 = L_{(i)} + L_{G(i)} + L_{D(i),max} - L_{D(i+1),max} \qquad [8–23]$$

Which in developed form will look like this:

$$0 = L_{(1)} + L_{G(1)} + L_{D(1),max} - L_{D(2),max}$$

$$0 = L_{(2)} + L_{G(2)} + L_{D(2),max} - L_{D(3),max}$$

.
.
.

$$0 = L_{(i)} + L_{G(i)} + L_{D(i),max} - L_{D(i+1),max} \qquad [8–24]$$

.
.
.

$$0 = L_{(n-1)} + L_{G(n-1)} + L_{D(n-1),max} - L_{D(n),max}$$

In order to express each $L_{D(i),max}$ as dependence from $L_{D(n),max}$ (deflection of inside/last pane) we will need to make sum from first to last, then from second to last, third to last and so on. This procedure will create the following set of equations:

$$L_{D(1),max} = \sum_{k=1}^{k=n-1} (L_{G(k)} - L_{(k)}) + L_{D(n),max}$$

$$L_{D(2),max} = \sum_{k=2}^{k=n-1} (L_{G(k)} - L_{(k)}) + L_{D(n),max} \qquad [8–25]$$

.
.
.

$$L_{D(i),max} = \sum_{k=i}^{k=n-1} (L_{G(k)} - L_{(k)}) + L_{D(n),max}$$

.
.
.

$$L_{D(n-1),max} = \sum_{k=n-1}^{k=n-1} (L_{G(k)} - L_{(k)}) + L_{D(n),max}$$

Now replacing this set of equations back to *[8–22]*:

$$\sum_{i=1}^{n-1} D_{(i)} \cdot \left(\sum_{k=i}^{k=n-1} \left(L_{G(k)} - L_{(k)}\right) + L_{D(n),max}\right) + D_{(n)} \cdot L_{D(n),max} = 0 \qquad \text{[8–26]}$$

Which solving by $L_{D(n),max}$ leads to the following equation:

$$L_{D(n),max} = \frac{\sum_{i=1}^{n-1}(D_{(i)} \cdot \sum_{k=i}^{k=n-1}\left(L_{(k)} - L_{G(k)}\right))}{\sum_{i=1}^{n} D_{(i)}} \qquad \text{[8–27]}$$

Calculating $L_{D(n),max}$ value from this equation and substituting it in *[8–25]* will enable calculation of the deflection of the remaining panes.

9. VACUUM INSULATING GLAZING - VIG

Vacuum insulating glazing, also referred to as evacuated glazing units (EGU) are an emerging technology, developed as a concept some 20-30 years ago, but only now approaching wide-spread commercialization and acceptance.

9.1. Thermal Conductance

The thermal Conductance of the space in an evacuated glazing unit (EGU) is the sum of the conductance of the low-pressure gas (air) and the radiation conductance.

$$C_{gas} = C_{COND} + C_{RAD} \qquad\qquad\qquad\qquad [9\text{-}1]$$

9.1.1. Conductance of the Low-Pressure Gas

The conductance of low pressure gasses is calculated using the formula by Corruccini (1959)

$$C_{COND} = \alpha \cdot \left[\frac{\gamma+1}{\gamma-1}\right] \cdot \left[\frac{R}{8 \cdot \pi \cdot M \cdot T}\right]^{\frac{1}{2}} \cdot P \qquad\qquad [9\text{-}2]$$

$$B = \alpha \cdot \left[\frac{\gamma+1}{\gamma-1}\right] \cdot \left[\frac{R}{8 \cdot \pi \cdot M \cdot T}\right]^{\frac{1}{2}} \qquad\qquad [9\text{-}3]$$

$$C_{COND} = B \cdot P \qquad\qquad\qquad\qquad [9\text{-}4]$$

Where:

$$\alpha = \frac{\alpha_1 \alpha_2}{\alpha_2 + \alpha_1 (1-\alpha_2)} \qquad\qquad\qquad\qquad [9\text{-}5]$$

α_1, α_2 = Accommodation coefficients of the gas molecules with the two surfaces. These values depend on the temperature, surface conditions, etc. For the present configuration and conditions, it is expected that α is approximately 0.5. If conservative value is needed than value of 1.0 could be used. With α_1, α_2 = 0.79, α= 0.652893

γ = Specific heat ratio, γ_{air} = 1.40. Table 2 lists specific heat ratios for other gasses.

R = Universal gas constant, R = 8,314.462175 J/mol·K

M = Molecular Weight, M_{air} = 28.97 [mol/g]

T = $(T_1 + T_2)/2$ [K]

$P`$ = Pressure of the gas [N/m²]

From the paper Collins and Robinson (1991), B is set at approximately 50 for Air, if pressure is given in torr. Therefore, according to Collins and Robinson (1991), for air and approximate conditions of EGU:

$$C_{COND} \approx 50 \cdot P \qquad\qquad\qquad\qquad [9\text{-}6]$$

Where P is in torr (i.e., mm Hg).

Note: Conversion from Pa to torr is accomplished by multiplying value in torr by 133.28.

Using Equation *[8–2]* and assuming T_1 to be 20 ºC and T_2 to be -18 ºC (expected temperatures of glass surfaces in the EGU, if one glass surface is low-e and the unit is exposed to NFRC standard environmental conditions), and using the SI system of units, B is calculated as 54.4, which is very close to the value of 50, proposed by Collins and Robinson (1991).

$$C_{COND} \approx 54.4 \cdot P \qquad\qquad [9\text{-}7]$$

We will use the exact value, calculated by the formula, so values will be input into the calculations, which enables a more flexible model that can account for special treatment of glass surfaces.

9.2. Radiation Conductance

Radiation conductance for the two parallel plates is given by:

$$C_{RAD} = \frac{1}{\varepsilon_1^{-1} + \varepsilon_2^{-1} - 1} \sigma \cdot \frac{\left(T_1^4 - T_2^4\right)}{T_1 - T_2} \qquad\qquad [9\text{-}8]$$

Where:

ε_1	= emissivity of the first facing glass surface, [-]
ε_2	= emissivity of the second facing glass surface, [-]
σ	= Stefan-Boltzmann Constant, 5.67×10^{-8}, $[W/(m^2 \cdot K^4)]$
T_1	= Temperature of the first facing glass surface, [K]
T_2	= Temperature of the second facing glass surface. [K]

Assuming glass surface temperatures of 20 ºC and -18 ºC, respectively, the following radiation conducatnces are obtained for the three different glass emissivities:

Clear Glass ($\varepsilon_1 = \varepsilon_2 = 0.84$):	C_{RAD} = 3.4 W/m²K
Hard Coat Low-e (ε_1 or $\varepsilon_2 = 0.15$):	C_{RAD} = 0.68 W/m²K
Soft Coat Low-e (ε_1 or $\varepsilon_2 = 0.04$):	C_{RAD} = 0.19 W/m²K

Note: C_{RAD} of 0.09 is theoretically possible using best low-e technology today (i.e., ε_1 or $\varepsilon_2 = 0.02$).

Note: Low-e values above are typical values, which will vary by manufacturer. Some more recent hard coat low-e values are at or below 0.1.

It should also be noted that the values above are based on the fixed set of temperatures, while in reality temperatures will depend on the environmental conditions and surface emissivities (e.g., it cannot be expected that clear glass will have same T_1 and T_2 as low-e glass).

Equation *[8–8]* is precise formulation for two parallel plates at the constant temperature. The simplified equation under these conditions is given in the form of:

$$C_{RAD} = 4\sigma \frac{1}{\varepsilon_1^{-1} + \varepsilon_2^{-1} - 1} T_m^3 \qquad\qquad [9\text{-}9]$$

Where:

T_m =   mean temperature, [K]

$$T_m = \frac{(T_1 + T_2)}{2}$$
                                                                                                    [9-10]

9.3. Calculation of the U-factor:

$$U = \frac{1}{R_{tot}} = \frac{1}{R_o + 2 \cdot R_{glass} + R_{gap} + R_i}$$
                                                                                                    [9-11]

$$R_{gap} = \frac{1}{C_{gap}} = \frac{1}{C_{COND} + C_{RAD}}$$
                                                                                                    [9-12]

$$R_{glass} = \frac{t_{glass}}{k_{glass}}$$
                                                                                                    [9-13]

Where:

t_{glass} = glass thickness; [m]

k_{glass} = glass conductivity; k_{glass} = 1 W/(m·K)

R_{glass} = 0.003 m²K/W (for 3 mm glass pane)

$R_o \approx 0.033$ m²K/W

$R_i \approx 0.14$ m²K/W

The U-factor of an EGU without any pillars (pretending that this is possible) would be calculated using C_{RAD} only. From the above radiation conductance calculations:

Clear Glass:	U = 2.64 W/(m² ·K) [0.464 Btu/(hr ·ft² ·°F)]
Hard Coat Low-e:	U = 0.62 W/(m² ·K) [0.109 Btu/(hr ·ft² ·°F)]
Soft Coat Low-e:	U = 0.19 W/(m² ·K) [0.034 Btu/(hr ·ft² ·°F)]

Adding conductance of the air at 0.001 torr (C_{COND} = 0.08 W/(m² ·K), using the analysis from "*Section 9.1.1. Conductance of the Low-Pressure Gas*", these values become:

Clear Glass:	U = 2.66 W/(m² ·K) [0.468 Btu/(hr ·ft² ·°F)]
Hard Coat Low-e:	U = 0.68 W/(m² ·K) [0.120 Btu/(hr ·ft² ·°F)]
Soft Coat Low-e:	U = 0.27 W/(m² ·K) [0.048 Btu/(hr ·ft² ·°F)]

In contrast, the U-factor of the same configuration with the air at atmospheric pressure will be (for the space width of 50 μm, $C_{COND} \approx 450$ W/m²K):

Clear Glass:	U = 5.52 W/(m² ·K) [0.468 Btu/(hr ·ft² ·°F)]
Hard Coat Low-e:	U = 5.52 W/(m² ·K) [0.120 Btu/(hr ·ft² ·°F)]
Soft Coat Low-e:	U = 5.52 W/(m² ·K) [0.048 Btu/(hr ·ft² ·°F)]

It is clear that the emissivity of the glass surface makes no difference, because of the dominant conductance of the air space. Also, it is worth noting that the U-factor of such configuration is very close to the U-factor of single glazing.

9.4. Thermal Conductance of Glass Support Elements:

Glass panes in an EGU are separated by an array of small support elements. Typically, these support elements have the cylindrical shape and are often referred to as "pillars". A typical geometry of the pillar is 0.5-1.0 mm diameter and 0.05 mm (50 μm) height. They are typically spaced 25 mm apart in the form of a square or staggered matrix.

9.4.1. Approximate Method for Determining Conductance of Support Pillars:

The conductance of these elements can be measured or numerically modeled to determine accurate thermal performance. An approximate method also exists and is based on the combination of modeling and analytical work for the conduction through small cylinders in contact with infinite parallel plates with thickness much larger than cylinder height.

The following formula can be used to determine the conductance of the single pillar, C_p (Collins and Fisher-Cripps 1991):

$$C_p = \frac{2ka}{1 + \frac{2h}{\pi a}} \qquad [9\text{-}14]$$

Where:

> k = conductivity of glass, W/(m·K)
>
> a = radius of the pillar (m)
>
> h = pillar height, m

For the square array of support pillars (Collins and Fischer-Cripps 1991) proposes the following formula for their conductance, C_{pa}:

$$C_{pa} = \frac{2ka}{\lambda^2\left(1 + \frac{2h}{\pi a}\right)} \qquad [9\text{-}15]$$

Where:

> λ = pillar spacing, m

This formula is approximate and does not include the effect of the conductivity of the pillar. An alternative method for determining the conductance for the square array of support pillars, which includes the conductivity of the pillars, was also proposed by Collins and Fischer-Cripps (1991).

$$C_{pa}^* = \frac{2ka}{\lambda^2\left(1 + \frac{2kh}{k_p\pi a}\right)} \qquad C_{pa}^* = \frac{2ka}{\lambda^2\left(1 + \frac{2kh}{k_p\,p\pi a}\right)} \qquad [9\text{-}16]$$

Where:

> k_p = conductivity of pillar [W/m·K]

Equation *[8–15]* gives a good approximation for common materials used in this technology, since the conductivity of the pillar does not play a substantial role for non-insulating pillars (where "non-insulating" would mean that the conductivity of the pillar is equal to or higher than the conductivity of the glass pane). Equation *[8–15]* is used to represent the pillar array for the remainder of this document.

The U-factor of the EGU with support pillars is then:

$$U = \frac{1}{R_{tot}} = \frac{1}{R_o + 2 \cdot R_{glass} + R_{gap} + R_i}$$

[9-17]

Where:

$$R_{gap} = \frac{1}{C_{gap}} = \frac{1}{C_{COND} + C_{RAD} + C_{pa}}$$

[9-18]

10. SHADING DEVICES

The ISO 15099 standard considers only layer types of shading devices, such as screens, curtains and blinds, which are located close and parallel to the glazing panes. The algorithm for the calculation of the thermal properties of glazing systems with shading devices differs from the algorithms for the other glazing system types, given in Chapter 5 due to modifications that the introduction of shading devices in the glazing system model requires. Differences, mainly related to the convective heat transfer through the glazing cavities surrounding the shading device, lead to adjustments that are made in the main thermal equations and, consequently, in the calculation procedure.

10.1. Modifications of basic energy balance equations

Since the shading device, shown as the ith layer in Figure 10-1, allows ventilation through the adjacent glazing cavities, the convective heat transfer in ventilated cavities cannot be described as simple heat transfer from one surface to another, as it was done in Chapter 5.
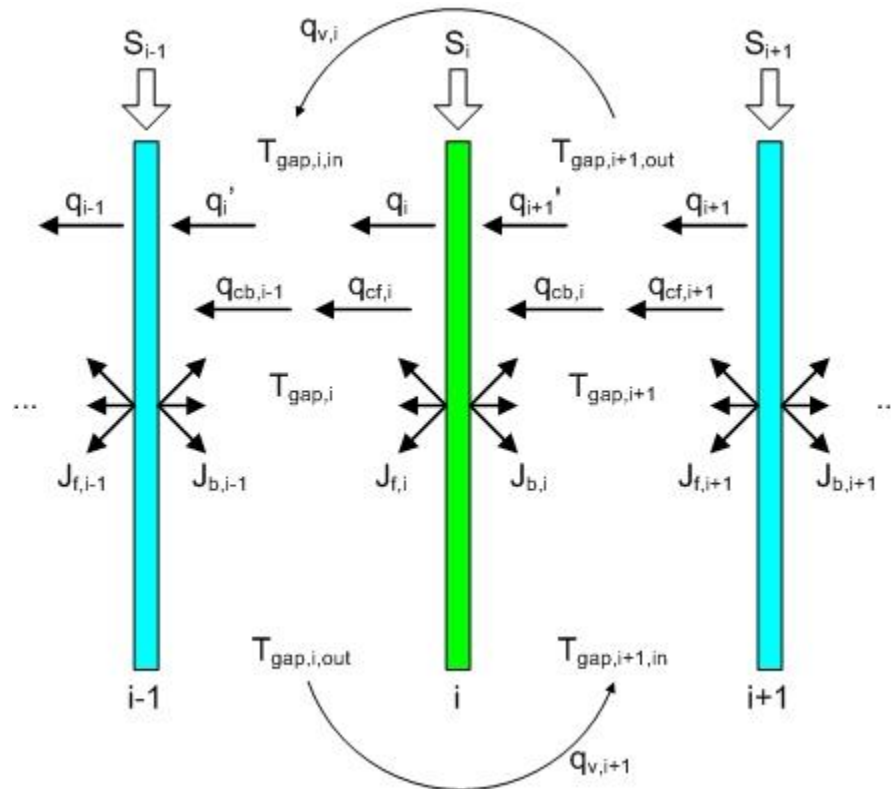
Figure 10-1. Numbering System and Energy Balance for Shading Layers in the Glazing System

In this case, the convective heat flux through the ventilated cavity must be divided into two parts, the convective heat flux from one layer to the gap space, and the convective heat flux from the gap space to another layer, where the mean gap temperature ($T_{gap,i}$) is a variable. Therefore, the convective heat flux through the ith glazing cavity can be described by the following equations:

$$q_{cf,i} = h_{cv,i}(T_{f,i} - T_{gap,i})$$

$$q_{cb,i-1} = h_{cv,i}(T_{gap,i} - T_{b,i-1})$$

[10–2]

where,

$q_{cf,i}$ = convective heat flux from one layer to the gap space

$q_{cb,i-1}$ = convective heat flux from the gap space to another layer

$T_{gap,i}$ = equivalent mean temperature of the gap space (see Equation *[10–28]*)

$T_{f,i}$ = temperature of the surface of the ith layer, facing the ith glazing cavity

$T_{b,i-1}$ = temperature of the surface of the layer i-1, facing the ith glazing cavity

$h_{cv,i}$ = convection heat transfer coefficient for ventilated cavities, given as:

$$h_{cv,i} = 2h_{cdv,i} + 4v_i$$

[10–3]

where,

$h_{cdv,i}$ = convection heat transfer coefficient for non-ventilated cavities (see *Chapter 5.1.2.3.3 Glazing Cavity Heat Transfer*)

v_i = mean air velocity in the glazing cavity (see *Chapter 10.1.2. Calculation of Air Velocity in Glazing*)
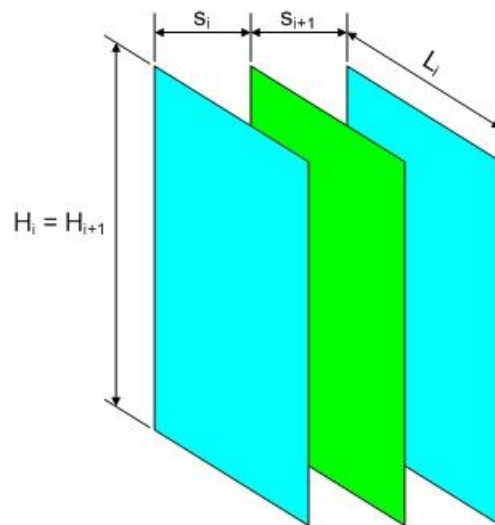
Figure 10-2. Main Dimensions of Glazing System Model with Shading Device

At the same time, the heat flux (i.e. $q_{v,i}$) supplied to or extracted from the ventilated cavity, determined as per following relation, must be included in main energy balance equations.

$$q_{v,i} = \frac{\rho_i \cdot c_{p,i} \cdot \varphi_{v,i} (T_{gap,i,in} - T_{gap,i,out})}{H_i \cdot L_i}$$

[10–4]

where,

ρ_i　　　= density of the gas space in the ith cavity at temperature $T_{gap,i}$

$c_{p,i}$　　= specific heat capacity of the gas space in the ith cavity at temperature $T_{gap,i}$

$T_{gap,i,in}$ = temperature at the inlet of the glazing cavity that depends on where the air comes from

$T_{gap,i,out}$ = temperature at the outlet of the glazing cavity (see equation [10–15])

H_i　　　= height of the ith glazing cavity (see Figure 10-2)

L_i　　　= depth of the ith glazing cavity (see Figure 10-2)

$\varphi_{v,i}$　　= air flow rate in the ith cavity, given as:

$$\varphi_{v,i} = v_i \cdot s_i \cdot L_i$$

[10–5]

where,

s_i = width of the ith glazing cavity (see Figure 10-2).

Using the equation [10–1], the total flux (including radiative part) leaving the front facing surface of the ith layer can be determined as:

$$q_i = q_{cf,i} + J_{f,i} - J_{b,i-1} = h_{cv,i}(T_{f,i} - T_{gap,i}) + J_{f,i} - J_{b,i-1}$$

[10–6]

Similarly, the heat flux leaving the layer i+1 is:

$$q_{i+1} = q_{cf,i+1} + J_{f,i+1} - J_{b,i} = h_{cv,i+1}(T_{f,i+1} - T_{gap,i+1}) + J_{f,i+1} - J_{b,i}$$

[10–7]

Finally, as a result of the mentioned modifications, made due to effects of ventilation on heat exchange in the glazing cavity, the basic energy balance equations for shading devices can be defined as the following system:

$$q_i = S_i + q_{i+1} + q_{v,i+1}$$

[10–8]

$$J_{f,i} = \varepsilon_{f,i}\sigma T_{f,i}^4 + \tau_i J_{f,i+1} + \rho_{f,i} J_{b,i-1}$$

[10–9]

$$J_{b,i} = \varepsilon_{b,i}\sigma T_{b,i}^4 + \tau_i J_{b,i-1} + \rho_{b,i} J_{f,i+1}$$

[10–10]

$$T_{b,i} - T_{f,i} = \frac{t_{sd,i}}{2k_{sd,i}}\left[2q_{i+1} + 2q_{v,i+1} + S_i\right]$$

[10–11]

10.1.1. Calculation of Glazing Cavity Temperature

The temperature in the glazing cavity can be determined by applying assumption about known value of mean velocity in the cavity to a model, which considers dependence of the temperature on the glazing cavity height (see Figure 10–3).
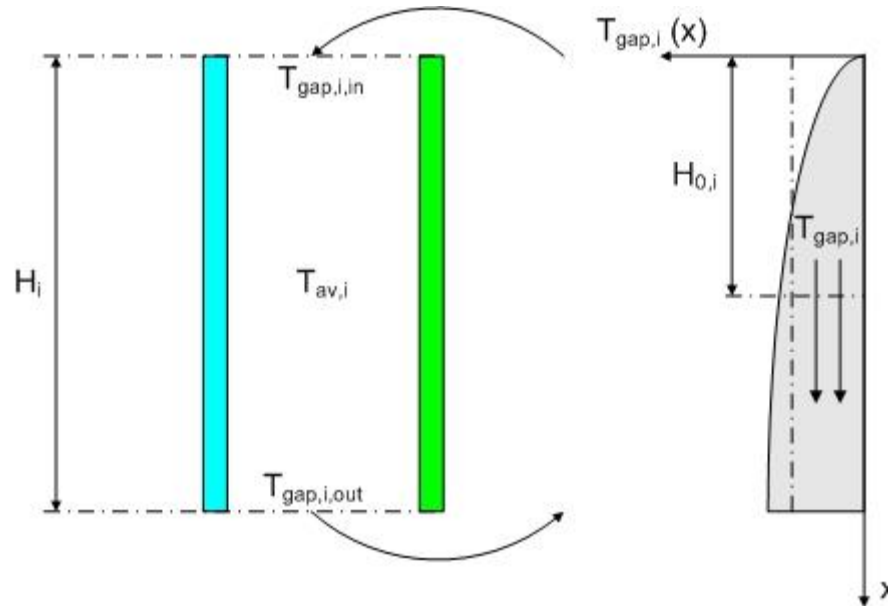
Figure 10–3. Temperature Profile in Ventilated Glazing Cavity

Temperature profile in the ventilated glazing cavity can be described as:

$$T_{gap,i}(x) = T_{av,i} - (T_{av,i} - T_{gap,i,in})e^{-x/H_{0,i}}$$

[10–12]

where,

x = distance from the inlet

$T_{gap,i}(x)$ = temperature in the glazing cavity at distance x

$T_{av,i}$ = average temperature of the layer surfaces bounding glazing cavity, given as:

$$T_{av,i} = \frac{T_{b,i-1} + T_{f,i}}{2}$$

[10–13]

$T_{gap,i,in}$ = air flow temperature at the inlet of the ventilated gap

$H_{0,i}$ = characteristic height (temperature penetration length) defined by:

$$H_{0,i} = \frac{\rho_i \cdot c_p \cdot s_i \cdot v_i}{2h_{cv,i}}$$

[10–14]

where,

ρ_i = density of the air at temperature $T_{gap,i}$

$c_{p,i}$ = specific heat capacity of the air at temperature $T_{gap,i}$

s_i = width of the ith glazing cavity (see Figure 10-2)

v_i = mean air velocity in the glazing cavity (see *Chapter 10.1.2. Calculation of Air Velocity in Glazing*)

$h_{cv,i}$ = convection heat transfer coefficient for ventilated cavities, presented in equation *[10–3]*

The following relation, which determines temperature of air flow leaving the ventilated glazing cavity, is obtained from the equation *[10–12]* by setting the glazing cavity height, H_i, for the distance from the inlet:

$$T_{gap,i,out} = T_{av,i} - (T_{av,i} - T_{gap,i,in})e^{-H_i/H_{0,i}}$$

[10–15]

The previous equation clearly shows that temperature of air flow leaving the ventilated cavity (i.e. $T_{gap,i,out}$) depends on temperature at the inlet of the glazing cavity (i.e. $T_{gap,i,in}$). In case of connected glazing cavities (as given in Figure 10–5), it means that the temperature at the inlet of ith cavity (i.e. $T_{gap,i,out}$) is a function of the temperature at the outlet of $i+1^{th}$ cavity, and vice versa. For the solution of this problem, the following model, shown in Figure 10–4, should be introduced.
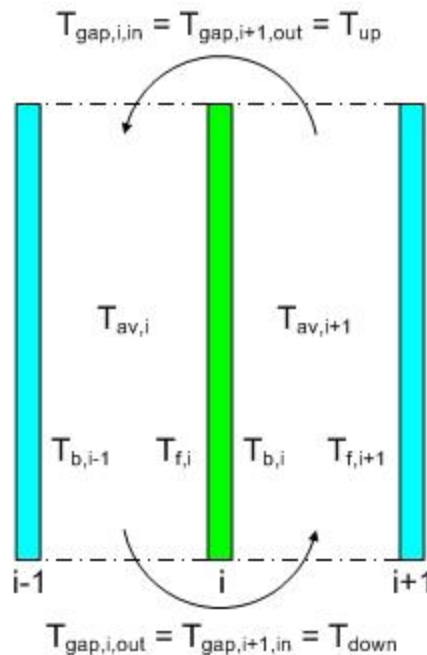
Figure 10–4. Model For Solving Inlet and Outlet Temperatures in Ventilated Cavities

Applying the notation from the Figure 10–4 in Equation *[10–15]* that is set for both ventilated cavities, gives the following relations:

$$T_{gap,i,out} = T_{down} = T_{av,i} - (T_{av,i} - T_{up})e^{-H_i/H_{0,i}}$$

[10–16]

$$T_{gap,i+1,out} = T_{up} = T_{av,i+1} - (T_{av,i+1} - T_{down})e^{-H_{i+1}/H_{0,i+1}}$$

[10–17]

After some re-arrangements, the following relations could be derived from the equations *[10–16]* and *[10–17]*:

$$T_{down} - \beta_i T_{up} = \alpha_i T_{av,i}$$

[10–18]

$$T_{up} - \beta_{i+1} T_{down} = \alpha_{i+1} T_{av,i+1}$$

[10–19]

where the terms α_i, α_{i+1}, β_i and β_{i+1} are:

$$\alpha_i = 1 - e^{-\frac{H_i}{H_{0,i}}}$$

[10–20]

$$\alpha_{i+1} = 1 - e^{-\frac{H_{i+1}}{H_{0,i+1}}}$$

[10–21]

$$\beta_i = e^{-\frac{H_i}{H_{0,i}}}$$

[10–22]

$$\beta_{i+1} = e^{-\frac{H_{i+1}}{H_{0,i+1}}}$$

[10–23]

By solving the equations *[10–18]* and *[10–19]*, temperatures at the inlet and outlet of ventilated glazing gaps can be found as:

$$T_{down} = T_{gap,i,out} = T_{gap,i+1,in} = \frac{\alpha_i T_{av,i} + \beta_i \alpha_{i+1} T_{av,i+1}}{1 - \beta_i \beta_{i+1}}$$

[10–24]

$$T_{up} = T_{gap,i,in} = T_{gap,i+1,out} = \alpha_{i+1} T_{av,i+1} + \beta_{i+1} \frac{\alpha_i T_{av,i} + \beta_i \alpha_{i+1} T_{av,i+1}}{1 - \beta_i \beta_{i+1}}$$

[10–25]

The above procedure is done in case of higher temperature in the cavity *i+1* (i.e. $T_{gap,i+1}$) than in the connected space *i* (i.e. $T_{gap,i}$).

Otherwise (i.e. if $T_{gap,i} > T_{gap,i+1}$), inlet and outlet temperatures for ventilated glazing cavities are:

$$T_{up} = T_{gap,i,out} = T_{gap,i+1,in} = \frac{\alpha_i T_{av,i} + \beta_i \alpha_{i+1} T_{av,i+1}}{1 - \beta_i \beta_{i+1}}$$

[10–26]

$$T_{down} = T_{gap,i,in} = T_{gap,i+1,out} = T_{av,i+1} \alpha_{i+1} + \beta_{i+1} \frac{\alpha_i T_{av,i} + \beta_i \alpha_{i+1} T_{av,i+1}}{1 - \beta_i \beta_{i+1}}$$

[10–27]

Finally, the equivalent average temperatures of the ventilated glazing cavities – $T_{gap,i}$ and $T_{gap,i+1}$ can be determined from the equation *[10–12]* by integration over the glazing cavity heights – H_i and H_{i+1}, respectively.

$$T_{gap,i} = \frac{1}{H_i} \int_0^H T_{gap,i}(x)dx = T_{av,i} - \frac{H_{0,i}}{H_i}(T_{gap,i,out} - T_{gap,i,in})$$

[10–28]

$$T_{gap,i+1} = \frac{1}{H_{i+1}} \int_0^H T_{gap,i+1}(x)dx = T_{av,i+1} - \frac{H_{0,i+1}}{H_{i+1}}(T_{gap,i+1,out} - T_{gap,i+1,in})$$

[10–29]

10.1.2. Calculation of Air Velocity in Glazing

The procedure for calculation of air flow velocity depends on the nature of the ventilation in the glazing cavity. Thus, different calculation methods are used in cases of thermally driven ventilation and forced ventilation.

10.1.2.1. Thermally Driven Ventilation

In this case air flow is caused by the stack or buoyancy effect, and the velocity can be found as a function of the driving pressure difference between connected spaces and the resistance to the air flow of the openings and the gas spaces itself.
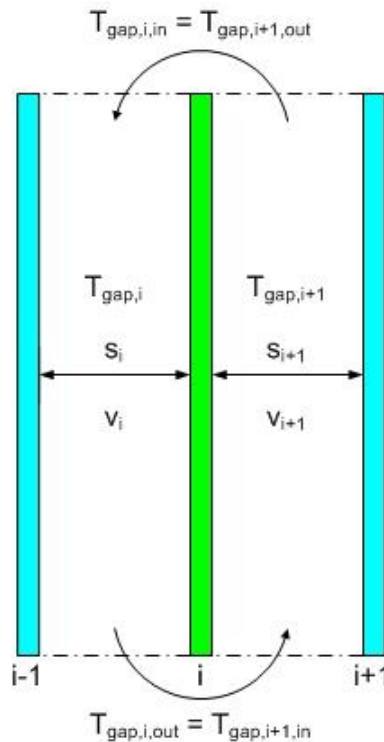
Figure 10–5. Schematic Presentation of the Thermally Driven Ventilation

The temperature difference between the glazing cavity, *i*, and the connected space, which can be either the outdoor or indoor environment, or another glazing cavity (as displayed in Figure 10-5), produces the driving pressure difference, $\Delta p_{T,i-i+1}$, that can be expressed as:

$$\Delta p_{T,i-i+1} = \rho_0 \cdot T_0 \cdot g \cdot H_i \cos\gamma_i \cdot \frac{\left|T_{gap,i} - T_{gap,i+1}\right|}{T_{gap,i} \cdot T_{gap,i+1}}$$

[10–30]

where,

$\rho_0 = $ density of the air at reference temperature T_0

T_0 =   reference temperature (283 K)

g =   acceleration due to gravity

H_i =   glazing cavity height

γ_i =   glazing system inclination (i.e. tilt angle) from vertical

$T_{gap,i}$ = mean temperature of the glazing cavity, given by equation *[10–28]*

$T_{gap,i+1}$ = mean temperature of the connected space (outdoor or indoor environment, or another glazing cavity)

The driving pressure difference $\Delta p_{T,i-i+1}$ shall be equal to the total pressure loss, which includes:

- Bernoulli pressure losses in spaces *i* and *i+1*, defined as:

$$\Delta p_{B,i} = 0.5\rho_i v_i^2$$

[10–31]

$$\Delta p_{B,i+1} = 0.5\rho_{i+1} v_i^2 \left(\frac{s_i}{s_{i+1}}\right)^2$$

[10–32]

- Hagen – Poiseuille pressure losses in spaces *i* and *i+1*, defined as:

$$\Delta p_{HP,i} = 12\mu_i \frac{H_i}{s_i^2} v_i$$

[10–33]

$$\Delta p_{HP,i+1} = 12\mu_{i+1} \frac{H_{i+1} \cdot s_i}{s_{i+1}^3} v_i$$

[10–34]

- pressure losses at the inlet and outlet of spaces *i* and *i+1*, defined as:

$$\Delta p_{Z,i} = 0.5\rho_i v_i^2 (Z_{in,i} + Z_{out,i})$$

[10–35]

$$\Delta p_{Z,i+1} = 0.5\rho_{i+1} v_i^2 (Z_{in,i+1} + Z_{out,i+1}) \left(\frac{s_i}{s_{i+1}}\right)^2$$

[10–36]

where,

ρ_i, ρ_{i+1} = density of the air at temperatures $T_{gap,i}$ and $T_{gap,i+1}$, respectively

v_i = mean air velocity in the ith glazing cavity that is being sought

H_i, H_{i+1} = height of ith and i+1th glazing cavity, respectively

s_i, s_{i+1} = width of ith and i+1th glazing cavity, respectively (see Figure 10-2)

μ_i, μ_{i+1} = dynamic viscosity of the air at temperatures $T_{gap,i}$ and $T_{gap,i+1}$, respectively

Z_i, Z_{i+1} = pressure loss factors of the ith and i+1th glazing cavity, found as per equations *[10–37] – [10–40]*

Note that all pressure losses for the space *i+1* are given in terms of air velocity in the space *i* (i.e. v_i) by setting velocity in the space *i+1* as: $v_{i+1} = v_i \cdot s_i / s_{i+1}$.

The pressure loss factors, Z_i and Z_{i+1}, can be found using the ratio of the equivalent opening areas ($A_{eq,i}$ and $A_{eq,i+1}$) to the cross sections of corresponding gas spaces ($A_{s,i}$ and $A_{s,i+1}$).
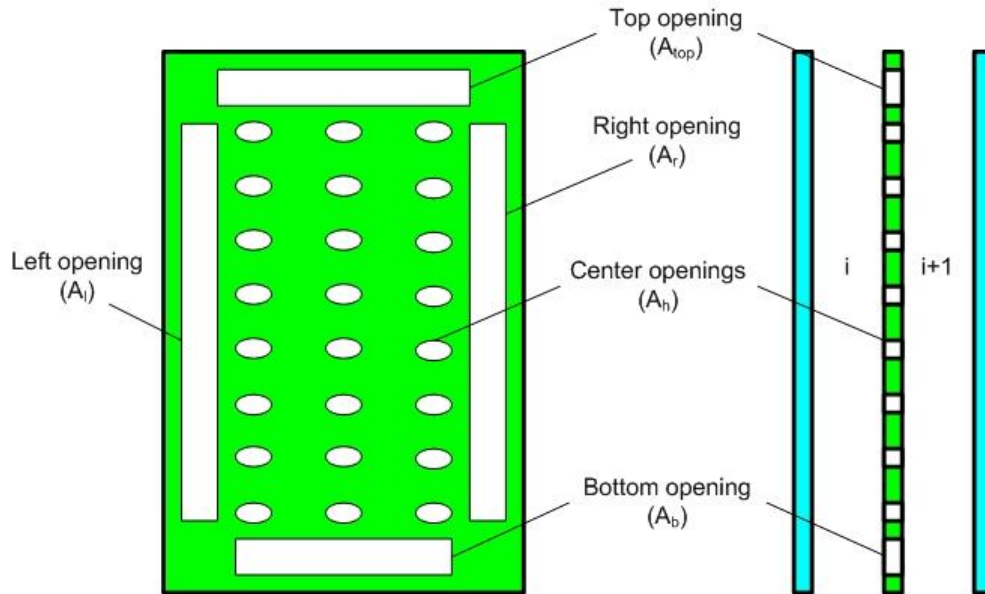
Figure 10–6. Openings in the Ventilated Glazing Cavity

$$Z_{in,i} = \left(\frac{A_{s,i}}{0.6 A_{eq,in,i}} - 1 \right)^2$$

[10–37]

$$Z_{in,i+1} = \left(\frac{A_{s,i+1}}{0.6 A_{eq,in,i+1}} - 1 \right)^2$$

[10–38]

$$Z_{out,i} = \left(\frac{A_{s,i}}{0.6 A_{eq,out,i}} - 1 \right)^2$$

[10–39]

$$Z_{out,i+1} = \left(\frac{A_{s,i+1}}{0.6 A_{eq,out,i+1}} - 1 \right)^2$$

[10–40]

where,

$A_{s,i}$, $A_{s,i+1}$ = cross section area of the ith and i+1th glazing cavity, respectively ($A_{s,i}$ and $A_{s,i} = si * L_i$;

$A_{s,i+1} =_{si+1} * L_{i+1}$) *[Length]*

s_i, s_{i+1} = width of ith and i+1th glazing cavity, respectively (see Figure 10-2) [Length]

L_i , L_{i+1} = depth of the ith and i+1th glazing cavity, respectively (see Figure 10-2) [Length]

Since the spaces *i* and *i+1* are connected, equivalent inlet opening area of the **ith** glazing cavity is, in fact, equivalent outlet opening area of the **i+1th** glazing cavity. Consequently, equivalent outlet opening area of the **ith** glazing cavity is equal to the equivalent inlet opening area of **i+1th** glazing cavity.

Calculation of equivalent inlet and outlet opening areas depends on temperature difference between adjacent glazing cavities (i.e. spaces *i* and *i+1*). If the temperature of the cavity *i* (i.e. $T_{gap,i}$) is higher than the temperature of the connected space *i+1* (i.e. $T_{gap,i+1}$), equivalent opening areas are:

$$A_{eq,in,i} = A_{eq,out,i+1} = A_{bot} + 0.5 \cdot \frac{A_{top}}{A_{bot} + A_{top}} (A_l + A_r + A_h)$$

[10–41]

$$A_{eq,out,i} = A_{eq,in,i+1} = A_{top} + 0.5 \cdot \frac{A_{bot}}{A_{bot} + A_{top}} (A_l + A_r + A_h)$$

[10–42]

Otherwise,

$$A_{eq,in,i} = A_{eq,out,i+1} = A_{top} + 0.5 \cdot \frac{A_{bot}}{A_{bot} + A_{top}} (A_l + A_r + A_h)$$

[10–43]

$$A_{eq,out,i} = A_{eq,in,i+1} = A_{bot} + 0.5 \cdot \frac{A_{top}}{A_{bot} + A_{top}} (A_l + A_r + A_h)$$

[10–44]

Where,

As	= is the cross section of the space, [Area];
Abot	= is the area of the bottom opening, [Area];
Atop	= is the area of the top opening, [Area];
Ah	= is the total area of the holes in the surface, [Area];
Al	= is the area of the left side opening, [Area];
Ar	= is the area of the right side opening, [Area];
Aeq,in,i	= is the equivalent inlet opening area of cavity I, [Area];
Aeq,out,i	= Equivalent outlet opening area of the cavity I, [Area]

Finally, air velocity in the space *i* (i.e. v_i) can be found from the following equation, which defines driving pressure difference (i.e. $\Delta p_{T,i-i+1}$) in terms of pressure losses.

$$\Delta p_{T,i-i+1} = \Delta p_{B,i} + \Delta p_{HP,i} + \Delta p_{Z,i} + \Delta p_{B,i+1} + \Delta p_{HP,i+1} + \Delta p_{Z,i+1}$$

[10–45]

After applying relation *[10–30]* for the driving pressure difference, as well as relations *[10–31]* − *[10–36]* for pressure losses, and some re-arrangements, the equation *[10–45]* becomes:

$$A_1 \cdot v_i^2 + A_2 \cdot v_i - A = 0 \qquad \text{[10–46]}$$

where the terms A, A_1 and A_2 are:

$$A = \rho_0 \cdot T_0 \cdot g \cdot H_i \cos\gamma_i \cdot \frac{\left| T_{gap,i} - T_{gap,i+1} \right|}{T_{gap,i} \cdot T_{gap,i+1}} \qquad \text{[10–47]}$$

$$A_1 = 0.5 \left[\rho_i \left(1 + z_{in,i} + z_{out,i} \right) + \rho_{i+1} \left(\frac{s_i}{s_{i+1}} \right)^2 \left(1 + z_{in,i+1} + z_{out,i+1} \right) \right] \qquad \text{[10–48]}$$

$$A_2 = 12 \left(\mu_i \frac{H_i}{s_i^2} + \mu_{i+1} \frac{H_{i+1} \cdot s_i}{s_{i+1}^3} \right) \qquad \text{[10–49]}$$

The air velocity v_i, as solution of the quadratic equation *[10–46]*, is given by the following relation:

$$v_i = \frac{\sqrt{A_2^2 + \left| 4 \cdot A \cdot A_1 \right|} - A_2}{2A_1} \qquad \text{[10–50]}$$

If the space *i+1* is exterior or interior environment, velocity v_{i+1} is set to zero, and the pressure losses $\Delta p_{B,i+1}$, $\Delta p_{HP,i+1}$ and $\Delta p_{Z,i+1}$ become zero, as well. In that case, the quadratic equation terms A_1 and A_2 will be:

$$A_1 = 0.5\rho_i \left(1 + z_{in,i} + z_{out,i} \right) \qquad \text{[10–51]}$$

$$A_2 = 12\mu_i \frac{H_i}{s_i^2} \qquad \text{[10–52]}$$

10.1.2.2. Forced Ventilation

In the case of forced ventilation, air flow velocity (i.e. v_i) can be determined from the known value of air flow rate, using the following relation:

$$v_i = \frac{\varphi_{v,i}}{s_i \cdot L_i} \qquad \text{[10–53]}$$

where,

s_i = width of the glazing cavity (see Figure 10-2)

L_i = length of the glazing cavity (see Figure 10-2)

$\phi_{v,i}$ = air flow rate in the glazing cavity (for the whole area), not normalized per m²

10.2. Airflow due to the Permeability of Shading Device

Validation has been performed for the ISO 15099 center-of-glass (COG) heat transfer correlations optimized for naturally ventilated cavities. Thermal transmittance was measured experimentally and simulated utilizing existing correlations from ISO 15099. Correlation coefficients to the ISO algorithm were proposed to better correlate simulation with experimental results. The focus is on impacts to system thermal transmittance due to variations in surface openness from room-side mounted screens and louvered horizontal (venetian) blinds.

10.2.1. Room-side mounted screens

Models and experimental analysis of pressure drop for flow through perforated surfaces has been extensively studied. The Darcy-Forchheimer Law, equation [10–54], is the relation used to describe velocity of a steady moving flow (Re > 1) under a pressure gradient, where Reynolds number (Re) is the ratio of inertial forces to viscous forces in a moving fluid. The linear term accounts for the momentum transfer from fluid to surface while the non-linear term accounts for the inertia effects,

$$\frac{\mu}{K}v + \rho\frac{Y}{K^{1/2}}v^2 = \frac{\partial p}{\partial x} \qquad\qquad [10\text{–}54]$$

where ρ is the fluid density, u is the dynamic viscosity, v is the velocity, p is the pressure, x is the direction vector of the pressure gradient, K is the permeability, and Y is the inertial factor (dependent on pore characteristics). K and Y can be correlated to a logarithmic model of the form shown in Equation *[10–55]* based on experimental analysis.

$$P = a \cdot d_{surface}^b \qquad\qquad [10\text{–}55]$$

d_surface represents openness of the shading system (fractional number 0-1). P represents the correlation constant K or Y and a & b are constants determined by regression analysis from measurements of perforated screen materials. Yarn shape and mesh geometry have negligible impact on airflow characteristics through screens, which allows the model to be dependent solely on $d_{surface}$ and thickness of the layer.

To improve the simulation correlation, correlation coefficients are proposed to the five ventilated layer opening parameters defined in ISO 15099; A_h, A_{top}, A_{bot}, A_{left}, and A_{right}. The proposed correlation coefficient for A_h is presented in Equation *[10–56]*. This model includes two correlation constants, C1 and C2 that are determined based on regression analysis of the measured dataset. An additional two constants, C3 and C4, are also optimized and used to correlate the left/right and top/bottom gaps respectively as shown in Equations *[10–57]* and *[10–58]*.

$$A_h = C1 \cdot d_{surface}^{C2} \cdot A_w \qquad\qquad [10\text{–}56]$$

$$A_{l,r}^* = C3 \cdot A_{l,r} \qquad\qquad [10\text{–}57]$$

$$A_{t,b}^* = C4 \cdot A_{t,b} \qquad\qquad [10\text{–}58]$$

Table 10–1. Calculated correlation coefficients for proposed WINDOW
simulation model of porous surfaces with perimeter gaps

Coefficient	Value
C1	0.078
C2	1.20
C3	1
C4	1

10.2.2. Room-side mounted horizontal louvered blinds

Seven parameters relative to horizontal blinds are considered in the model; slat width, pitch, rise, conductivity, tilt angle, slat-window gap width, and left and right gap dimensions.

Table 10–2. Measurement parameters for horizontal blind investigation

Variable	Parameter
w	slat width
p	pitch
r	rise
k_s	conductivity
d_{left}, d_{right}	side gap width
φ	tilt angle
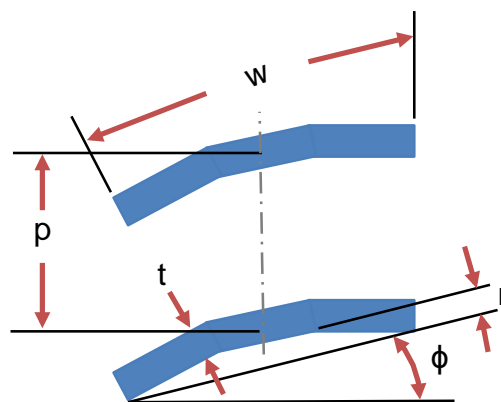
Figure 10–7. Horizontal blind slat geometry

The proposed model for A_h in Equation *[10–59]* is of the logarithmic form. The openness in Equation *[10–60]* is the ratio of slat to open area of the blind layer. This model includes four correlation constants D1, D2, D3, and D4 that are calculated based on the measured dataset according to optimization procedure based on experimental analysis.

Proposed:

$$A_h = D1 \cdot [d_{surface} \cdot (\cos \varphi)^{D2}]^{D3} \cdot A_s \qquad\qquad [10–59]$$

$$d_{surface} = 1 - \frac{t}{(\cos \varphi) \cdot (\rho - t)} \qquad\qquad [10–60]$$

$$t^* = D4 \cdot w \cdot \cos \varphi \qquad\qquad [10–61]$$

$$d_{top} = 0 \qquad\qquad [10–62]$$

$$d_{left,right} = d_{gap} \quad \text{for outside mount} \qquad\qquad [10–63]$$

$$d_{left,right} = 0 \quad\quad \text{for inside mount} \qquad\qquad [10–64]$$

$$d_{bot} = d_{gap} \quad\quad \text{for outside mount} \qquad\qquad [10–65]$$

$$d_{bot} = 0 \quad\quad\quad \text{for inside mount} \qquad\qquad [10–66]$$

where t^* and k^* are the revised layer thickness and equivalent conductivity and k_c is the conductivity of the gas between slats at the average blind layer temperature. The calculated openness by Equation *[10–60]* for horizontal blind systems typically results in openness greater than 90%. With the tested inside mount blinds the top, bottom, and side gaps are zero.

Utilizing the revised algorithm as described by Equations *[10–59]* - *[10–66]*, and optimizing the correlation coefficients based on measured data, the accuracy of the simulation increases greatly. The resulting correlation coefficients are listed in Table 10–3. Calculated correlation coefficients for proposed WINDOW simulation model for horizontal louvered blinds. The proposed revisions to WINDOW show much less sensitivity to openness. This is achieved by significantly reducing openness weighting in the algorithm through D1.

Table 10–3. Calculated correlation coefficients for proposed WINDOW
simulation model for horizontal louvered blinds

Coefficient	Value
D1	0.016
D2	-0.63
D3	0.53
D4	0.043

10.3. System of Equations for Glazing Systems Incorporating Shading Devices

The non-linear system of energy balance equations for shading devices, given in equations *[10–8] - [10–11]*, can become linear if solved in terms of black emissive power instead of temperature. In this case, differences from glazing systems with monolithic layers are related to convective heat transfer through ventilated cavities, so the *heat transfer coefficient based on emissive power for ventilated cavities* must be introduced, instead of the previous one (i.e. for non-ventilated cavities), given in equation *[10–67]*:

$$\hat{h}_{v,i} = h_{cv,i} \frac{T_{f,i} - T_{gap,i}}{E_{bf,i} - E_{bgap,i}}$$

[10–67]

Applying the methodology, described for monolithic layers, in conjunction with relations *[10–8]*–*[10–11]* and *[10–67]* for shading layers, gives the following system of linear equations for glazing systems incorporating shading devices:

$$J_{f,1} + \hat{h}^{out}E_{bf,1} + \hat{h}_2 E_{bb,1} + J_{b,1} - J_{f,2} - \hat{h}_2 E_{bf,2} = S_1 + G_{out} + \hat{h}^{out}G_{out}$$

[10–68]

$$-J_{f,1} + \varepsilon_{f,1}E_{bf,1} + \tau_1 J_{f,2} = -\rho_{f,1}G_{out}$$

[10–69]

$$\varepsilon_{b,1}E_{bb,1} - J_{b,1} + \rho_{b,1}J_{f,2} = -\mathrm{T}_1 G_{out}$$

[10–70]

$$\hat{h}_1^{gl} E_{bf,1} + (\hat{h}_1^{gl} + \hat{h}_2)E_{bb,1} + J_{b,1} - J_{f,2} - \hat{h}_2 E_{bf,2} = 0.5 S_1$$

[10–71]

…

$$-J_{b,i-1} + J_{f,i} + \hat{h}_{v,i}E_{bf,i} + J_{b,i} - J_{f,i+1} - \hat{h}_{v,i+1}E_{bf,i+1} = S_i + \hat{h}_{v,i}E_{bgap,i} - \hat{h}_{v,i+1}E_{bgap,i+1} + q_{v,i+1}$$

[10–72]

$$\rho_{f,i}J_{b,i-1} - J_{f,i} + \varepsilon_{f,i}E_{bf,i} + \tau_i J_{f,i+1} = 0$$

[10–73]

$$\tau_i J_{b,i-1} + \varepsilon_{b,i}E_{bb,i} - J_{b,i} + \rho_{b,i}J_{f,i+1} = 0$$

[10–74]

$$-\hat{h}_i^{gl} E_{bf,i} + \hat{h}_i^{gl} E_{bb,i} + J_{b,i} - J_{f,i+1} - \hat{h}_{v,i+1}E_{bf,i+1} = 0.5 S_i + q_{v,i+1} - \hat{h}_{v,i+1}E_{bgap,i+1}$$

[10–75]

…

$$-\hat{h}_n E_{bb,n-1} - J_{b,n-1} + J_{f,n} + \hat{h}_n E_{bf,n} + \hat{h}^{in}E_{bb,n} + J_{b,n} = S_n + G_{in} + \hat{h}^{in}G_{in}$$

[10–76]

$$\rho_{f,n}J_{b,n-1} - J_{f,n} + \varepsilon_{f,n}E_{bf,n} = -\tau_n G_{in}$$

[10–77]

$$\tau_n J_{b,n-1} + \varepsilon_{b,n}E_{bb,n} - J_{b,n} = -\rho_{b,n}G_{in}$$

[10–78]

$$\hat{h}_n^{gl} E_{bf,n} + (\hat{h}_n^{gl} + \hat{h}^{in})E_{bb,n} + J_{b,n} = 0.5 S_n + G_{in} + \hat{h}^{in}G_{in}$$

[10–79]

The system of equations *[10–68] – [10–79]* can also be transformed into a matrix form [A] [X] = [B] for the whole glazing system.

$$[A] = \begin{bmatrix}
1 & \hat{h}^{out} & \hat{h}_2 & 1 & \dots & 0 & 0 & 0 & 0 & \dots & 0 & 0 & 0 & 0 \\
-1 & \varepsilon_{f,1} & 0 & 0 & \dots & 0 & 0 & 0 & 0 & \dots & 0 & 0 & 0 & 0 \\
0 & 0 & \varepsilon_{b,1} & -1 & \dots & 0 & 0 & 0 & 0 & \dots & 0 & 0 & 0 & 0 \\
0 & -\hat{h}_1^{gl} & \hat{h}_1^{gl}+\hat{h}_2 & 1 & \dots & 0 & 0 & 0 & 0 & \dots & 0 & 0 & 0 & 0 \\
\dots & \dots & \dots & \dots & \dots & \dots & \dots & \dots & \dots & \dots & \dots & \dots & \dots & \dots \\
0 & 0 & 0 & 0 & \dots & 1 & \hat{h}_{v,i} & 0 & 1 & \dots & 0 & 0 & 0 & 0 \\
0 & 0 & 0 & 0 & \dots & -1 & \varepsilon_{f,i} & 0 & 0 & \dots & 0 & 0 & 0 & 0 \\
0 & 0 & 0 & 0 & \dots & 0 & 0 & \varepsilon_{b,i} & -1 & \dots & 0 & 0 & 0 & 0 \\
0 & 0 & 0 & 0 & \dots & 0 & -\hat{h}_i^{gl} & \hat{h}_i^{gl} & 1 & \dots & 0 & 0 & 0 & 0 \\
\dots & \dots & \dots & \dots & \dots & \dots & \dots & \dots & \dots & \dots & \dots & \dots & \dots & \dots \\
0 & 0 & 0 & 0 & \dots & 0 & 0 & 0 & 0 & \dots & 1 & \hat{h}_n & \hat{h}^{in} & 1 \\
0 & 0 & 0 & 0 & \dots & 0 & 0 & 0 & 0 & \dots & -1 & \varepsilon_{f,n} & 0 & 0 \\
0 & 0 & 0 & 0 & \dots & 0 & 0 & 0 & 0 & \dots & 0 & 0 & \varepsilon_{b,n} & -1 \\
0 & 0 & 0 & 0 & \dots & 0 & 0 & 0 & 0 & \dots & 0 & -\hat{h}_n^{gl} & \hat{h}_n^{gl}+\hat{h}^{in} & 1
\end{bmatrix}$$

$$[X] = \begin{bmatrix}
J_{f,1} \\
E_{bf,1} \\
E_{bb,1} \\
J_{b,1} \\
\dots \\
J_{f,i} \\
E_{bf,i} \\
E_{bb,i} \\
J_{b,i} \\
\dots \\
J_{f,n} \\
E_{bf,n} \\
E_{bb,n} \\
J_{b,n}
\end{bmatrix}
\qquad
[B] = \begin{bmatrix}
S_1 + G_{out} + \hat{h}^{out} G_{out} \\
-\rho_{f,1} G_{out} \\
-\tau_1 G_{out} \\
0.5 S_1 \\
\dots \\
S_i + \hat{h}_{v,i} E_{bgap,i} - \hat{h}_{v,i+1} E_{bgap,i+1} + q_{v,i+1} \\
0 \\
0 \\
0.5 S_i + q_{v,i+1} - \hat{h}_{v,i+1} E_{bgap,i+1} \\
\dots \\
S_n + G_{in} + \hat{h}^{in} G_{in} \\
-\tau_n G_{in} \\
-\rho_{b,n} G_{in} \\
0.5 S_n + G_{in} + \hat{h}^{in} G_{in}
\end{bmatrix}$$

The matrix equation [A] [X] = [B] is solved and the glazing layer temperatures determined, using the same iterative procedure as for glazing systems with monolithic layers (see Chapter 5).

10.4. Actual Cavity Width Convection Model

In this model, convection around the SD is treated as if shading device is just another impermeable layer, and the width of this layer and the corresponding gap space width between this layer and the glass is assumed to be equal to the actual width. This means that if the SD is venetian blind and if the venetian blind is open, the width of the venetian blind layer is assumed to be the width from the tip to tip of venetian blind slats. For example, if 16 mm wide venetian blinds are installed in 20 mm glazing cavity, and if venetian blind is at 0 degrees angle, which means that slats are horizontal (fully opened), the venetian blind layer width will be 16

mm, while each gap around the venetian blind will be 2 mm wide.   If on the other hand that same blind is at the 45 degree, the width of the venetian blind layer will be 16·cos(45) = 11.31 mm, while each gap around the blind will be 4.34 mm. Fort the fully closed blind, the thickness of the venetian blind layer will be the thickness of the blind material.

Treatment of SD on indoor and outdoor side is similar, where actual cavity width is calculated by subtracting half the width of the shading device (tip to tip) from the distance of the center of SD to the surface of the glass.

Conductivity of such layer is ignored, meaning that thermal resistance of the layer itself is negligible. This model has been compared with the limited set of measurements from published technical papers and it gave reasonable agreement.

10.5. Scalar Convection

Scalar convection is an alternative methodology for calculating convective heat transfer in the presence of shading devices.   In this model, the convection in gaps around the SD is treated as an intermediate case between two extreme cases, set with the use of convection scalar, with range from 0 to 1. The two extreme cases are:

1. Existence of SD is ignored for the convection heat transfer and convection equations for unobstructed glazing cavity are solved in each iteration.

2. SD is assumed to be fully closed and is treated as impermeable layer with the negligible thickness. Two gaps are formed as a result and convection heat transfer is solved as if solid layer is placed between two glass layers (making effectively triple glazing out of double glazing with SD in between.

When the convective scalar is set to 0, case 1 is solved. When the convective scalar is set to 1, case 2 is solved. When the convective scalar is set to the value in-between 0 and 1 (e.g., 0.5), then the linear interpolation between the two cases is performed at each iteration.

A similar procedure is employed for indoor and outdoor venetian blinds, except that the blind in those cases form one additional cavity on indoor or outdoor, respectively.

10.5.1. "No SD" Case

Case "No SD" treats a glazing system without SD layer in terms of convection. As a first step, SD layer is removed from the glazing system and calculation is performed for two glass layers (equation *[10–80]*) where gap thickness S_{gg} equals a distance between first and third layer (sum of first and second gap thickness and SD thickness).
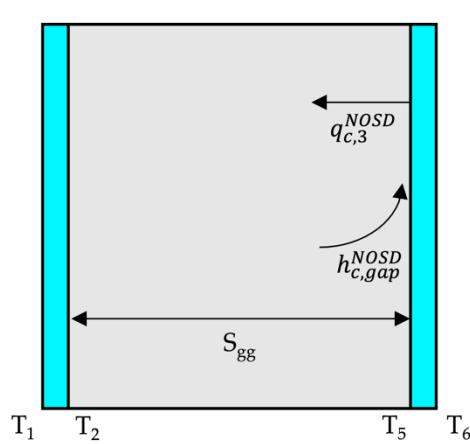
Figure 10–8. Glazing system with two glass glazing pane

Convective heat transfer coefficient for this case depends on glazing layer temperatures and gap thickness:

$$h_{c,gap}^{NOSD} = f(T_2, T_5, S_{gg}) = N_{u,i} \cdot \frac{k_g}{S_{gg}}$$

$$[10–80]$$

where:

S_{gg} is thickness of glazing cavity which is equal to the sum of thickness of first, second gap and SD thickness.

k_g is thermal conductivity of the fill gas in the cavity. Convective heat flux through the glazing cavity is determined as:

$$q_{c,3}^{NOSD} = h_{c,gap}^{NOSD} \cdot (T_5 - T_2)$$

$$[10–81]$$

In the original configuration, with SD present, convective parts of heat fluxes in two gaps can be expressed as (Figure 10–9. Glazing system without SD influence on convection):

$$q_{c,2}^{o} = h_{c,gap1}^{o} \cdot (T_3 - T_2)$$

$$[10–82]$$

$$q_{c,3}^{o} = h_{c,gap2}^{o} \cdot (T_5 - T_4)$$

$$[10–83]$$

In order to form a glazing system in which existence of SD layer does not affect convective heat transfer (Figure 10–9. Glazing system without SD influence on convection), the resulting convective parts of heat fluxes in two gaps, expressed as in equation *[10–84]* and *[10–85]*, must be equal to heat flux from the "no SD" configuration:

$$q_{c,2}^{o} = q_{c,3}^{NOSD}$$

$$[10–84]$$

$$q_{c,3}^{o} = q_{c,3}^{NOSD}$$

$$[10–85]$$
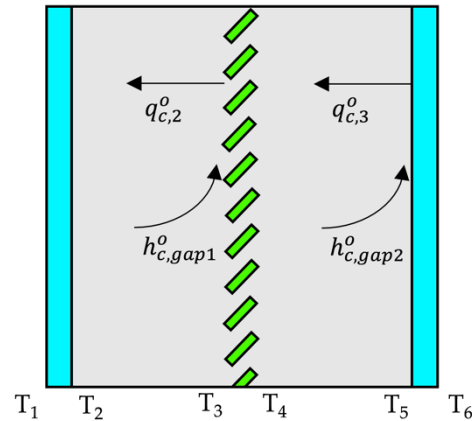
Figure 10–9. Glazing system without SD influence on convection

Therefore, convective heat transfer coefficients for a "No SD" case become:

$$h^o_{c,gap1} = h^o_{c,gap2} = h^{NOSD}_{c,gap} \qquad [10–86]$$

10.5.2. "Closed SD" Case

"Closed SD" case (Figure 10–10. Glazing system with closed SD which is treated as glass layer) treats SD layer as closed, which means it will be treated as glass layer with SD thickness and conductivity of SD material. Glazing cavity convective heat transfer coefficients $h^1_{c,gap1}$ and $h^1_{c,gap2}$ will be calculated in a "standard" way, as in a case of two glass layers with a gap between them – as explained in chapter 10.5.1. "No SD" Case.
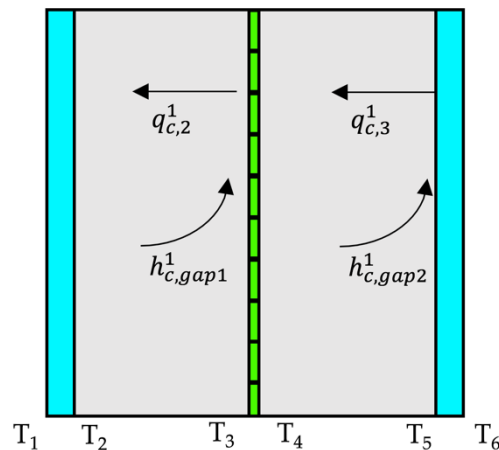
Figure 10–10. Glazing system with closed SD which is treated as glass layer

Combination of the extreme cases "NO SD" and "Closed SD" which were presented above will be obtained by introducing new scalar parameter – Alpha:

$$h^\alpha_{c,gap1} = \alpha \cdot (h^1_{c,gap1} - h^0_{c,gap1}) + h^0_{c,gap1} \qquad [10–87]$$

$$h^\alpha_{c,gap2} = \alpha \cdot (h^1_{c,gap2} - h^0_{c,gap2}) + h^0_{c,gap2} \qquad [10–88]$$

These convective heat transfer coefficients will be used in "standard" energy balance equations instead of convection heat transfer coefficients for ventilated cavities $h_{cv,1}$ and $h_{cv,2}$, so equation *[10–67]* will become:

$$\hat{h}^{\alpha}{}_{gap1} = h^{\alpha}_{c,gap1} \cdot \frac{T_3 - T_2}{E_{bf,2} - E_{bb,1}}$$

[10–89]

$$\hat{h}^{\alpha}{}_{gap2} = h^{\alpha}_{c,gap2} \cdot \frac{T_5 - T_4}{E_{bf,3} - E_{bb,2}}$$

[10–90]
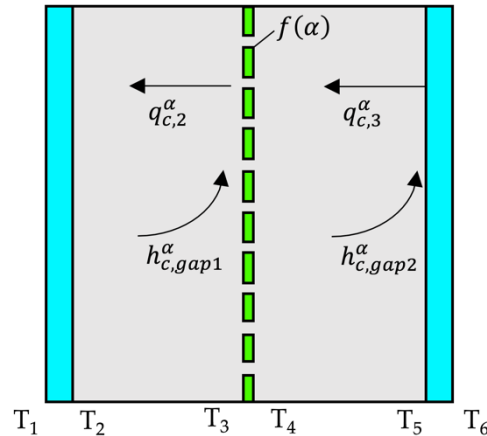
Figure 10–11. Glazing system with new convection coefficients

When factor Alpha is set to zero new model will calculate convection as if there was no SD layer. If Alpha is set to one, convective coefficient will correspond to second extreme case – ''Closed SD''.

10.5.3. Calculation of U – factor and SHGC

The U–factor of glazing systems with shading devices is calculated using essentially the same method as for other glazing system types (i.e. with monolithic or laminated layers), since it is, again, defined as the reciprocal of the total glazing system thermal resistance – R_{tot}. As for other glazing system types, the R_{tot} is, also, determined as a sum of the thermal resistance on the outdoor side of the glazing system, thermal resistances of the glazing layers and glazing cavities and the thermal resistance on the indoor side of the glazing system.

The thermal resistance on the glazing system outdoor side – R_{out}, thermal resistances of glazing layers – $R_{g1,i}$ and thermal resistance on the glazing system indoor side – R_{in}, are calculated using the same relations as for glazing system with monolithic layers (see chapter 5). At the same time, thermal resistance – $R_{gap,i}$, of ventilated glazing cavities is calculated differently from the thermal resistance of non-ventilated cavities. In case of ventilated cavities, heat transfer in the cavities is divided into two parts due to ventilation and, therefore, thermal resistance of ventilated cavities should be expressed in the same way.

$$R_{gap,i} = R_{gap,f,i} + R_{gap,b,i-1}$$

[10–91]

where,

$R_{gap,f,i}$ – resistance to heat transfer between the glazing layer and ventilated cavity, given as:

$$R_{gap,f,i} = \frac{T_{f,i} - T_{gap,i}}{h_{cv,i}(T_{f,i} - T_{gap,i}) + J_{f,i} - J_{b,i-1}}$$

[10–92]

$R_{gap,b,i-1}$ – resistance to heat flow between the ventilated cavity and another glazing layer, given as:

$$R_{gap,b,i-1} = \frac{T_{gap,i} - T_{b,i-1}}{h_{cv,i}(T_{gap,i} - T_{b,i-1}) + J_{f,i} - J_{b,i-1}}$$

[10–93]

The calculation of solar heat gain coefficient (SHGC) is performed in the same manner as for glazing systems with monolithic layers.

11. OPTICAL PROPERTIES: LOUVERED BLIND

Venetian is a set of procedures for the calculation of the optical properties for the Venetian blind type of shading devices. These calculations are performed for ultraviolet (UV), visible (VIS) and near infra-red (NIR) wavelengths (UV/VIS/NIR), jointly referred to as the solar or SOL range in this document, and also separately for the far infra-red range, referred to as FIR in this document.

The calculations of SOL properties (transmittance, reflectance at the front and at the back side of the blind) are done for the set of incident radiation and outgoing radiation angles, and the results are recorded in two BTDF (forward and back transmittance) and two BRDF matrices (forward and back reflectance). BTDF/BRDF stands for Bi-directional Transmittance/Reflectance Distribution Functions. The calculations in the SOL range are done for the discrete wavelengths, whose spacing depends on the quality of the spectral data available.

These matrices are later used in the calculation of the overall glazing system solar-optical properties using the procedure detailed in Klems, J.H. 1994a and Klems, J.H. 1994b. The Venetian blind is treated as just one layer in the glazing system, albeit having both specular and diffuse transmission/reflection properties, as opposed to a "simple" transparent layer, which is assumed to have purely specular properties.

Venetian also calculates the FIR properties of the Venetian blind: FIR transmittance, emissivity at the front and at the back side of the blind. These properties are diffuse values and are calculated for the single band comprising the entire FIR range from 2.5 µm to 50 µm.

11.1. Input data for Venetian BLINDS procedure

Input data for the Venetian blind procedure can be divided into four categories: slat geometry data, slat optical properties, angle coordinates and calculation parameters (see *Table 11-1*). Slat geometry data and slat optical properties describe the blind, while angular coordinates define all incident and outgoing directions, which must be the same for each layer in the glazing system. The calculation parameters define which calculation method will be used and whether the View Factor (VF) values should be calculated and stored in memory, or previously stored VF values would be used.
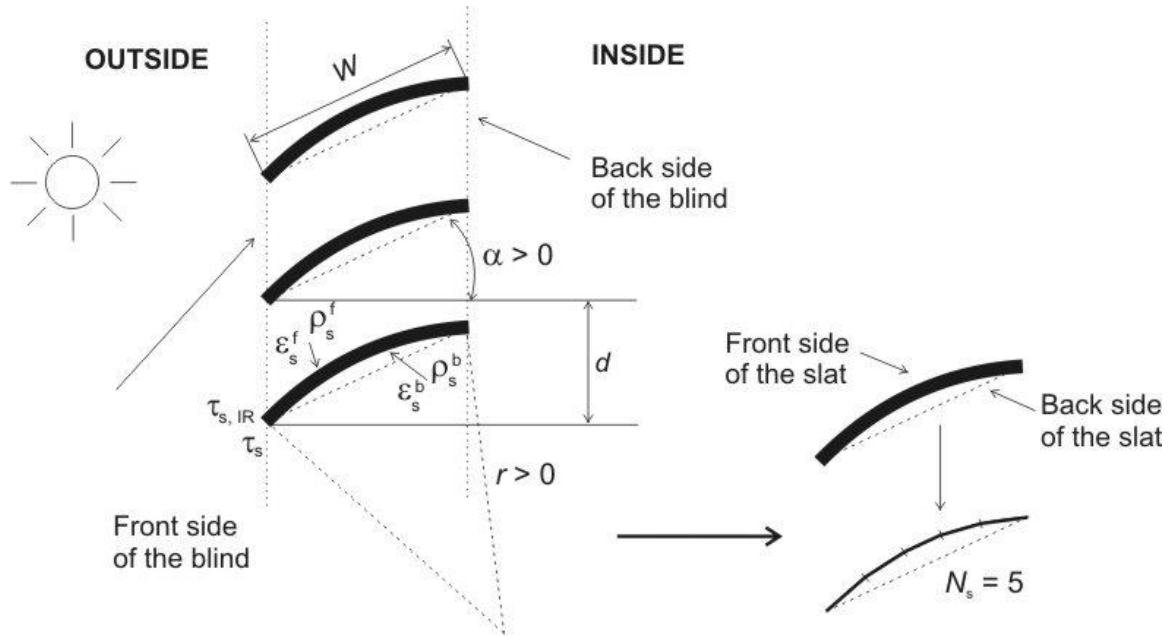
Figure 11-1. Slat geometry and optical properties

11.1.1. Slat Geometry Data

Figure 11-1 describes the slat geometry data which defines the geometry of the Venetian blind. It shows a 2-D cross-section of the slats, perpendicular to the plane of the window. It also shows definitions for the "front" and "back" side of the Venetian blind, as well as for the "front" and "back" surface of each slat, which will be used throughout this document.

Table 11-1 shows definitions and ranges for all input parameters needed for Venetian's calculations.

Table 11-1. Definition of Terms for Venetian Blinds

Type of data	Designator	Description	Unit	Limitations
Slat geometry data	W	Width of the slat (without curvature)	m	$W > 0$
	d	Distance between adjacent slats	m	$d > 0$
	a	Slat tilt angle	°	$-90° \leq \alpha \leq 90°$
	r	Radius of slat curvature	m	$r > W / 2$
	N_{seg}	Number of slat segments		$N_s > 0$
Slat material properties	ρ_s^f	Front reflectance		$0 < \rho_s^f < 1$
	ρ_s^b	Back reflectance		$0 < \rho_s^b < 1$
	τ_s	Transmittance		$0 < \tau_s < 1$
	ε^f	Front emissivity FIR		$0 < \varepsilon^f < 1$
	ε^b	Back emissivity FIR		$0 < \varepsilon^b < 1$

	τ_{IR}	Transmittance FIR		$0 < \tau_{IR} < 1$
	N_θ	Number of angles θ		$N_\theta > 0$
Angle coordinates	θ_i	Array of θ values $(i = 1, \ldots, N_\theta)$	o	$0° \leq \theta_i < 90°$
	$N_{\varphi,i}$	Number of φ angles for each θ_i		
	φ_i	Array of φ values for each θ_i	o	$0° \leq \varphi_i < 360°$

The slat tilt angle α has positive values for the slat configuration shown in Figure 11-1 (the dashed line "above horizon"), and negative values for configurations in which the cross-section of the slat lies below the defined horizontal line. The value $\alpha = 0$ corresponds to horizontal slats (an open blind). For describing flat slats, the curvature radius $r = 0$ is used. The curvature radius r can have both positive and negative values. A positive r corresponds to a curved slat, such as the one in Figure 11-1 , i.e. configuration in which the slats are curved towards the outside, and a negative r means that the slats are curved towards the inside. For the purpose of the calculations, slats are divided into N_{seg} smaller segments, where more segments provide better accuracy. For curved slats, the cross-section is treated as piece-wise linear, with N_{seg} linear segments (see Figure 11-1). The optimal number of slats was determined to be $N_{seg} = 5$, which gives a good compromise between accuracy and the number of calculations.

11.1.2. Properties of Slat Material

Slat material properties are divided into two groups: **SOL** properties (used for calculations in the SOL range, covering wavelengths from 0.3 μm to 2.5 μm) and **FIR** properties, used for calculations in the far infra-red range, covering wavelengths from 2.5 μm to 50 μm).

SOL properties of the slat are the transmittance of the slat – τ_s , and the reflectance of the slat at the front and back surface of the slat (Figure 11-1) – ρ_s^f and ρ_s^b , respectively. SOL properties are normally given for discrete values of wavelengths, providing spectral distribution.

FIR properties are the FIR transmittance of the slat material in the FIR range – τ_{IR} , emissivity at the front surface and at the back surface of the slat in FIR range – ε^f and ε^b , respectively. FIR properties are normally prescribed for a single band covering the entire FIR range.

11.1.3. Definition of Angle Coordinates

Figure 11-2 shows two coordinate systems: xyz (we will refer to it as a "forward" system) and $x^r y^r z^r$ (a "reversed" or "reflected" system).
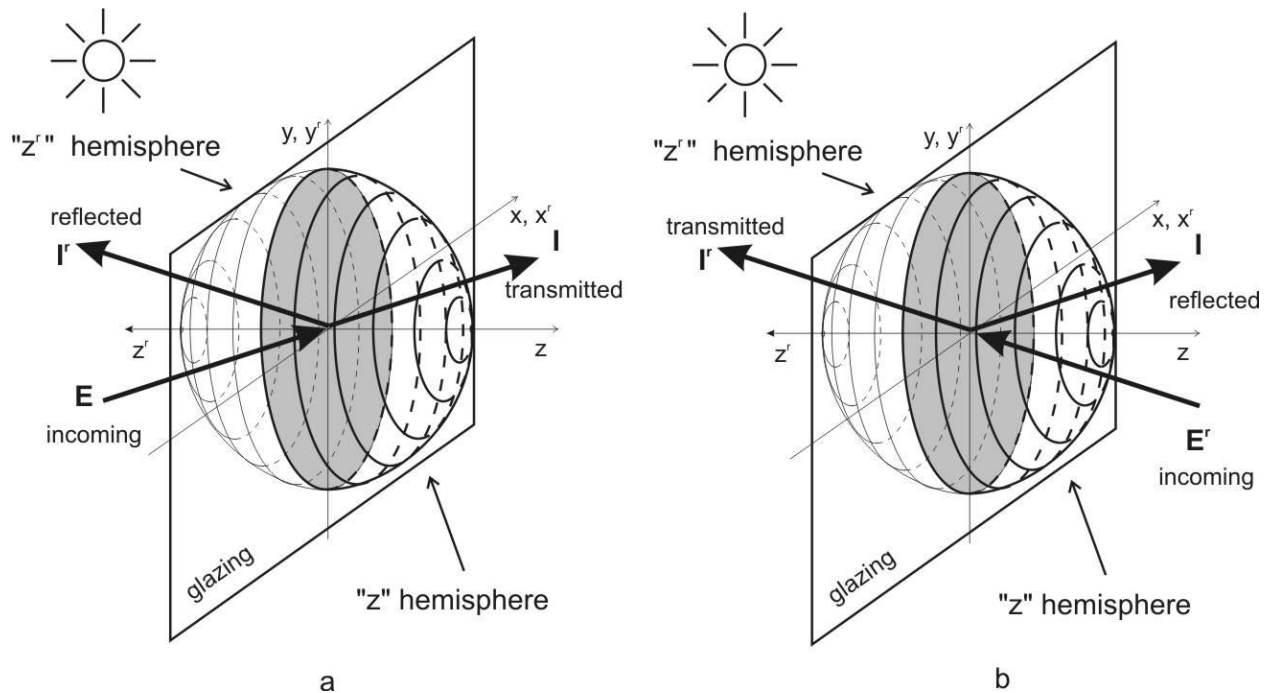
Figure 11-2. Two hemispheres, with corresponding coordinate systems

Axis *z* points towards the indoor side, while axis *z*^{r} points towards the outdoor side. These two axes define two hemispheres. All directions that correspond to radiation that travels forward ("left-to-right" with regards to the Venetian blind, where 'left' is outdoor side and 'right' is indoor side) are defined in the *xyz* coordinate system, using "*z*" hemisphere (incident and transmitted radiation – *E* and *I* in Figure 11-2a, or reflected radiation *I* in Figure 11-2b), and directions that correspond to backward-going radiation ("right-to-left" or toward the outdoor side) are defined in the reflected *x*^{r}*y*^{r}*z*^{r} coordinate system, using "*z*^{r}" hemisphere (reflected radiation *I*^{r} in Figure 11-2a, or incident and transmitted radiation *E*^{r} and *I*^{r} in Figure 11-2b).
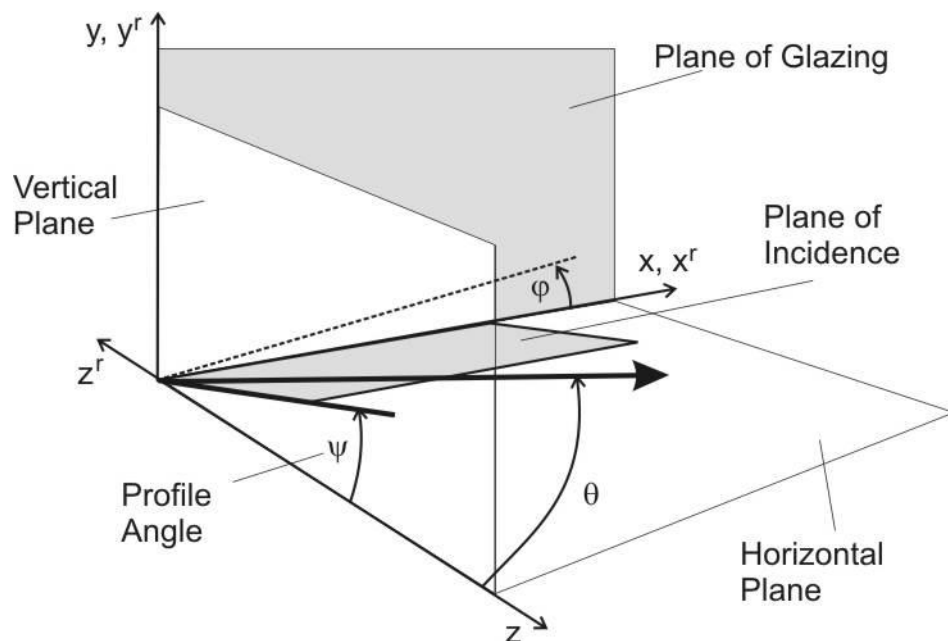
Figure 11-3. Angles definitions – forward-going light
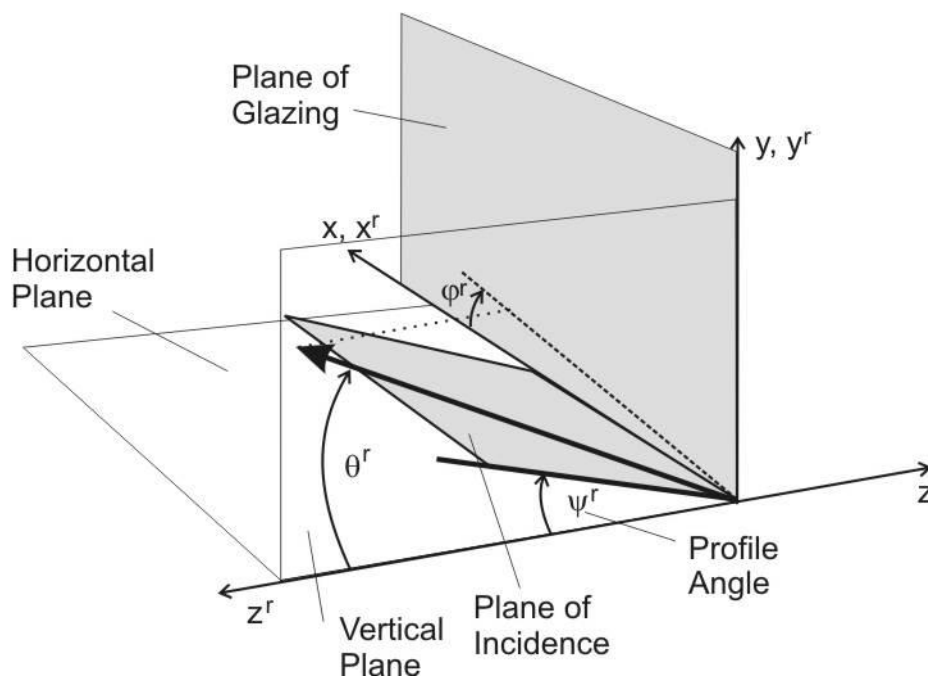
Figure 11-4. Angles definitions – backward-going light

Directions of interest are defined using angular coordinates θ (latitude angle) and φ (azimuth angle) for forward-going radiation (Figure 11-3), and θ^r and φ^r for backward going radiation (Figure 11-4). Latitude angle θ is the angle between the z axis and the direction of interest, φ is the angle between the *x* axis and the *x0y* projection of the direction of interest. Angle θ^r is the angle between the z^r axis and the direction of interest, and angle φ^r is in fact equal to φ, because the *x* and *y* axes are the same in both coordinate systems. To illustrate this: $\theta = 0^\circ$ lies on the z axis; all directions defined as ($\theta > 0^\circ$, $\varphi = 0^\circ$) lie in the horizontal (*x0z*) plane; all directions defined as ($\theta > 0^\circ$, $\varphi = 90^\circ$) lie in the vertical (*y0z*) plane, etc. Values of θ and φ are defined within following limits:

$$0° \le \theta < 90°$$
$$0° \le \varphi < 360°$$

[11–1]

The same restrictions apply to θ^r and φ^r.

Figure 11-5 shows an example with directions of interest in the planar projection of the "*z*" hemisphere in the *x0y* plane, with the *z* axis pointing towards the viewer. The diameters of the circles representing θ angles are growing with the θ value. The value of angle φ grows in a positive (counter-clockwise) direction. Numbers 1 – 49, shown in Figure 11-5, correspond to a set of pre-defined bins, defined by 7 θ angles and 8 φ angles. This set of 49 bins has been given only as an example to illustrate the concept, since full angular set consists of 145 bins. In this example, direction 15 (or D_{15}) is defined as ($\theta_{15} = 45^\circ$, $\varphi_{15} = 225^\circ$). For backward directions, Figure 11-5 can also be used: axes x^r and y^r are oriented the same as axes *x* and *y*, and axis z^r points away from the viewer. In this frame of reference, the numbers in Figure 11-5 correspond to backward-going directions.
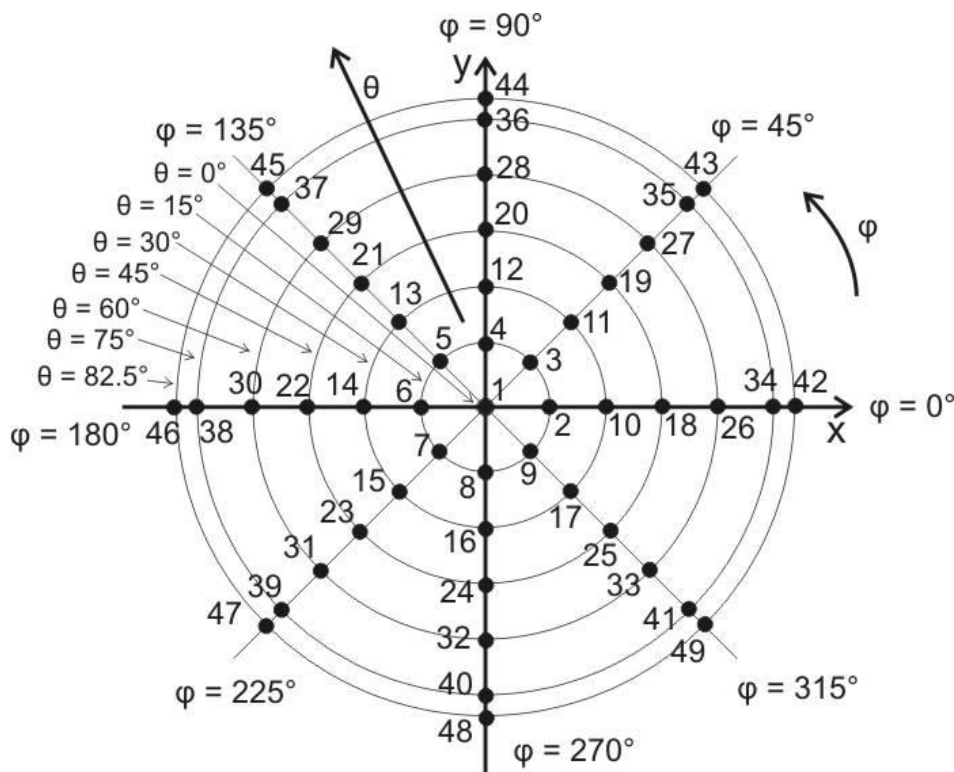
Figure 11-5. Projection of "z" hemisphere in x0y plane, viewed from the indoor side

Each direction *i*, in the forward or reversed coordinates, is determined by its angular coordinates, as (θ_i, φ_i) or $(\theta_i^r, \varphi_i^r)$, where i = 1, … , N_{dir} (number of directions).

The calculations for Venetian blinds are essentially done in 2-D space, ignoring edge effects in the x and y directions. The transition from 3D to 2D space is carried out through the introduction of profile angles ψ (for forward-going radiation) and ψ^r (for backward-going radiation). The profile angle is the angle between the plane of incidence and the horizontal plane, when projected on a vertical plane. Profile angles for forward- and backward-going directions are shown in Figure 11-3 and Figure 11-4, respectively. The connection between angular coordinates and profile angle in general is given by:

$$\tan\psi = \sin\varphi \cdot \tan\theta$$

[11–2]

One of the consequences of using angular coordinates defined in two coordinate systems, as shown in Figure 11-3 and Figure 11-4, is that incident directions are being defined in the "z" hemisphere. For example, the incident direction coming from the outdoor side from above the horizontal plane will actually be defined in the "z" hemisphere. Therefore, the associated profile angle for this direction, calculated using equation *[11–2]* will have a negative value. For incident radiation, the profile angles will be defined as:

$$\psi_i = -\arctan(\sin\varphi_i \cdot \tan\theta_i)$$
$$\psi_i^r = -\arctan(\sin\varphi_i^r \cdot \tan\theta_i^r)$$

[11–3]

Where ψ_i is the profile angle of the i-th incident direction for forward-going radiation, and ψ_i^r is the profile angle of the i-th incident direction, for backward-going radiation.

For outgoing angles, the profile angles will be defined as:

$$\psi_j = \arctan\left(\sin\varphi_j \cdot \tan\theta_j\right)$$
$$\psi_j^r = \arctan\left(\sin\varphi_j^r \cdot \tan\theta_j^r\right)$$

[11–4]

where ψ_j is the profile angle of the j-th outgoing direction for forward-going radiation, and ψ_j^r is the profile angle of the j-th outgoing direction, for backward-going radiation.

All 2D calculations are performed using these profile angles, and the results are stored in the resulting bi-directional matrices (BTDF/BRDF matrices) in places that correspond to the particular (θ, φ) bin and its associated profile angle.

Figure 11-6 shows examples of incident and outgoing profile angles, for forward- and backward-going radiation.
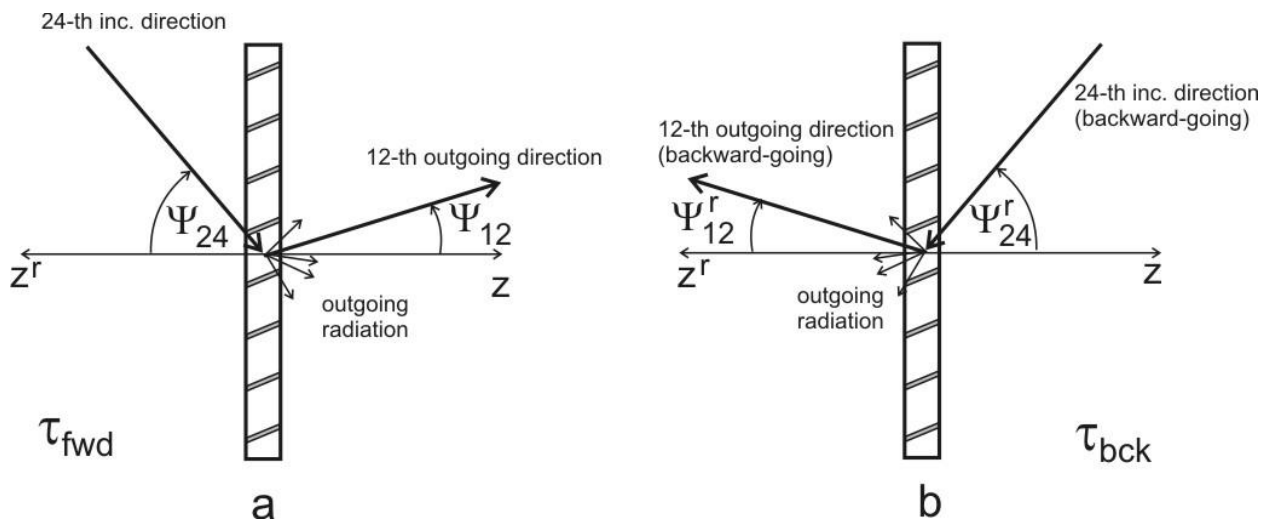
Figure 11-6. Profile angles for incident and outgoing light [Note that particular incident and outgoing directions (i.e., 24ᵗʰ incident and 12ᵗʰ outgoing directions) are given for illustrative purposes as an example]

11.1.4. Irradiance and Outgoing Radiance in 2-D Space

All incident and outgoing directions are defined in 3-D space using angular coordinates (θ, φ). However, incident irradiance and outgoing radiance can be calculated for actual 3-D directions based on corresponding profile angles, ψ, thus allowing all calculations to be essentially performed in 2-D space, using vertical cross-section of the Venetian blind, as indicated in Section 11.1.3.

Bi-directional scattered properties are defined with assumed unit irradiance at the plane of glazing (Figure 11-7, Entry point). For a given incident direction *i*, irradiance at a flat segment *p* of the slat is given by:

$$E_{p,i} = \frac{1}{\cos\theta_i} \left| \left(\mathbf{s}_i \cdot \mathbf{n}_p\right)\right| \cdot \frac{A_p'}{A_p}$$

[11–5]

where:

$\mathbf{s}_i$ = unit vector of incident direction i

$\mathbf{n}_p$ = normal vector for segment p

A_p = area (length in 2D) of segment p

A_p' = irradiated area (length in 2D) of segment p

$\dfrac{1}{\cos\theta_i}$ - flux of incident radiation, coming from direction i, which results in unit irradiance at the front side of the blind

Vector $\mathbf{s}_j$ is a 3D vector, defined by θ and φ angles of the incident direction j. However, the two dot products in equation *[11–5]* can be rearranged:

$$\frac{1}{\cos\theta_i}\cdot\left|\left(\mathbf{s}_i\cdot\mathbf{n}_p\right)\right| = \frac{1}{\cos\theta_i}\left(\cos\beta_p\sin\theta_i\sin\varphi_i - \sin\beta_p\cos\theta_i\right) =$$
$$= \cos\beta_p\tan\theta_i\sin\varphi_i - \sin\beta_p = \cos\beta_p\tan\psi_i - \sin\beta_p \qquad\qquad [11\text{–}6]$$

where β_p is the angle between segment normal $\mathbf{n}_p$ and y axis (which is equal to tilt angle of segment p with respect to z axis), and ψ_i is the profile angle of incident direction with respect to the z^r axis (Figure 11-8). Therefore, equation *[11–5]* has an equivalent 2D form:

$$E_{p,i} = (\cos\beta_p\tan\psi_i - \sin\beta_p)\cdot\frac{A'_p}{A_p} \qquad\qquad [11\text{–}7]$$
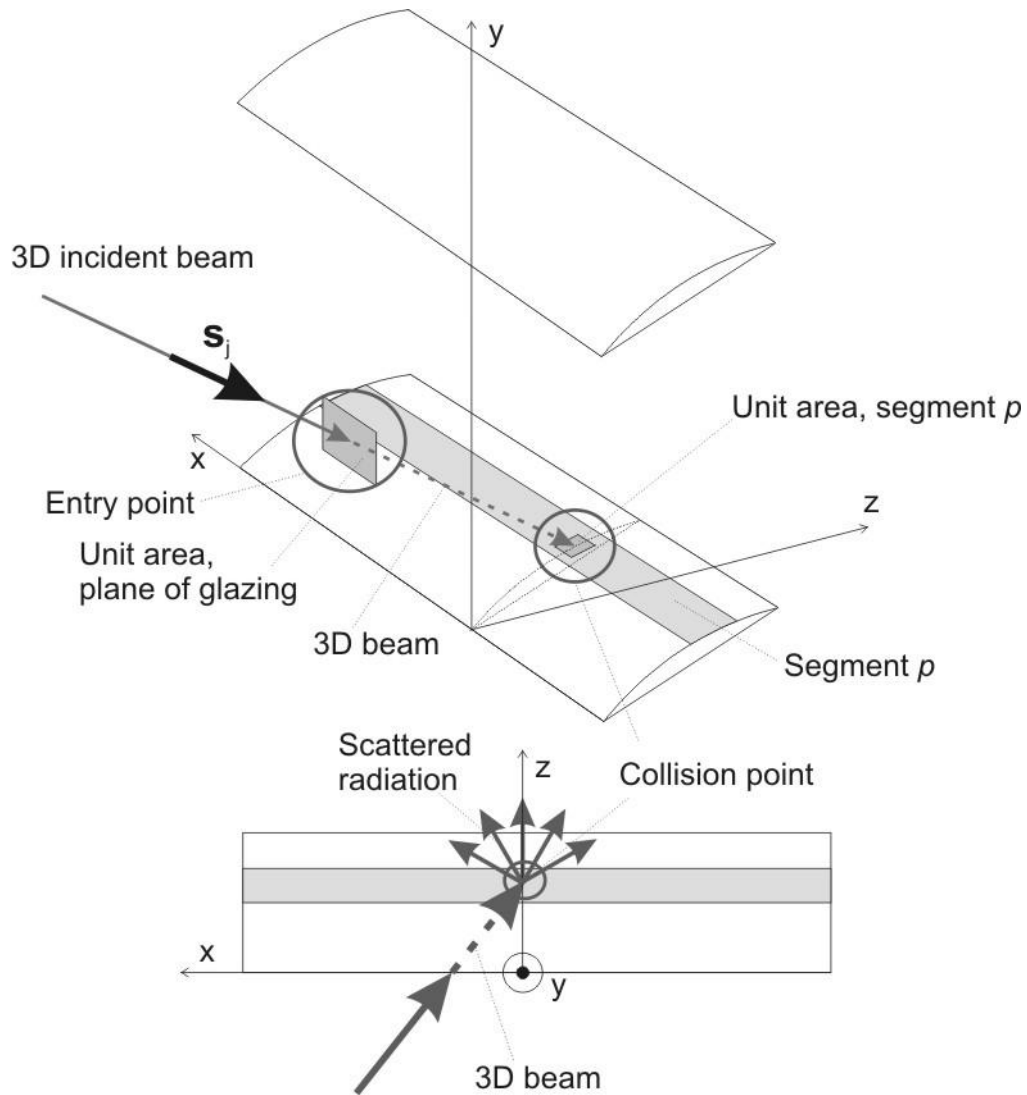
Figure 11-7. 3D representation and top view of incident radiation beam
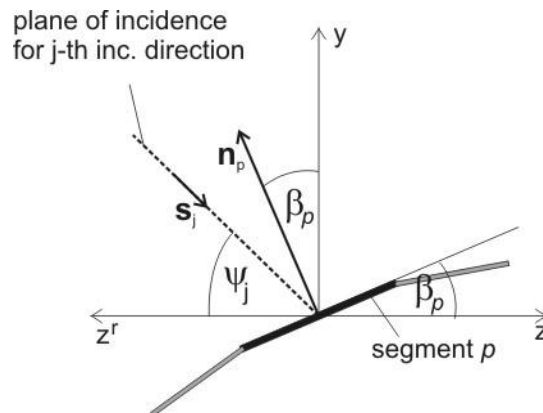

Figure 11-8. Angles in vertical plane used in calculation of irradiance

An irradiated segment is assumed to emit energy equally in each direction (which is the basic assumption in a purely diffuse model). For segment p, the total emitted radiosity is $J_{p,i}$ (Figure 11-9). Outgoing radiance, which

is a result of the incident radiation coming from the incident direction i is given as $\dfrac{J_{p,i}}{\pi}$. Radiant intensity $\iota_{p,j}$ (radiant energy transmitted per unit time and per unit solid angle), coming from segment p at outgoing direction j, is given as:

$$\iota_{p,j} = \frac{J_{p,i}}{\pi} \cdot A_p \cdot \left(\mathbf{s}_j \cdot \mathbf{n}_p\right)$$

[11–8]

The total contribution of this segment to outgoing radiance for the outgoing direction k with respect to the plane of the glazing is given by:

$$I_{p,j} = \frac{J_{p,i}}{\pi} \cdot \left(\mathbf{s}_j \cdot \mathbf{n}_p\right) \cdot \frac{1}{\cos\theta_j}$$

[11–9]

where:

$\mathbf{s}_j$ = unit vector of outgoing direction j

$\mathbf{n}_p$ = normal vector for segment p

$J_{p,i}$ = outgoing radiosity emerging from slat segment p, as a result of incident radiation from incident direction i

A_p = area (length in 2D) of segment p

θ_j = latitude angle of outgoing direction j

As shown in the case of irradiance (Eq. *[11–6]*), this formula can be rearranged into a 2D form:

$$I_{p,j} = \frac{J_{p,i}}{\pi} \cdot \left(\cos\beta_p \tan\psi_j - \sin\beta_p\right)$$

[11–10]

where $\mathbf{b}_p$ is the angle between segment normal $\mathbf{n}_p$ and y axis (or tilt angle of segment p), and $\mathbf{y}_j$ is the profile angle of the outgoing direction j with respect to the z axis (Figure 11-9).
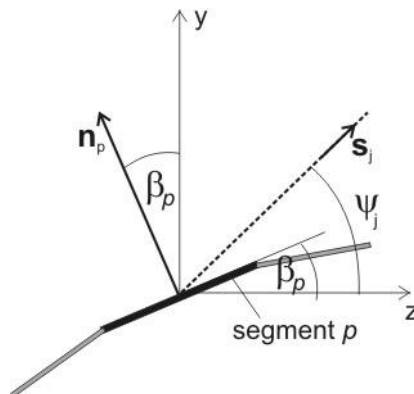
Figure 11-9. Angles in vertical plane used in calculation of outgoing radiance

2D formulas for the calculation of incident irradiances and outgoing radiances are significant because they allow a reduction of calculation iterations, as it is sufficient to carry out a single calculation for all the incident/outgoing directions that have the same combination of profile angles.

11.2. Solar-Optical Mathematical Models for Venetian Blinds

This chapter provides information about the mathematical models used in calculating the solar-optical properties of Venetian blinds. Two different models are presented in this section; a) ISO 15099, Section 7 (ISO 15099) method and b) Bi-Directional method.

The ISO 15099 method calculates integrated properties for transmittance, front reflectance and back reflectance. The Bi-Directional method calculates transmittance and front and back reflectance for each incident and outgoing angle (when integrated over all angles, the Bi-Directional method should produce same integrated values as ISO 15099 method). In the FIR range, which will be presented in Section 11.4, both methods calculate the integrated IR transmittance and front and back emissivity for a single band comprising the entire FIR range.

11.2.1. Basic Naming Conventions

Quantities, symbols, directions and their notation are presented in *Table 11-2*. Directions of interest are shown in Figure 11-10.

Figure 11-10. Incident irradiance, reflected and transmitted radiance, for 2 directions of incident radiation: a) forward-going (FWD) and b) backward-going (BCK)

Table 11-2. Symbols and indexes used

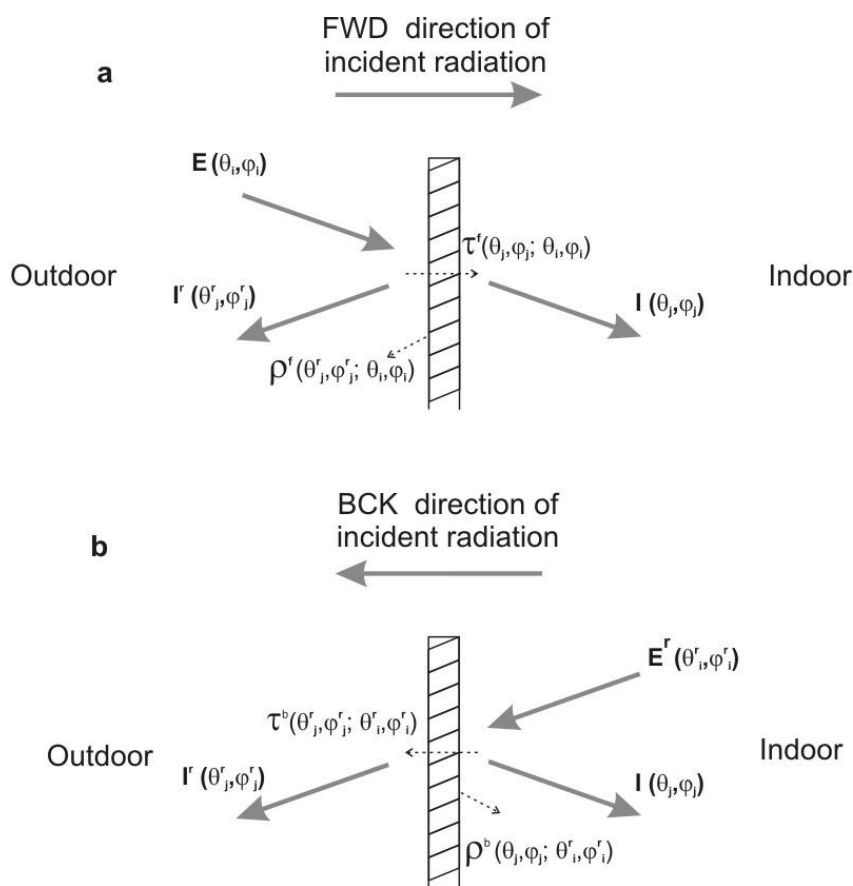| Symbol (index)	Meaning
r	"in reversed coordinates", used for vector quantities defined in $x^r y^r z^r$ system (in z^r hemisphere)
f	index indicating front side of the slat segment and/or Venetian blind
b	index indicating back side of the slat segment and/or Venetian blind
E	incident irradiance – for FWD going light only; in ISO model, E denotes total irradiance arriving at a slat segment
E^r	incident irradiance in reversed coordinates – for BCK going light only
I	radiance – always in FWD (L2R) direction: transmitted part of E reflected part of E^r
I^r	radiance – always in BCK (R2L) direction: transmitted part of E^r reflected part of E ;
J	radiosity

11.2.2. ISO 15099 Method

ISO 15099, Section 7 outlines methods for calculating the optical properties of Venetian blinds (ISO 2003). These methods are based on the following assumptions:

1. Diffuse radiation transmitted or reflected by the solar shading device is assumed to remain diffuse ("dif-dif" transmission/reflection).

2. Beam radiation transmitted or reflected by the solar shading device is considered in two parts:

   - undisturbed part (specular transmission – "dir-dir" transmission)
   - disturbed part, approximated as anisotropic diffuse (Lambertian – "dir-dif" transmission/reflection)

This section describes in detail how all three types of optical properties ("dir-dir", "dir-dif" and "dif-dif") for the blind are calculated. These methods can be used both for flat and curved Venetian blind slats.

11.2.2.1. Dir-Dir Portion

Dir-Dir transmittance is defined as the portion of the incident beam light that goes undisturbed through the shading device. It can be defined as (Figure 11-11 – FWD going incident beam):

$$\tau_{dir-dir} = \frac{J_{dir-dir}}{J_{inc}}$$

[11–11]

where J_{inc} is the incident external radiosity, and $J_{dir-dir}$ is the part of the incident radiation that reaches the back side (an imaginary surface) of the blind without interaction with the slat material (i.e., the undisturbed part).
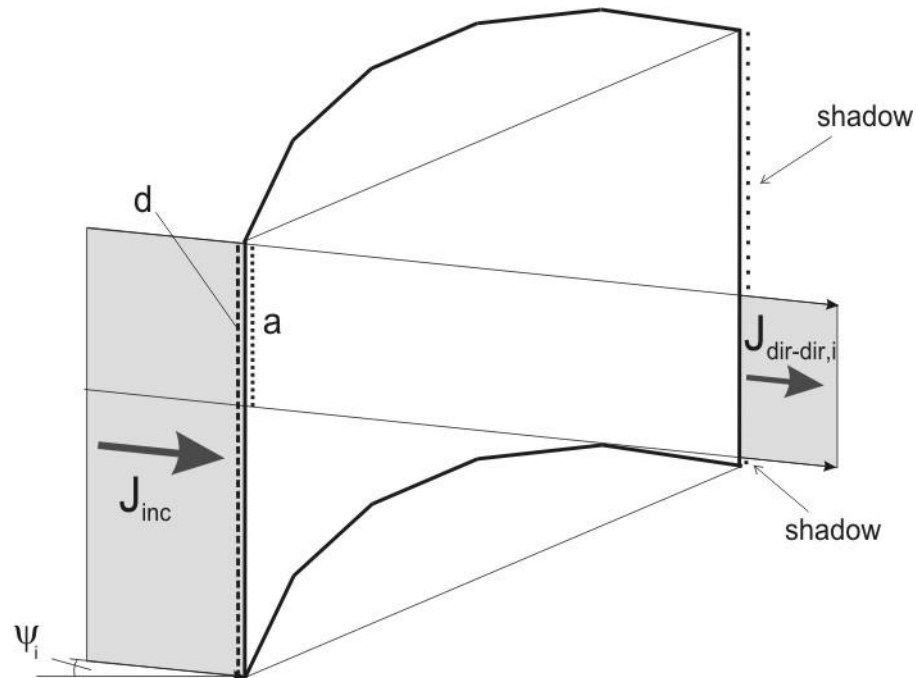
Figure 11-11. Direct-direct transmission

The Dir-Dir portion depends on the profile angle of the incident light beam. Following the notation from Figure 11-11, the Dir-Dir portion of the transmittance for the incident direction i can be expressed geometrically as:

$$\tau_{dir-dir,i} = \frac{a}{d} \cdot \cos \psi_i \qquad\qquad [11-12]$$

where d is the distance between two adjacent slats.

11.2.2.2. Dif-Dif Portion

Dif-Dif transmittance and reflectance are used in cases where the incident and outgoing radiation is diffuse. It can be defined as the ratio of the outgoing and incident radiant energy. Figure 11-12 explains Dif-Dif transmittance and reflectance in general, for forward-going incident radiation:

$$\tau_{dif-dif} = \frac{J_{out}}{J_{inc}}, \quad \rho_{dif-dif} = \frac{J_{out}^r}{J_{inc}} \qquad\qquad [11-13]$$

where J_{inc} is the incident external radiosity, J_{out} and J^r_{out} are portions of the incident radiation that leave from the back and the front side of the blind, respectively, after a series of diffuse Lambertian reflections off the slat surfaces.
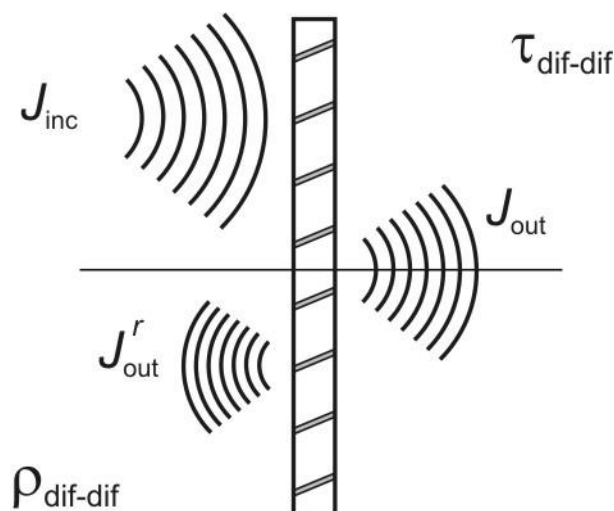
Figure 11-12. Dif-Dif Propagation

If a single slat enclosure, defined by the two adjacent slats, is considered, the diffuse transmittance at the front side can be defined as the ratio of the outgoing radiance Jout, leaving the back opening of the enclosure, and the incident irradiance E reaching the front opening of the enclosure (Figure 11-13). If unit irradiance at the front side of the blind is assumed, the transmittance becomes equal to the outgoing radiance, leaving the back opening.
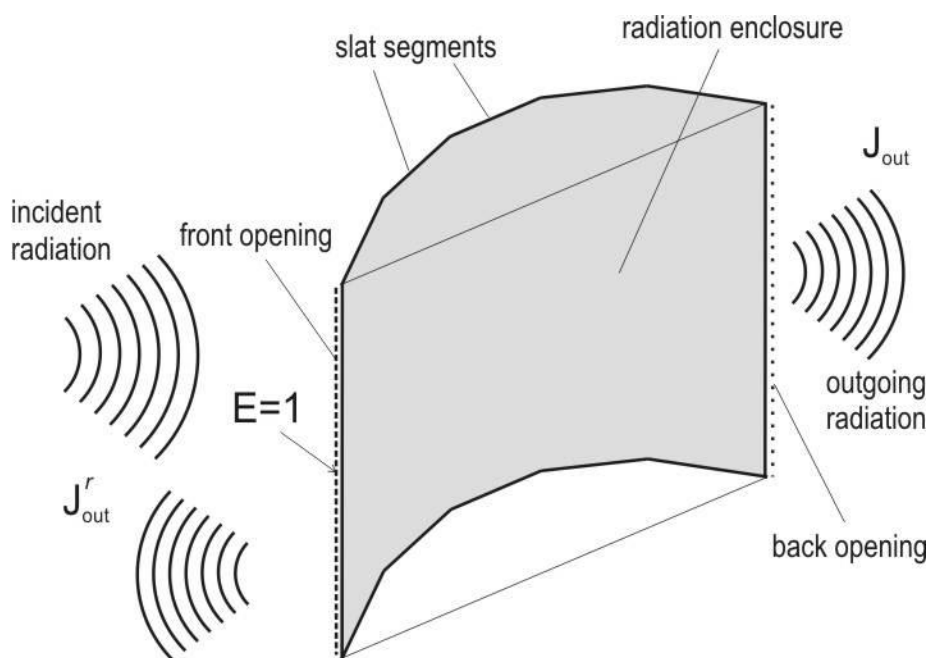
Figure 11-13. Radiation enclosure formed by two adjacent slats

Similarly, diffuse reflectance at the front side can be expressed as Jrout, outgoing radiance, leaving the front opening.

The radiation enclosure shown in Figure 11-13 (also referred to as "slat enclosure") is formed by the flat segments of the slats, and virtual segments that represent the front and back opening. Slat surfaces are assumed to scatter incident radiation diffusely, and have uniform temperatures. For such an enclosure, a set of energy balance equations is formed in order to calculate the outgoing radiance at front and back openings.

The procedure is based on a model, shown in Figure 11-14, which considers two adjacent slats divided into Nseg equal parts (default Nseg = 5) and forming "slat enclosure", together with the front opening ("segment" 0) and the back opening ("segment" Nseg+1, i.e. segment 6). Every segment may have different surface optical properties, which is given through different values of surface reflectance and transmittance: ρf,i and ρb,i (the diffuse reflectance of the material at the front and back side of the slat segment i) and τi (the diffuse transmittance of the material of slat segment i). "Special" segments – front and back opening – are defined with zero reflectances and unit transmittance: τ0 = τ6 = 1, ρf,0 = ρb,0 = ρf,6 = ρb,6 = 0.
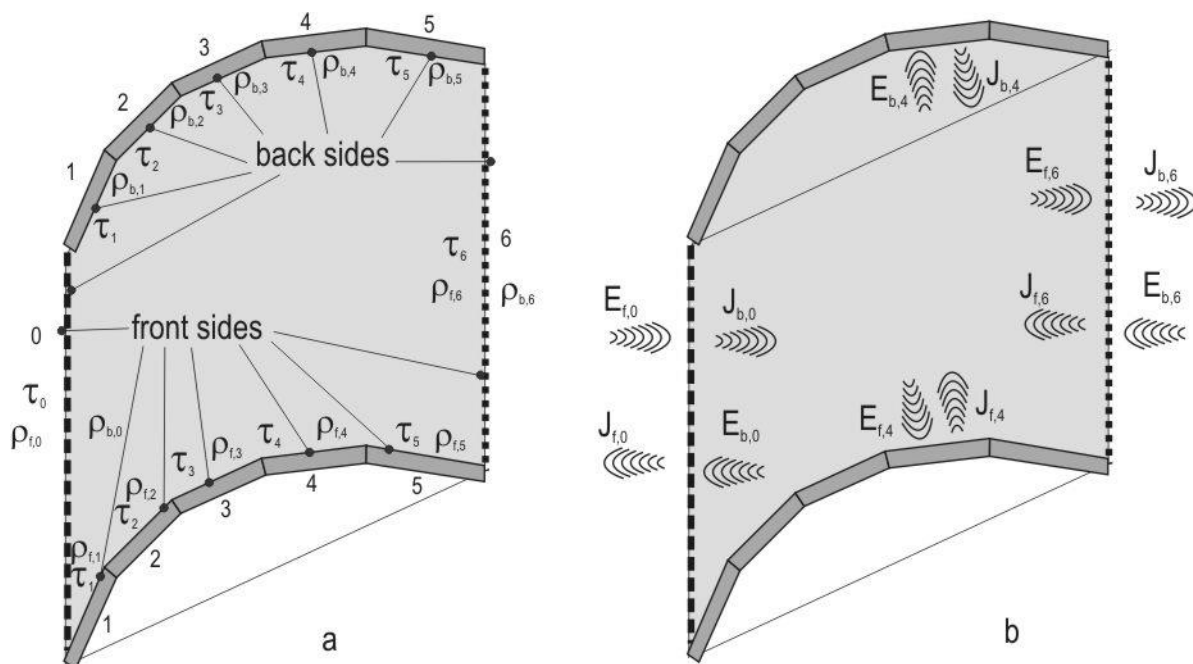
Figure 11-14. Segments of the enclosure and their indexing

The following naming convention will be used in the energy balance equations (Figure 11-14):

f = indicates front surface of enclosure segment

b = indicates back surface of enclosure segment

Jf,i = radiosity leaving the front surface of enclosure segment i

Jb,i = radiosity leaving the back surface of enclosure segment i

Ef,i = irradiance at the front surface of enclosure segment i

Eb,i = irradiance at the back surface of enclosure segment i

Using this notation, the radiant outgoing fluxes (i.e. radiosities) – Jf,i and Jb,i for each enclosure segment, is given by the following set of equations:

$$J_{f,0} = \rho_{f,0}E_{f,0} + \tau_{b,0}E_{b,0} = E_{b,0} \quad (\rho_{f,0} = 0; \tau_{b,0} = 1)$$

[11–14]

$$J_{f,1} = \rho_{f,1}E_{f,1} + \tau_{b,1}E_{b,1}$$

[11–15]

$$J_{f,2} = \rho_{f,2}E_{f,2} + \tau_{b,2}E_{b,2}$$

[11–16]

$$J_{f,3} = \rho_{f,3}E_{f,3} + \tau_{b,3}E_{b,3}$$

[11–17]

$$J_{f,4} = \rho_{f,4}E_{f,4} + \tau_{b,4}E_{b,4}$$

[11–18]

$$J_{f,5} = \rho_{f,5}E_{f,5} + \tau_{b,5}E_{b,5} \tag{11-19}$$

$$J_{f,6} = \rho_{f,6}E_{f,6} + \tau_{b,6}E_{b,6} = E_{b,6} \quad (\rho_{f,6} = 0 \; ; \; \tau_{b,6} = 1) \tag{11-20}$$

$$J_{b,0} = \rho_{b,0}E_{b,0} + \tau_{f,0}E_{f,0} = E_{f,0} \quad (\rho_{b,0} = 0 ; \tau_{f,0} = 1) \tag{11-21}$$

$$J_{b,1} = \rho_{b,1}E_{b,1} + \tau_{f,1}E_{f,1} \tag{11-22}$$

$$J_{b,2} = \rho_{b,2}E_{f,2} + \tau_{f,2}E_{f,2} \tag{11-23}$$

$$J_{b,3} = \rho_{b,3}E_{b,3} + \tau_{f,3}E_{f,3} \tag{11-24}$$

$$J_{b,4} = \rho_{b,4}E_{b,4} + \tau_{f,4}E_{f,4} \tag{11-25}$$

$$J_{b,5} = \rho_{b,5}E_{b,5} + \tau_{f,5}E_{f,5} \tag{11-26}$$

$$J_{b,6} = \rho_{b,6}E_{b,6} + \tau_{f,6}E_{f,6} = E_{f,6} \quad (\rho_{b,6} = 0 \; ; \; \tau_{f,6} = 1) \tag{11-27}$$

It should be noted that, for front transmittance and reflectance, irradiance on the back surface of the boundary of a shading device from the indoor environment – Eb,6 is set to zero (Eb,6 = 0) due to the lack of radiosity from the internal environment. At the same time, irradiance on the front surface of boundary between the shading device and the external environment – Ef,0 is set to 1.

After introducing these assumptions, equations *[11–20]* and *[11–21]* become:

$$J_{f,6} = 0 \tag{11-28}$$

$$J_{b,0} = 1 \tag{11-29}$$

On the other hand, the relation between radiosities from each segment and irradiances at any other segment can be defined by means of view factors. The view factor represents a fraction of energy leaving one surface, that arrives at a second surface.

For surfaces with finite area, view factors are generally defined by:

$$F_{i \to j} = \frac{1}{A_i} \int\limits_{A_i} \int\limits_{A_j} \frac{\cos\theta_i \cos\theta_j}{\pi S^2} dA_i dA_j \tag{11-30}$$

where S is a distance from a point on surface Aj to a point on surface Ai. The angles θ_j and θ_k are measured between the line S and the normal to the surface. $F_{i \to j}$ represents "view factor between segments i and j".

Figure 11-15 illustrates terms from equation *[11–30]*, for two surfaces in a radiation enclosure:
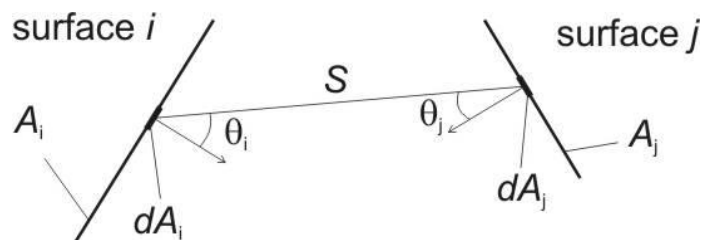
Figure 11-15. Cross section of two segments in radiation enclosure

View factors between two flat segments in a 2-D radiation enclosure can be calculated based on lengths in a vertical cross-section of the enclosure, according to the *cross-string* rule:

$$F_{i \to j} = \frac{r_{12} + r_{21} - (r_{11} + r_{22})}{2L_i}$$

[11–31]

where L_i is the length of segment i, and r are distances between endpoints of segments i and j.
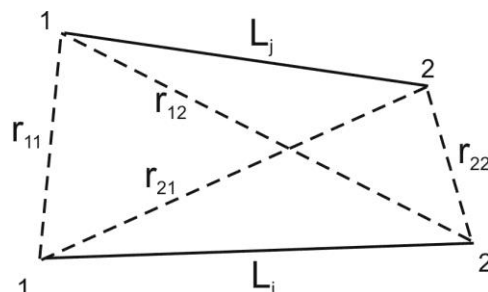
Figure 11-16. Illustration of the Cross String Rule for Calculating View Factors

Two view factors exist for two given segments i and j: view factor from i to j - $F_{i \to j}$, and view factor from j to

i – $F_{j \to i}$. These two values are related as:

$$L_i \cdot F_{i \to j} = L_j \cdot F_{j \to i}$$

[11–32]

In case there is a shadowing, caused by a third, blocking surface (as in Figure 11-17), the view factor between two segments can be calculated by dividing each segment into a finite number n of sub-segments. If a pair of sub-segments p and q (where one sub-segment belongs to segment i, and the other belongs to segment j) are mutually visible, which means that line rpq (which is a line between midpoints of these sib-segments) does not intersect the blocking segment (Figure 11-17a), the view factor between p and q is calculated using equation *[11–30]*. Otherwise, $F_{p \to q}$ is set to zero (Figure 11-17b). This is repeated for each pair of sub-segments belonging to segments i and j. Finally, the view factor between segments i and j is obtained as:

$$F_{i \to j} = \sum_{p=1}^{n} \sum_{q=1}^{n} F_{p \to q}$$

[11–33]
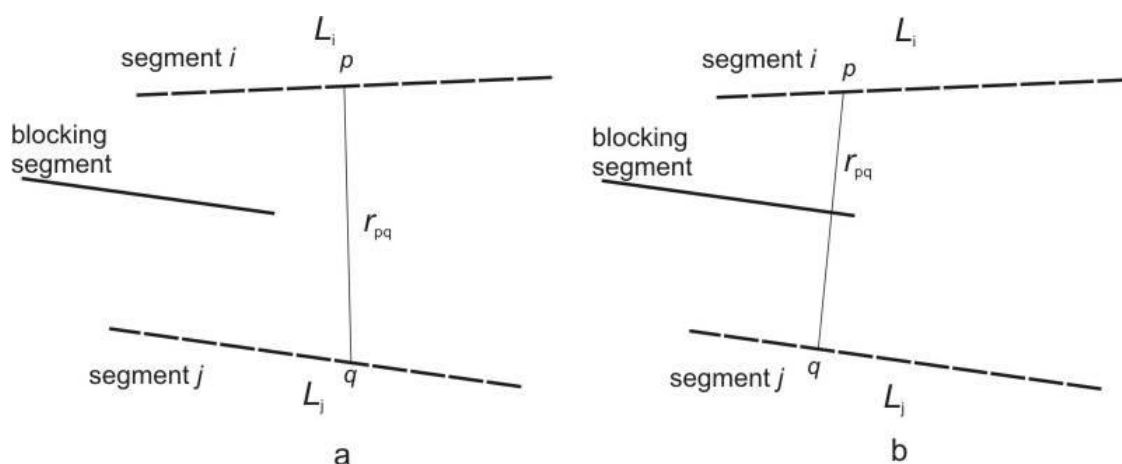
Figure 11-17. Third surface shadowing: a) "un-shadowed" sub-segments, b) "shadowed" sub-segments

In the case of a slat enclosure, as shown in Figure 11-14, the view factors between segment surfaces are given as:

$$F_{a,b \to c,d} \qquad\qquad [11-34]$$

where a and c indicate the front (f) or back (b) side of each segment, and b and d are the indices of the two segments. For example, the view factor between the back side of segment 1 of the upper slat, and the front side of segment 3 of the lower slat is given as $F_{f,1 \to b,3}$. Non-zero view factors exist only between segment surfaces that are facing the interior of the enclosure. View factors from the front side of segment 0 (front opening segment) to any other segment of the enclosure are zero: $F_{f,0 \to f,i} = F_{f,0 \to b,i} = 0$. The same applies to the back side of segment 6 (the back opening segment): $F_{b,6 \to f,i} = F_{b,6 \to b,i} = 0$.

After introducing view factors, irradiances – Ef,i and Eb,i can be defined as:

$$E_{f,0} = 1 \qquad\qquad [11-35]$$

$$E_{f,1} = J_{f,0}F_{f,0\to f,1} + J_{f,1}F_{f,1\to f,1} + ... + J_{f,6}F_{f,6\to f,1} + J_{b,0}F_{b,0\to f,1} + J_{b,1}F_{b,1\to f,1} + ... + J_{b,6}F_{b,6\to f,1} \quad [11-36]$$

$$E_{f,2} = J_{f,0}F_{f,0\to f,2} + J_{f,1}F_{f,1\to f,2} + ... + J_{f,6}F_{f,6\to f,2} + J_{b,0}F_{b,0\to f,2} + J_{b,1}F_{b,1\to f,2} + ... + J_{b,6}F_{b,6\to f,2} \quad [11-37]$$

$$E_{f,3} = J_{f,0}F_{f,0\to f,3} + J_{f,1}F_{f,1\to f,3} + ... + J_{f,6}F_{f,6\to f,3} + J_{b,0}F_{b,0\to f,3} + J_{b,1}F_{b,1\to f,3} + ... + J_{b,6}F_{b,6\to f,3} \quad [11-38]$$

$$E_{f,4} = J_{f,0}F_{f,0\to f,4} + J_{f,1}F_{f,1\to f,4} + ... + J_{f,6}F_{f,6\to f,4} + J_{b,0}F_{b,0\to f,4} + J_{b,1}F_{b,1\to f,4} + ... + J_{b,6}F_{b,6\to f,4} \quad [11-39]$$

$$E_{f,5} = J_{f,0}F_{f,0\to f,5} + J_{f,1}F_{f,1\to f,5} + ... + J_{f,6}F_{f,6\to f,5} + J_{b,0}F_{b,0\to f,5} + J_{b,1}F_{b,1\to f,5} + ... + J_{b,6}F_{b,6\to f,5} \quad [11-40]$$

$$E_{f,6} = J_{f,0}F_{f,0\to f,6} + J_{f,1}F_{f,1\to f,6} + ... + J_{f,6}F_{f,6\to f,6} + J_{b,0}F_{b,0\to f,6} + J_{b,1}F_{b,1\to f,6} + ... + J_{b,6}F_{b,6\to f,6} \quad [11-41]$$

$$E_{b,0} = J_{b,0}F_{b,0\to b,0} + J_{b,1}F_{b,1\to b,0} + ... + J_{b,6}F_{b,6\to b,0} + J_{f,0}F_{f,0\to b,0} + J_{f,1}F_{f,1\to b,0} + ... + J_{f,6}F_{f,6\to b,0} \quad [11-42]$$

$$E_{b,1} = J_{b,0}F_{b,0\to b,1} + J_{b,1}F_{b,1\to b,1} + ... + J_{b,6}F_{b,6\to b,1} + J_{f,0}F_{f,0\to b,1} + J_{f,1}F_{f,1\to b,1} + ... + J_{f,6}F_{f,6\to b,1} \quad [11-43]$$

$$E_{b,2} = J_{b,0}F_{b,0\to b,2} + J_{b,1}F_{b,1\to b,2} + ... + J_{b,6}F_{b,6\to b,2} + J_{f,0}F_{f,0\to b,2} + J_{f,1}F_{f,1\to b,2} + ... + J_{f,6}F_{f,6\to b,2} \quad [11-44]$$

$$E_{b,3} = J_{b,0}F_{b,0\to b,3} + J_{b,1}F_{b,1\to b,3} + ... + J_{b,6}F_{b,6\to b,3} + J_{f,0}F_{f,0\to b,3} + J_{f,1}F_{f,1\to b,3} + ... + J_{f,6}F_{f,6\to b,3} \quad [11-45]$$

$$E_{b,4} = J_{b,0}F_{b,0\to b,4} + J_{b,1}F_{b,1\to b,4} + ... + J_{b,6}F_{b,6\to b,4} + J_{f,0}F_{f,0\to b,4} + J_{f,1}F_{f,1\to b,4} + ... + J_{f,6}F_{f,6\to b,4} \quad [11-46]$$

$$E_{b,5} = J_{b,0}F_{b,0\to b,5} + J_{b,1}F_{b,2\to b,5} + ... + J_{b,6}F_{b,6\to b,5} + J_{f,0}F_{f,0\to b,5} + J_{f,1}F_{f,1\to b,5} + ... + J_{f,6}F_{f,6\to b,5} \quad [11-47]$$

$$E_{b,6} = 0 \qquad\qquad [11-48]$$

The system of equations *[11-35]*– *[11-48]* defines irradiances (Ef,i and Eb,i), in term of radiosities and associated view factors.

General expressions for the irradiances Ef,i and Eb,i can be derived from the energy balance, shown in equations *[11-36]* – *[11-47]*:

$$E_{f,i} = \sum_{\substack{k=0 \\ k \neq i}}^{N_{seg}+1} J_{f,k}F_{f,k \to f,i} + \sum_{k=0}^{N_{seg}+1} J_{b,k}F_{b,k \to f,i} \qquad\qquad [11-49]$$

$$E_{b,i} = \sum_{\substack{k=0 \\ k \neq i}}^{N_{seg}+1} J_{b,k} F_{b,k \rightarrow b,i} + \sum_{k=0}^{N_{seg}+1} J_{f,k} F_{f,k \rightarrow b,i} \qquad [11-50]$$

where Nseg is the number of slat segments. Note the exclusion of terms for k=i in the left-hand sums in equations *[11–49]* and *[11–50]*. This is done because there is no transfer of radiation if the source surface is the same as the target surface.

Applying expressions for the radiosities Jf,i and Jb,i, given in equations *[11–14]* – *[11–27]*, and substituting them into equations *[11–36]* and *[11–37]*, the irradiances Ef,i and Eb,i become:

$$E_{f,i} = \sum_{\substack{k=0 \\ k \neq i}}^{N_{seg}+1} (\rho_{f,k} E_{f,k} + \tau_{b,k} E_{b,k}) F_{f,k \rightarrow f,i} + \sum_{k=0}^{N_{seg}+1} (\rho_{b,k} E_{b,k} + \tau_{f,k} E_{f,k}) F_{b,k \rightarrow f,i} \qquad [11-51]$$

$$E_{b,i} = \sum_{\substack{k=0 \\ k \neq i}}^{N_{seg}+1} (\rho_{b,k} E_{b,k} + \tau_{f,k} E_{f,k}) F_{b,k \rightarrow b,i} + \sum_{k=0}^{N_{seg}+1} (\rho_{f,k} E_{f,k} + \tau_{b,k} E_{b,k}) F_{f,k \rightarrow b,i} \qquad [11-52]$$

Where the first term in the equation *[11–51]* is the amount of radiant energy, transmitted through the back surface of the lower slat's segment k and reflected from the front surface of that same segment, while the second term in that equation is the amount of radiant energy, transmitted through the front surface of the upper slat's segment k and reflected from the back surface of the same segment, which combined reaches the front surface of the lower slat's segment i. Correspondingly, the first term in equation *[11–52]* is the amount of radiant energy, transmitted through the front surface of the upper slat's segment k and reflected from the back surface of that same segment, while the second term in that equation is the amount of radiant energy, transmitted through the back surface of the lower slat's segment k and reflected from the front surface of the same segment, which combined reaches the back surface of upper slat's segment i. In the example in Figure 11-18, i =2 and k = 4.
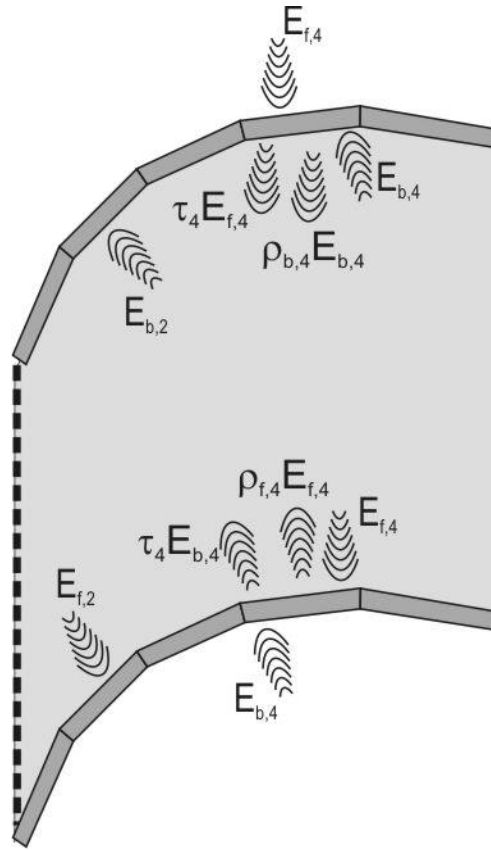
Figure 11-18. Example of Radiation Exchange Between Segments 2 and 4 (equations [11–51] *and* [11–52])

After solving 2 x (N_{seg} + 1) system of equations, expanded from equations *[11–51]* and *[11–52]*, the resulting front transmittance is calculated as:

$$\tau^f_{dif-dif} = \frac{E_{f,6}}{E_{f,0}} = \frac{E_{f,6}}{1} = E_{f,6} \qquad\qquad [11–53]$$

The resulting front reflectance becomes:

$$\rho^f_{dif-dif} = \frac{E_{b,0}}{E_{f,0}} = \frac{E_{b,0}}{1} = E_{b,0} \qquad\qquad [11–54]$$

Note that the results in equations *[11–53]* and *[11–54]* represent Dif-Dif optical properties for FWD case. For BCK case, certain adjustments have to be made. Equations *[11–28]* and *[11–29]* become:

$$J_{f,6} = J_{ex} = 1 \Rightarrow E_{b,6} = 1 \qquad\qquad [11–55]$$

$$J_{b,0} = 0 \qquad\qquad [11–56]$$

After solving the system for BCK case, resulting back transmittance becomes:

$$\tau^b_{dif-dif} = \frac{E_{b,0}}{E_{b,6}} = \frac{E_{b,0}}{1} = E_{b,0} \qquad\qquad [11–57]$$

Resulting BCK reflectance becomes:

$$\rho^{b}_{dif-dif} = \frac{E_{f,6}}{E_{b,6}} = \frac{E_{f,6}}{1} = E_{f,6}$$

[11–58]

11.2.2.3. Dir-Dif Portion

In contrast to the diffuse radiation coming from all directions uniformly in the Dif-Dif portion of radiation, presented in Section 11.2.2.2, Dir-Dif means that there is a "beam" incident radiation source that produces diffuse transmitted and reflected radiance (Figure 11-19). Note that Dir-Dif properties depend on the profile angle of the incident radiation.

Basically, Dir-Dif properties can be obtained using the system of equations defined for the Dif-Dif case. However, since now there is a "beam" input instead of diffuse input, certain modifications have to be made; modifications of view factors between the front side of the front opening segment ("0th" segment) and all other segments within the slat enclosure, in the case of forward-going incident radiation (incident radiation coming from the outdoor environment), and the back opening segment ("Nseg+1st" segment, in the default case, 6th" segment) and all other segments in the slat enclosure, in the case of backward-going incident radiation (the incident radiation coming from the indoor environment).
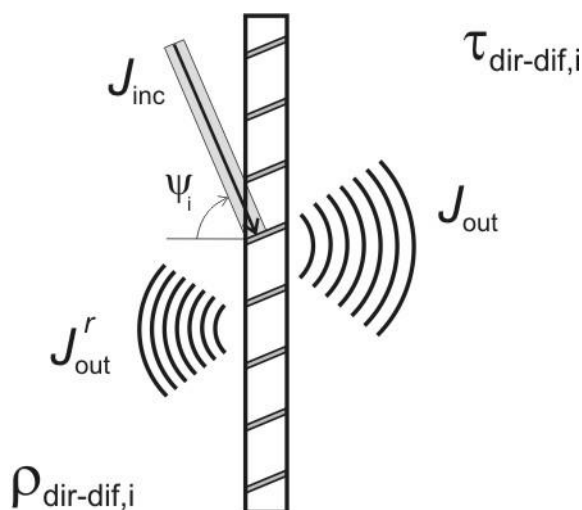
Figure 11-19. Dir-Dif propagation

As in the case of dif-dif propagation, unit irradiance at the front side of the blind is assumed. View factors, used in Equations *[11–51]* and *[11–52]*, which are used for the calculations of Dif-Dif properties will mostly be used here as well since from the moment after direct beam hits any surface, it is reflected fully diffusely. The exception to this are imaginary surfaces 0 and Nseg+1 (the front and back opening of the blind), since they represent the beam radiation source at the outer side and the diffuse view factors between the front surface of segment 0 and other slat segments in the case of forward-going incident radiation (or the back surface of segment 6 and other slat segments in the case of backward-going incident radiation) cannot be used. Instead, it is necessary to determine which part of the incident beam radiation hits each slat segment, and use those values instead of the corresponding view factors. We will call these quantities "Beam view factors", or BF.

Figure 11-20 shows an example of 5 segment slats (the default). Incident radiation hits the front sides of slat segments 1, 2 and partially 3 (dotted line). The BF for those surfaces are defined as fractions of the incident radiation that hit the segment of interest. In our example, the BF of the aforementioned slat segment surfaces are equal to the ratio of lengths of b1, b2 and b3, respectively (dashed lines) to the slat distance d.
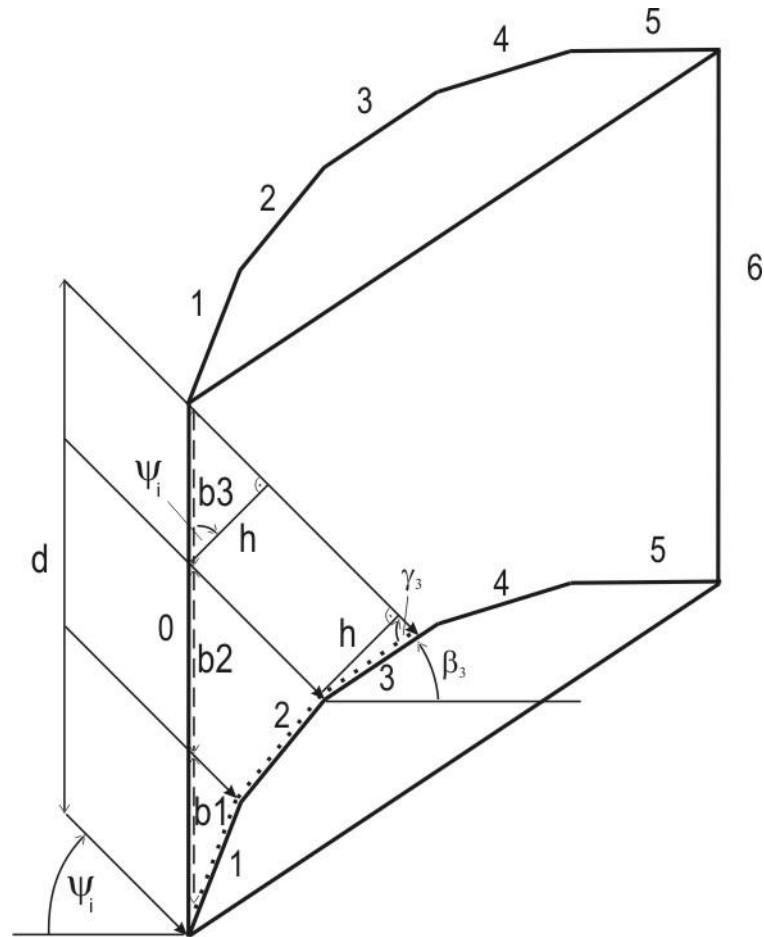
Figure 11-20. Calculation of Beam view factors

BF for the front surface of segment 3 is given as:

$$BF_{f,3} = \frac{h}{d \cdot \cos\psi_i}$$

[11–59]

Where:

$$h = A_3' \cdot \sin\gamma_3$$

$$\gamma_3 = \beta_3 + \psi_i$$

[11–60]

A_3' = length of segment 3 which is directly irradiated

β_3 = tilt angle of segment 3 (with respect to horizontal plane)

ψ_i = profile angle of incident direction i

d = slat spacing

f = indicates front surface of the segment

Finally:

$$BF_{f,3} = \frac{A_3' \cdot \sin(\beta_3 + \psi_i)}{d \cdot \cos\psi_i}$$

[11–61]

*BF*s for the front surfaces of segments 1 and 2 ($BF_{f,1}$ and $BF_{f,2}$) can be calculated the same way. The rest of the slat segments shown in Figure 11-20 are not directly irradiated, so the remaining *BF*s (including *BF*s for the back sides of segments 1-5) are equal to zero:

$$BF_{f,4} = BF_{f,5} = BF_{b,1} = BF_{b,2} = BF_{b,3} = BF_{b,4} = BF_{b,5} = 0$$

[11–62]
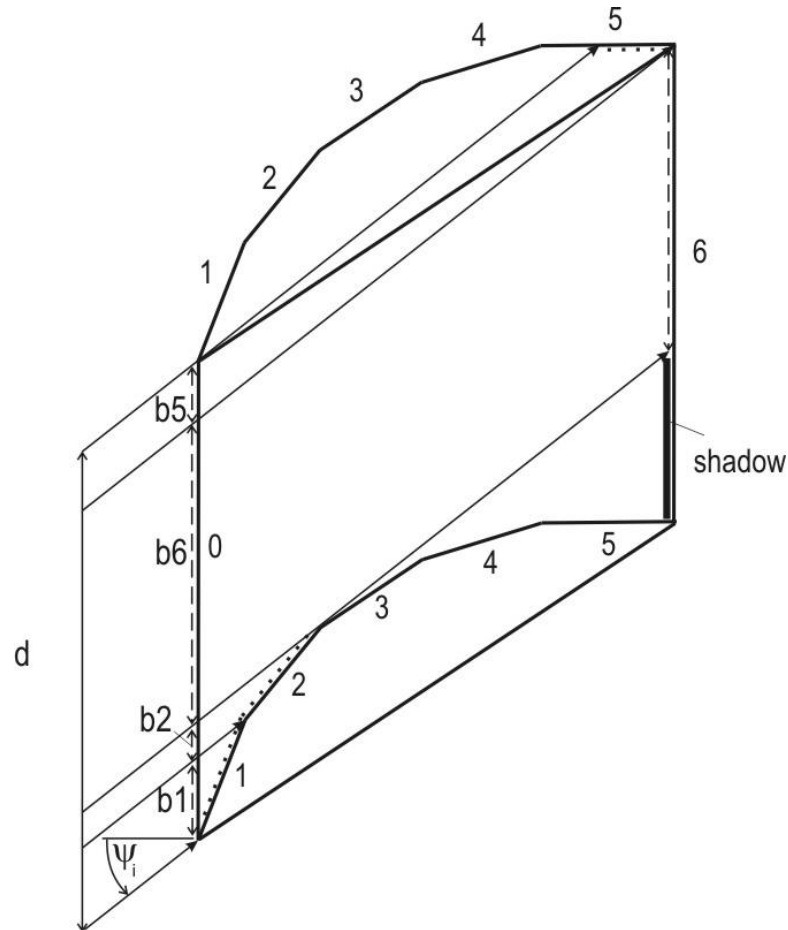
Figure 11-21. Beam view factors and Dir-Dir transmittance

For extreme negative profile angles of incident light, some of the upper slat segments are irradiated. As a result, some of the *BF*s for the back surfaces of segments ($BF_{b,\,i}$) will have non-zero values. This is the case shown in Figure 11-21: non-zero *BF* are $BF_{f,1}$, $BF_{f,2}$ and $BF_{b,5}$. Note that according Figure 11-21, a part of the incident beam passes through the blind without hitting the slats. The ratio of b6 to the slat distance *d* corresponds to the dir-dir portion of transmitted light – $\tau_{\text{dir-dir}}$, as defined in Section 11.2.1.1:

$$\tau_{dir-dir} = \frac{b6}{d}$$

[11–63]

The sum of all *BF* and $\tau_{\text{dir,dir}}$ must equal 1:

$$\sum_{i=1}^{N_{seg}} BF_{f,i} + \sum_{i=1}^{N_{seg}} BF_{b,i} + \tau_{dir-dir} = 1 \qquad\qquad [11–64]$$

After BF are calculated for all slat segments using formulas similar to equation *[11–61]*, in the case of the forward-going incident light, these BF are used to substitute certain view factors F in equations *[11–51]-[11–52]*:

$$F_{f,0->f,i} = BF_{f,i} \ , \ F_{f,0->b,i} = BF_{b,i} \ , \ i = 1,...,N_{seg} \qquad\qquad [11–65]$$

As in the case of the dif-dif portion, unit irradiance at the front side of the blind is assumed: Ef,0 = 1, with no incidence at the back side: Eb,6 = 0. After making these changes, the system of equations is solved for Ef,i and Eb,i. The resulting Dir-Dif transmittance for the front side of the blind is then calculated for i-th incident direction as:

$$\tau^{f}_{dir-dif,i} = \frac{E_{f,6}}{E_{f,0}} = \frac{E_{f,6}}{1} = E_{f,6} \qquad\qquad [11–66]$$

The resulting front-side reflectance becomes:

$$\rho^{f}_{dir-dif,i} = \frac{E_{b,0}}{E_{f,0}} = \frac{E_{b,0}}{1} = E_{b,0} . \qquad\qquad [11–67]$$

In the case of backward-going incident light, BF are calculated using the same geometry approach at the back side of the blind. View factors are then replaced as:

$$F_{b,6->f,i} = BF_{f,i} \ , \ F_{b,6->b,i} = BF_{b,i} \ , \ i = 1,...,N_{seg} \qquad\qquad [11–68]$$

The unit irradiance at the back side of the blind is assumed: $E_{f,0} = 0$, $E_{b,6} = 1$. After solving the modified system of equations, dir-dif transmittance for iʳ-th incident direction at the back-side is given as:

$$\tau^{b}_{dir-dif,i^r} = \frac{E_{b,0}}{E_{b,6}} = \frac{E_{b,0}}{1} = E_{b,0} \qquad\qquad [11–69]$$

Back-side reflectance becomes:

$$\rho^{b}_{dir-dif,i^r} = \frac{E_{f,6}}{E_{b,6}} = \frac{E_{f,6}}{1} = E_{f,6} . \qquad\qquad [11–70]$$

11.3. Bi-Directional Method

11.3.1. Introduction

This section presents an overview of the bi-directional properties (transmittances and reflectances) calculation for the optical layer which can be specular and diffuse at the same time (i.e., the directly transmitted portion in the Venetian blind is considered specular, while dif-dif and dir-dif are diffuse). These properties are defined for each combination of incident and outgoing directions, and they form BTDF and BDRF matrices: square matrices, with equal number of columns and rows defined by the total number of different angular coordinates (θ,φ), described in Section 11.1.3. These matrices describe a single specular and diffusing layer and they are used for calculation of the SOL properties of the glazing system that contains one or more of these layers, and which is described in detail in Klems, J.H. 1994a and Klems, J.H. 1994b. It should be noted that for purely specular optical layers, all non-diagonal terms are zero (diffuse terms), producing diagonal

matrices. For partially or fully diffuse layers, the non-diagonal terms in the bi-directional matrices can be non-zero.

In the case of forward-going incident radiation, E, coming from the i-th direction, the following equations apply for the forward-going transmitted radiation in direction j, I, and the backward-going reflected radiation, I^r in direction j^r (see Figure 11-10a):

$$I(\theta_j,\varphi_j) = \tau^f(\theta_j,\varphi_j;\theta_i,\varphi_i)E(\theta_i,\varphi_i)$$
$$I^r(\theta_j^r,\varphi_j^r) = \rho^f(\theta_j^r,\varphi_j^r;\theta_i,\varphi_i)E(\theta_i,\varphi_i)$$

[11–71]

After introducing matrix notations, we can define **TAU_F:** a BTDF matrix that contains bi-directional transmittances for **FWD** going incident radiation:

$$\mathbf{I} = \mathbf{TAU\_F} \times \mathbf{E}$$

$$\begin{bmatrix} I_1 \\ I_2 \\ I_3 \\ ... \\ I_N \end{bmatrix} = \begin{bmatrix} \tau^f_{1,1} & \tau^f_{1,2} & \tau^f_{1,3} & ... & \tau^f_{1,N} \\ \tau^f_{2,1} & \tau^f_{2,2} & \tau^f_{2,3} & ... & \tau^f_{2,N} \\ \tau^f_{3,1} & \tau^f_{2,2} & \tau^f_{3,3} & ... & \tau^f_{3,N} \\ ... & ... & ... & & ... \\ \tau^f_{N,1} & \tau^f_{N,2} & \tau^f_{N,3} & ... & \tau^f_{N,N} \end{bmatrix} \times \begin{bmatrix} E_1 \\ E_2 \\ E_3 \\ ... \\ E_N \end{bmatrix}$$

[11–72]

where $\tau^f_{j,i}$ is short notation used for the front bidirectional transmittance $\tau^f(\theta_j,\varphi_j;\theta_i,\varphi_i)$ (radiation coming from direction i, and transmitted in direction j), and N is the number of incident/outgoing directions defined as (θ, φ) pairs (in our case, shown in Figure 11-5, $N = 49$).

For reflected radiation, we have **RHO_F**: a BRDF matrix that contains bi-directional reflectances for **FWD** going incident radiation:

$$\mathbf{I^r} = \mathbf{RHO\_F} \times \mathbf{E}$$

$$\begin{bmatrix} I_1^r \\ I_2^r \\ I_3^r \\ ... \\ I_N^r \end{bmatrix} = \begin{bmatrix} \rho^f_{1,1} & \rho^f_{1,2} & \rho^f_{1,3} & ... & \rho^f_{1,N} \\ \rho^f_{2,1} & \rho^f_{2,2} & \rho^f_{2,3} & ... & \rho^f_{2,N} \\ \rho^f_{3,1} & \rho^f_{3,2} & \rho^f_{3,3} & ... & \rho^f_{3,N} \\ ... & ... & ... & & ... \\ \rho^f_{N,1} & \rho^f_{N,2} & \rho^f_{N,3} & ... & \rho^f_{N,N} \end{bmatrix} \times \begin{bmatrix} E_1 \\ E_2 \\ E_3 \\ ... \\ E_N \end{bmatrix}$$

[11–73]

where $\rho^f_{j,i}$ is short notation used for the front bidirectional reflectance $\rho^f(\theta_j^r,\varphi_j^r;\theta_i,\varphi_i)$ (radiation coming from direction i, and reflected in direction j^r, which is in reversed coordinates, in z^r hemisphere), and N is the number of incident/outgoing directions.

As for the backward-going incident radiation, E^r, the following equations apply for backward-going transmitted radiation, I^r and forward-going reflected radiation, I, (see Figure 11-10b):

$$I^r(\theta_j^r,\varphi_j^r) = \tau^b(\theta_j^r,\varphi_j^r;\theta_i^r,\varphi_i^r)E^r(\theta_i^r,\varphi_i^r)$$
$$I(\theta_j,\varphi_j) = \rho^b(\theta_j,\varphi_j;\theta_i^r,\varphi_i^r)E^r(\theta_i^r,\varphi_i^r)$$

[11–74]

After introducing matrix notations, we can define **TAU_B:** a BTDF matrix that contains bi-directional transmittances for **BCK** going incident radiation:

$$\mathbf{I^r = TAU\_B \times E^r}$$

$$
\begin{bmatrix} I_1^r \\ I_2^r \\ I_3^r \\ \dots \\ I_N^r \end{bmatrix} =
\begin{bmatrix}
\tau_{1,1}^b & \tau_{1,2}^b & \tau_{1,3}^b & \dots & \tau_{1,N}^b \\
\tau_{2,1}^b & \tau_{2,2}^b & \tau_{2,3}^b & \dots & \tau_{2,N}^b \\
\tau_{3,1}^b & \tau_{2,2}^b & \tau_{3,3}^b & \dots & \tau_{3,N}^b \\
\dots & \dots & \dots & & \dots \\
\tau_{N,1}^b & \tau_{N,2}^b & \tau_{N,3}^b & \dots & \tau_{N,N}^b
\end{bmatrix}
\times
\begin{bmatrix} E_1^r \\ E_2^r \\ E_3^r \\ \dots \\ E_N^r \end{bmatrix}
$$

[11–75]

where $\tau_{j,i}^b$ represents bidirectional transmittance at the back side $\tau^b\left(\theta_j^r,\varphi_j^r;\theta_i^r,\varphi_i^r\right)$ (radiation coming from direction i^r, and transmitted in direction j^r, both of which are defined in reversed coordinates, in z^r hemisphere), and *N* is the number of incident/outgoing directions defined as (θ,φ) pairs (in our case, *N* = 49).

For reflected radiation, we have **RHO_B:** a BRDF matrix that contains bi-directional reflectances for **BCK** going incident radiation:

$$\mathbf{I = RHO\_B \times E^r}$$

$$
\begin{bmatrix} I_1 \\ I_2 \\ I_3 \\ \dots \\ I_N \end{bmatrix} =
\begin{bmatrix}
\rho_{1,1}^b & \rho_{1,2}^b & \rho_{1,3}^b & \dots & \rho_{1,N}^b \\
\rho_{2,1}^b & \rho_{2,2}^b & \rho_{2,3}^b & \dots & \rho_{2,N}^b \\
\rho_{3,1}^b & \rho_{3,2}^b & \rho_{3,3}^b & \dots & \rho_{3,N}^b \\
\dots & \dots & \dots & & \dots \\
\rho_{N,1}^b & \rho_{N,2}^b & \rho_{N,3}^b & \dots & \rho_{N,N}^b
\end{bmatrix}
\times
\begin{bmatrix} E_1^r \\ E_2^r \\ E_3^r \\ \dots \\ E_N^r \end{bmatrix}
$$

[11–76]

where $\rho_{j,i}^b$ represents the bidirectional reflectance at the back side $\rho^b\left(\theta_j,\varphi_j;\theta_i^r,\varphi_i^r\right)$ (radiation coming from direction i^r, which is given in reversed coordinates, in z^r hemisphere, and reflected in direction j, which is defined by "regular" coordinates, in *z* hemisphere), and N is the number of incident/outgoing directions.

It is important to note that BTDF (Tau) matrices should be represented as sums of two matrices which correspond to two transfer mechanisms (undisturbed, or directly transmitted, dubbed "dir" and Lambertian diffuse reflections from slats, dubbed "dif"), as shown in equations *[11–77]* and *[11–78]*, which describe **TAU_F** and **TAU_B** matrices, defined in equations *[11–72]* and *[11–75]*, respectively:

$$\mathbf{TAU\_F = TAU\_F\_dir + TAU\_F\_dif} \qquad\qquad \textit{[11–77]}$$

$$\mathbf{TAU\_B = TAU\_B\_dir + TAU\_B\_dif} \qquad\qquad \textit{[11–78]}$$

On the other hand, reflected radiation contains only "dif" part.

11.3.2. Directly Transmitted Radiation

The specular portion (**t^f** **dir** for FWD going incident radiation, or **t^b** **dir** for BCK going incident radiation) is a portion of incident radiation that travels through the blind without interaction with the slat material. It is calculated for each incident profile angle, using the Dir-Dir methodology, explained in Section 11.2.2.1. These

values are affected only by the geometry of the blind and incident profile angle; slat material properties have no influence. After calculating the portion of light that goes undisturbed through the venetian blind for a certain incident profile angle ψ_i, which corresponds to i-th incident direction of forward-going radiation, this value is divided by Lambda, and placed in the appropriate place in a diagonal TAU_F_dir matrix:

$$\tau_{i,i\,dir}^f = \frac{\tau_{dir-dir,i}^f}{\Lambda_i}, \quad i = 1,..., N \qquad\qquad [11-79]$$

Lambda in equation [11–79] represents propagation operators, elements of a matrix which transforms radiance vectors emerging from one layer into irradiance vectors incident on the next layer. Lambda values are geometrical quantities associated with the partitioning of a solid angle, as described in Klems, J.H. 1994a and Klems, J.H. 1994b. Each $\Delta\Omega$ bin has a corresponding Lambda value. They can be expressed as:

$$\Lambda_i = \frac{1}{2}\left(\sin^2\theta_i^{hi} - \sin^2\theta_i^{lo}\right)\Delta\varphi_i, \quad i = 1,..., N_\theta \qquad\qquad [11-80]$$

If directions are equally spaced along each strip defined by θ angle, we have:

$$\Lambda_i = \frac{1}{2}\left(\sin^2\theta_i^{hi} - \sin^2\theta_i^{lo}\right)\frac{2\pi}{N_{\varphi_i}}, \quad i = 1,..., N_\theta \qquad\qquad [11-81]$$

where $N\varphi_i$ is the number of directions in one θ strip.

Lambda values are stored in a matrix. Indexes *lo* and *hi* in equation [11–80] stand for "lower" and "higher" bounding angles of $\Delta\Omega$ bins. Figure 11-22 shows one $\Delta\Omega$ bin with corresponding bounding angles (using planar projection of the hemisphere).

The "*z*" hemisphere is divided into N_θ spherical strips (the first of which is actually a spherical cap). Each strip is defined by the two boundary angles: θ^{lo} and θ^{hi}. The relation between these boundary angles and corresponding θ angle is:

$$\theta_1^{lo} = 0°; \quad \theta_{N_\theta}^{hi} = 90°;$$
$$\theta_i^{lo} = \theta_{i-1}^{hi} = 2\theta_i - \theta_i^{hi}, \quad i = N_\theta,...,2; \qquad\qquad [11-82]$$

Note that bounding angles should be calculated from the highest θ angle towards the lowest θ.

Figure 11-23 shows one spherical strip, an area bordered with "low" and "high" boundary angles.
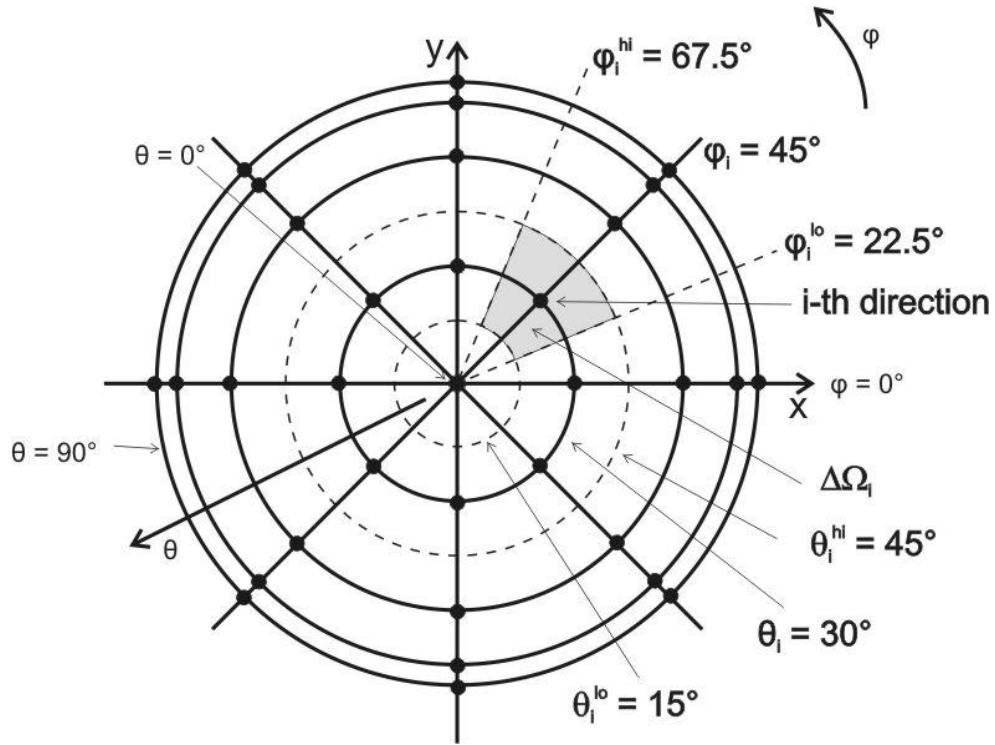
Figure 11-22. Angle Definitions for Calculation of Lambda values
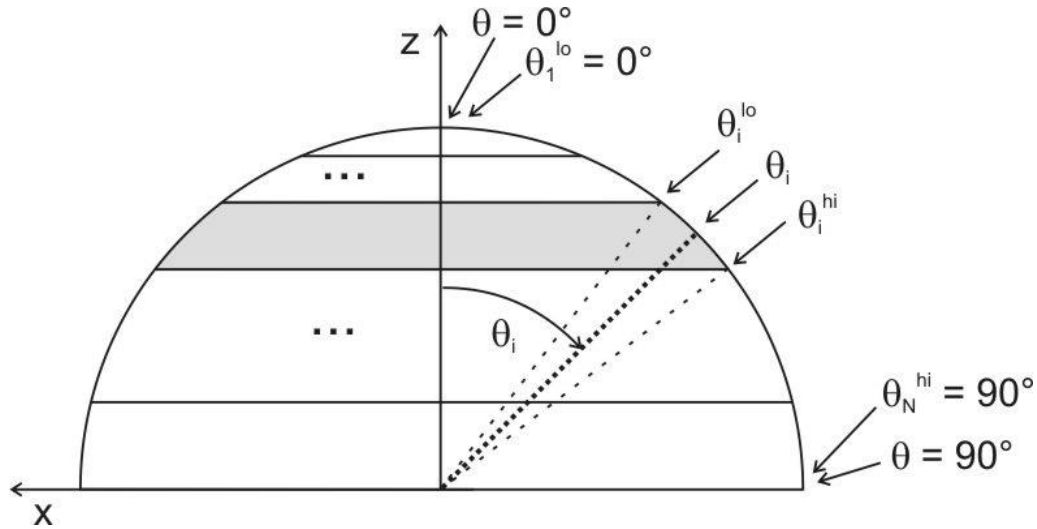
Figure 11-23. Theta limits which form a spherical strip ("z" hemisphere)

In our example, shown in Figure 11-22, i=3, and Λ_3 would be:

$$\Lambda_3 = \frac{1}{2}\left(\sin^2 \theta_3^{hi} - \sin^2 \theta_3^{lo}\right)\frac{2\pi}{N_{\varphi_3}} = \frac{1}{2}\left(\sin^2 \frac{\pi}{4} - \sin^2 \frac{\pi}{12}\right)\cdot\frac{2\pi}{8} = \frac{\pi}{8}\left(\sin^2 \frac{\pi}{4} - \sin^2 \frac{\pi}{12}\right) = 0.17$$

[11–83]

11.3.3. Diffusely Transmitted and Reflected Radiation

The diffuse (or "dif") transmitted or reflected portion of the incident radiation is a portion of the incident radiation that arrives at the slat surface(s), and leaves the blind at the other, or at the same side, after a series of Lambertian reflections off slat surfaces.

In all calculations of SOL range diffuse properties of the Venetian blind, SOL properties of the slat material are used (τ_s, ρ_s^f and ρ_s^b).

Two different methods for calculations of diffuse portion of solar-optical properties in SOL range are presented; a) Uniform Diffuse method and b) Directional Diffuse method.

Uniform-Diffuse Method

This method utilizes the Dir-Dif methodology, presented in Section **Error! Reference source not found.**

For each incident direction *i*, or to be more precise, for each incident direction's profile angle ψ_i, $\tau_{dir-dif,i}$ and $\rho_{dir-dif,i}$ are calculated twice, for FWD and BCK going incident radiation. $\tau_{dir-dif,i}$ and $\rho_{dir-dif,i}$ are obtained after solving systems of equations, defined by equations *[11–51]-[11–52]*.

These results are hemispherical values, averaged across the hemisphere. Therefore, they need to be divided by π before placing in BTDF/BRDF matrices.

Note that this calculation method gives uniform distribution of diffuse values for one incident profile angle ψ_i. This results in **RHO** matrices, **TAU_F_dif** and **TAU_B_dif** matrices having equal values within any column.

When "dir" and "dif" results are summed, **TAU_F** from equation *[11–72]* becomes:

$$
\textbf{TAU\_F} = \begin{bmatrix}
\dfrac{\tau_{dir-dir,1}^f}{\Lambda_1} + \dfrac{\tau_{dir-dif,1}^f}{\pi} & \dfrac{\tau_{dir-dif,2}^f}{\pi} & \cdots & \dfrac{\tau_{dir-dif,N}^f}{\pi} \\[2ex]
\dfrac{\tau_{dir-dif,1}^f}{\pi} & \dfrac{\tau_{dir-dir,2}^f}{\Lambda_2} + \dfrac{\tau_{dir-dif,2}^f}{\pi} & \cdots & \dfrac{\tau_{dir-dif,N}^f}{\pi} \\[2ex]
& & \cdots & 0 \\[2ex]
\cdots & \cdots & \cdots & \cdots \\[2ex]
\dfrac{\tau_{dir-dif,1}^f}{\pi} & \dfrac{\tau_{dir-dif,2}^f}{\pi} & \cdots & \dfrac{\tau_{dir-dir,N}^f}{\Lambda_N} + \dfrac{\tau_{dir-dif,N}^f}{\pi}
\end{bmatrix}
\qquad [11–84]
$$

Figure 11-24 shows how the TAU_F matrix is formed.

Elements of **RHO_F** matrix from equation *[11–73]* are:

$$
\rho_{j,i}^f = \frac{\rho_{dir-dif,i}^f}{\pi}, \quad i,j = 1,...,N
\qquad [11–85]
$$

The **RHO_F** is:

$$
\mathbf{RHO\_F} = \begin{bmatrix} \dfrac{\rho^f_{dir-dif,1}}{\pi} & \dfrac{\rho^f_{dir-dif,2}}{\pi} & \cdots & \dfrac{\rho^f_{dir-dif,N}}{\pi} \\[2ex] \dfrac{\rho^f_{dir-dif,1}}{\pi} & \dfrac{\rho^f_{dir-dif,2}}{\pi} & \cdots & \dfrac{\rho^f_{dir-dif,N}}{\pi} \\[2ex] & & \cdots & \\ \cdots & \cdots & \cdots & \cdots \\[2ex] \dfrac{\rho^f_{dir-dif,1}}{\pi} & \dfrac{\rho^f_{dir-dif,2}}{\pi} & \cdots & \dfrac{\rho^f_{dir-dif,N}}{\pi} \end{bmatrix}
$$

[11–86]
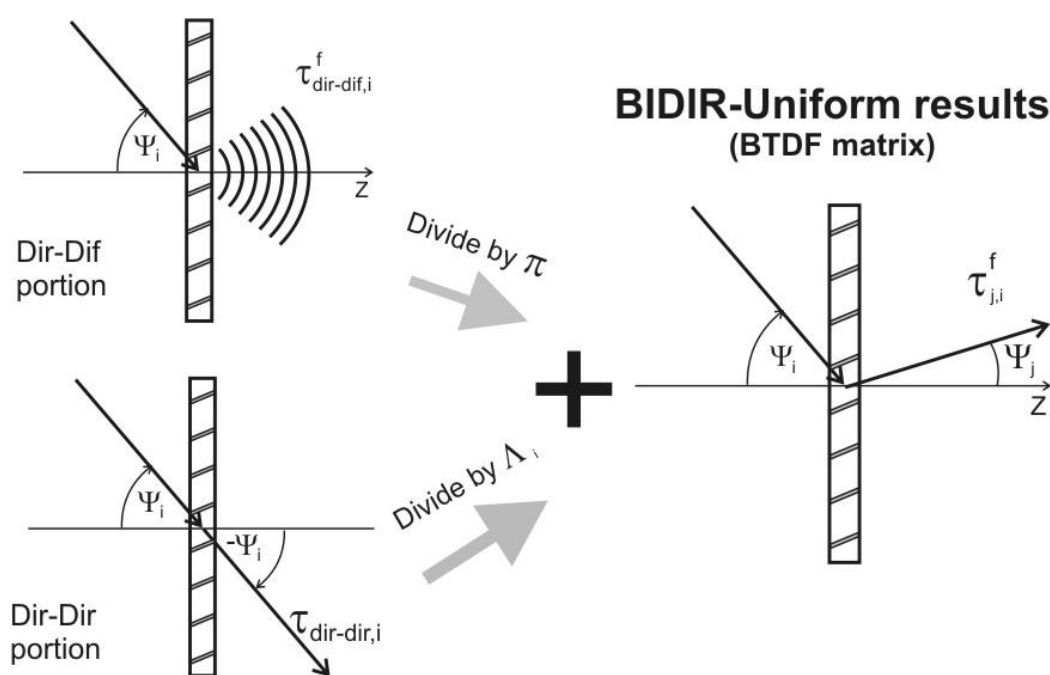
Figure 11-24. Overview of BiDir – Uniform Diffuse calculation method
(FWD transmittance)

Matrices for backward radiation direction are formed by following the same pattern, only in reversed coordinates. Calculations of $\tau_{dir-dir,i}$, $\tau_{dir-dif,i}$ and $\rho_{dir-dif,i}$ are performed for BCK direction of incident radiation, and stored in the appropriate result matrices in a previously described manner.

More examples with elements of BSDF matrices, based on a full angular set of 145 directions, are available in Section 11.5.

Directional-Diffuse Method

Unlike the Uniform-Diffuse Method, which gives uniform distribution of diffusely transmitted and reflected radiance across all outgoing directions for a given incident direction, the Directional-Diffuse method calculates the diffuse component for each outgoing direction taking into account which segments are "visible" and which segments are "shielded" by the other slat, when considered at the outgoing angle. In other words, the procedure considers the cut-off angle and adjusts the diffuse radiation intensity based on that cut-of angle. This approach provides a more realistic angular distribution of the diffuse radiation.

However, in the average sense, the integrated, or hemispherical value of diffuse transmittance or reflectance of an isolated layer, such as a Venetian blind, should be the same, regardless of the approach taken. The improved accuracy comes from the fact that the matrix method for determining solar-optical properties of multiple layer systems, consisting of specular, diffuse, or partially diffuse layers, described in Klems, J.H. 1994a and Klems, J.H. 1994b, considers individual outgoing directions in the process of calculating the system properties, so having more accurate angular distribution of the diffuse radiation improves the accuracy of the method.

Figure 11-25 shows how outgoing radiance (and hence transmittance) changes with the outgoing profile angle, for a simple case of a flat-slat Venetian blind. It shows a situation in which the blind is irradiated by light that arrives at an incident profile angle ψ_{in}. The incident radiation is diffusely reflected off both slats. When the radiation reaches the indoor facing imaginary plane, four different bands can be identified for the outgoing directions which lay in a vertical plane, starting from the lowest outgoing angle of -90° (-π/2):

1. Increasing radiance: the total outgoing radiance increases with ψ_{out}, from zero to $I_{max,1}$, achieved at outgoing angle ψ_{max1}, as the larger part of the upper slat becomes visible

2. Decreasing radiance, as the angle between outgoing direction and upper slat normal vector decreases, from ψ_{max1} to zero at slat tilt angle ψ_{slat}

3. Increasing radiance: when ψ_{out} increases past slat tilt angle ψ_{slat}, the lower slat is no longer visible, and the lower slat becomes completely visible, the outgoing radiance increases from zero to $I_{max,2}$, which is achieved at outgoing angle ψ_{max2}

4. Decreasing radiance: as the outgoing angle increases past ψ_{max2}, the decrease of the total visible part of the lower slat outweighs the decrease of angle between the outgoing direction and the normal vector of the lower slat in terms of an overall contribuiton to outgoing radiance, which results in decreasing of the total outgoing radiance from $I_{max,2}$, to zero for $\psi_{out} = -90°$ (-π/2).
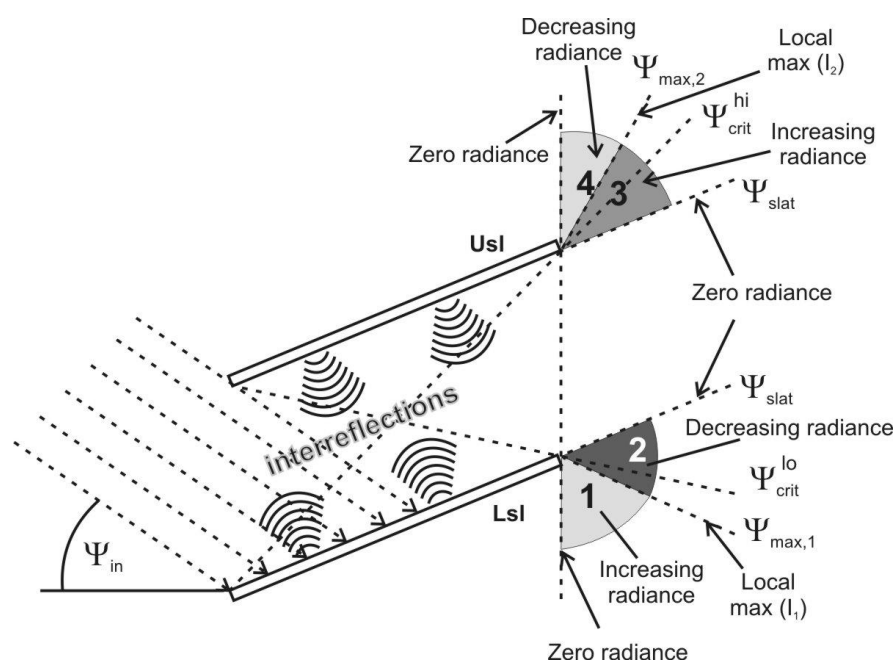
Figure 11-25. Illustration of directional-diffuse transmittance
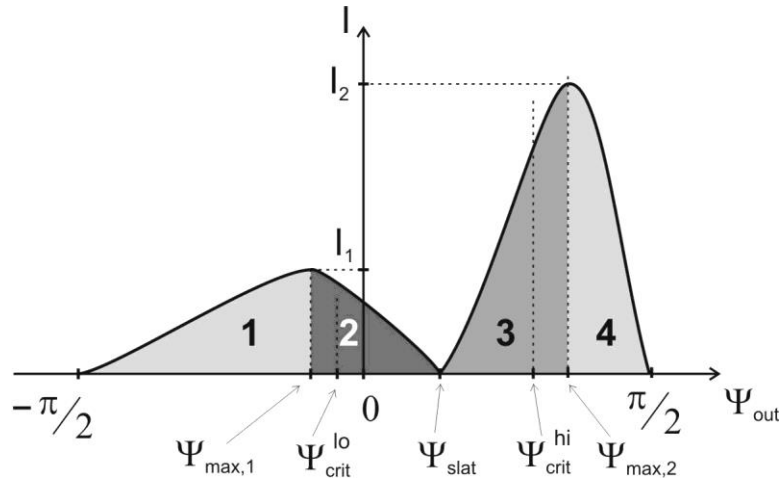
Figure 11-26. Outgoing radiance vs. outgoing profile angle for directional-diffuse transmittance in vertical outgoing plane

Figure 11-26 shows the plot of outgoing radiance against outgoing profile angle, for the example from Figure 11-25. The shape of the curve is highly influenced by several factors: the incident direction, the overall geometry of the slat (width, distance, curvature, tilt) and the optical properties of slat material (at both sides).

Although individual basic energy balance equations are essentially the same as the ones used in Section 11.2.1.3, equations *[11–35]-[11–48]*, there are certain differences in the resulting equation systems:

- Unlike the "slat enclosure" model (Figure 11-14), there are no "virtual" segments for the front and back opening; therefore, the dimension of this system is reduced by 2.

- The system of equations is formed and solved for radiosities leaving slat segments, instead of irradiances arriving at slat segments.

- The resulting outgoing radiation is calculated as a sum of contributions of each segment of the two adjacent slats, using radiosities leaving each slat segment instead of irradiance reaching the "virtual" segment "6", used in the Uniform-Diffuse approach.

- Although the physical meaning is similar, this system uses a slightly different notation for slat segments, which is more appropriate for the Directional-Diffuse approach described in this section.

The system of energy-balance equations in the Directional-Diffuse method has the following form (see also Klems, J.H. 2004):

for each segment p of the lower slat (Lsl):

$$\sum_q \left[\delta_{pq} - \left(r_p^f \cdot F_{p,q} + t_p \cdot F_{p',q} \right) \right] \cdot J_{q,i} = \left(r_p^f \cdot E_{p,i} + t_p \cdot E_{p',i} \right)$$

[11–87]

for each segment p' of the upper slat (Usl):

$$\sum_q \left[\delta_{p'q} - \left(r_{p'}^b \cdot F_{p',q} + t_{p'} \cdot F_{p',q} \right) \right] \cdot J_{q,i} = \left(r_{p'}^b \cdot E_{p',i} + t_{p'} \cdot E_{p,i} \right)$$

[11–88]

where:

$$\delta_{pq} = \begin{cases} 1, \ p = q \\ 0, \ p \neq q \end{cases}$$

q = any slat segment (of both Lsl and Usl)

p, p' = slat segment of the lower and upper slat, respectively

i = indicates i-th incident direction

$r_{p1}^f r_p^b$ = reflectance of the front and back side of slat segment p, respectively

t_p = transmittance of slat segment p

$f_{p,q}$ = view factor from segment p towards q

$E_{p,i}$ = irradiance incident on a slat segment p, radiation coming from incident direction i

$J_{q,i}$ = outgoing radiosity from slat segment q, which comes from incident radiation coming from incident direction i

Front Transmittance:
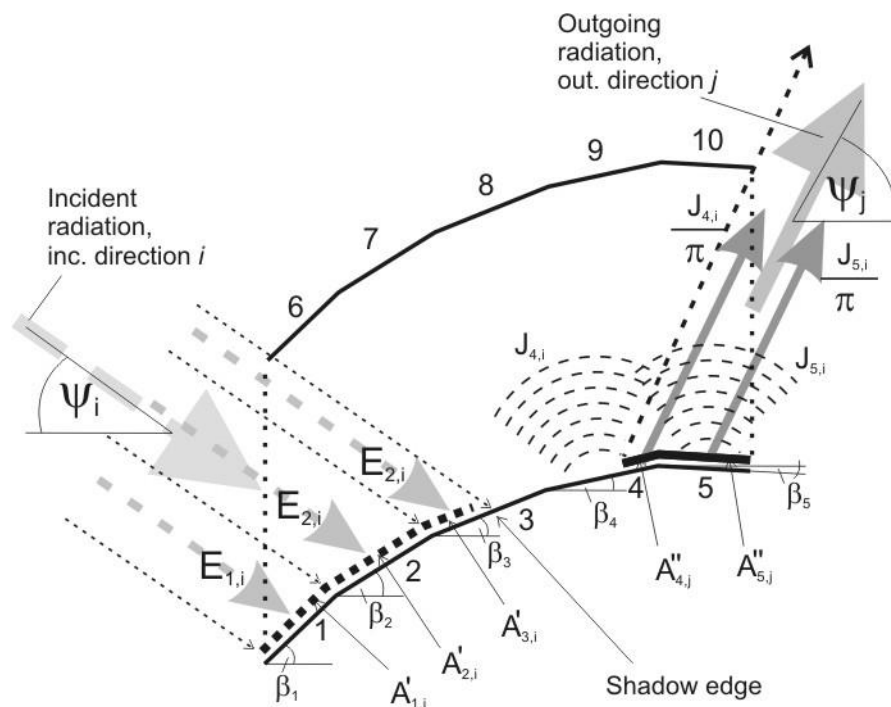
Figure 11-27. Explanation of terms in calculation of front bi-directional transmittance

Figure 11-27 explains the terms in the calculation of front bi-directional transmittance, for the forward-going incident direction i and the forward-going outgoing direction j. These directions are transformed into profile angles ψ_i and ψ_i, respectively. The thick dotted line represents the irradiated parts of the lower slat, while the thick full line marks parts of the lower slat visible in the outgoing direction.

As previously shown in Section 11.1.4, irradiances on each slat segment p (caused by radiation from incident direction i), needed for the energy-balance equations, can be calculated in 2D space, using:

$$E_{p,i} = (\cos \beta_p \tan \psi_i - \sin \beta_p) \cdot \frac{A'_{p,i}}{A_p}$$

[11–89]

where:

β_p = tilt angle of slat segment p

ψ_i = profile angle of incident direction i

$A'_{p,j}$ = area (length in 2D) of segment p that is irradiated by radiation coming from incident direction i

A_p = area of slat segment p (length in 2D)

With regards to equation [11–89], following values correspond to our example shown in Figure 11-27:

$$A'_{1,i} = A_1,$$
$$A'_{2,i} = A_2,$$
$$A'_{3,i} < A_3,$$
$$A'_{p,i} = 0, \quad p > 3$$

[11–90]

In order to calculate the front transmittance for a given outgoing direction (profile angle), it is necessary to solve the set of equations defined by equations [11–87]-[11–88]), with irradiances E calculated using Equation [11–7]. After that, it is necessary to determine which slat segments (or parts of certain slat segments) are visible from that particular outgoing direction, as shown in Figure 11-27.

The contribution of each slat to the total outgoing radiance in the outgoing direction k is given by equation [11–10]. The total outgoing transmittance is calculated as an averaged sum of these contributions, with regards to the area of back opening:

$$\tau^f_{j,i} = \frac{1}{A_d \cos\theta_j} \sum_p \left[\left(\cos\beta_p \cdot \tan\psi_j - \sin\beta_p \right) A''_{p,j} \frac{J_{p,i}}{\pi} \right]$$

[11–91]

where:

A_d = area of slat opening (slat distance in 2D)

θ_j = latitude angle of outgoing direction j

β_p = tilt angle of slat segment p

ψ_i = profile angle of outgoing direction j

$J_{p,i}$ = outgoing radiosity from slat segment p (as a result of irradiance at all slat segments, coming from incident direction i) – solution of set of equations [11–87]-[11–88]

$A''_{p,j}$ = area (length in 2D) of segment p that is visible from outgoing direction j

With regards to equation [11–91], following values would be used in our example:

$$A''_{5,j} = A_5,$$
$$A''_{4,j} < A_4,$$
$$A''_{p,j} = 0, \quad p \in \{1,2,3,6,7,8,9,10\}$$

[11–92]

As shown in equation [11–91], the transmitted part is calculated as a sum of the contributions (diffuse radiosities divided by π) of each slat segment visible from the outgoing direction j, and this is calculated for

each outgoing direction. This results in a non-uniform distribution of results, unlike the distribution of results present in Uniform-Diffuse method.

This calculation can be summarized for front-side transmittance as:

- calculate incident and outgoing profile angles: ψ_i (forward-going) and ψ_j (forward-going), respectively

- determine visible areas $A'_{p,i}$ for each slat segment p (from incident direction i)

- calculate irradiance $E_{p,i}$ of each slat segment p

- calculate radiosities $J_{p,i}$ for each slat segment p, by solving set of *[11–87]-[11–88]*

- determine parts $A''_{p,j}$ of each slat segment p, visible from the outgoing direction j.

- use equation *[11–91]* to calculate front bi-directional transmittance.

These steps are repeated for each pair of (ψ_i, ψ_j), and results of these calculations are stored in the appropriate places in TAU_F_dif bi-directional matrix.

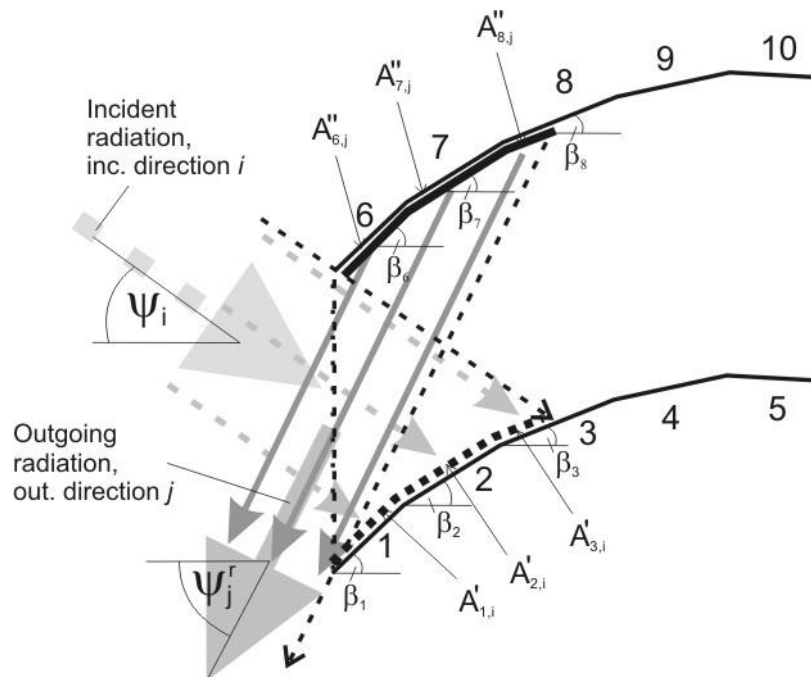**Front Reflectance:**

Figure 11-28. Explanation of terms in calculation of front bi-directional reflectance

Front bi-directional reflectance is calculated for the forward-going incident direction i and the backward-going outgoing direction j (Figure 11-28), as:

$$\rho^f_{j,i} = \frac{1}{A_d} \sum_p \left(\cos\beta_p \tan\psi^r_j - \sin\beta_p \right) A''_{p,j} \frac{J_{p,i}}{\pi}$$
[11–93]

Calculation of the **RHO_F** bi-directional matrix is done using the same procedure as shown for the **TAU_F_dif** bi-directional matrix.

Back-side transmittances and reflectances are calculated after applying the same procedure shown for the front-side transmittances and reflectances to the backward-going incident directions. The resulting bi-directional matrices are TAU_B_dif and RHO_B.

Again, directly transmitted values (TAU_F_dir and TAU_B_dir) are added to matrices TAU_F_dif and TAU_B_dif to form the full set of bid-directional matrices TAU_F and TAU_B.

11.3.4. Direct to Hemispherical Solar-optical Properties

Direct to hemispherical solar-optical properties (transmittances and reflectances) of the blind are integrated properties calculated from bi-directional results for each incident angle or direction. These properties represent transmitted/reflected radiation integrated over the outgoing hemisphere, which is a result of the incident directional radiation (a beam), coming from a certain incident direction (Figure 11-29).
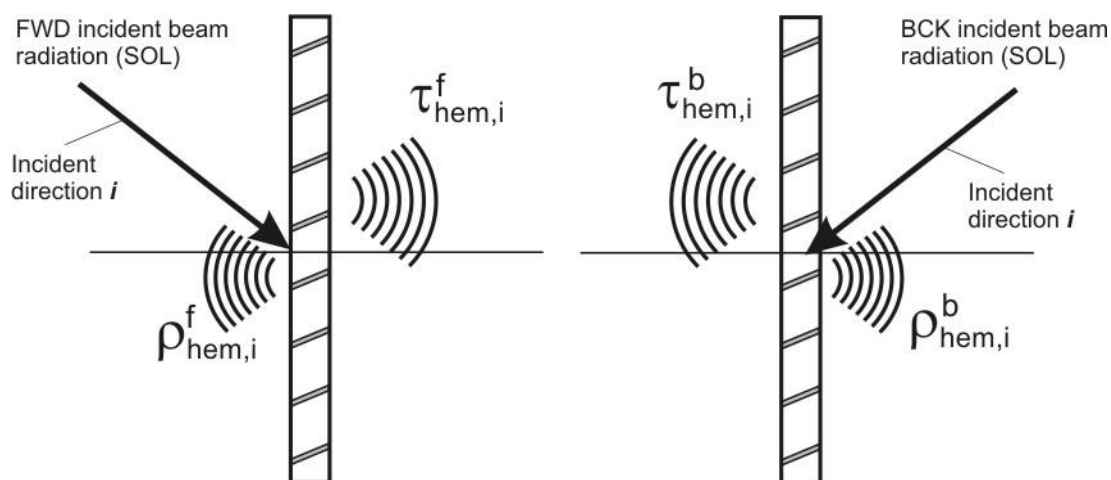
Figure 11-29. Directional-to-hemispherical properties at front and back side of the Venetian blind

Due to the inherent asymmetry of the geometry and the slat material properties of the blind with respect to incident angles, integrated transmittances and reflectances are calculated separately for the front and for the back side of the blind. Thus, we define 4 different sets of direct to hemispherical properties:

- Hemispherical transmittances at the front side of the blind, $\tau^f_{hem,i}$

- Hemispherical transmittances at the back side of the blind, $\tau^b_{hem,i}$

- Hemispherical reflectances at the front side of the blind, $\rho^f_{hem,i}$

- Hemispherical reflectances at the back side of the blind, $\rho^b_{hem,i}$

As equation *[11–72]* shows, an element of the bi-directional transmittance matrix for the front side of the blind **TAU_F** is defined as $\tau^f_{j,i}$ – radiation coming from direction *i*, and transmitted in direction *j* – (*i,j* = 1, … , *N*, where *N* is the number of incident/outgoing directions). The same matrix format is used in other three matrices with bi-directional properties (**TAU_B**, **RHO_F**, and **RHO_B**).

Direct-to-Hemispherical transmittance (front or back) for *i*-th incident direction $\tau^f_{hem,i}$ and $\tau^b_{hem,i}$ are defined as the hemispherical average of the bi-directional transmittances, over an outgoing hemisphere:

$$\tau_{hem,i} = \frac{\displaystyle\int_{\substack{outgoing \\ hemisphere}} \tau_{j,i}\cos\theta_j\, d\omega_j}{\displaystyle\int_{\substack{outgoing \\ hemisphere}} \cos\theta_j\, d\omega_j} \qquad\qquad [11\text{--}94]$$

Where for $\tau^f_{hem,i}$, $\tau^f_{j,i}$ is used and for $\tau^b_{hem,i}$, $\tau^b_{j,i}$ is used. The solid angle of the outgoing hemisphere Ω can be expressed in terms of θ and ω:

$$d\omega_j = \frac{1}{2\pi}\sin\theta_j d\theta_j d\varphi_j \qquad\qquad [11\text{--}95]$$

After re-arranging:

$$\tau_{hem,i} = \frac{1}{\pi}\int_{\theta_j=0}^{\pi/2}\int_{\varphi_j=0}^{2\pi} \tau_{j,i}\cos\theta_j\sin\theta_j\, d\theta_j\, d\varphi_j \qquad\qquad [11\text{--}96]$$

For a finite number of directions, a summation formula is used:

$$\tau_{hem,i} = \frac{\displaystyle\sum_{j=1}^{N}\tau_{j,i}\left(\sin^2\theta_j^{hi} - \sin^2\theta_j^{lo}\right)\cdot\Delta\varphi_j}{2} \qquad\qquad [11\text{--}97]$$

where N is number of (incident and outgoing) directions. This again applies to both front and back directions. This can be written as:

$$\tau^f_{hem,i} = \sum_{j=1}^{N}\tau^f_{j,i}\Lambda_j \qquad\qquad [11\text{--}98]$$

$$\tau^b_{hem,i} = \sum_{j=1}^{N}\tau^b_{j,i}\Lambda_j \qquad\qquad [11\text{--}99]$$

where $\tau_{j,i}^f$ and $\tau_{j,i}^b$ correspond to $\tau_{j,i}$ elements of **TAU_F** or **TAU_B** matrix, and Λ_j is a Lambda value that corresponds to j-th outgoing direction, calculated using equation *[11–80]*. Essentially, the front hemispherical transmittance for i-th incident direction is obtained by averaged summation of the i-th column of **TAU_F** matrix.

Similarly, front/back hemispherical reflectances are obtained using:

$$\rho_{hem,i} = \frac{\displaystyle\sum_{j=1}^{N}\rho_{j,i}\left(\sin^2\theta_j^{hi} - \sin^2\theta_j^{lo}\right)\cdot\Delta\varphi_j}{2} \qquad\qquad [11\text{--}100]$$

This can be written as:

$$\rho^f_{hem,i} = \sum_{j=1}^{N} \rho^f{}_{j,i} \Lambda_j \qquad \text{[11–101]}$$

$$\rho^b_{hem,i} = \sum_{j=1}^{N} \rho^b{}_{j,i} \Lambda_j \qquad \text{[11–102]}$$

11.3.5. Hemispherical to Hemispherical Solar-optical Properties

Hemispherical to hemispherical (also referred to as *diffuse*) solar-optical properties (transmittances and reflectances) of the venetian blind layer are full integrated quantities, giving a scalar result independent from incident or outgoing directions. These scalar quantities are calculated from bi-directional results as well, by performing double integration, and they represent the amount of transmitted/reflected diffuse radiation as a result of diffuse incident radiation (Figure 11-30).
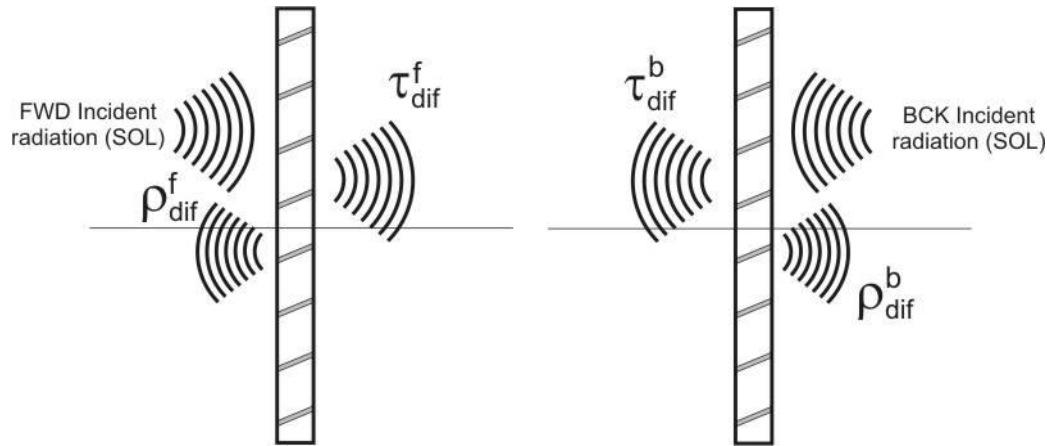
Figure 11-30. Diffuse (hemispherical-to-hemispherical) properties at front and back side of the Venetian blind

Hemispherical to hemispherical properties are easily calculated from the directional to hemispherical properties, as their integral sum over all incident angles. Transmittance is calculated as:

$$\tau_{dif} = \int_{\substack{incident \\ hemisphere}} \tau_{hem,i} \cdot \cos\theta_i \, d\omega_i \qquad \text{[11–103]}$$

Where $\tau_{hem,i}$ is direct to hemispherical transmittance for *i*-th incident direction, and ω_i is the unit solid angle of the hemisphere at the incident side of the blind.

After rearranging:

$$\tau_{dif} = \frac{1}{2\pi} \int_{\theta_i=0}^{\pi/2} \int_{\varphi_i=0}^{2\pi} \tau_{hem,i} \cdot \cos\theta_i \sin\theta_i \, d\theta_i \, d\varphi_i \qquad \text{[11–104]}$$

For a finite number of directions, *N*, a summation formula is used:

$$\tau_{dif} = \frac{1}{\pi} \sum_{i=1}^{N} \tau_{hem,i} \cdot \Lambda_i \qquad \text{[11–105]}$$

where Λ_i is a Lambda value that corresponds to i-th incident direction. This applies to both front and back directions:

$$\tau_{dif}^{f} = \frac{1}{\pi} \sum_{i=1}^{N} \tau_{hem,i}^{f} \cdot \Lambda_i \qquad [11-106]$$

$$\tau_{dif}^{b} = \frac{1}{\pi} \sum_{i=1}^{N} \tau_{hem,i}^{b} \cdot \Lambda_i \qquad [11-107]$$

where $\tau_{hem,i}^{f}$ and $\tau_{hem,i}^{b}$ represent the front and back directional to hemispherical transmittance for i-th incident direction, calculated using equations *[11−98]* and *[11−99]*, respectively. Note that τ_{dif}^{f} must be equal to τ_{dif}^{b}, so it is sufficient to calculate diffuse transmittance for one side of the blind only.

Similarly, front and back diffuse reflectances are calculated as:

$$\rho_{dif}^{f} = \frac{1}{\pi} \sum_{i=1}^{N} \rho_{hem,i}^{f} \cdot \Lambda_i \qquad [11-108]$$

$$\rho_{dif}^{b} = \frac{1}{\pi} \sum_{i=1}^{N} \rho_{hem,i}^{b} \cdot \Lambda_i \qquad [11-109]$$

where $\rho_{hem,i}^{f}$ and $\rho_{hem,i}^{b}$ are front and back directional to hemispherical reflectance for i-th incident direction, calculated using equations *[11−101]* and *[11−102]*, respectively.

11.4. Far Infra-RED (FIR) Mathematical Models

11.4.1. Introduction

Optical properties of the Venetian blind in far infra-red (FIR) range are:

- IR transmittance, τ IR

- IR emissivity of the front side of the blind, ε f

- IR emissivity of the back side of the blind, ε b

These are hemispherical-to-hemispherical, which means that they are not angle dependent. In addition to material properties, which are purely diffuse, just like in SOL range, in the FIR range the incident radiation is also always diffuse, which means that calculation of layer properties are done using only the Dif-Dif procedure. The transmittance and reflectance are ratios of outgoing diffuse radiation with incident diffuse radiation and they are a single scalar value for forward and backward directions. Note that τ IR must be equal for both directions, front and back:

$$\tau_{IR} = \tau_f = \tau_b \qquad [11-110]$$
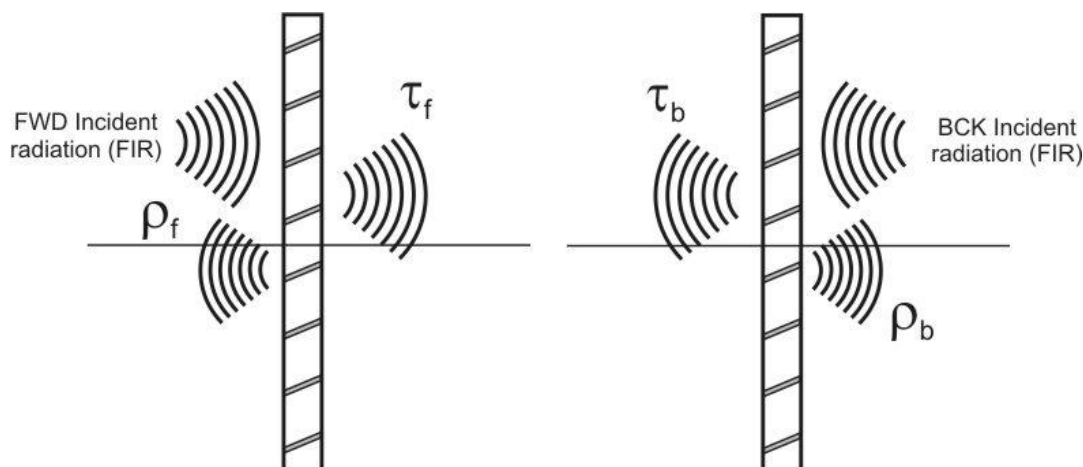
Figure 11-31. FIR properties (front and back) of the Venetian blind

Following the notations from Figure 11-31, the appropriate values for emissivities can be obtained using:

$$\tau_{IR} = \tau_{IR}^f = \tau_{IR}^b$$
$$\varepsilon^f = 1 - \tau_{IR} - \rho_{IR}^f \qquad\qquad [11–111]$$
$$\varepsilon^b = 1 - \tau_{IR} - \rho_{IR}^b$$

In these calculations, single band FIR range properties of the slat material are used (τ_{IR}, ρ_{IR}^f, and ρ_{IR}^b).

Transmittance and front and back reflectance in FIR range of the Venetian blind layer can be calculated using either a) ISO 15099 Dif-Dif methodology; b) BTDF/BRDF uniform diffuse method and then doing hemispherical-to-hemispherical integration, presented in Section 11.3.3; or c) BTDF/BRDF directional diffuse method and then doing hemispherical-to hemispherical integration. Each of these methods is expected to produce identical final results.

11.4.2. ISO15099 Method

ISO15099 FIR method is a direct implementation of Dif-Dif calculation procedure from Section 11.2.2.2. The calculations are done for a single band using FIR properties of the slat material.

11.4.3. Bi-Directional Methods

These methods use BTDF/BRDF matrices, obtained using either Uniform Diffuse or Directional Diffuse bi-directional calculation method. This calculation is done for a single set of FIR slat material properties.

Bidirectional results are integrated over the two hemispheres (in which all incident and outgoing directions are defined), resulting in three hemispherical FIR values: τ, ρ^f and ρ^b. These integrations are done the same way as in the case of hemispherical to hemispherical solar optical properties, as shown in Section 11.3.3. Transmittance, τ, can be calculated from either front or back transmittance matrix, using equation *[11–106]* or *[11–107]*. Reflectances, ρ, can be calculated from front and back reflectance matrices, using equations *[11–108]* and *[11–109*.

11.4.4. Vertical LOUVERED blinds

Venetian blinds are common name for relatively narrow (i.e., 1-2 in.) horizontally oriented louvered blinds. In order to model vertical louvered blinds, which are more typical for taller fenestration systems and are typically wider (i.e., 4 in. or wider), the coordinate system of the horizontal blind needs to be rotated by 90°

around the z axis (in xOy plane).   Adopting the convention that positive venetian blind rotation is in a counterclockwise direction, that means that the coordinate system of the BSDF hemisphere needs to be rotated in the opposite direction, or by -90° (90° clockwise). The result is that φ = 0° becomes φ = -90° (or 270°), and φ = 90° becomes φ = 0, etc.

11.4.5. Other Angles

The rotation of the Venetian blind around the z axis may not be restricted to the vertical direction only. Theoretically, we can rotate it by any angle increment. In this case, the BSDF hemisphere rotation needs to be done by an equal but opposite rotation. So if the Venetian blind is rotated by x°, the BSDF hemisphere coordinate system needs to be rotated by -x°. It is not clear if this arbitrary angle of the louvered blind (i.e., angles other than horizontal or vertical) has any practical application, however this functionality is provided so that it is fairly general.

Note that φ angles need to be kept in the range from 0 to 360, so when the rotation of the BSDF hemisphere coordinate system results in negative values they will need to be recalculated "back" to 0-360 range. For example, an angle of -45⁰ is equal to 315⁰, etc..

11.5. Indexing of Incident and Outgoing Directions in BSDF Matrices

The following figures illustrate the indexing of incident and outgoing directions in BSDF matrices. The full angular basis, which consists of 145 directions, was assumed. The full angular basis contains a normal direction, plus 8 strips defined by a latitude angle θ, with each θi strip divided into Nφi equal bins (i = 1, … , 8), as shown in Table 11-3.

Table 11-3. *Number of directions per one θ strip*

Theta index i	θ_i	$N\varphi_i$	$\Delta\varphi_i$
1	0°	1	360°
2	10°	8	45°
3	20°	16	22.5°
4	30°	20	18°
5	40°	24	15°
6	50°	24	15°
7	60°	24	15°
8	70°	16	22.5°
9	82.5°	12	30°

Directions are numbered 1-145, with direction 1 being the normal direction (θ=0°), followed by directions from each strip, beginning with $\varphi = 0°$, and ending with $\varphi = (N\varphi_i - 1) \cdot \Delta\varphi_i$.

For example:

- direction 31 is defined by (θ = 30°, φ = 90°);

- direction 41 is defined by (θ = 30°, φ = 270°);

- direction 100 is defined by (θ = 60°, φ = 90°);

- direction 112 is defined by (θ = 60°, φ = 270°);

The dimension of four BSDF matrices for the full angular basis is 145.

Figure 11-32 describes an element of front BTDF matrix **TAU_F**, placed in 112th column of the 31st row. This element represents a ratio of forward-going radiance, leaving the blind at outgoing direction 31, to incident forward-going irradiance, coming from incident direction 112. Note that both incident and outgoing directions are defined in *z* hemisphere. Figure 11-33 and Figure 11-34 show elements **TAU_F**(41,112) and **TAU_F**(31,31), respectively.
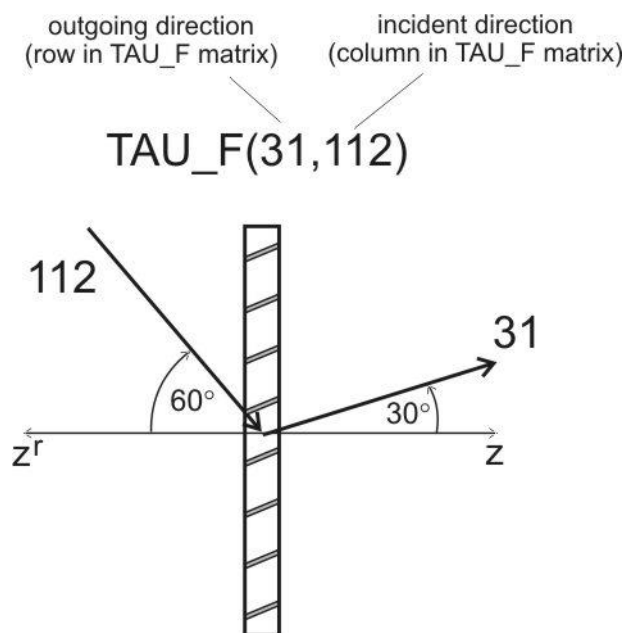
Figure 11-32. Front bi-directional transmittance, inc. direction 112, out. dir. 31
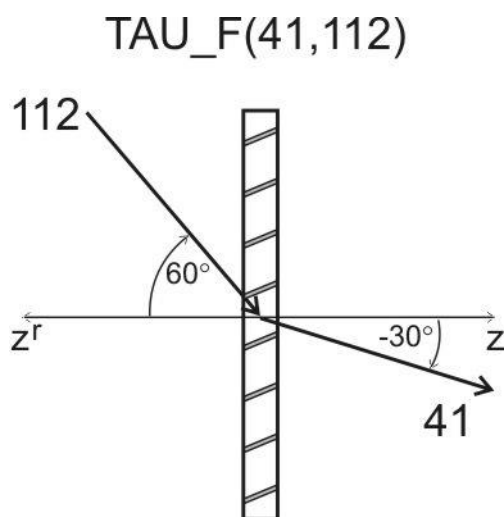
Figure 11-33. Front bi-directional transmittance, inc. direction 112, out. dir. 41

Figure 11-35 shows a member of front reflectance matrix – **RHO_F**(31,112). In this case, the outgoing direction 31^r is defined in z^r hemisphere.

TAU_F(31,31)
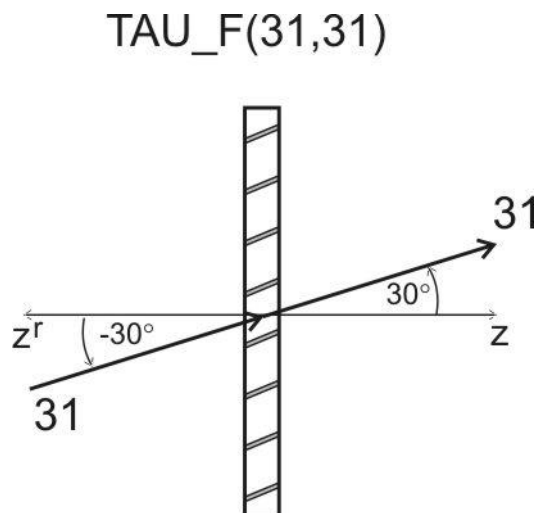
Figure 11-34. Front bi-directional transmittance, inc. direction 31, out. dir. 31

RHO_F(31,112)
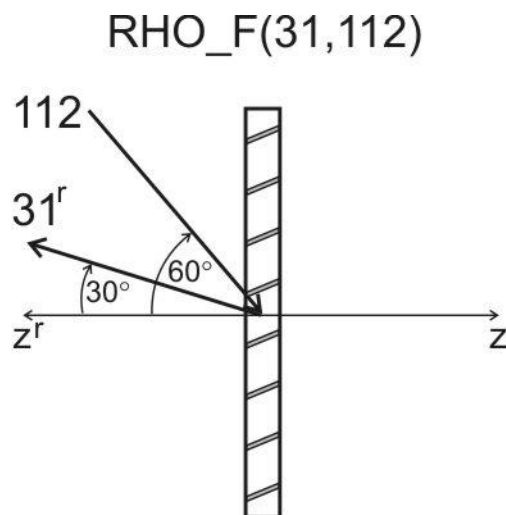
Figure 11-35. Front bi-directional reflectance, inc. direction 112, out. dir. 31ʳ

Figure 11-36 shows a member of back transmittance matrix – **TAU_B**(31,112). In this case, both incident and outgoing directions (112^r and 31^r, respectively) are defined in z^r hemisphere.

Figure 11-37 shows a member of back reflectance matrix – **RHO_B**(100,112). Incident direction 112^r is defined in z^r hemisphere, while outgoing direction 100 is defined in z hemisphere.

TAU_B(31,112)
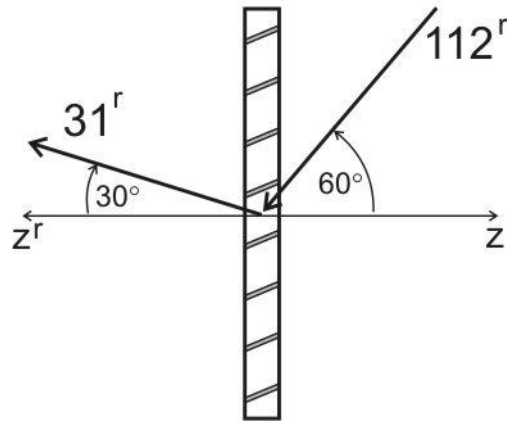
Figure 11-36. *Back bi-directional transmittance, inc. direction 112ʳ, out. dir. 31ʳ*

RHO_B(100,112)
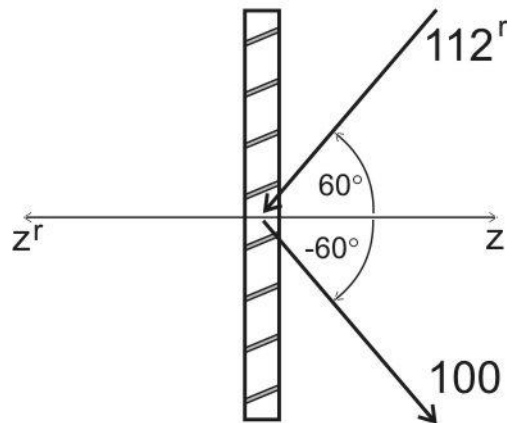
Figure 11-37. *Back bi-directional reflectance, inc. direction 112ʳ, out. dir. 100*

12. WOVEN SHADE TYPE OF SHADING DEVICE

Woven shades are types of shading devices that are typically installed on the interior of the building façade but this model allows the shade to be placed in any position (exterior, interior or between glass).

The purpose of this document is to present a proposal for the implementation of a calculation of bi-directional solar optical properties of woven shade devices in LayerOptics.dll, which is based on the direct transmittance model by Klems (2006) and the diffuse reflectance model by FSEC (McCluney 2006). This methodology will be implemented in a function called WovenShade. The input arguments for this function are the geometry of a woven shade device, the front and back diffuse reflectance and transmittance of the shade material, and the definition of the directions of interest, for which the bi-directional properties of the device will be calculated. The output arguments are four matrices: BTDF (Bi-directional Transmittance Distribution function) and BRDF (Bi-directional Reflectance Distribution function), with bi-directional properties at the front and back side of the device.

12.1. Direct transmittance model

The geometry of a simple woven shade of evenly-spaced threads in a cross-sectional plane perpendicular to one of the thread directions is shown in Figure 12-1. (It is assumed that the threads of the weave run horizontally and vertically). It can be seen from the figure that this simple geometry is characterized by the periodicity, L, of the weave, which here is the center-to-center distance between the threads, and the radius, r, of the thread. The projected transmittance at normal incidence in this two-dimensional model is simply the ratio d_0.
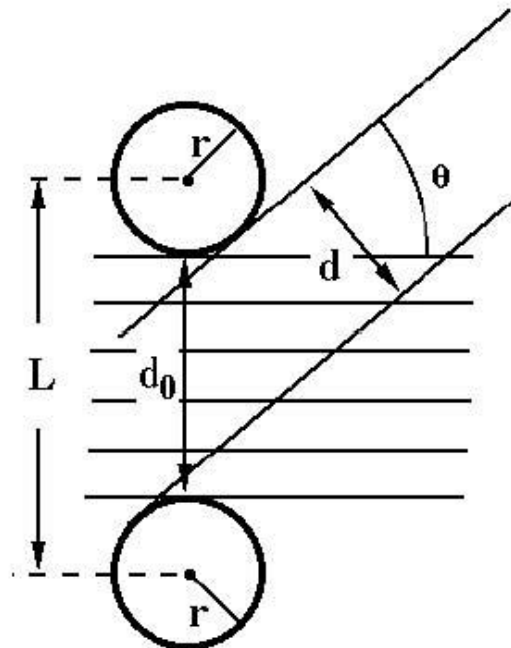
Figure 12-1. Simplified Two-Dimensional Geometry for a Simple Woven Screen.
Horizontal lines indicate normal-incidence radiation. Taken from Klems (2006)
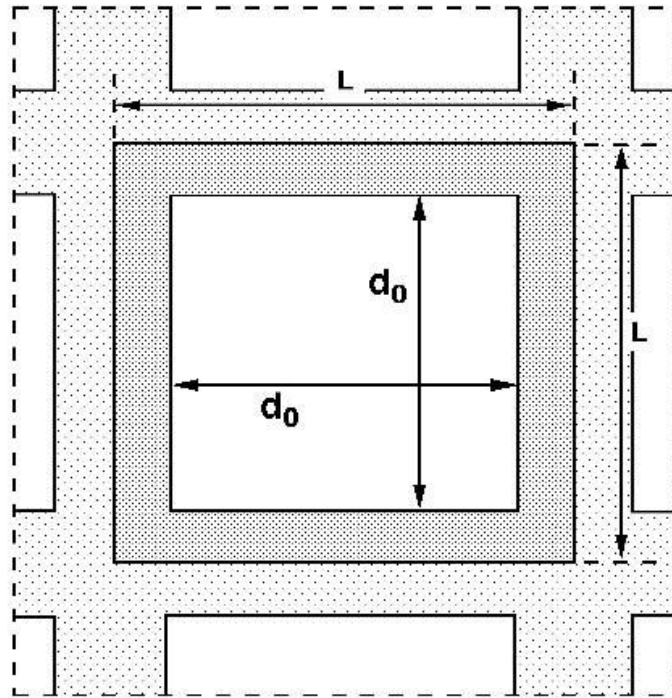
Figure 12-2. Typical Unit Cell of a Simple Square-weave Screen. Taken from Klems (2006)

Considering that the woven shade is made of transparent materials, the transmittance can be divided into two parts: direct-direct and direct-diffuse.

12.1.1. Direct-direct transmittance

By assuming a regular square weave pattern as shown in Figure 12-2, the normal transmittance gives the necessary ratio,

$$T_{dir-dir}(0) = \left(\frac{d_0}{L}\right)^2 \qquad \text{[12-1]}$$

For an incident direction with the angles (θ,φ), where the azimuthal angle is defined with the φ= 0 axis in the horizontal plane,

$$\cos\theta_{H,sol} = \frac{\cos\theta_{sol}}{\sqrt{\sin^2\theta_{sol}\cos^2\phi_{sol} + \cos^2\theta_{sol}}} \qquad \text{[12-2]}$$

$$\cos\theta_{V,sol} = \frac{\cos\theta_{sol}}{\sqrt{\sin^2\theta_{sol}\sin^2\phi_{sol} + \cos^2\theta_{sol}}} \qquad \text{[12-3]}$$

And the transmittance as a function of incidence direction is then:

$$T_{dir-dir}(\theta_{sol},\phi_{sol}) = MAX \begin{Bmatrix} \left[\cos\theta_{H,sol} - \left(1 - \sqrt{T_{dir-dir}(0)}\right)\right] \cdot \\ \left[\cos\theta_{V,sol} - \left(1 - \sqrt{T_{dir-dir}(0)}\right)\right], 0 \end{Bmatrix} \qquad \text{[12-4]}$$

And the condition $T_{dir-dir}(\theta_{sol},\phi_{sol})=0$ defines a cutoff contour in $(\theta_{sol},\phi_{sol})$ that reflects the rectilinear geometry of the weave. Angles θ_{sol} and ϕ_{sol} are relative solar azimuth and relative solar altitude (see Figure 12-7).

Using the same procedure to calculate directly transmitted radiation, McCluney (2006), gives the comparison between the result of such analytical model and ray tracing, as shown in Figure 12-3.
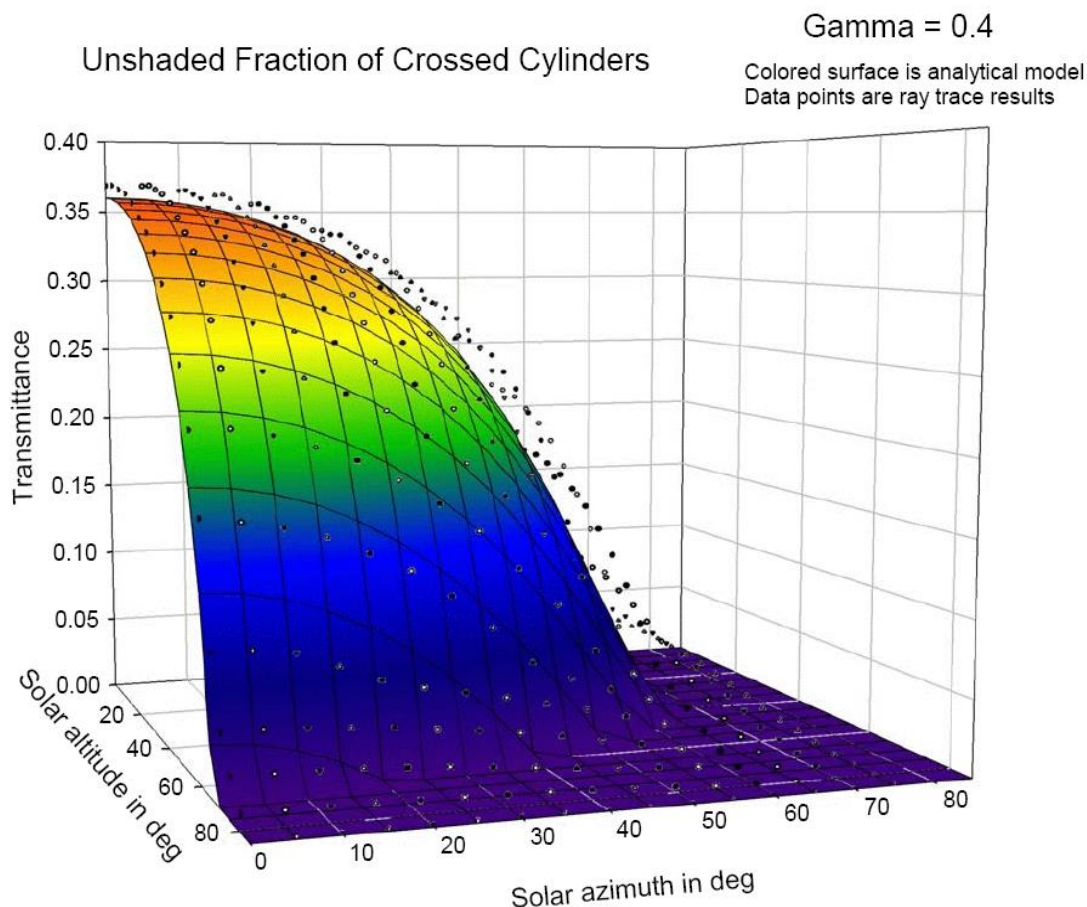
Figure 12-3. Analytical model output for Unshaded Fraction (transmittance).
Taken from McCluney (2006)

12.1.2. Direct-diffuse transmittance

The direct to diffuse transmittance is calculated as the transmittance through the woven thread in addition to the component of the beam reflected off the thread.
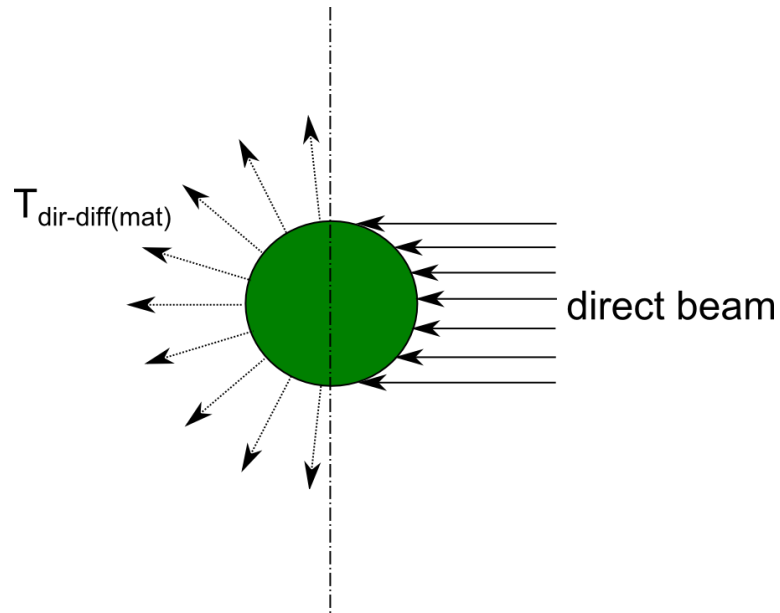
Figure 12-4. *Direct to diffuse transmittance through woven thread*

12.1.2.1. Direct-diffuse transmittance through woven thread

Considering that the unobstructed beam through the woven layer is calculated by Equation [12-1], then the transmitted beam from beam hitting material is simply equal to:

$$T_{dir-diff(mat)}(\theta,\phi) = (1 - T_{dir-dir}(\theta,\phi)) \cdot T_{material}$$

[12-5]

Where $T_{dir-diff(mat)}(\theta,\phi)$ is the transmittance through the material thread for given (θ,ϕ) incident angles (see Figure 12-7), $T_{dir-dir}(\theta,\phi)$ is defined by Equation [12-4] and $T_{material}$ is the transmittance of the woven thread.

12.1.2.2. Direct-diffuse transmittance reflected off woven thread

For some angles, a certain part of the incident beam hits the back side of the woven thread and gets reflected off the thread to the back side. That part of the reflected beam makes direct-diffuse transmittance.
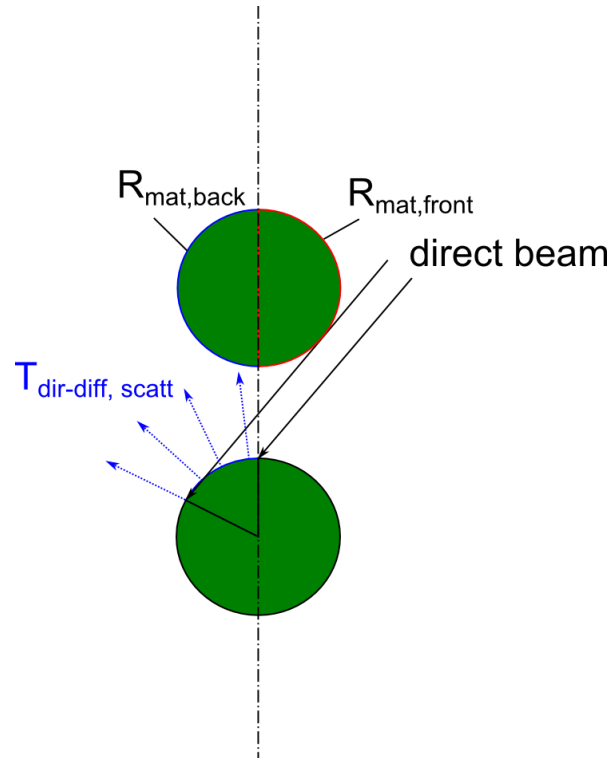
Figure 12-5. Scattered transmittance

The FSEC window screen model calculates diffuse (scattered) transmittance using the geometry of the woven shade material and the relative position of the sun with respect to the surface outward $T_{scatter}$, a part of the beam solar radiation which is reflected inward from the cylinder's surface.

The scattering contribution to the transmittance in Figure 12-6 is equivalent to $T_{scatter}$. Figure 12-6 shows the additive component for the scattered transmittance for a screen material having an aspect ratio of 0.4 and a material reflectance of 0.4. Although this component is shown to be highly directional, the magnitude (0.055) is small compared to the transmittance of a totally absorbing surface. For this reason, the scattered transmittance due to a reflective screen material surface will be added directly to the transmittance of a totally-absorbing screen material (or could be considered as beam-to-diffuse transmittance). Figure 12-6 shows distribution of $T_{scatter}$ for Aspect ratio 0.4.
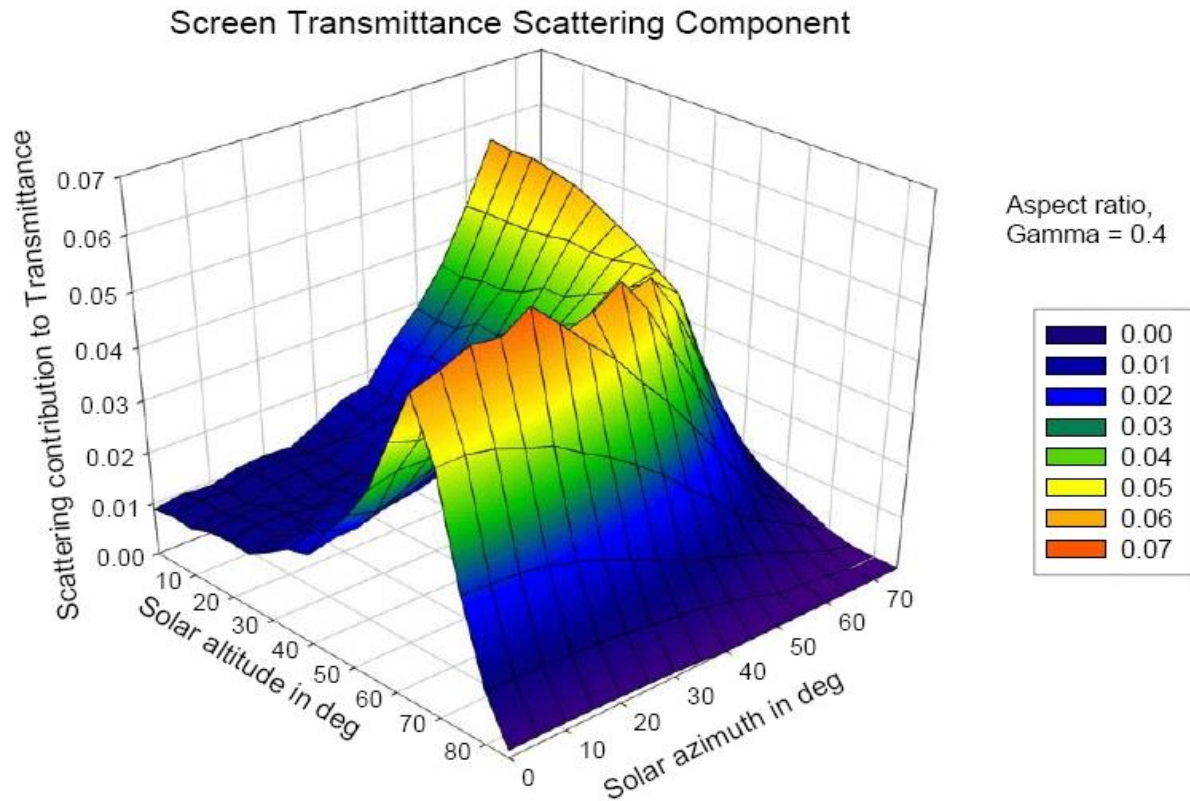
Figure 12-6. Transmittance due to reflective property of screen material

Diffuse transmittance is calculated for each time step based on sun position and surface orientation. To account for the variation in the front surface reflectance for varying sun angles, a simplified model is used. The front surface reflectance model is based on the geometry of the screen material and the reflectance property of the screen material cylinders. The following equations are used for the calculation of front and back $T_{scatter}$:

$$\gamma = D/S \hfill \text{[12-6]}$$

where D is the thread diameter and S is the thread spacing.

$$T_{scatt,front,MAX} = 0.0229 \cdot \gamma + 0.2971 \cdot R_{mat,back} - 0.03624 \cdot \gamma^2 + 0.04763 \cdot R_{mat,back}^2 - 0.44416 \cdot \gamma \cdot R_{mat,back} \hfill \text{[12-7]}$$

where $R_{mat,back}$ is the thread material reflectance on the back side of the woven shade (see Figure 12-5). The same equation is used for the back side with the difference that $R_{mat,\text{front}}$ will be used instead.

$$PeakRatio_{front} = \frac{1}{(0.2 \cdot R_{mat,back} \cdot (1-\gamma))} \hfill \text{[12-8]}$$

$$TscFactor_{front} = 0.2 \cdot R_{mat,\text{back}} \cdot T_{scatt,front,\text{MAX}} \cdot (1-\gamma) \hfill \text{[12-9]}$$

$$\delta_{\deg} = \sqrt{\theta_{sol,\deg}^2 + \phi_{sol,\deg}^2} \hfill \text{[12-10]}$$

where $\theta_{sol,\text{deg}}$ and $\phi_{sol,\text{deg}}$ are relative solar azimuth and relative solar altitude given in degrees.

$$\delta_{\max} = 89.7 - 10 \cdot \frac{\gamma}{0.16} \qquad\qquad [12\text{-}11]$$

$$E_1 = -\frac{\left|\delta_{\text{deg}} - \delta_{\max}\right|^2}{600} \qquad\qquad [12\text{-}12]$$

$$E_2 = -\frac{\left|\delta_{\text{deg}} - \delta_{\max}\right|^{2.5}}{600} \qquad\qquad [12\text{-}13]$$

$$\delta = \frac{\delta_{\text{deg}} - \delta_{\max}}{90 - \delta_{\max}} \qquad\qquad [12\text{-}14]$$

and finally the scattered part of the transmittance is calculated as:

$$\delta_{\text{deg}} \le \delta_{\max}$$

$$T_{scatt,front} = TscFactor_{front} \cdot (1 + (PeakRatio_{front} - 1) \cdot e^{E_1}) \qquad\qquad [12\text{-}15]$$

$$\delta_{\text{deg}} > \delta_{\max}$$

$$T_{scatt,front} = TscFactor_{front} \cdot (1 + (PeakRatio_{front} - 1) \cdot e^{E_2} - TscFactor_{front} \cdot \delta \qquad\qquad [12\text{-}16]$$
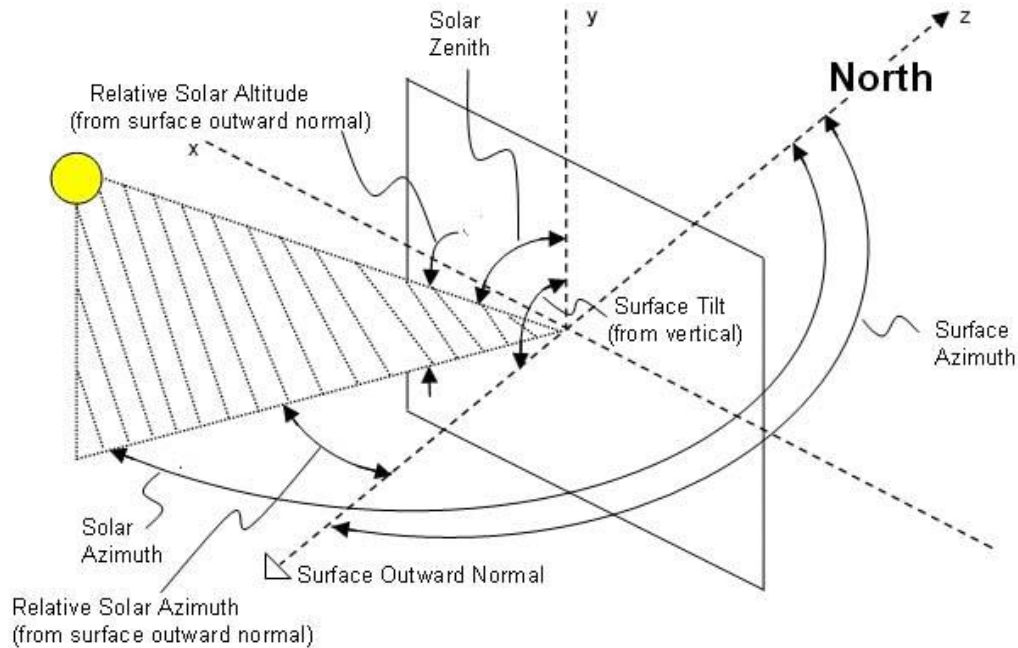
Figure 12-7. Schematic of window screen facing due south

12.2. Diffuse reflectance model

The FSEC model calculates the reflectance of the screen as:

$$R_{scatter,front} = R_{mat,front} \cdot \left(1 - T_{direct,front}\right) - T_{scatter,front} \qquad \text{[12-17]}$$

where r is the reflectance of the window screen material.

It should be noted that the form of this equation in McCluney (2006) is somewhat different due to an error in the derivation. Within the simplifying assumptions, this is the correct version of the equation.

The overall absorptance of the woven shade material is then:

$$A_{front} = 1 - \left(T_{direct,front} + T_{scatter,front} + R_{scatter,front}\right) \qquad \text{[12-18]}$$

Which reduces to:

$$A_{front} = \left(1 - R_{mat,front}\right) \cdot \left(1 - T_{direct,front}\right) \qquad \text{[12-19]}$$

12.3. Conversion from BSDF to solar coordinate system

To calculate BSDF values one needs to convert the BSDF coordinate system into the solar coordinate system. This can be done by applying the equations described in this chapter.

θ and φ are angles as described in "*Chapter 11. Louvered Blinds*", and θ_{solar} and ϕ_{solar} are relative solar azimuth and relative solar altitude as previously explained.

$\varphi \in [90, 270]$

$$\theta_{solar} = \arctan(\frac{\sin(\theta) \cdot \cos(\varphi)}{\cos(\theta)}) \qquad \text{[12-20]}$$

$\varphi \in [0, 90] \, or \, \varphi \in [270, 360]$

$$\theta_{solar} = -\arctan(\frac{\sin(\theta) \cdot \cos(\varphi)}{\cos(\theta)}) \qquad \text{[12-21]}$$

$\varphi \in [0, 180]$

$$\phi_{solar} = -\arccos(\sqrt{\cos(\theta)^2 + \sin(\theta)^2 \cdot \cos(\varphi)^2}) \qquad \text{[12-22]}$$

$\varphi \in [180, 360]$

$$\phi_{solar} = \arccos(\sqrt{\cos(\theta)^2 + \sin(\theta)^2 \cdot \cos(\varphi)^2}) \qquad \text{[12-23]}$$

12.4. Wovenshade function

The WovenShade function will calculate the bi-directional properties, transmittance and reflectance, which are defined for each combination of incident and outgoing direction, and as a result will form BTDF and BRDF matrices.

The WovenShade function will perform calculations according to the Klems and the FSEC model. Because the FSEC model provides properties for a single incident direction, the WovenShade method must perform a

series of calculations in order to produce bi-directional properties for all incident and outgoing directions. The directions of interest will be defined as in the Venetian blind function.

For a given incident direction i, defined by the pair of angle coordinates (Theta$_i$, Phi$_i$), transmittances $T_{direct,i}$ and $T_{scatter,i}$ are calculated. In order to get the bi-directional transmittance, $T_{direct,i}$ must be divided with the Lambda factor before putting into the appropriate place in the result matrix, which is at the diagonal (as the directly transmitted component exists only for the outgoing direction that is collinear with the incident direction). Lambda is the propagation operator which transforms the radiance vector emerging from one layer into irradiance vectors incident on the next layer. $T_{scatter,i}$ which is a hemispherical property, must be divided with Pi in order to obtain the bi-directional transmittance (Pi transforms diffuse outgoing radiance into direct outgoing radiance). These values will be placed in the i-th column of a BTDF matrix, which corresponds to the i-th incident direction.

This procedure is repeated for each incident direction. Direct and scattered components of the bi-directional transmittances are summed to form the **TAU_F** matrix, (Equation [12-24]).

$$
TAU\_F = \begin{bmatrix}
\dfrac{T^f_{direct,1}}{\Lambda_1} + \dfrac{T^f_{scatter,1}}{\pi} & \dfrac{T^f_{scatter,2}}{\pi} & \cdots & \dfrac{T^f_{scatter,N}}{\pi} \\[4mm]
\dfrac{T^f_{scatter,1}}{\pi} & \dfrac{T^f_{direct,2}}{\Lambda_2} + \dfrac{T^f_{scatter,2}}{\pi} & \cdots & \dfrac{T^f_{scatter,N}}{\pi} \\[4mm]
 & & \cdots & \\
\cdots & \cdots & \cdots & \cdots \\[4mm]
\dfrac{T^f_{scater,1}}{\pi} & \dfrac{T^f_{scatter,2}}{\pi} & \cdots & \dfrac{T^f_{direct,N}}{\Lambda_N} + \dfrac{T^f_{scatter,N}}{\pi}
\end{bmatrix}
$$

[12-24]

The same procedure is applied for backward incident directions. The **TAU_B** matrix, (Equation [12-25]), consists of backward bi-directional transmittances.

$$
TAU\_B = \begin{bmatrix}
\dfrac{T^b_{direct,1}}{\Lambda_1} + \dfrac{T^b_{scatter,1}}{\pi} & \dfrac{T^b_{scatter,2}}{\pi} & \cdots & \dfrac{T^b_{scatter,N}}{\pi} \\[4mm]
\dfrac{T^b_{scatter,1}}{\pi} & \dfrac{T^b_{direct,2}}{\Lambda_2} + \dfrac{T^b_{scatter,2}}{\pi} & \cdots & \dfrac{T^b_{scatter,N}}{\pi} \\[4mm]
 & & \cdots & \\
\cdots & \cdots & \cdots & \cdots \\[4mm]
\dfrac{T^b_{scatter,1}}{\pi} & \dfrac{T^b_{scatter,2}}{\pi} & \cdots & \dfrac{T^b_{direct,N}}{\Lambda_N} + \dfrac{T^b_{scatter,N}}{\pi}
\end{bmatrix}
$$

[12-25]

Scattered reflectances $R_{scatter,i}$ are hemispherical values, calculated according to Equation ([12-17]). As in the case of scattered transmittance, these values must be divided with Pi in order to get bi-directional reflectances. The **RHO_F** matrix (Equation [12-26]) contains front bi-directional reflectances, while **RHO_B** matrix (Equation [12-27]) contains back bi-directional reflectances.

$$
\text{RHO\_F} = \begin{bmatrix}
\dfrac{R^f_{scatter,1}}{\pi} & \dfrac{R^f_{scatter,2}}{\pi} & \cdots & \dfrac{R^f_{scatter,N}}{\pi} \\[2ex]
\dfrac{R^f_{scatter,1}}{\pi} & \dfrac{R^f_{scatter,2}}{\pi} & \cdots & \dfrac{R^f_{scatter,N}}{\pi} \\[2ex]
& & \cdots & \\[1ex]
\cdots & \cdots & \cdots & \cdots \\[2ex]
\dfrac{R^f_{scatter,1}}{\pi} & \dfrac{R^f_{scatter,2}}{\pi} & \cdots & \dfrac{R^f_{scatter,N}}{\pi}
\end{bmatrix}
$$

[12-26]

$$
\text{RHO\_B} = \begin{bmatrix}
\dfrac{R^b_{scatter,1}}{\pi} & \dfrac{R^b_{scatter,2}}{\pi} & \cdots & \dfrac{R^b_{scatter,N}}{\pi} \\[2ex]
\dfrac{R^b_{scatter,1}}{\pi} & \dfrac{R^b_{scatter,2}}{\pi} & \cdots & \dfrac{R^b_{scatter,N}}{\pi} \\[2ex]
& & \cdots & \\[1ex]
\cdots & \cdots & \cdots & \cdots \\[2ex]
\dfrac{R^b_{scatter,1}}{\pi} & \dfrac{R^b_{scatter,2}}{\pi} & \cdots & \dfrac{R^b_{scatter,N}}{\pi}
\end{bmatrix}
$$

[12-27]

13. PERFORATED SCREEN TYPE OF SHADING DEVICE

Perforated screens are types of shading devices that are typically installed on the exterior of a commercial building façade. Figure 13-1 shows an example of a perforated screen product.

The solar optical performance of these shading devices depends on the geometry and the properties of the material that these devices are made of. In the first approximation, it will be assumed that the transmittance of these products is based on the geometry of the openings alone and on the bulk transmittance and reflectance of the material. Any diffuse reflections from the edge of the openings will be ignored. This assumption is believed to produce very small errors, because the thickness of these devices is normally quite small and the openings are well defined, without much scattering back.
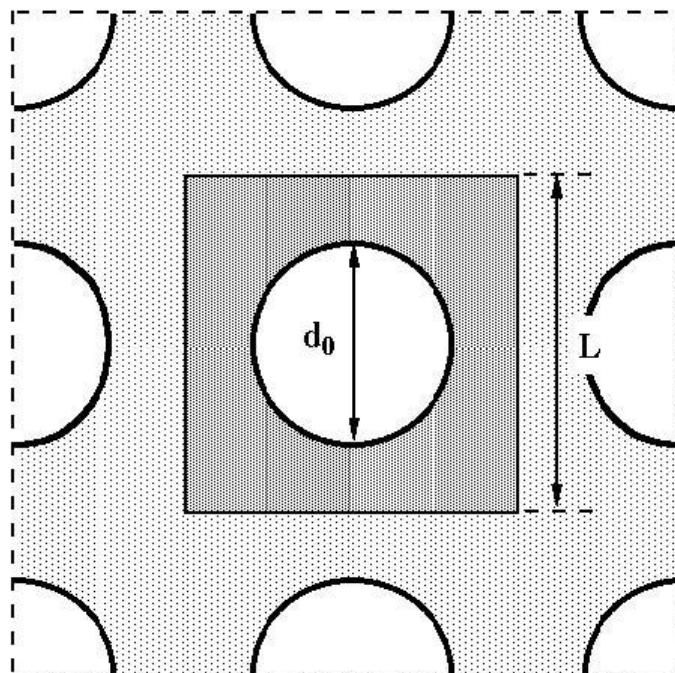
Figure 13-1. Typical unit cell of a circular perforated screen
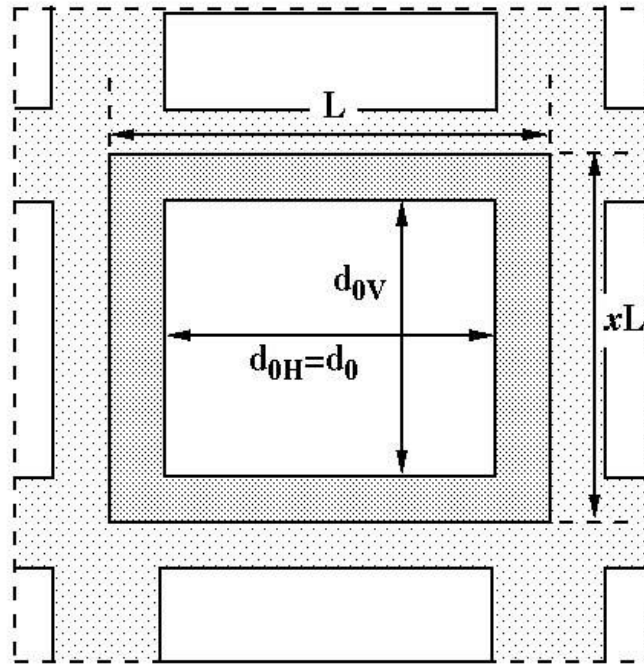
Figure *13-2. Typical unit cell of a rectangular perforated screen*

13.1. Direct-direct transmittance

13.1.1. Circular holes

The circular holes are fully symmetrical, so we can express the transmittance of the perforated screen with circular holes in terms of an incidence angle, θ

Profile angle:

$$T_{dir-dir}(\theta) = \frac{A_\theta^{hole}}{A_\theta^{cell}} \tag{13-1}$$

To calculate area of the hole at incidence angle θ

$$r_o' = r_o \cdot \cos\theta - t \cdot \sin\theta \tag{13-2}$$

The projected area of the opening consists of two semi-ellipses.

$$A_1 = \frac{\pi}{2} \cdot r_o \cdot r_o \cdot \cos\theta = \frac{\pi}{2} \cdot r_o^2 \cdot \cos\theta \tag{13-3}$$

$$A_2 = \frac{\pi}{2} \cdot r_o \cdot r_o' = \frac{\pi}{2} \cdot (r_o^2 \cdot \cos\theta - r_o \cdot t \cdot \sin\theta) \tag{13-4}$$

$$A_\theta^{hole} = A_1 + A_2 = \frac{\pi}{2} \cdot (2 \cdot r_o^2 \cdot \cos\theta - r_o \cdot t \cdot \sin\theta) \qquad [13\text{-}5]$$

$$A_\theta^{hole} = \pi \cdot r_o^2 \cdot \cos\theta \cdot (1 - \frac{t}{2 \cdot r_o} \cdot \tan\theta) \qquad [13\text{-}6]$$

$$A_\theta^{cell} = S_x \cdot S_y \cdot \cos\theta \qquad [13\text{-}7]$$

These formulas are valid between cutoff angles defined as:

$$\theta \in [0, \tan^{-1}\frac{2 \cdot r_o}{t}] \qquad [13\text{-}8]$$

Therefore,

$$T_{dir-dir}(\theta) = MAX([\pi \cdot (\frac{r_o}{L})^2 \cdot (1 - \frac{t}{2 \cdot r_o} \cdot \tan\theta)], 0) \qquad [13\text{-}9]$$

13.1.2. Quadratic holes

Quadratic holes do not exhibit the symmetry of the circular holes, so we will consider projections of the incident direction onto horizontal and vertical planes, commonly denoted as profile angle ψ, and azimuth angle η (see "*Chapter 15. BSDF Properties*" on the coordinates transformation).

Profile angle:

$$d_o' = d_o \cdot \cos\psi - t \cdot \sin\psi \qquad [13\text{-}10]$$

$$T_{dir-dir}^V(\psi) = \frac{d_o'}{S_y \cdot \cos\psi} = \frac{d_o}{S_y} - \frac{t}{S_y} \cdot \tan\psi \qquad [13\text{-}11]$$

These formulas are valid between cutoff angles defined as:

$$\psi \in [-\tan^{-1}\frac{d_o}{t}, \tan^{-1}\frac{d_o}{t}] \qquad [13\text{-}12]$$

Azimuth angle:

$$d_o' = d_o \cdot \cos\eta - t \cdot \sin\eta \qquad [13\text{-}13]$$

$$T_{dir-dir}^H(\eta) = \frac{d_o'}{S_x \cdot \cos\eta} = \frac{d_o}{S_x} - \frac{t}{S_x} \cdot \tan\eta \qquad [13\text{-}14]$$

These formulas are valid between cutoff angles defined as:

$$\eta \in [-\tan^{-1}\frac{d_o}{t}, \tan^{-1}\frac{d_o}{t}] \qquad [13\text{-}15]$$

Therefore, transmittance T can be expressed in terms of both angles:

$$T_{dir-dir}(\psi, \eta) = MAX([\frac{d_o}{S_y} - \frac{t}{S_y} \cdot \tan\psi], 0) \cdot MAX([\frac{d_o}{S_x} - \frac{t}{S_x} \cdot \tan\eta], 0) \qquad [13\text{-}16]$$

13.1.3. Rectangular holes

Rectangular holes are similar to square holes, except that the dimension in the x and y directions are not the same. We will still consider the projections of the incident direction onto horizontal and vertical planes, commonly denoted as profile angle ψ, and azimuth angle η (see *Chapter 15. BSDF Properties* on coordinates transformation).

Profile angle:

$$d'_{ov} = d_{ov} \cdot \cos\psi - t \cdot \sin\psi \qquad\qquad\qquad\text{[13-17]}$$

$$T^V_{dir-dir}(\psi) = \frac{d'_{ov}}{S_y \cdot \cos\psi} = \frac{d_{ov}}{S_y} - \frac{t}{S_y} \cdot \tan\psi \qquad\qquad\qquad\text{[13-18]}$$

These formulas are valid between cutoff angles defined as:

$$\psi \in [-\tan^{-1}\frac{d_{ov}}{t}, \tan^{-1}\frac{d_{ov}}{t}] \qquad\qquad\qquad\text{[13-19]}$$

Azimuth angle:

$$d'_{oh} = d_{oh} \cdot \cos\eta - t \cdot \sin\eta \qquad\qquad\qquad\text{[13-20]}$$

$$T^H_{dir-dir}(\eta) = \frac{d'_{oh}}{S_x \cdot \cos\eta} = \frac{d_{oh}}{S_x} - \frac{t}{S_x} \cdot \tan\eta \qquad\qquad\qquad\text{[13-21]}$$

These formulas are valid between cutoff angles defined as:

$$\eta \in [-\tan^{-1}\frac{d_{oh}}{t}, \tan^{-1}\frac{d_{oh}}{t}] \qquad\qquad\qquad\text{[13-22]}$$

Therefore, transmittance T can be expressed in terms of both angles:

$$T_{dir-dir}(\psi,\eta) = MAX([\frac{d_{ov}}{S_y} - \frac{t}{S_y} \cdot \tan\psi],0) \cdot MAX([\frac{d_{oh}}{S_x} - \frac{t}{S_x} \cdot \tan\eta],0) \qquad\text{[13-23]}$$

13.2. Direct-diffuse transmittance

Once the direct-direct transmittance is calculated (for circular and rectangular holes), the following equations are applied for the direct-diffuse components of transmittance and reflectance:

$$T_{dir-dif} = (1 - T_{dir-dir}) \cdot \tau_{mat} \qquad\qquad\qquad\text{[13-24]}$$

and

$$R_{dir-dif} = (1 - T_{dir-dir}) \cdot \rho_{mat} \qquad\qquad\qquad\text{[13-25]}$$

14. FRITTED GLAZING

Fritted glazing (also known as "frits") is a special type of glazing which consists of a glazing substrate (usually specular glass) and diffuse patterns on the glass, commonly referred to as frits. The frit layer consists of glass and in some cases colored pigments that are melted to bond to the substrate surface. This process can easily be masked so that a pattern of the fritted surface is created. Because of the presence of diffuse material, the whole glazing layer is considered to be a complex glazing, which requires a more sophisticated calculation of the glazing system optical properties, which incorporates the fritted glazing layer. These more complex calculations also require more detailed optical data, because the incoming direction of solar radiation is no longer equal to the outgoing direction, which is the case in specular glazing layers. The optical data for each complex glazing layer is provided in four matrices, one for front transmittance, one for back transmittance, one for front reflectance and one for back reflectance. Each matrix has data for 145 incident directions and 145 outgoing directions for each incident direction, therefore forming a 145 x 145 matrix of data, or 21,025 data points. These matrices are provided for each wavelength.

In the case of a highly spectrally selective layer, which is characterized by 300 wavelengths, the total amount of data is 4 x 21,025 x 300 or 215,230,000 data points. In comparison, specular glazing layer of the same spectral selectivity will have 300 transmittances, 300 front reflectances and 300 back reflectances, for a total of 900 data points.   Note that for a specular glazing layer, only one set of transmittance data is needed, as front and back transmittances in specular transmission are identical.

The WINDOW software, developed by Lawrence Berkeley National Laboratory, implements calculations for fritted glazing using the matrix data discussed above. In WINDOW, the spectral data for fritted glazing is stored in the WINDOW database in a table called SpectralData. In order to generate spectral data for a fritted glazing layer, measured optical data from the frit substrate glazing layer without the frit and from the frit substrate with the frit covering are combined using special algorithms, called "Fritted glazing composition", detailed in this report. The fritted glazing composition optical calculations use a two layer optical model. Data for each layer is stored in a database. The first layer is for the substrate data, and the second layer is for the frit data. However, frits can have a diffuse and specular portion. Both the diffuse and specular portion of frits are obtained by importing data from two different files (one for the front side and one for the back side measurements), for a total of four individual optical data files.

Columns of interest stored in the SpectralData table are:

- Wavelength
- T
- Rf
- Rb
- Tb

This document describes the algorithms and procedures for the fritted glazing composition optical calculations.

14.1. Optical data

The introduction of transmittance back is necessary since unlike for specular glazings, the transmittance does not have to be identical from the front and the back. All these matrices are three dimensional with the following dimensions:

1. (Glazing) Layer

2. Component

3. Index

(Glazing) Layer is used to denote the fritted glazing layer position in an Insulated Glazing Unit (IGU). For example, if the fritted glazing layer is glazing layer 2 in an IGU, then the (Glazing) Layer index will be equal to 1 (note that numbering starts from zero).

Component part is used to store the layer data representing the Frit layer. Since there are three layers used to represent one Frit, there will be three components stored in these arrays:

Component = 0 – Substrate data

Component = 1 – Specular data

Component = 2 – Diffuse data

Index is used to represent the data for each wavelength.

14.1.1. BSDF Data Model

Each fritted glazing layer has its optical data stored in a Bi-Directional Scattering Function (BSDF) format. BSDFs are matrices of transmittance and reflectance, where each matrix contains columns of incident directions and rows of outgoing directions. At the maximum, the BSDF is a 145 x 145 matrix, corresponding to the 145 incident and 145 outgoing directions (solid angles). For a smaller angular basis, the number of directions is reduced. Currently we have half basis (72 x 72 matrix) and quarter basis (36 x 36 matrix). Half and quarter basis may be used in calculations for improved speed, but the optical data for a layer is still stored in a full 145 x 145 matrix. One BSDF Matrix is created for each wavelength.

Optical calculations in WINDOW, using the Matrix calculation approach (mandatory for scattering glazing layers or shading devices) can be done for different wavelength ranges and for different angular bases definitions, as specified in Optical Calcs Preferences. Since frits are considered non-specular (i.e., diffuse) glazing layers, the matrix calculations will be performed independent of the setting for "Use matrix method for specular systems (glazing systems without shading devices)".

14.1.2. Specular properties

Matrices for a specular layer will have zero values, except for the values on the diagonal. The diagonal values will be calculated by using following equation:

$$BTDF_{(i)} = \frac{T(\lambda, i)}{\Lambda_i}$$

[14-1]

Where BTDF$_{(i)}$ represents the BSDF value for transmittance in the i-th direction, Λ_i Λ_i represents the solid angle partition for i-th direction, and $T(\lambda, i)$ is the transmittance for a specific wavelength (read from the spectral data tables) and adjusted for specific angular dependence. Note that Equation [14-1] is valid for back and front transmittance as well as for front and back reflectance. The matrix presentation of Equation [14-1] is:

$$
BTDF = \left\| \begin{array}{cccc} \dfrac{T(\lambda,1)}{\Lambda_1} & 0 & ... & 0 \\[2mm] 0 & \dfrac{T(\lambda,2)}{\Lambda_2} & ... & 0 \\[2mm] ... & ... & ... & 0 \\[2mm] 0 & 0 & ... & \dfrac{T(\lambda,N)}{\Lambda_N} \end{array} \right\|
$$

[14-2]

14.1.3. Fritted glazing composition optical calculations

Fritted glazing composition optical calculations consist of the following steps:

1. Specular optical properties of the frit layer readout

2. Diffuse optical properties of the frit layer readout

3. Create resultant frit layer matrix from the specular and diffuse optical properties

4. Substrate optical properties readout

5. Create fritted glazing BSDF by area weighting

After performing the above steps, the transmittance and reflectance (front and back) BSDF matrices (i.e., BTDF$_F$, BTDF$_B$, BRDF$_F$, BRDF$_B$) are created and are ready to be incorporated into the calculation of the glazing system, which may involve one or more specular glazing layers.

14.1.3.1. Specular optical properties of the frit layer

Specular optical properties are stored in a diagonal matrix, as described in previous section. Note that all four matrices are stored using the same diagonal matrix form.

14.1.3.2. Diffuse optical properties of the frit layer

For the diffuse portion of the BSDF there is no angular dependence. This means that transmittance and reflectance is uniform and identical for all angles and is only wavelength dependent. The values on the diagonal of this matrix are not used in the creation of the resultant matrix, and can be ignored.

Note: Because specular optical data is measured by subtracting diffuse from total radiation, where diffuse radiation is measured by the opening port in an integrating sphere, the specular component intrinsically includes the diffuse portion in the specular direction.

$$
BTDF_{res} = \left\| \begin{array}{cccc} 0 & \dfrac{T(\lambda)}{\pi-\Lambda_2} & ... & \dfrac{T(\lambda)}{\pi-\Lambda_N} \\[3mm] \dfrac{T(\lambda)}{\pi-\Lambda_1} & 0 & ... & \dfrac{T(\lambda)}{\pi-\Lambda_N} \\[3mm] ... & ... & ... & ... \\[3mm] \dfrac{T(\lambda)}{\pi-\Lambda_1} & \dfrac{T(\lambda)}{\pi-\Lambda_2} & ... & 0 \end{array} \right\|
$$

[14-3]

Equation [14-3] is valid for front and back transmittance as well as for front and back reflectance.

14.1.3.3. Frit layer optical matrix

The resultant matrices of the optical properties for the frit layer are created by adding the specular and diffuse matrices. The resultant matrix contains terms in a diagonal which are equal to the specular values, while the rest of the matrix is filled with the diffuse part.

$$BTDF = \begin{Vmatrix} \dfrac{T(\lambda)}{\Lambda_1} & \dfrac{T(\lambda)}{\pi - \Lambda_2} & \cdots & \dfrac{T(\lambda)}{\pi - \Lambda_N} \\ \dfrac{T(\lambda)}{\pi - \Lambda_1} & \dfrac{T(\lambda)}{\Lambda_2} & \cdots & \dfrac{T(\lambda)}{\pi - \Lambda_N} \\ \cdots & \cdots & \cdots & \cdots \\ \dfrac{T(\lambda)}{\pi - \Lambda_1} & \dfrac{T(\lambda)}{\pi - \Lambda_2} & \cdots & \dfrac{T(\lambda)}{\Lambda_N} \end{Vmatrix} \qquad [14\text{-}4]$$

This matrix is also valid for reflectance.

14.1.3.4. Substrate optical properties

Fritted glazing substrate data have the same format as the specular portion of the frit layer. Only the diagonal terms are non-zero.

14.1.3.5. Final fritted glazing properties

The substrate matrix is added to the frit layer optical matrix by weighting the area of the frit coverage. If the frit layer matrix is marked as $BTDF(\lambda)_{res}$ BTDF(λ)$_{res}$ and the substrate matrix is marked as $BTDF(\lambda)_{sub}$ then the final fritted glazing BSDF is created using following equation:

$$BTDF(\lambda)_{final} = FritCoverage \cdot BTDF(\lambda)_{res} + (1 - FritCoverage) \cdot BTDF(\lambda)_{sub} \qquad [14\text{-}5]$$

Where *FritCoverage* is a number between 0 and 1, and denotes the area fraction of frit coverage (i.e., 0.2 is 20% frit coverage, 0.5 is 50% frit coverage, etc.).

14.1.4. Angular dependence

Each term in the diagonal of the specular matrices correspond to an optical property at a given incidence angle. Since specular properties are only dependent on the overall incidence angle, without the consideration of solar azimuth, the only angular dependence is given with respect to incidence angle θ. Angular dependence for specular glazing is not measured, rather it is calculated.

14.2. Hemispherical Transmittance

Hemispherical transmittance is an integrated property at the outgoing direction, representing the overall optical properties for each incidence angle (i.e., each fritted glazing will have 145 hemispherical data points for each optical property (i.e., 145 Transmittances, 145 Reflectances)). The hemispherical transmittance is calculated for each incident direction by using the following equation:

$$T_{hem,i} = \frac{\sum_{j=1}^{N} \int T_{i,j} * cos(\theta_j) * d\omega_j}{\sum_{j=1}^{N} \int cos(\theta_j) * d\omega_j} \qquad [14\text{-}6]$$

Where $T_{i,j}$ is the transmittance between the incoming direction "i" and outgoing direction "j", θ_j is the angle between surface normal and direction "j", N is the number of outgoing directions, and both integrations in *[14-6]* are performed over the outgoing direction.

14.2.1. Solid Angle Transformation

In order to calculate the integration given by *[14-6]*, a spherical coordinate system is used. In order to do integration in a spherical coordinate system, the infinitesimal angle dω needs to be transferred into the spherical coordinate system. Since all outgoing rays are covered by outgoing half-sphere, integration of the solid angle over the half-sphere should be equal to 1. Therefore, we can calculate the solid angle by simple division of dA and A:

$$dω = \frac{dA}{A}$$

[14-7]

Where A is area of the half-sphere while dA is area of the infinitesimal surface covered by solid angle dω.
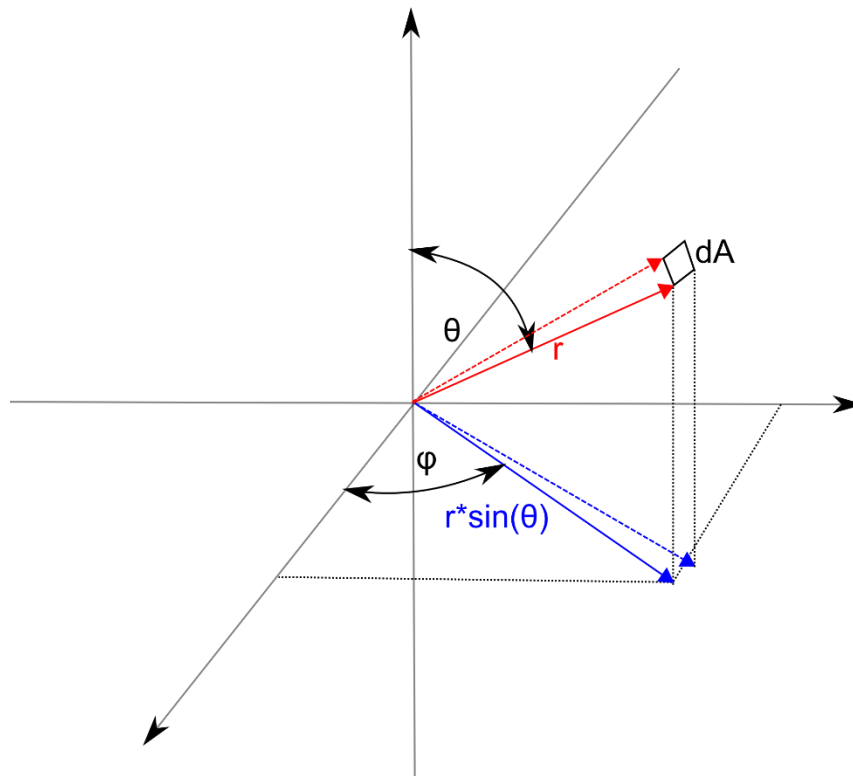
Figure 14-1: Spherical Coordinates

The area of surface *dA* is calculated by following equation:

$$dA = dθ * r * \sin(θ) * dφ * r$$

[14-8]

and since the half-sphere surface is equal to 2πr², *[14-7]* becomes:

$$dω = \frac{1}{2π}\sin(θ)\,dθ\,dφ$$

[14-9]

14.2.2. Hemispherical Transmittance Integration

Integration of *[14-6]* can be performed in two parts: the nominator and the denominator.

Integration over the denominator is fairly simple and it can be represented with the following equation:

$$\sum_{j=1}^{N} \int cos(\theta_j) * d\omega_j$$

$$= \int cos(\theta) * d\omega = \frac{1}{2\pi} \int_{\theta=0}^{\pi/2} \int_{\varphi=0}^{2\pi} cos(\theta) \sin(\theta) \, d\theta d\varphi \qquad [14\text{-}10]$$

$$= \frac{1}{2}$$

Substituting back into *[14-6]* and integrating over direction "j":

$$T_{hem,i} = 2 * \sum_{j=1}^{N} \int T_{j,i} * cos(\theta_j) * d\omega_j$$

$$= 2 * \sum_{j=1}^{N} \int_{\theta=\theta_{j,LO}}^{\theta=\theta_{j,HI}} \int_{\varphi=\varphi_{j,LO}}^{\varphi=\varphi_{j,HI}} T_{j,i} * cos(\theta_j) * d\omega_j \qquad [14\text{-}11]$$

then replacing $d\omega_j$ with *[14-9]* and performing both integrations, the following equation is obtained:

$$T_{hem,i} = \frac{1}{2} \sum_{j=1}^{N} \tau_{j,i} ((\sin \theta_{j,HI})^2 - (\sin \theta_{j,LO})^2) \, \Delta\varphi_j \qquad [14\text{-}12]$$

where $\tau_{j,i} = \frac{T_{j,i}}{\pi}$ and $\Delta\varphi_j = \varphi_{j,HI} - \varphi_{j,LO}$.

Introducing lambda coefficient as:

$$\Lambda_j = \frac{1}{2} ((\sin \theta_{j,HI})^2 - (\sin \theta_{j,LO})^2) \Delta\varphi_j \qquad [14\text{-}13]$$

then *[14-12]* can be written as:

$$T_{hem,i} = \sum_{j=1}^{N} \tau_{j,i} \Lambda_j \qquad [14\text{-}14]$$

It is also noteworthy that following equation is valid:

$$\pi = \sum_{j=1}^{N} \Lambda_j \qquad [14\text{-}15]$$

14.3. Spectral Data Measurements

There are two types of measurements taken from the samples. The first measurement is performed over the closed sphere as shown in Figure 14-2 which we will call total transmittance T_{total}. In the second measurement, the sphere is open at the direction normal to the sample (see Figure 14-3), which is used to let the specular portion of the incident radiation escape, thus providing the diffuse transmittance portion T_{diff}.
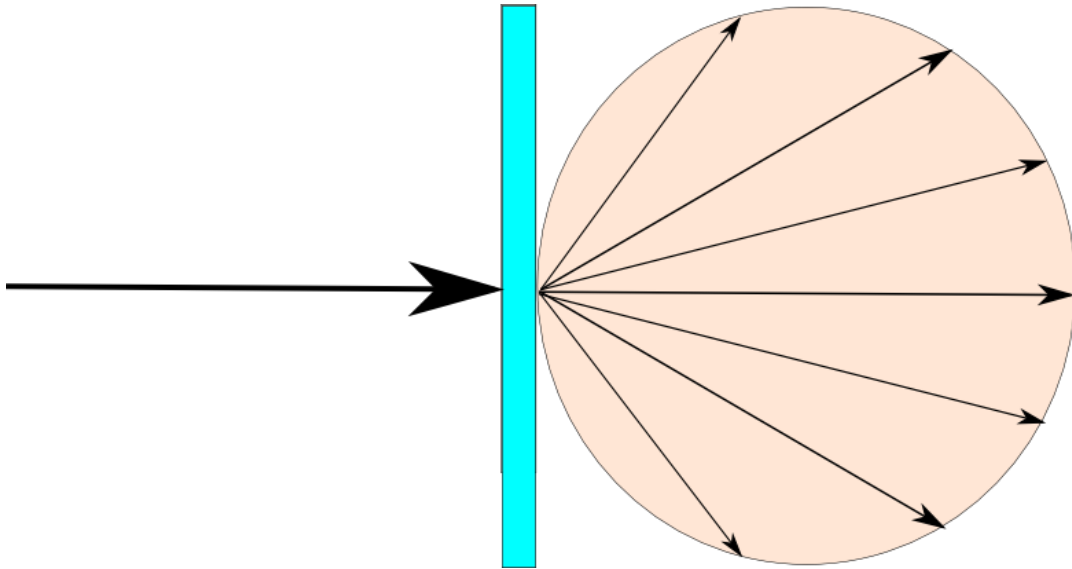
Figure 14-2. Total Transmittance Measurement
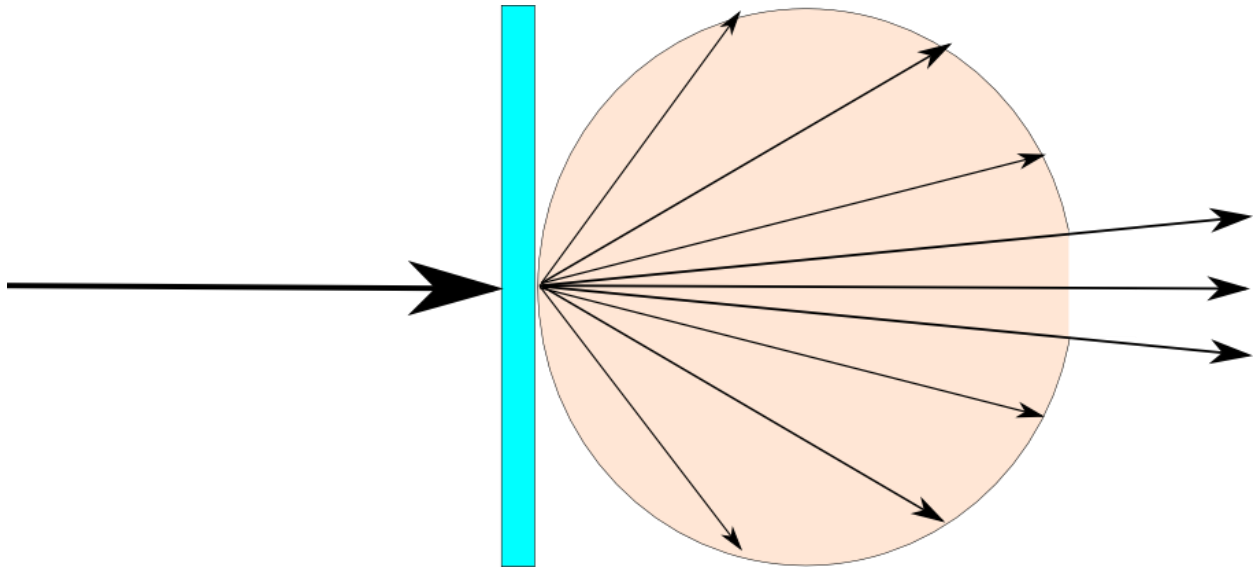
*Figure 14-3. **Diffuse Transmittance Measurement***

The difference between the measured total transmittance and the diffuse transmittance is the specular transmittance:

$$T_{i,specular} = T_{i,total} - T_{i,diffuse}$$

[14-16]

Note that while *[14-16]* is true for each incoming direction, the measurement is done for normal incident direction or i=1.

$T_{1,total}$, and $T_{1,diff}$ are measured in a spectrophotometer and are reported as a result of the measurement for each wavelength. If we consider how these quantities are calculated by the internal instrument's software, we can prove that their difference is equal to the members of diagonal component in a specular matrix (see Section 14.1.2. The following formulas are applicable to these two quantities:

$$T_{1,total} = \sum_{j=1}^{N} \tau_{j,1} \Lambda_j \qquad \text{[14-17]}$$

while for diffuse measurement:

$$T_{1,diff} = \sum_{j=2}^{N} \tau_{j,1} \Lambda_j \qquad \text{[14-18]}$$

which leads to the equation for specular transmittance:

$$T_{1,specular} = T_{1,total} - T_{1,diff} = \tau_{1,1} \Lambda_1 \qquad \text{[14-19]}$$

From which:

$$\tau_{1,1} = \frac{T_{1,total} - T_{1,diff}}{\Lambda_1} = \frac{T_{1,specular}}{\Lambda_1} \qquad \text{[14-20]}$$

$$\tau_{i,i} = \frac{T_{i,specular}}{\Lambda_i} \qquad \text{[14-21]}$$

$\tau_{1,1}$ and the rest of $\tau_{i,i}$ are diagonal elements in a specular matrix.

Note that value $T_{1,specular}$ in *[14-20]* is measured for normal incidence and therefore the equation can be applied only to $\tau_{1,1}$. For specular samples, the normal incidence measurement is usually the only measurement done. For other angles of incidence, formulas are used that correlate normal to off normal incidence angles (See Section 7.7). It is also possible to measure at different angles of incidence, in which case values do not need to be correlated.

The following set of equations details the elements of diffuse matrix, $\tau_{diff,i}$. Rewriting *[14-18]* for any incidence direction "i":

$$T_{i,diff} + \tau_{diff,i} \Lambda_i = \tau_{diff,i} \sum_{j=1}^{N} \Lambda_j \qquad \text{[14-22]}$$

$$\tau_{diff,i} = \frac{T_{i,diff}}{\pi - \Lambda_i} \qquad \text{[14-23]}$$

where $T_{1,diff}$ is angular dependent.

15. BI-DIRECTIONAL SCATTERING DISTRIBUTION FUNCTION

The **B**idirectional **S**cattering **D**istribution **F**unction (BSDF) is used to name the general mathematical function which describes the way in which the light is scattered by a surface. In practice this phenomenon is usually split into the reflected and transmitted components which are then treated separately as BRDF (**B**idirectional **R**eflectance **D**istribution **F**unction) and BTDF (**B**idirectional **T**ransmittance **D**istribution **F**unction).

The concept behind all BxDF functions could be described as a black box with the inputs being any two angles, one for incoming (incident) ray and one for the outgoing (reflected or transmitted) ray at a given point of the surface. The output of the black box is the value defining the ratio between the incoming and the outgoing light energy for the given couple of angles. The content of the black box may be a mathematical formula which more or less accurately tries to model and approximate the actual surface behavior, or an algorithm which produces the output based on discrete samples of measured data.

In fenestration systems, modeling BxDF functions are used to describe non-specular systems such as shading devices and systems constructed of shading devices.

15.1. Definition of BSDF matrices

To properly analyze BSDF properties, fenestration systems are set to have two hemispheres (Figure 15-1) with a finite number of incident and outgoing patches (Figure 15-2). A patch represents a 2D surface in a 3D hemisphere that is used to calculate the energy going through the patch surface. In this way the matrix of incoming and outgoing energies can be defined and calculated or measured. In this way it is possible to define the amount of energy incoming through the patch N and exiting through the patch M.

Hemispherical coordinate system is used to set up angles and define surface of each patch.
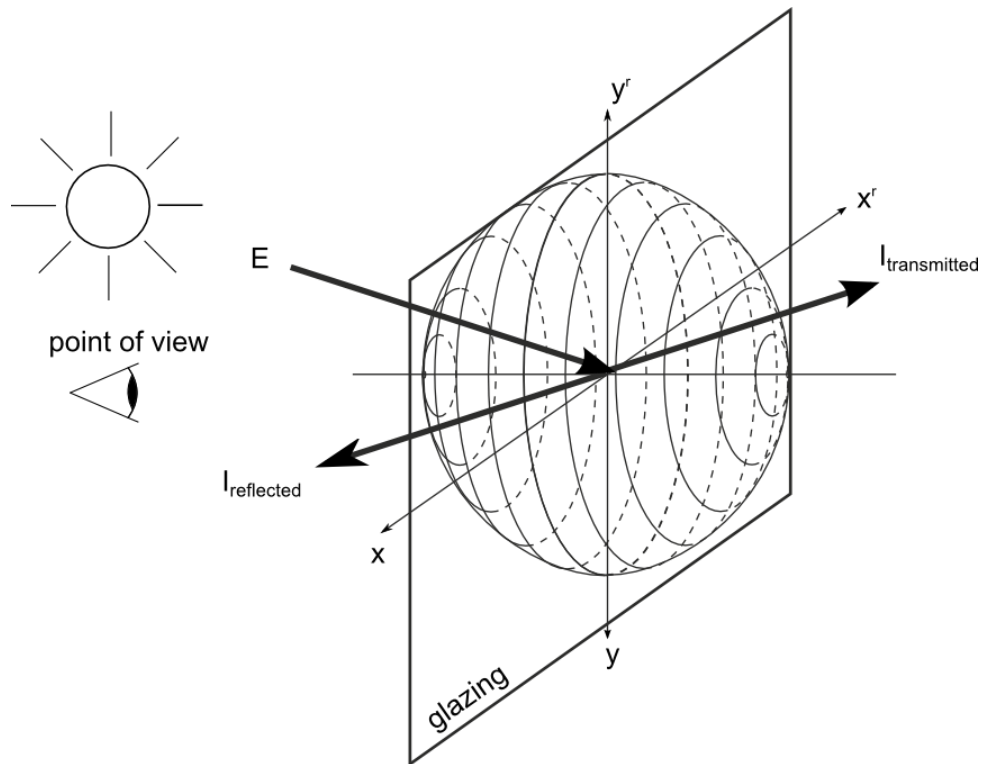
Figure 15-1. BSDF hemispheres with corresponding coordinate systems

The mathematical model or measurements will be expected to have two angles as input parameters and to produce a set of outputs for every outgoing patch with the given angles.

The number of incoming and outgoing patches (directions) are usually defined through these standard definitions:

- Full basis (145 x 145)
- Half basis (77 x 77)
- Quarter basis (41 x 41)
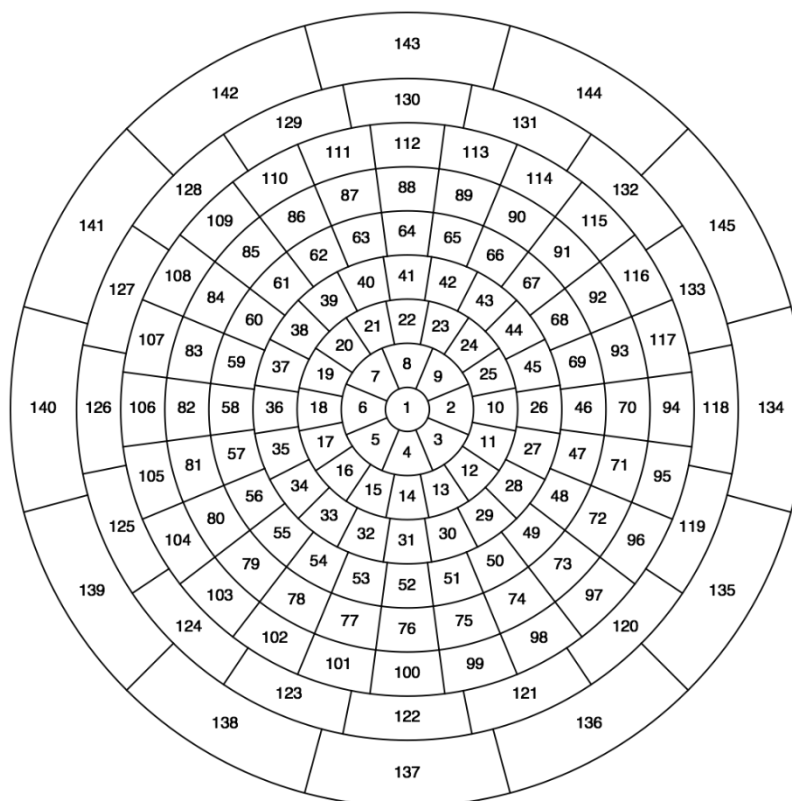
Figure 15-2. Full incoming BSDF (145 x 145) definition

Results will be kept in the form of matrices where the incoming and outgoing directions will be represented by columns and rows respectively.
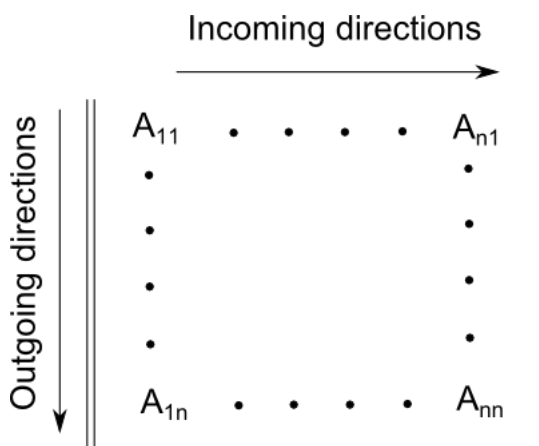
Figure 15-3. BSDF Matrix Representation

Patches numbering will be set up in a way that the following is satisfied:

- Every specular system will be presented as a diagonal matrix with all non-diagonal terms equal to zero

- When a BSDF matrix (layer) is used in glazing system, equivalent optical properties will be calculated by applying the same mathematical equations as used for the non-BSDF layers. For example, the equivalent transmittance of a two layer system will simply be multiplication of the two transmittance matrices.

To have these two rules satisfied, bins for incoming and outgoing directions must be mirrored (Figure 15-4).

a)   b)
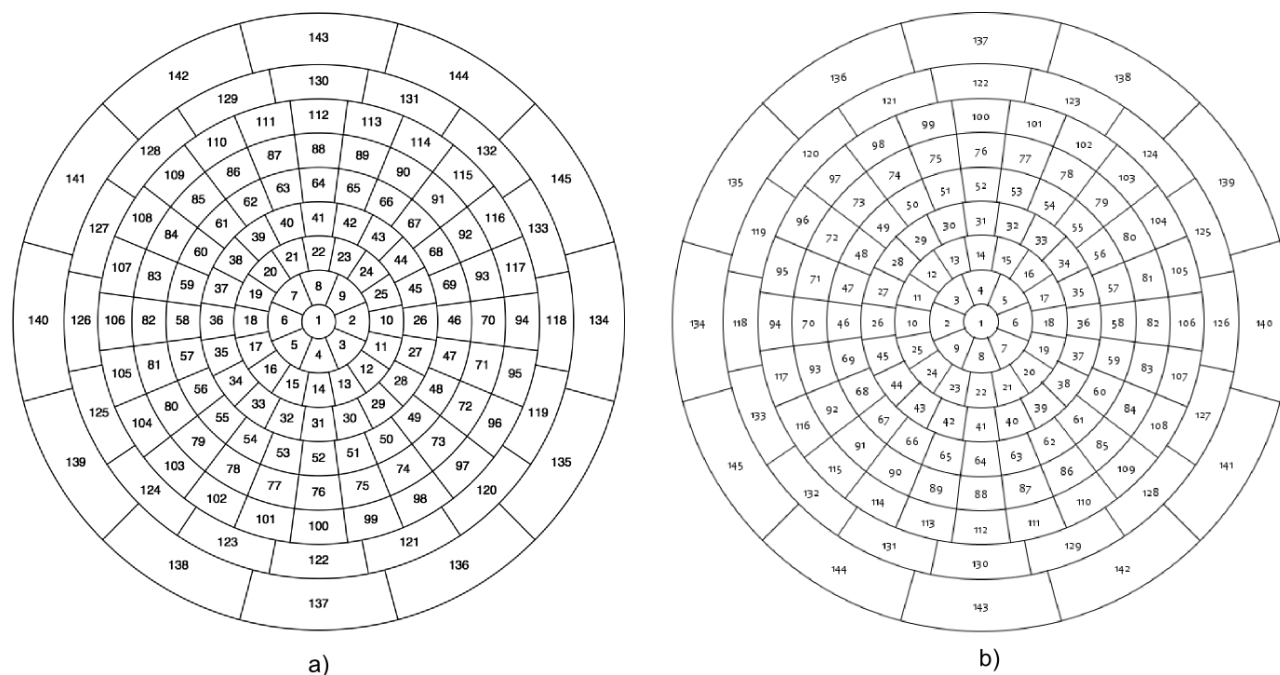
Figure 15-4. BSDF patches for a) incoming and b) outgoing directions

In this way the specular component that is entering (incoming) through a certain patch number will also leave through the same patch number. The same will be true for the specular component reflecting off the surface.

15.2. Definition of angle coordinates

Figure 15-1 shows two coordinate systems: xyz (we will refer to it as a "incoming" system) and x^{r}y^{r}z^r ("reversed" or "outgoing" system). Coordinate systems are set up in a way to satisfy incoming and outgoing patches symmetry (Figure 15-4).

Axis z points into the opposite direction of the incoming ray, while axis z^r points in the same direction as the reflected and transmitted ray. Note that z^r axis orientations point to opposite directions for reflected and transmitted rays. In this way we have defined three different coordinate systems, one for the incoming ray and two for the outgoing (reflected and transmitted) directions.
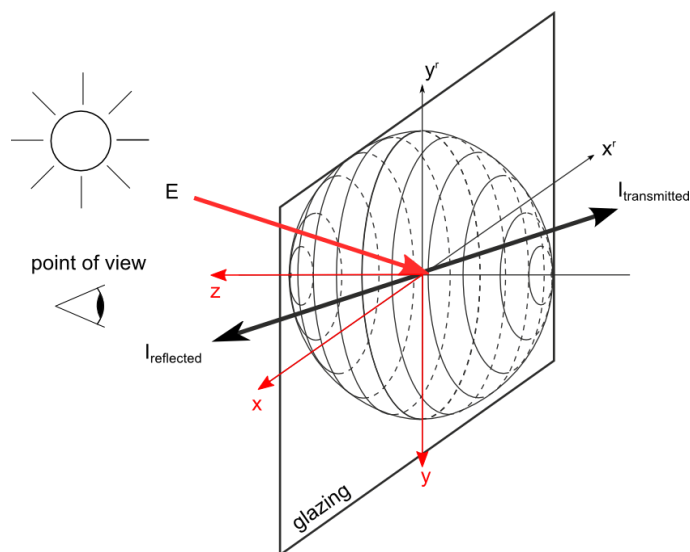
Figure 15-5. Incoming directions coordinate system
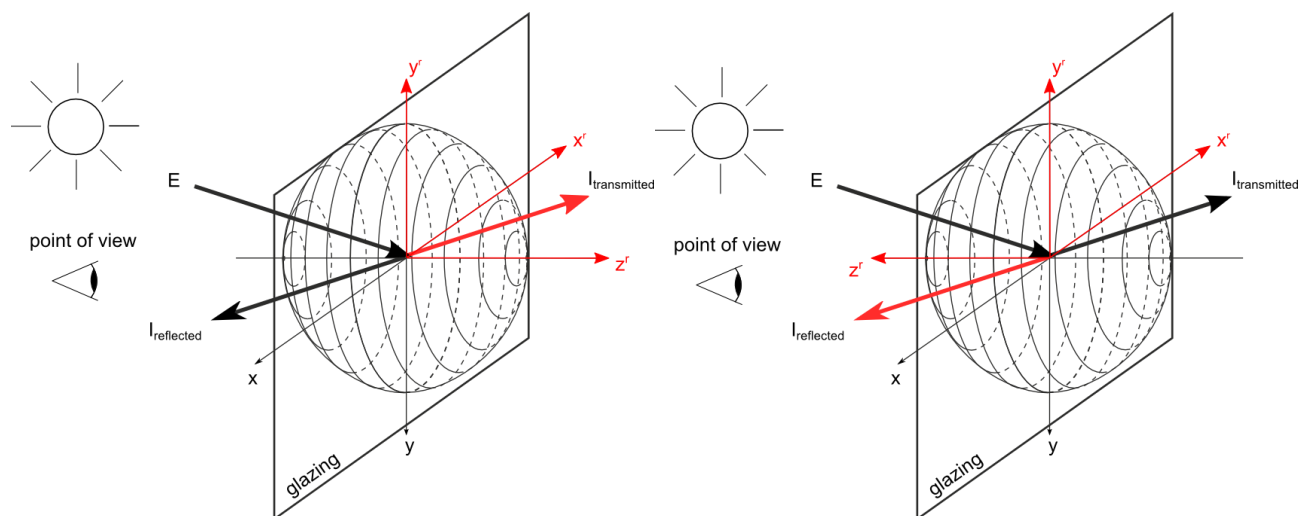
Figure 15-6. Outgoing directions coordinate system (transmittance and reflectance)

Directions of interest are defined using angular coordinates θ (latitude angle) and φ (azimuth angle). Values of θ and φ are defined within the following limits:

$$0° \leq \theta < 90°$$

$$0° \leq \varphi < 360°$$

[15-1]

Figure 15-7 shows an example with directions of interest in a planar projection of the "z" hemisphere in the $x0y$ plane, with z axis pointing towards the viewer. The diameters of the circles representing θ angles are growing with the θ value. Value of angle φ grows in a positive (clockwise) direction. Numbers 1 – 49, shown in Figure 15-7, correspond to a set of pre-defined bins, defined by seven θ angles and eight φ angles. This set of 49 bins had been given only as an example to illustrate the concept, since the full angular set consists of 145 bins. In this example, direction 15 (or D_{15}) is defined as ($\theta_{15} = 45°$, $\varphi_{15} = 225°$).
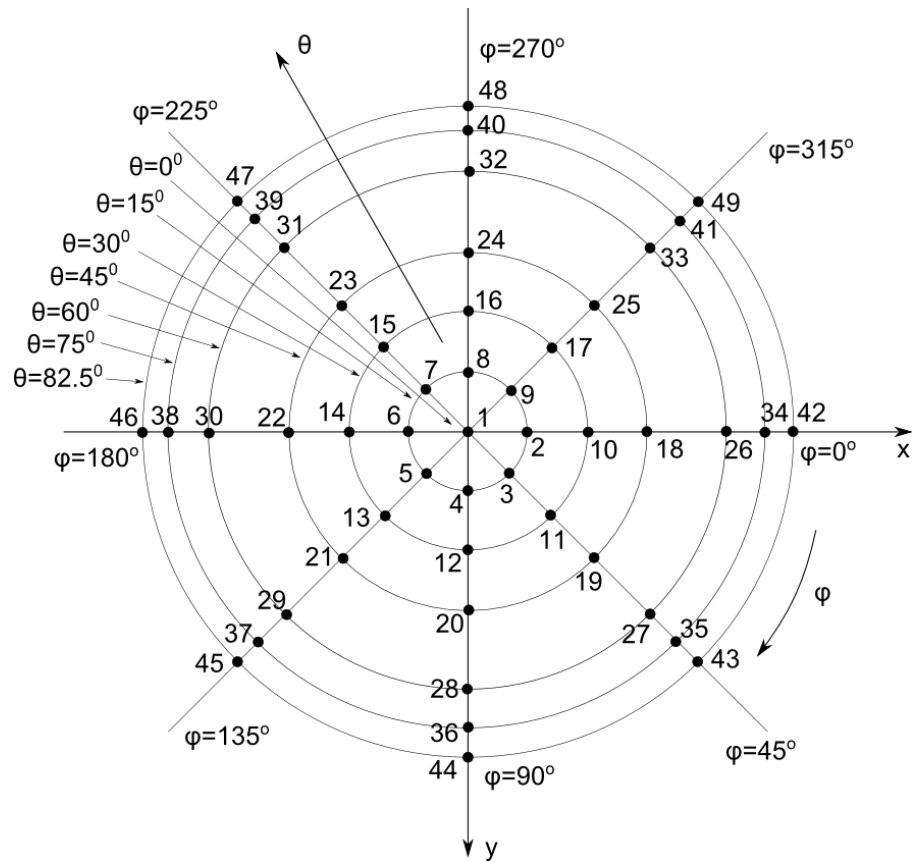
Figure 15-7. Projection of "z" hemisphere in x0y plane, viewed from incoming direction

For outgoing directions the coordinate system shown in Figure 15-8 should be used.
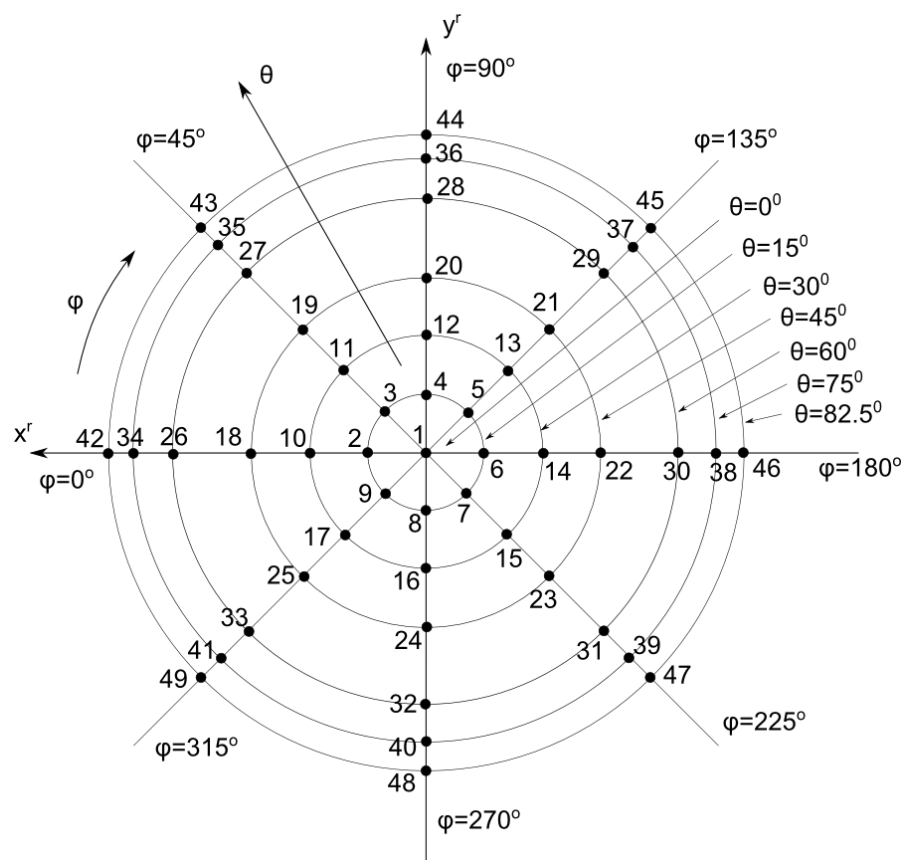
Figure 15-8. Projection of "z" hemisphere in x0y plane, viewed from outgoing direction

It is important to note that these hemispheres are not fixed to outdoor and indoor sides. They are connected with the direction of the light (hence the name incoming and outgoing). If for example, back transmittance is calculated, then the incoming hemisphere is placed on the indoor side and the outgoing hemisphere is placed at the outdoor side. Also, when calculating front reflectance the incoming hemisphere is set at the outdoor side and the outgoing hemisphere is also placed at the outdoor side.

15.3. BSDF patch and solid angle

Every patch is defined through two angles θ (latitude angle) and φ (azimuth angle) given in the hemispherical coordinate system.
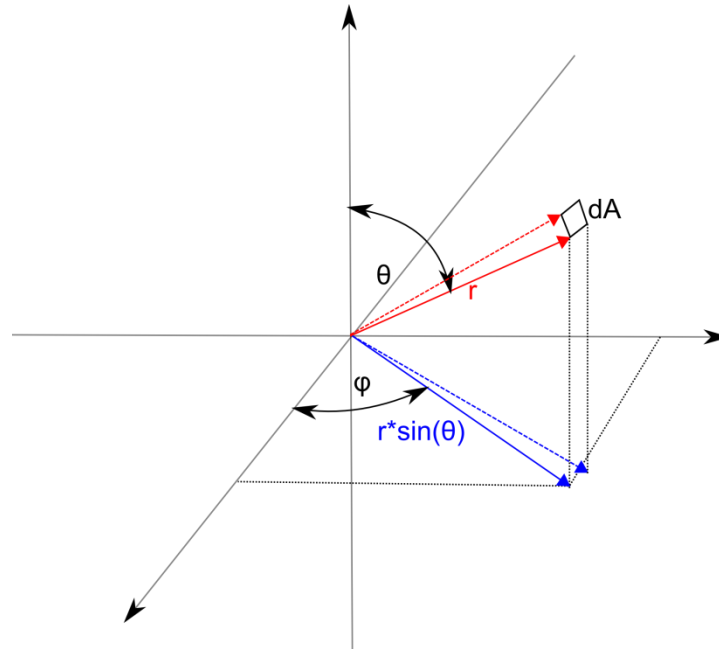
Figure 15-9. Spherical coordinates and patch

A patch defined in this way will have two sides with following dimensions:

$$side_1 = r \cdot \sin(\theta) \cdot d\theta \qquad\qquad\qquad\qquad \textit{[15-2]}$$

$$side_2 = r \cdot d\varphi \qquad\qquad\qquad\qquad \textit{[15-3]}$$

This infinitely small patch will have surface area:

$$dA = side_1 \cdot side_2 = d\theta \cdot r \cdot \sin(\theta) \cdot d\varphi \cdot r \qquad\qquad \textit{[15-4]}$$

The solid angle of the patch is then equal to:

$$d\omega = \frac{dA}{r^2} = \sin(\theta) \cdot d\theta \cdot d\varphi \qquad\qquad\qquad \textit{[15-5]}$$

Simple integration of the solid angles over the BSDF hemisphere is equal to 2π (see Equation [15-6]). Note that the solid angle of the sphere is equal to 4π.

$$\int_{\theta=0}^{\theta=\frac{\pi}{2}} \int_{\varphi=0}^{\varphi=2\pi} \sin(\theta) \cdot d\theta \cdot d\varphi = 2\pi \qquad\qquad \textit{[15-6]}$$

15.3.1. Hemispherical properties and integration

Hemispherical values are a simplification of BSDF properties into a single value. While there is a lot if information available from BSDF matrices, some calculations requires single number values. For example, there is no need to calculate heat transfer through the fenestration layer for every BSDF direction. Those calculations would be quite extensive and unnecessary since the previous integration of BSDF properties into a single value would produce identical results.

15.3.1.1. Hemispherical to hemispherical

Any hemispherical property is calculated by applying the following integration:

$$P_{hem} = \frac{\displaystyle\iint_{i\ j} P_{i,j} \cdot \cos(\theta_i) \cdot \cos(\theta_j) \cdot d\omega_i \cdot d\omega_j}{\displaystyle\iint_{i\ j} \cos(\theta_i) \cdot \cos(\theta_j) \cdot d\omega_i \cdot d\omega_j} \qquad \textit{[15-7]}$$

where "i" represents incoming direction, "j" outgoing directions, $P_{i,j}$ property value for given incoming-outgoing direction, θ_i, θ_j are angle between direction of the energy flow and incoming and outgoing directions and solid angle and $d\omega_i$, $d\omega_j$ are infinitesimal value of the solid angles at given position of the incoming and outgoing directions respectively. Integration over the hemisphere will produce a single value called *hemispherical value*. Such properties are useful when performing diffuse to diffuse calculations.

15.3.1.2. Directional to hemispherical

Sometimes it is required to calculate hemispherical properties for a certain direction. Such integration is performed for a certain incoming direction and over all outgoing directions.

$$P_{hem,i} = \frac{\displaystyle\int_j P_{i,j} \cdot \cos(\theta_j) \cdot d\omega_j}{\displaystyle\int_j \cos(\theta_j) \cdot d\omega_j} \qquad \textit{[15-8]}$$

This equation represents the directional hemispherical value for a certain incoming direction "i". Such a value is very useful when performing direct to diffuse calculations. For example, when calculating heat transfer through a fenestration layer it is important to know the position of the sun and the optical properties of the system in the direction of the sun.

In order to correctly calculate energy going through it, the patch view factor must be considered from the view of "z" axis (energy always travels parallel with the z axis).

15.3.1.3. Lambda values

Since the angle between the patch and the z axis is simply defined with θ, the solid angle of the patch viewed from the direction of the energy flow is equal to:

$$d\omega_j = d\omega \cdot \cos(\theta) \qquad \textit{[15-9]}$$

where "j" denotes the patch number and $d\omega_j$ is the solid angle as viewed in the direction parallel to the z axis.

Using of one of the standard BSDF definitions would require each patch to have defined limit angles ($\theta_{LO}, \theta_{HI}, \varphi_{LO}, \varphi_{HI}$). That would convert equation [15-9] into:

$$\Delta\omega_j = \int_{\theta_{LO,j}}^{\theta_{HI,j}} \int_{\varphi_{LO,j}}^{\varphi_{HI,j}} \cos(\theta) \cdot d\omega = \int_{\theta_{LO,j}}^{\theta_{HI,j}} \int_{\varphi_{LO,j}}^{\varphi_{HI,j}} \cos(\theta) \cdot \sin(\theta) \cdot d\theta \cdot d\varphi \qquad \textit{[15-10]}$$

$$= \frac{1}{2} \cdot (\sin^2(\theta_{HI,j}) - \sin^2(\theta_{LO,j})) \cdot \Delta\varphi_j = \Lambda_j$$

Where Λ_j is coefficient for the patch "j".

$$\Lambda_j = \frac{1}{2}(\sin^2(\theta_{HI,j}) - \sin^2(\theta_{LO,j})) \cdot \Delta\varphi_j \qquad \textit{[15-11]}$$

It is also noteworthy that the following equation is valid:

$$\pi = \sum_{j=1}^{N} \Lambda_j \qquad\qquad [15\text{-}12]$$

where N represents the number of all patches in single BSDF definition.

15.3.1.4. Hemispherical values and BSDF

Having a finite number of BSDF values and defined lambda values it is simple to calculate hemispherical values for any BSDF system.

Hemispherical to hemispherical

This is obtained by using discrete values when performing the calculation as displayed in Equation [15-7]:

$$
P_{hem} = \frac{\iint_{i\ j} P_{i,j} \cdot \cos(\theta_i) \cdot \cos(\theta_j) \cdot d\omega_i \cdot d\omega_j}{\iint_{i\ j} \cos(\theta_i) \cdot \cos(\theta_j) \cdot d\omega_i \cdot d\omega_j}
$$

$$
= \frac{\displaystyle\sum_i \sum_j \int_{\theta_{LO,i}}^{\theta_{HI,i}} \int_{\varphi_{LO,i}}^{\varphi_{HI,i}} \int_{\theta_{LO,j}}^{\theta_{HI,j}} \int_{\varphi_{LO,j}}^{\varphi_{HI,j}} P_{i,j} \cdot \cos(\theta_i) \cdot \cos(\theta_j) \cdot d\omega_i \cdot d\omega_j}{\displaystyle\sum_i \sum_j \int_{\theta_{LO,i}}^{\theta_{HI,i}} \int_{\varphi_{LO,i}}^{\varphi_{HI,i}} \int_{\theta_{LO,j}}^{\theta_{HI,j}} \int_{\varphi_{LO,j}}^{\varphi_{HI,j}} \cos(\theta_i) \cdot \cos(\theta_j) \cdot d\omega_i \cdot d\omega_j}
$$

$$[15\text{-}13]$$

Applying Equation [15-10] and considering that $P_{i,j}$ is constant over the entire patch, Equation [15-13] becomes:

$$
P_{hem} = \frac{\displaystyle\sum_i \sum_j P_{i,j} \cdot \Lambda_i \cdot \Lambda_j}{\displaystyle\sum_i \sum_j \Lambda_i \cdot \Lambda_j} \qquad\qquad [15\text{-}14]
$$

Direct to hemispherical

Similarly to the case of hemispherical to hemispherical, this value is obtained by discretization of Equation [15-8] and Equation [15-10]:

$$
P_{hem,i} = \frac{\displaystyle\sum_j P_{i,j} \cdot \Lambda_j}{\displaystyle\sum_j \Lambda_j} \qquad\qquad [15\text{-}15]
$$

15.3.2. Fenestration BSDF properties

15.3.2.1. BSDF layer transmittance and reflectance

All equations described in this chapter can be simply applied to fenestration properties such as transmittance and reflectance where for each incoming BSDF direction number of outgoing directions can be applied. Simply replacing $P_{i,j}$ with the corresponding value for transmittance and/or reflectance will perform the calculations for the given property.

15.3.2.2. BSDF layer absorptances

Absorptance of the layer is a physical property that can only have an incoming direction and not outgoing. For this reason it is not possible to represent BSDF layer absorptances as a matrix of incoming and outgoing directions. The only correct way to represent absorptances is through the vector, where each value in the vector represents the absorptance of the layer for a certain incoming direction.

15.4. Calculating BSDF matrices

When providing a mathematical model for a custom shading layer it is important to understand how to create the BSDF properties of such a layer. For any given incoming direction, the model must be able to calculate the direct-direct and direct-diffuse properties. Note that the diffuse-diffuse properties are calculated by applying Equations [15-14] and [15-15].
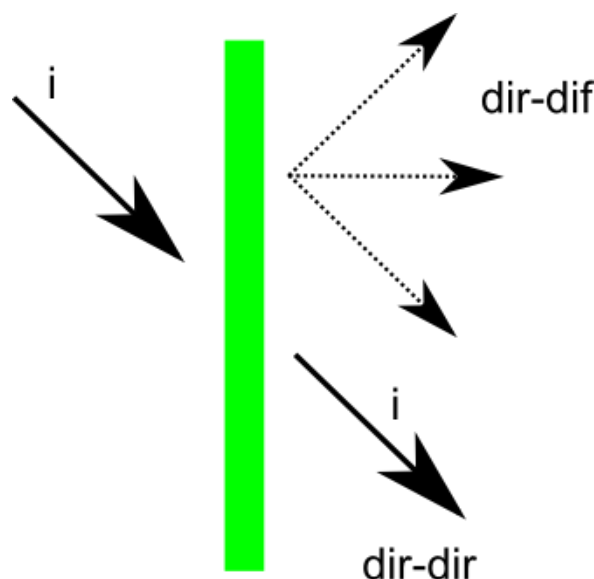
Figure 15-10. Mathematical model of shading cell

When the model calculates the properties of the shading, that must be done for each incoming direction "i" and the results must be provided for every outgoing direction "j". The calculation of the **direct-direct component** usually come down to calculating the openness of the hole in the shading fabric and the ratio of the direct ray that passes through the shading device. Before supplying the results of the direct-direct component to the matrix, it is important to divide the result with the corresponding lambda coefficient.

$$\tau_{i,i} = \frac{T_{i,i}}{\Lambda_i} \qquad\qquad\qquad [15\text{-}16]$$

where $T_{i,i}$ is calculated as the ratio of the direct-direct component. The direct-direct component is usually visible on the matrix diagonals. It is, however, possible to work with systems that would scatter rays into different directions in which casethe number must be divided with the corresponding lambda value.

$$T_{dir-dir} = \begin{Vmatrix} \tau_{1,1} & 0 & ... & 0 \\ 0 & \tau_{2,2} & ... & 0 \\ ... & ... & ... & ... \\ 0 & 0 & ... & \tau_{n,n} \end{Vmatrix} \qquad\qquad [15\text{-}17]$$

Direct-diffuse component is calculated by scattering through the material. In most of the cases, scattering through the material will be considered to be *perfectly diffuse*. In this case the incoming ray will be equally distributed in every direction. Since the sum of all lambdas at the outgoing direction is equal to π (Equation [15-12]), the measured number must be divided with π.

$$\tau_i = \frac{T_i}{\pi}$$
[15-18]

Since the obtained number is valid for the outgoing direction, every column in the matrix (a column represents outgoing directions) will be filled with the same numbers.

$$T_{dir-dif} = \begin{Vmatrix} \tau_1 & \tau_2 & \dots & \tau_n \\ \tau_1 & \tau_2 & \dots & \tau_n \\ \dots & \dots & \dots & \dots \\ \tau_1 & \tau_2 & \dots & \tau_n \end{Vmatrix}$$
[15-19]

Finally, the total transmittance matrix is obtained by the summation of the two previously calculated matrices (direct-direct and direct-diffuse).

$$BTDF = T_{dir-dir} + T_{dir-dif}$$
[15-20]

15.5. Measuring BSDF matrices

There are two types of measurements taken from the samples. The first measurement is performed over the closed sphere as shown in Figure 15-11, which we will call total transmittance (T_{total}). In the second measurement, the sphere is open at direction normal to the sample (see Figure 15-12), which is used to let the specular portion of incident radiation to escape, thus providing the diffuse transmittance portion (T_{diff}).
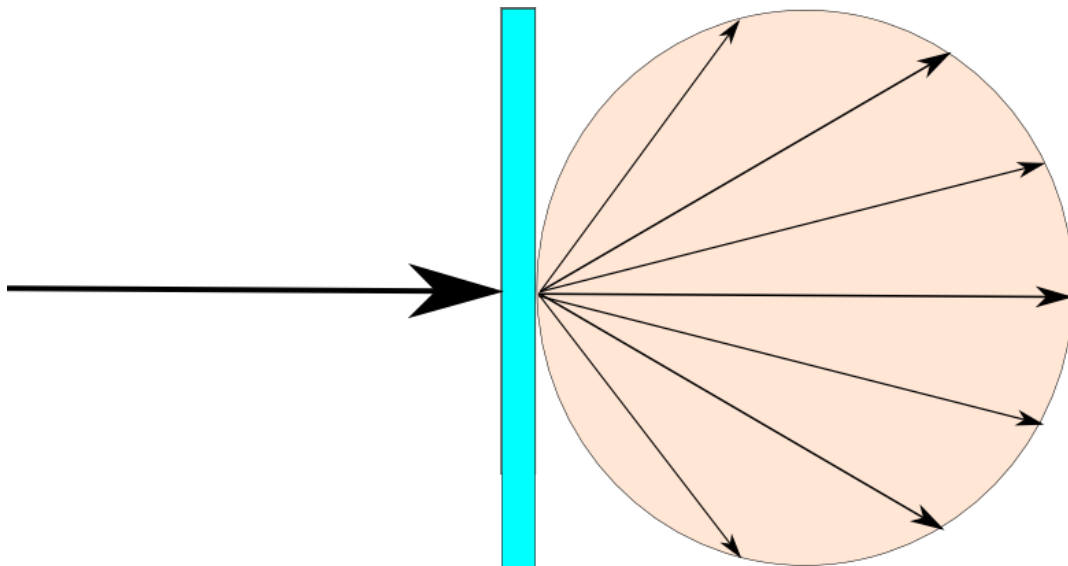
Figure 15-11. Measurement of total transmittance
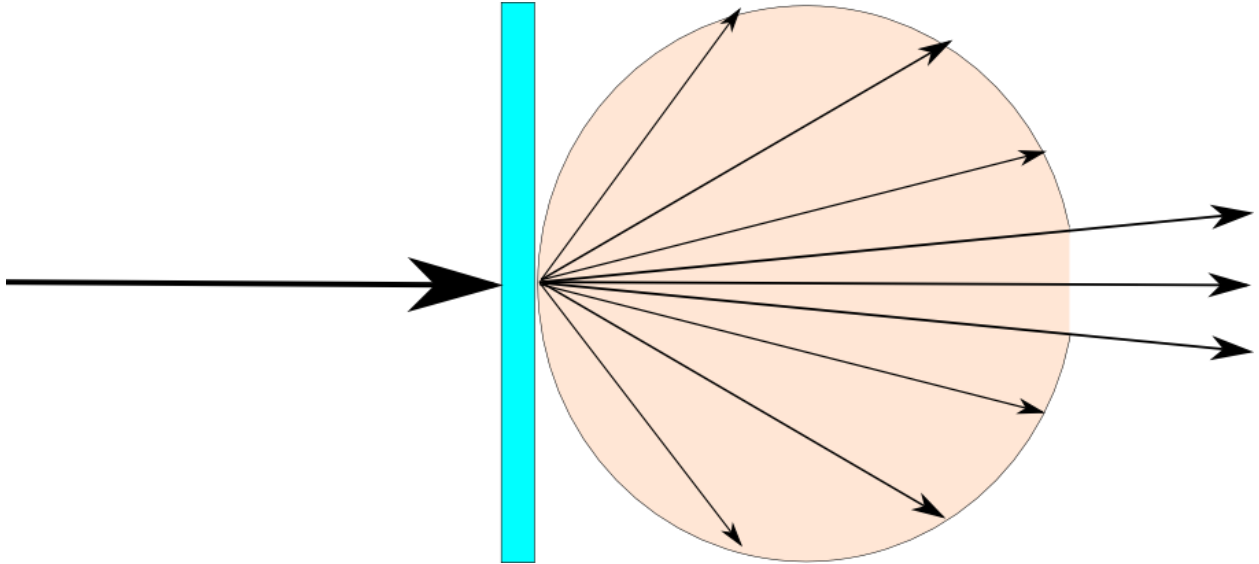
Figure 15-12. Measurement of diffuse transmittance

The difference between the measured total transmittance and the diffuse transmittance is the specular transmittance:

$$T_{i,specular} = T_{i,total} - T_{i,diffuse}$$
<div align="right">[15-21]</div>

Note that while [15-21] is true for each incoming direction, the measurement is done for the normal incident direction or i=1.

$T_{1,total}$, and $T_{1,diff}$ are measured in a spectrophotometer and are reported as a result of the measurement for each wavelength. If we consider how these quantities are calculated by the internal instrument's software, we can prove that their difference is equal to the members of the diagonal component in a specular matrix (see "Section 15.4. Calculating BSDF matrices"). The following formulas are applicable to these two quantities:

$$T_{1,total} = \sum_{j=1}^{N} \tau_{j,1} \cdot \Lambda_j$$
<div align="right">[15-22]</div>

while for diffuse measurement:

$$T_{1,diff} = \sum_{j=2}^{N} \tau_{j,1} \cdot \Lambda_j$$
<div align="right">[15-23]</div>

which leads to the equation for specular transmittance:

$$T_{1,specular} = T_{1,total} - T_{1,diff} = \tau_{1,1} \cdot \Lambda_1$$
<div align="right">[15-24]</div>

from which:

$$\tau_{1,1} = \frac{T_{1,total} - T_{1,diff}}{\Lambda_1} = \frac{T_{1,specular}}{\Lambda_1}$$
<div align="right">[15-25]</div>

$$\tau_{i,i} = \frac{T_{i,specular}}{\Lambda_i}$$
<div align="right">[15-26]</div>

$\tau_{1,1}$ and the rest of $\tau_{i,i}$ are diagonal elements in a specular matrix.

Note that value $T_{1,specular}$ in Equation [15-25] is measured for normal incidence and therefore the equation can be applied only to $\tau_{1,1}$. For specular samples, normal incidence measurement is usually the only measurement done. For other angles of incidence, formulas are used that correlate normal to off normal incidence angles. It is also possible to measure at different angles of incidence, in which case the values do not need to be correlated.

The following set of equations details the elements of the diffuse matrix, $\tau_{diff,i}$. Rewriting Equation [15-23] for any incidence direction "i":

$$T_{i,diff} + \tau_{diff,i} \cdot \Lambda_i = \tau_{diff,i} \cdot \sum_{j=1}^{N} \Lambda_j \qquad \text{[15-27]}$$

$$\tau_{diff,i} = \frac{T_{i,diff}}{\pi - \Lambda_i} \qquad \text{[15-28]}$$

where $T_{i,diff}$ is angular dependent.

Finally, BSDF matrix is equal:

$$BTDF = \left\| \begin{array}{cccc} \dfrac{T_{1,specular}}{\Lambda_1} & \dfrac{T_{2,diff}}{\pi - \Lambda_2} & \cdots & \dfrac{T_{n,diff}}{\pi - \Lambda_n} \\[3mm] \dfrac{T_{1,diff}}{\pi - \Lambda_1} & \dfrac{T_{2,specular}}{\Lambda_2} & \cdots & \dfrac{T_{n,diff}}{\pi - \Lambda_n} \\[3mm] \cdots & \cdots & \cdots & \cdots \\[3mm] \dfrac{T_{1,diff}}{\pi - \Lambda_1} & \dfrac{T_{2,diff}}{\pi - \Lambda_2} & \cdots & \dfrac{T_{n,specular}}{\Lambda_n} \end{array} \right\| \qquad \text{[15-29]}$$

15.6. Transformation of spherical to profile angles

Some mathematical models are symmetrical from the vertical point of view and because of that calculations can be performed once for several incoming directions. For example, a horizontal venetian blind will produce identical results for incoming patches number 7 and number 9 (see Figure 15-2a). In that case, the 3D spherical coordinate system can be converted to a 2D coordinate system.
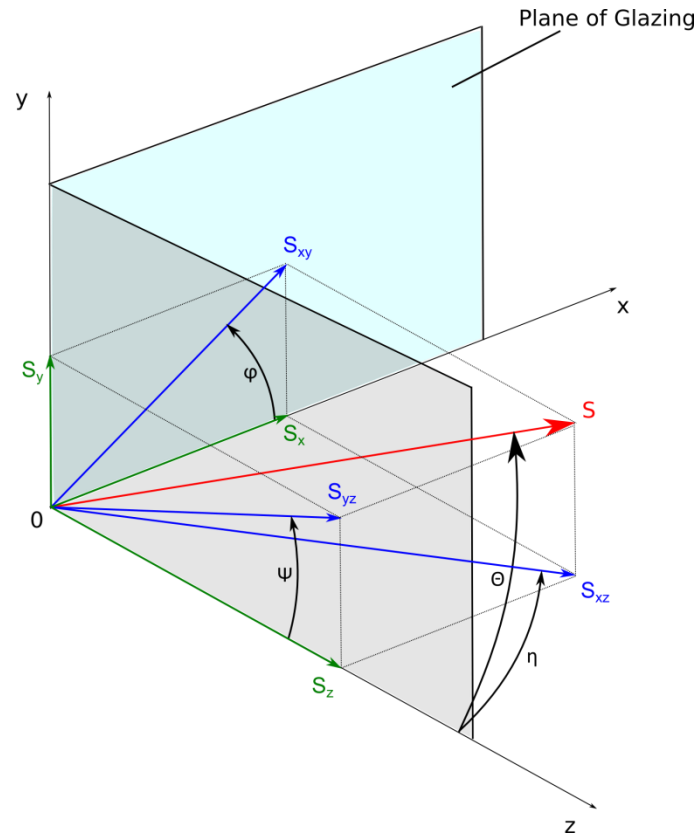
Figure 15-13. Conversion of spherical coordinate system to 2D and profile angle

Figure 15-13 shows the conversion of (θ, φ) coordinate system (spherical) into (ψ, η) coordinate system. Directional vector "S" and its projections to the Cartesian coordinate system planes and axis needs to be calculated. First the projection of interest is the projection of "S" to the y-axis (S_y). The first step is to calculate the projection of "S" to the xz plane:

$$S_{xy} = S \cdot \sin \theta \qquad\qquad [15\text{-}30]$$

and then the projection to y-axis:

$$S_y = S_{xy} \cdot \sin \varphi \qquad\qquad [15\text{-}31]$$

which leads to the equation for "S_y":

$$S_y = S \cdot \sin \theta \cdot \sin \varphi \qquad\qquad [15\text{-}32]$$

Similarly the equation of S_z (projection to z-axis) is calculated as:

$$S_z = S \cdot \cos \theta \qquad\qquad [15\text{-}33]$$

Since,

$$\frac{S_y}{S_z} = \tan \psi \qquad\qquad [15\text{-}34]$$

S_y can be expressed as:

$$S_y = S \cdot \cos\theta \cdot \tan\psi \qquad\qquad [15\text{-}35]$$

From which the following expression can be obtained:

$$\tan\psi = \tan\theta \cdot \sin\varphi \qquad\qquad [15\text{-}36]$$

This gives the first coordinate system conversion equation. For the second coordinate system conversion equation, we will calculate the projection of s on the x-axis:

$$\frac{S_x}{S_z} = \tan\eta \qquad\qquad [15\text{-}37]$$

and since $S_z = S \cdot \cos\theta$, S_x becomes:

$$S_x = S \cdot \cos\theta \cdot \tan\eta \qquad\qquad [15\text{-}38]$$

Also:

$$S_x = S_{xy} \cdot \cos\varphi = S \cdot \sin\theta \cdot \cos\varphi \qquad\qquad [15\text{-}39]$$

which leads to the second equation of coordinates transformation:

$$\tan\eta = \tan\theta \cdot \cos\varphi \qquad\qquad [15\text{-}40]$$

16. CELLULAR SHADES

The simulation of cellular shades as they are implemented in WINDOW, THERM, and Radiance is divided into thermal properties (Section 16.1) and optical properties (Section 16.2).

16.1. Thermal properties definition and implementation in WINDOW and THERM

Section 1 of this document outlines a review and validation of the ISO 15099 center-of-glass (COG) heat transfer correlations for cellular shades through measurement and simulation. The impact of system thermal transmittance due to dimensional and material variations of the shades is measured experimentally, simulated using CFD analysis, and simulated utilizing simplified correlations from ISO 15099 with the Berkeley Lab WINDOW and THERM software.

16.1.1. Geometry

Two aspects of cellular shade geometry are studied; the cells themselves and the layer as a whole. The four cell geometries considered are single-cell, cell-in-cell, cell-in-cell-in-cell, and stacked double cell. These geometries are shown in Figure 16-1a-d. The significant dimensions include the cell width (w), cell height or pitch (p), side length (ls), and glue-line length (lg). In all cases the comparable side lengths are considered to be equal, as shown in Figure 16-1a. Cell wall thickness has insignificant impact on overall layer thermal performance for the materials considered, so a typical thickness of 0.2 mm is assumed. Interior, or room-side, mounted cellular shades are studied exclusively in this work. The typical geometry relative to the glazing system is shown in Figure 16-1e.
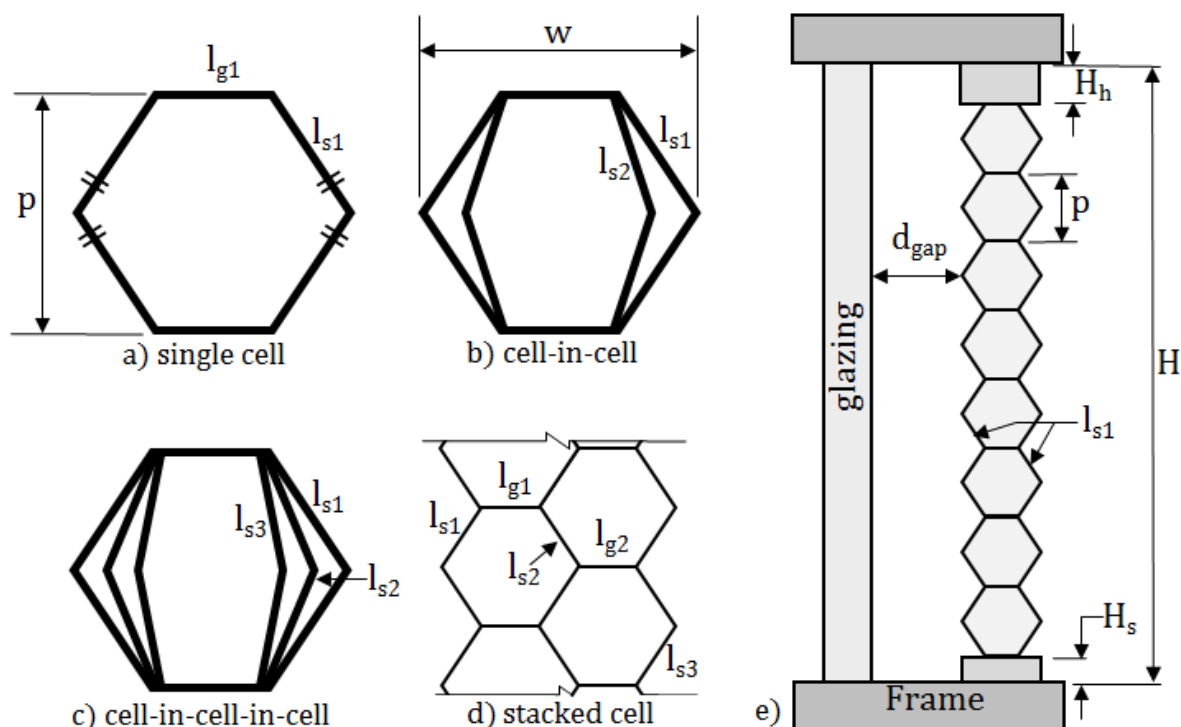
Figure 16-1. Geometry of a) single-cell, b) cell-in-cell, c) cell-in-cell-in-cell, d) stacked double cell, and e) side view of room-side mounted shade installed in window.

p :	Height (pitch) of cell	[m]
w :	Width of cell	[m]
H :	Height of shade	[m]
H_h :	Height of shade head rail	[m]
H_s :	Height of shade sill rail	[m]
d_{gap} :	Shade-window gap depth	[m]
l_{g1} :	Glue-line length number 1	[m]
l_{g2} :	Glue-line length number 2 (if present)	[m]
l_{s1} :	Length 1st cavity wall	[m]
l_{s2} :	Length 2nd cavity wall (if present)	[m]
l_{s3} :	Length 3rd cavity wall (if present)	[m]

16.1.2. Simulation Methodology

The correlations developed in ISO 15099 to predict the heat flux through window systems have been implemented in one and two dimensions with the Berkeley Lab WINDOW and THERM software programs. The process for simulating a glazing system with cellular shades utilizing the software is shown in Figure 16-2. First, the relevant thermal and optical material properties of glue-lines and cavity walls are entered into the

WINDOW shade material database. The properties may be measured spectral data or integrated into solar, visible, and thermal infrared groups. The cell geometry is defined in THERM with the cell wall properties appropriated from the previously defined shade material database. The THERM geometry and material properties are then used as an input for the ray-tracing program Radiance, where 1D equivalent layer optical properties are calculated. The calculated shade layer properties are then combined with the remainder of the glazing system and boundary conditions to determine the 1D center-of-glazing thermal performance. The THERM program determines the 1D equivalent thermal properties of the shading layer based on the 2D geometry. Since the solution is solved for iteratively, the previously defined THERM cell geometry is called repeatedly to ensure accurate thermal boundary conditions and cavity convection within cells during the calculation.
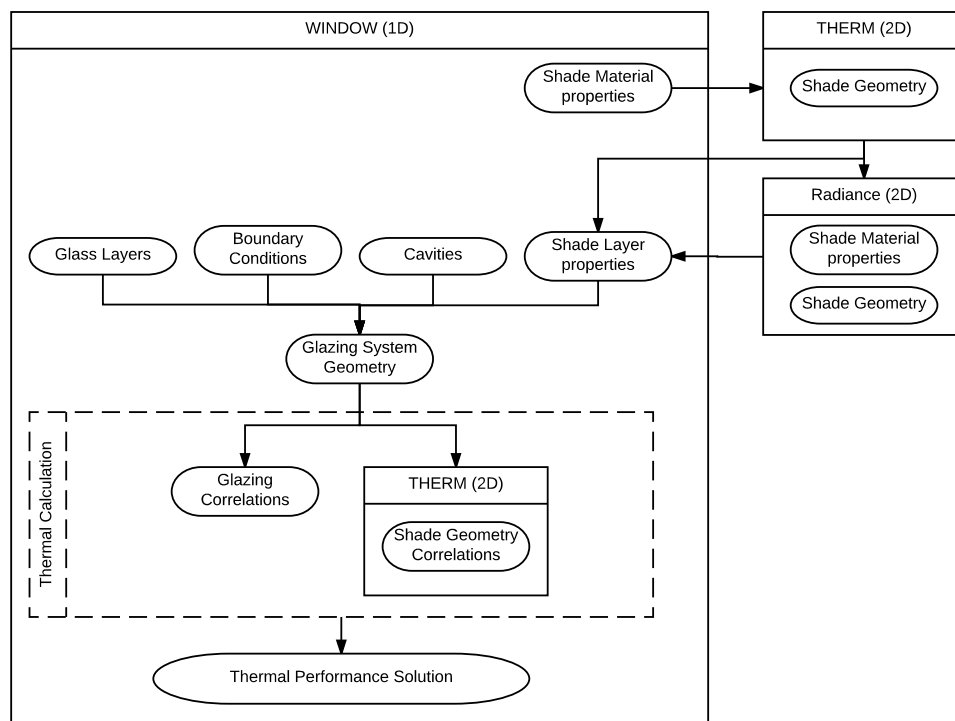
Figure 16-2. Cellular shade simulation algorithm flow used by LBNL WINDOW and THERM software.

16.1.3. Finite Element Analysis (FEA)

In the multiphysics analysis program COMSOL, the finite element method is used to solve the coupled heat and fluid-flow equations in two dimensions. Conduction, convection and radiation are simulated numerically. COMSOL default meshing is used to construct the computational domains. Sensitivity analysis of the results to mesh size is performed and determined to be less than 1%. Viscous dissipation is not addressed and all thermophysical properties are assumed to be constant except for the buoyancy term of the y-momentum equation where the Boussinesq approximation is used. The parallel direct iterative sparse solver (PARDISO) is used.

Fluid heat transfer for constant temperature walls of four geometries is studied as shown in Figure 16-3. Geometry (a) represents the cavity between glass and cellular shade; Geometry (b) is a rectangular cell and is the baseline geometry used in the ISO 15099 correlation; Geometry (c) represents a hexagonal cellular shade cell; and Geometry (d) represents natural convection along the triangular wave surface of a cellular shade.
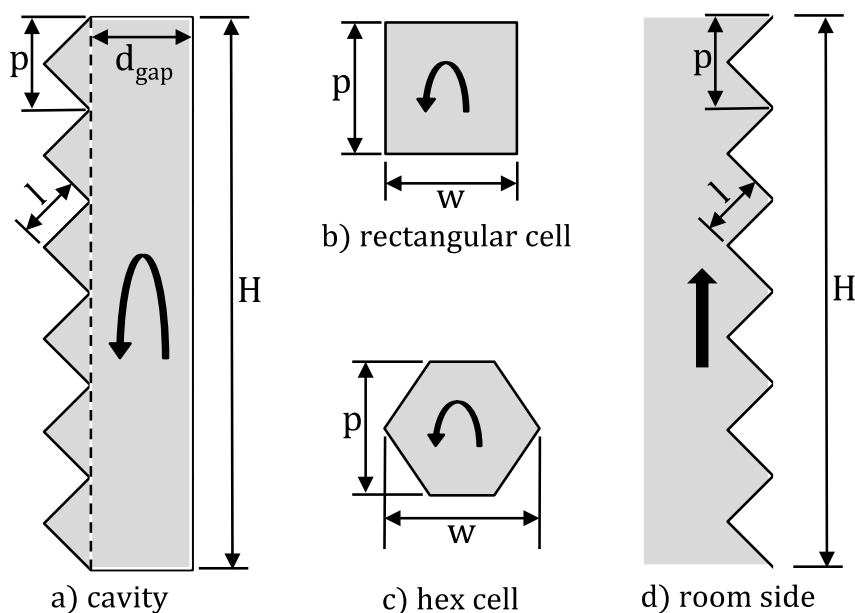
Figure 16-3. 2D geometries utilized in FEA simulations for fluid heat transfer with constant temperature walls. Fluid areas shown in grey.

Heat flux through rectangular fluid filled cavities has been extensively studied by others. The work by El Sherbiny et al. is the basis for the sealed cavity model in the ISO 15099 standard. All of these studies provide a means to calculate average heat flux based on definitions of the non-dimensional Nusselt (Nu) and Rayleigh (Ra) numbers as shown in Equations *[16–1]-[16–2]*; where Nu is the ratio of convective to conductive heat transfer across the cavity and Ra designates strength of the buoyancy driven flow. An empirical correlation between them is determined for specific geometries in the form of Equation *[16–3]*.

$$Nu = \frac{q \cdot L}{k \cdot \Delta T} \qquad\qquad\qquad [16–1]$$

$$Ra = \frac{\rho^2 \cdot g \cdot C_p \cdot \beta \cdot \Delta T \cdot L^3}{k \cdot \mu} \qquad\qquad [16–2]$$

$$Nu = f(Ra) \qquad\qquad\qquad [16–3]$$

where:

Nu :	Nusselt number	[-]
Ra :	Rayleigh number	[-]
q :	Heat flux	[W m^{-2}]
L :	Characteristic length	[m]
k :	Thermal conductivity	[W m^{-1} K^{-1}]
T :	Temperature	[K]
ρ :	Density	[Kg m^{-3}]
g :	Gravity	[m s^{-2}]
C_p :	Heat capacity	[J kg^{-1} K^{-1}]
β :	Coefficient of thermal expansion	[K^{-1}]

μ :   Dynamic viscosity   [Pa s]

Detailed FEA is used to determine the heat flux through the geometries shown in Figure 16-3 for a wide range of temperatures. The simulations are performed non-dimensionally per Equations *[16–1]*-*[16–3]* in order to generalize the solutions. The resulting steady state heat flux, represented here by the non-dimensional Nusselt number (Equation *[16–1]*), is determined and plotted against the Rayleigh number (Equation *[16–2]*). Figure 16-4 shows the correlation between the current FEA simulations and ISO 15099 for rectangular and hexagonal cells at height-to-width aspect ratios (AR) of 0.5 and 1. There is a large error between the two models for AR=1 within the typical Ra range encountered in this work. This discrepancy is due to an interpolation error in the ISO model. This divergence shows that we should anticipate a significant under-prediction of the cellular shade Nu, and in turn, system heat flux in some cases. The error will be greatest when Ra is smallest, principally with smaller cells and low temperature difference between cell walls. Similar correlations are shown in Figure 16-5 and Figure 16-6 for the glass-shade cavity (wave cavity) and natural convection from the shade (wave surface) to the room. The expected error for these configurations also appears to be significant, but offsetting, to the expected error from the cell cavity models.
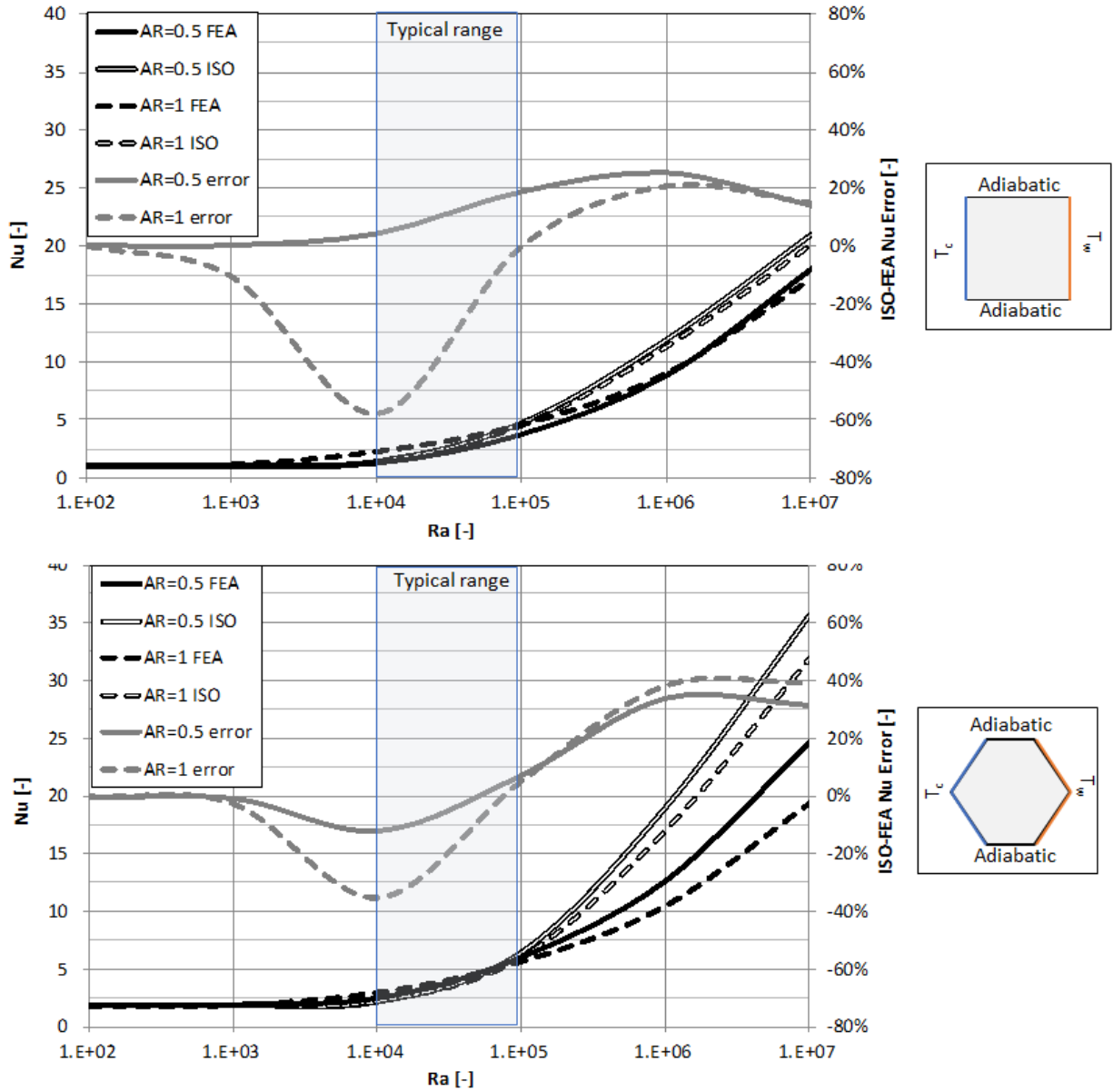
Figure 16-4. Nu = f(Ra) correlation curves solved by FEA of cell geometries at aspect ratios (AR) of 0.5 and 1 compared to ISO 15099. The typical Ra range encountered during measurements is highlighted.
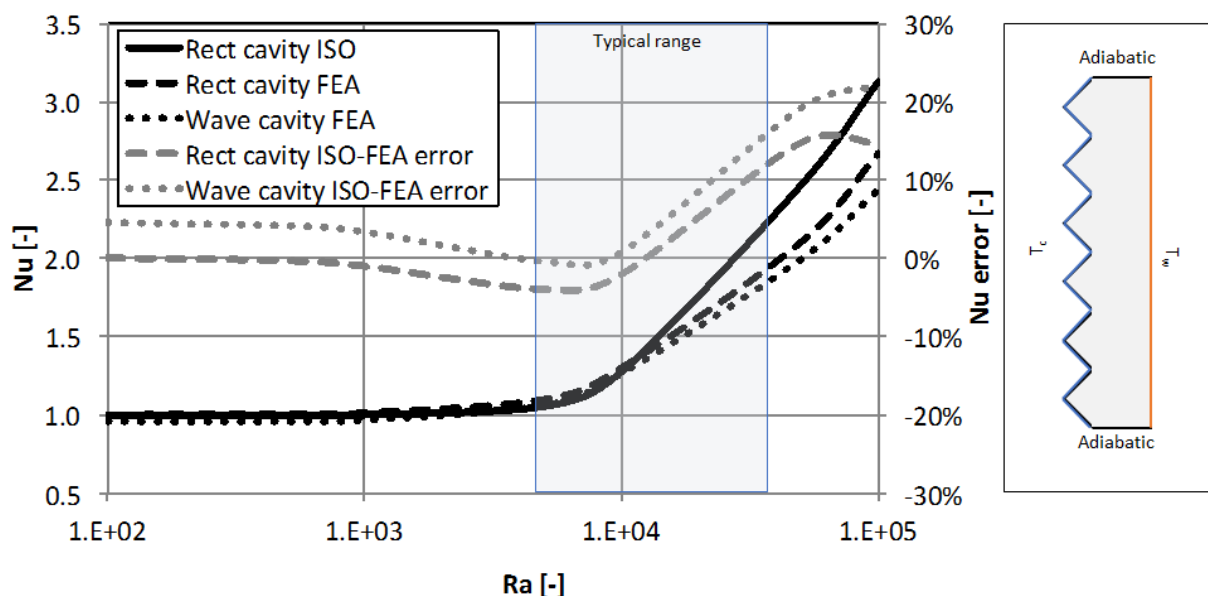
Figure 16-5. Nu = f(Ra) correlation curves solved by FEA for rectangular (flat wall to flat wall) and wave (wave wall to flat wall) cavities at AR=40 compared to ISO 15099. The typical Ra range encountered during measurements is highlighted.
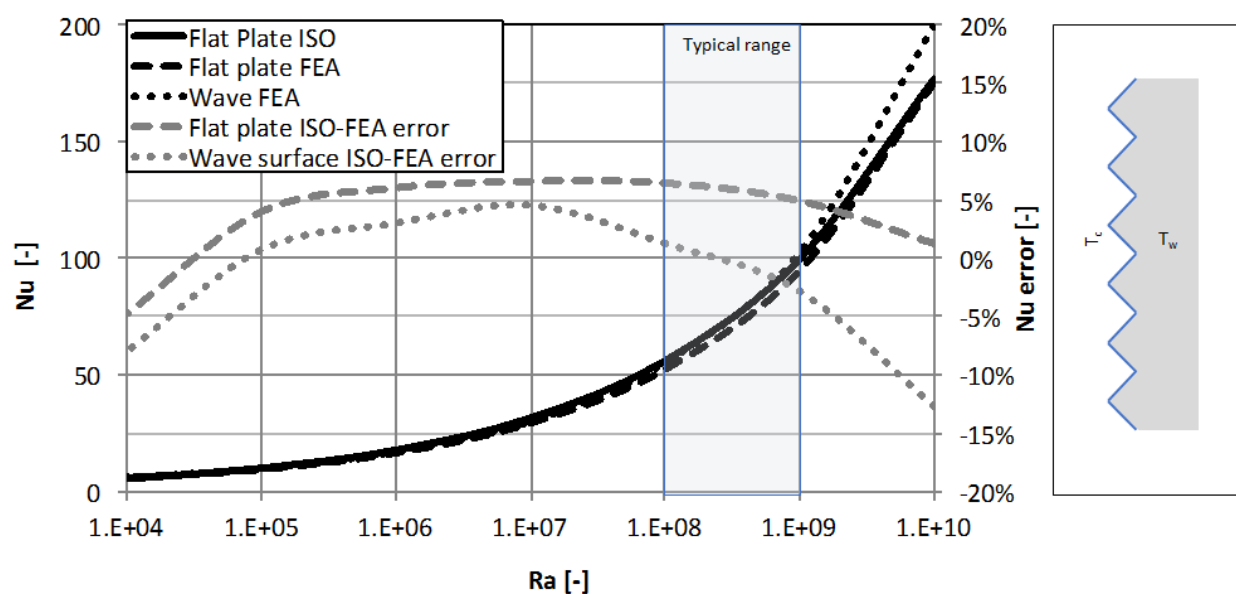
Figure 16-6. Nu = f(Ra) correlation curves solved by FEA of natural convection on vertical flat plate and wave surfaces compared to ISO 15099. The typical Ra range encountered during measurements is highlighted.

16.1.4. Correlations

Cellular shades do not hang uniformly as is commonly assumed. Typically, the top most cells are significantly stretched due to the weight of cells below and correspondingly the bottom cells lie nearly flat, as shown in Figure 16-7a. This scenario results in a variable dgap*. In the majority of test configurations dgap is large (>25mm) resulting in low dgap sensitivity. Window heat flux is sensitive to dgap at dimensions < 25mm

though. A revised method to calculate dgap (Equation *[16–4]*) is proposed as dgap* in Equation *[16–5]*. It is based on the midpoint between fully extended and fully flat cells. The geometry is described in Figure 16-7b.

$$d_{gap} = d_h + \frac{w_h - l_{g1}}{2} - \sqrt{l_{s1}^2 - \left(\frac{p}{2}\right)^2}$$

[16–4]

$$d_{gap*} = d_h + \frac{w_h - l_{g1} - \sqrt{l_{s1}^2 - \left(\frac{p}{2}\right)^2}}{2}$$

[16–5]
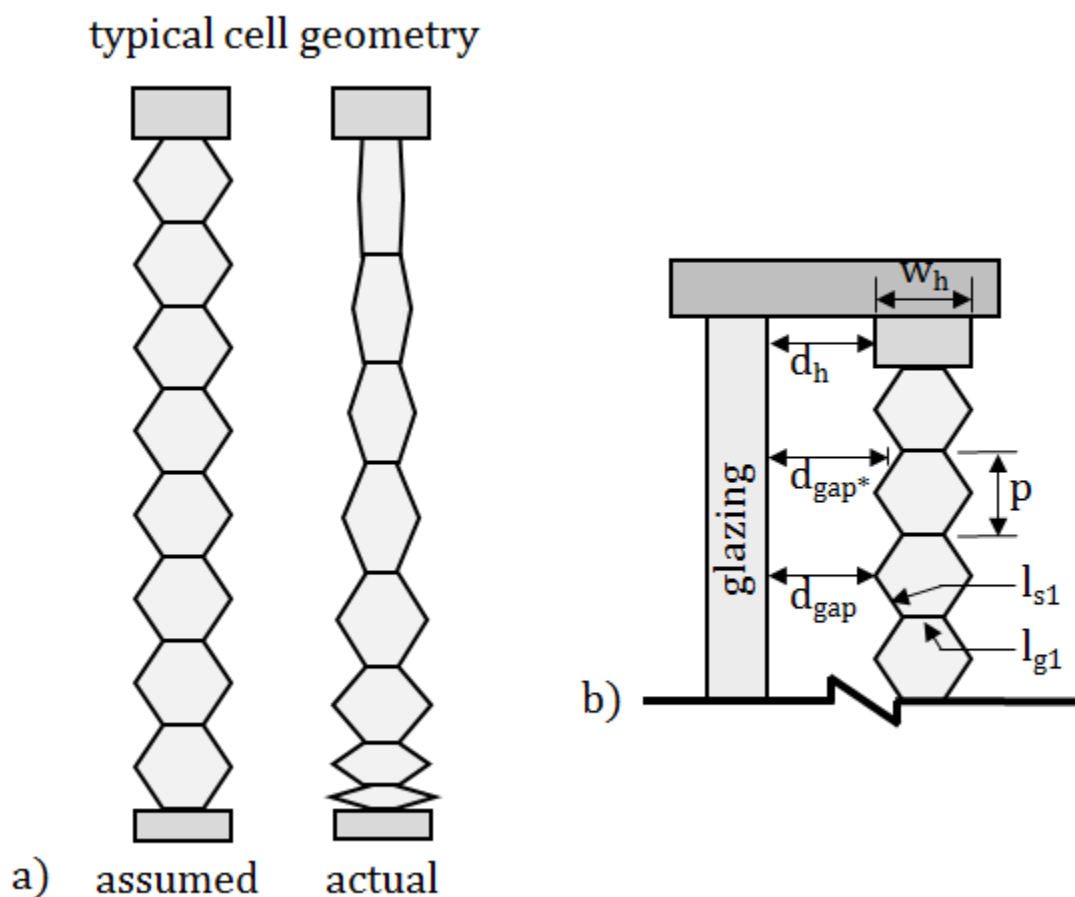
Figure 16-7. (a) End view of the assumed and actual cellular shade geometry when mounted to a window. (b) Geometry defining the distance from glazing surface to cellular shade.

Correlation between WINDOW simulation and measured heat flux for 94 measured cellular shade combinations is shown in Figure 16-8. Analysis is performed on the basis of heat flux in lieu of thermal transmittance (U-factor) since this property is used in WINDOW for simulation convergence. This way it is possible to perform a quantitative correlation between the measured and simulated values in an attempt to validate the model. The measured to simulated heat flux difference is 0.5 percent, with a typical spread of ±6 percent.
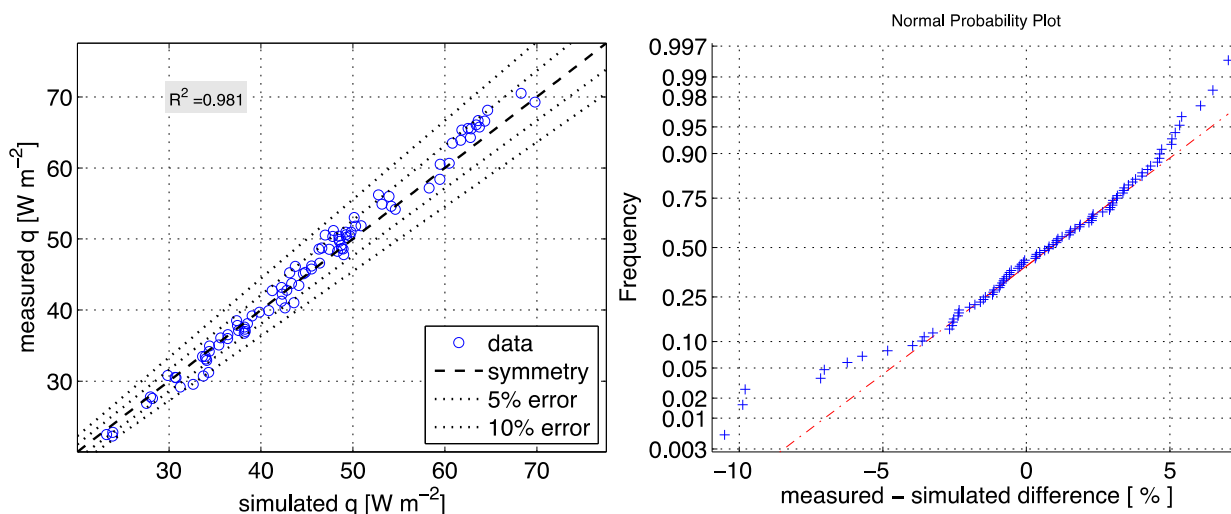
Figure 16-8. Measured to simulated heat flux comparison for 94 cellular shade configurations based on data corrected for CTS measurement error and cell shade mounting hardware.

16.2. Optical properties implementation in WINDOW, THERM, and Radiance

Cellular shade calculations are done in several steps. First the geometry is drawn in THERM, then it is exported to Radiance format which is used in genBSDF to generate the layer properties in three wavelength bands. For each band, genBSDF is run to produce data files in the Klems coordinate system. Thermal IR properties are integrated to hemipspherical values (TIR and emissivity). Finally visible and solar BSDFs are combined with the integrated thermal IR values to a single XML file that can be used in the multi-layer calculations of WINDOW.

16.2.1. Using THERM for drawing geometry

A drawing of the cellular shade geometry references materials in the WINDOW shade layer library for each surface of the cellular shade. The drawing contains straight line *segments*.

THERM in radiance mode require that a boundry is defined as the illuminated area (defining a single period of a periodic material). This boundry definition is passed to the –DIM parameter of the genBSDF call.

16.2.2. Exporting THERM model to .RAD format

The spectral data from the shade layer library is divided into three wavelength bands: visible, solar, and TIR. A Radiance .RAD file is created for each of the three bands. Each segment is represented in the file by the following parts

1. Two material descriptions, one for front, and one for back surface, using the trans description. E.g.

    ```
    void trans trans_segment_303
    0 0 7
    0.0    0.000000 0.000000 0.414161 0.000000 1.000000 1.000000
    ```

    The trans parameters are described in the Rendering with Radiance reference book page 325.

2. Mixfunc modifiers that make the segment invisible to rays coming from the wrong direction (i.e. rays incident on the front does not interact with the back side properties). E.g.

    ```
    void mixfunc segment_303
    ```

```
4 trans_segment_303 void if(Rdot,1,0) .

0

0
```

3. Polygons describing the space coordinates of the segment, extending it from 2D to 3D. E.g.

```
segment_303 polygon polygon_303

0 0 12

1 0.093316 -0.018937 1 0.093316 -0.017417 -1 0.093316 -0.017417 -1
0.093316 -0.018937
```

16.2.3. Running genBSDF

genBSDF is a PERL script distributed with Radiance. The input parameters used by WINDOW are

+f +b	
-r "-ad 400 –lw 0.001"	rtcontrib/rtrace parameters, ad = ambient divisions, lw = limit weight
-c 1000	Number of rays traced
-dim x0 x1 y0 y1 z0 z1	Illumination box
Solar.rad	Input geometry

The rcontrib parameters were based on experimentation with cellular shades to get reasonable runtime for 2015 desktop processors (hours rather than days)

16.2.4. Combining Visible, Solar, and Thermal IR parts

Hemispherical emissivity and TIR are obtained by integrating the BSDFs for the IR band. The Visilbe and Solar bands are kept as is and all are merged into one large XML file as described below.

The header of the file contains information about the product in the following format.

```xml
<?xml version="1.0" encoding="UTF-8"?>
<WindowElement xmlns="http://windows.lbl.gov" xmlns:xsi=
"http://www.w3.org/2001/XMLSchema-instance"
xsi:schemaLocation="http://windows.lbl.gov BSDF-v1.4.xsd">
      <WindowElementType>Layer</WindowElementType>
      <FileType>BSDF</FileType>
      <Optical>
            <Layer>
            <Material>
                  <Name>World's best fabric</Name>
                  <Manufacturer>World's best company</Manufacturer>
                  <Thickness unit="Millimeter">1</Thickness>
                  <DeviceType>Woven Shade</DeviceType>
                  <ThermalConductivity>0.15</ThermalConductivity>
                  <EmissivityFront>0.7</EmissivityFront>
                  <EmissivityBack>0.3</EmissivityBack>
                  <TIR>0.15</TIR>
                  <PermeabilityFactor>0.145</ PermeabilityFactor >
                  <Color>brown</Color>
                  <Comments></Comments>
            </Material>
```

The angle basis is defined after the initial information, the Klems coordinate system that is used in WINDOW would look like

```
<DataDefinition>
        <IncidentDataStructure>Columns</IncidentDataStructure>
                <AngleBasis>
                <AngleBasisName>LBNL/Klems Full</AngleBasisName>
                <AngleBasisBlock>
                        <Theta>0</Theta>
                        <nPhis>1</nPhis>
                        <ThetaBounds>
                                <LowerTheta>0</LowerTheta>
                                <UpperTheta>5</UpperTheta>
                        </ThetaBounds>
                </AngleBasisBlock>
                <AngleBasisBlock>
                        <Theta>10</Theta>
                        <nPhis>8</nPhis>
                        <ThetaBounds>
                                <LowerTheta>5</LowerTheta>
                                <UpperTheta>15</UpperTheta>
                        </ThetaBounds>
                </AngleBasisBlock>
                <!-- and so forth until-->
                <AngleBasisBlock>
                <Theta>82.5</Theta>
                <nPhis>12</nPhis>
                <ThetaBounds>
                        <LowerTheta>75</LowerTheta>
                        <UpperTheta>90</UpperTheta>
                </ThetaBounds>
                </AngleBasisBlock>
                </AngleBasis>
        </DataDefinition>
```

After the header the same style block is repeated for each wavelength band (visible and solar) and property (reflectance/transmittance).

```
<WavelengthData>
<LayerNumber>System</LayerNumber>
<Wavelength unit="Integral">Visible</Wavelength>
<SourceSpectrum>CIE D65 standard illuminant</SourceSpectrum>
<DetectorSpectrum>CIE 1931 2deg observer Y</DetectorSpectrum>
<WavelengthDataBlock>
        <WavelengthDataDirection>Reflection Front
                                </WavelengthDataDirection>
        <ColumnAngleBasis>LBNL/Klems Full</ColumnAngleBasis>
        <RowAngleBasis>LBNL/Klems Full</RowAngleBasis>
        <ScatteringDataType>BTDF</ScatteringDataType>
        <ScatteringData>
        <!-- Data block goes here 145x145 matrix of BSDF values-->
        </ScatteringData>
</WavelengthDataBlock>
</WavelengthData>
```

This block will come back in 8 permutation with all possible combinations of three variables

- Wavelength: This can be Visible or Solar

- WavelengthDataDirection: This has two parts Reflection or Transmittance and Front or Back.

For each permutation there will be a 145 by 145 matrix with BSDF values in the data block. Each column corresponds to an incident direction and each row corresponds to the outgoing direction resulting in all specular directions being located on the main diagonal. The tail of the document only closes the blocks started in the header

```
            </Layer>
        </Optical>

    </WindowElement>
```

17. PLEATED SHADES

The simulation of pleated shades as they are implemented in WINDOW, THERM, and Radiance is divided into "*Section 17.1. Thermal properties definition and implementation in WINDOW and THERM*" and "*Section 17.2. Optical properties implementation in WINDOW, THERM, and Radiance*".

17.1. Thermal properties definition and implementation in WINDOW and THERM

Section 1 of this document outlines a review and validation of the ISO 15099 center-of-glass (COG) heat transfer correlations for cellular shades through measurement and simulation. The impact of system thermal transmittance due to dimensional and material variations of the shades is measured experimentally, simulated using CFD analysis, and simulated utilizing simplified correlations from ISO 15099 with the Berkeley Lab WINDOW and THERM software.

17.1.1. Geometry

Pleated shades are treated similarly to cellular shades (chapter 16). In the case of pleated shades though, only the air layer as a whole was considered. The significant dimensions include the height or pitch (p) and side length (l_s). In all cases, the comparable side lengths are considered to be equal, as shown in Figure 17-1a. Side wall thickness has insignificant impact on overall layer thermal performance for the materials considered, so a typical thickness of 0.2 mm is assumed. Interior, or room-side, mounted pleated shades are studied exclusively in this work. The typical geometry relative to the glazing system is shown in Figure 17-1b.
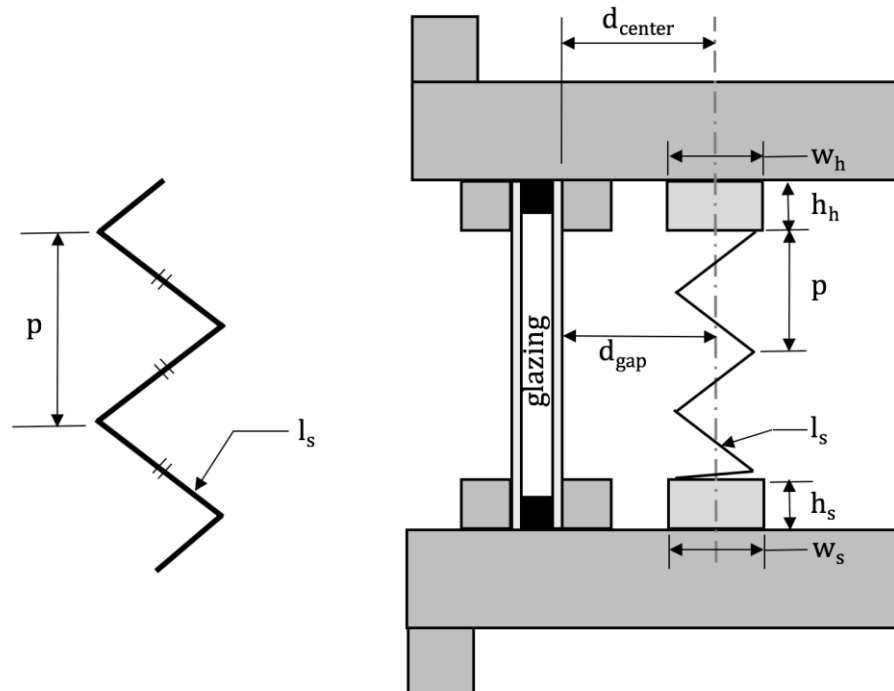

Figure 17-1. a) Geometry of a pleated shade and b) side view of room-side mounted shade installed in window.

p: Height (pitch) of "pleat"   [m]

H: Height of shade   [m]
H_h: Height of shade head rail   [m]
H_s: Height of shade sill rail   [m]
d_{gap}: Shade-window gap depth   [m]
l_{s1}:   Length of side wall   [m]

17.1.2. Simulation Methodology

The correlations developed in ISO 15099 to predict the heat flux through window systems have been implemented in one and two dimensions with the Berkeley Lab WINDOW and THERM software programs. The process for simulating a glazing system with pleated shades utilizing the software is shown in Figure 17-2. First, the relevant thermal and optical material properties of fabric walls are entered into the WINDOW shade material database. The properties may be measured spectral data or integrated into solar, visible, and thermal infrared groups. The pleated shade geometry is defined in THERM with the pleated shade wall properties appropriated from the previously defined shade material database. The THERM geometry and material properties are then used as an input for the ray-tracing program Radiance, where 1D equivalent layer optical properties are calculated. The calculated shade layer properties are then combined with the remainder of the glazing system and boundary conditions to determine the 1D center-of-glazing thermal performance.
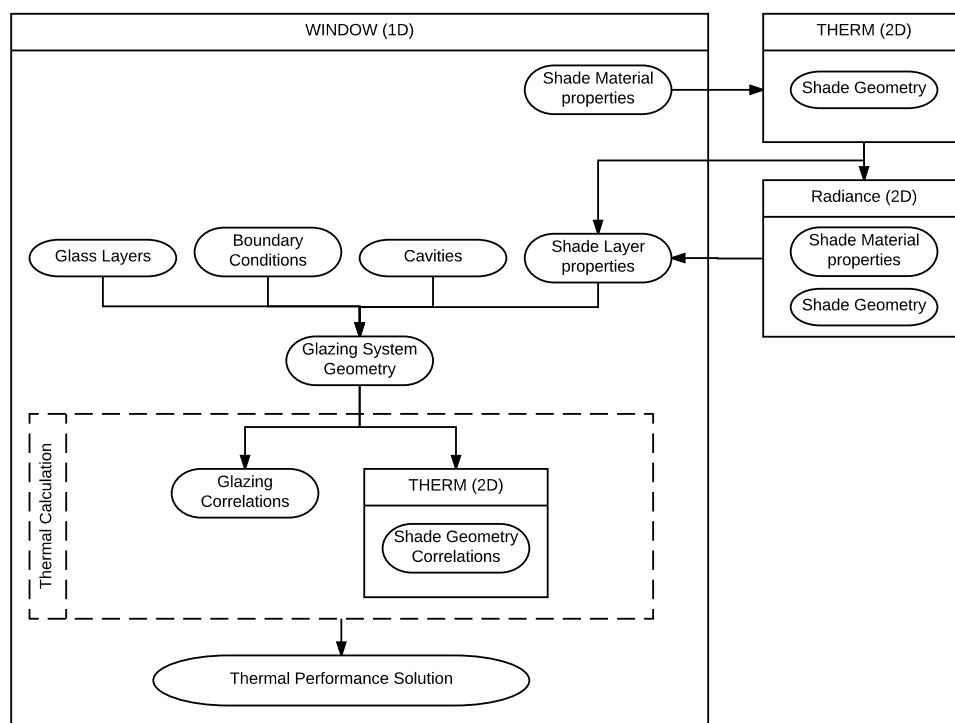
Figure 17-2. Pleated shade simulation algorithm flow used by LBNL WINDOW and THERM software.

17.1.3. Finite Element Analysis (FEA)

In the multiphysics analysis program COMSOL, the finite element method is used to solve the coupled heat and fluid-flow equations in two dimensions. Conduction, convection and radiation are simulated numerically. COMSOL default meshing is used to construct the computational domains. Sensitivity analysis of the results to mesh size is performed and determined to be less than 1%. Viscous dissipation is not addressed and all thermophysical properties are assumed to be constant except for the buoyancy term of the y-momentum equation where the Boussinesq approximation is used. The parallel direct iterative sparse solver (PARDISO) is used.

Fluid heat transfer for constant temperature walls of four geometries is studied as shown in Figure 17-3. Geometry (a) represents the cavity between glass and pleated shade; and Geometry (d) represents natural convection along the triangular wave surface of a pleated shade.
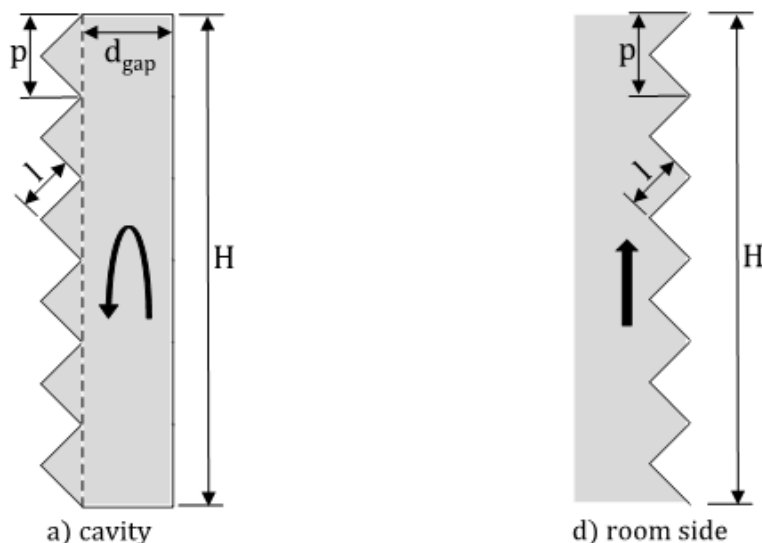

a) cavity   d) room side

Figure 17-3. 2D geometries utilized in FEA simulations for fluid heat transfer with constant temperature walls. Fluid areas shown in grey.

Heat flux through rectangular fluid filled cavities has been extensively studied by others. The work by El Sherbiny et al. is the basis for the sealed cavity model in the ISO 15099 standard. All of these studies provide a means to calculate average heat flux based on definitions of the non-dimensional Nusselt (Nu) and Rayleigh (Ra) numbers as shown in Equations [17–1] - [17–3]; where Nu is the ratio of convective to conductive heat transfer across the cavity and Ra designates strength of the buoyancy driven flow. An empirical correlation between them is determined for specific geometries in the form of equation [17–3].

$$Nu = \frac{q \cdot L}{k \cdot \Delta T}$$ [17–1]

$$Ra = \frac{\rho^2 \cdot g \cdot C_p \cdot \beta \cdot \Delta T \cdot L^3}{k \cdot \mu}$$ [17–2]

$$Nu = f(Ra)$$ [17–3]

where:

Nu:	Nusselt number	[-]
Ra:	Rayleigh number	[-]
q:	Heat flux	[W m^{-2}]
L:	Characteristic length	[m]
k:	Thermal conductivity	[W m^{-1} K^{-1}]
T:	Temperature	[K]
ρ:	Density	[Kg m^{-3}]
g:	Gravity	[m s^{-2}]
C_p:	Heat capacity	[J kg^{-1} K^{-1}]
β:	Coefficient of thermal expansion	[K^{-1}]
μ:	Dynamic viscosity	[Pa s]

Detailed FEA is used to determine the heat flux through the geometries shown in Figure 17-3 for a wide range of temperatures. The simulations are performed non-dimensionally per Equations [17–1] - [17–2] in order to generalize the solutions. The resulting steady state heat flux, represented here by the non-dimensional Nusselt number (Equation [17–1]), is determined and plotted against the Rayleigh number (Equation [17–2]). Correlations are shown in Figure 16-4 and Figure 16-5 for the glass-shade cavity (wave cavity) and natural

convection from the shade (wave surface) to the room. The discrepancy between these correlations and ISO 15099 for flat surfaces appears to be significant, but offsetting.
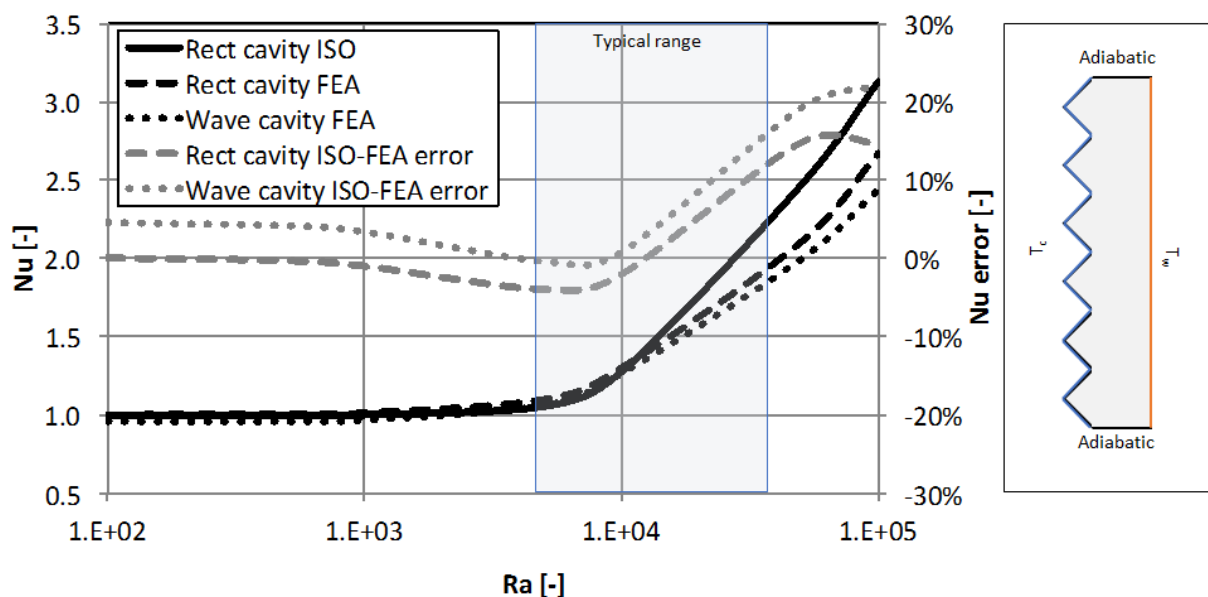
Figure 17-4. Nu = f(Ra) correlation curves solved by FEA for rectangular (flat wall to flat wall) and wave (wave wall to flat wall) cavities at AR=40 compared to ISO 15099. The typical Ra range encountered during measurements is highlighted.
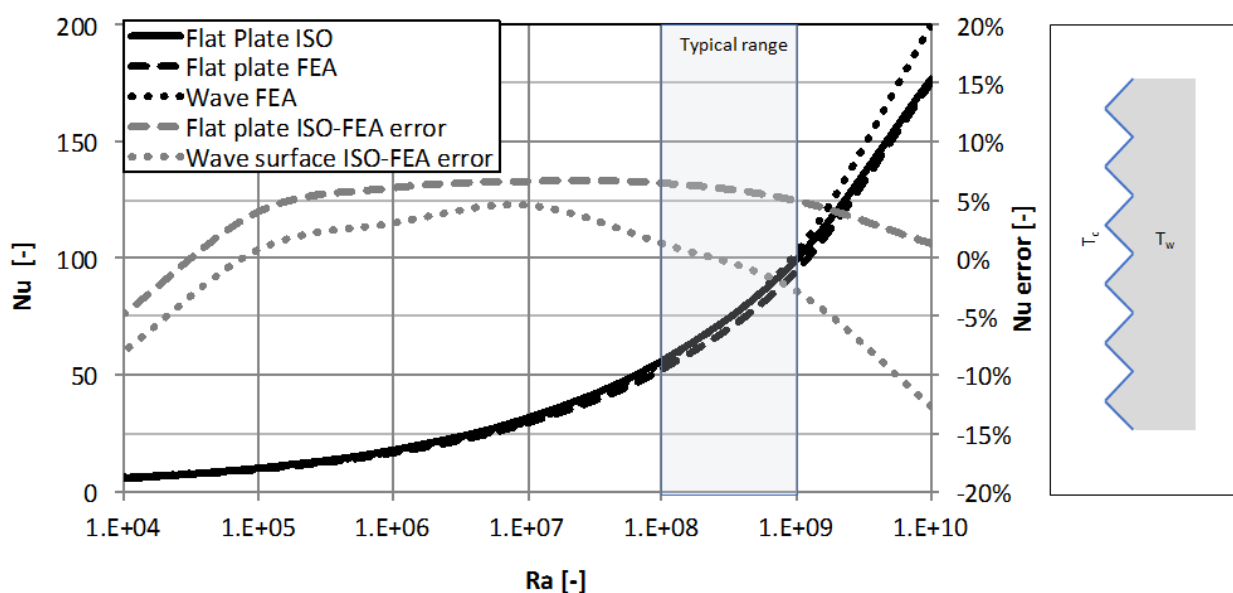
Figure 17-5. Nu = f(Ra) correlation curves solved by FEA of natural convection on vertical flat plate and wave surfaces compared to ISO 15099. The typical Ra range encountered during measurements is highlighted.

17.1.4. Correlations

Just like cellular shades, pleated shades do not hang uniformly as is commonly assumed. Typically, the top most "pleats" are more stretched due to the weight of pleats below and correspondingly the bottom pleats lie

nearly flat, as shown in Figure 16-6a. This scenario results in a variable dgap*. In the majority of test configurations dgap is large (>25 mm) resulting in low dgap sensitivity. Window heat flux is sensitive to dgap at dimensions < 25 mm though. A revised method to calculate dgap (Equation [17–4]) is proposed as dgap* in Equation [17–5]. It is based on the midpoint between fully extended and fully flat pleats. The geometry is described in Figure 16-6b.

$$d_{gap} = d_h + \frac{w_h}{2} - \sqrt{l_s^2 - \left(\frac{p}{2}\right)^2} \qquad\qquad [17\text{–}4]$$

$$d_{gap*} = d_h + \frac{w_h - \sqrt{l_s^2 - \left(\frac{p}{2}\right)^2}}{2} \qquad\qquad [17\text{–}5]$$
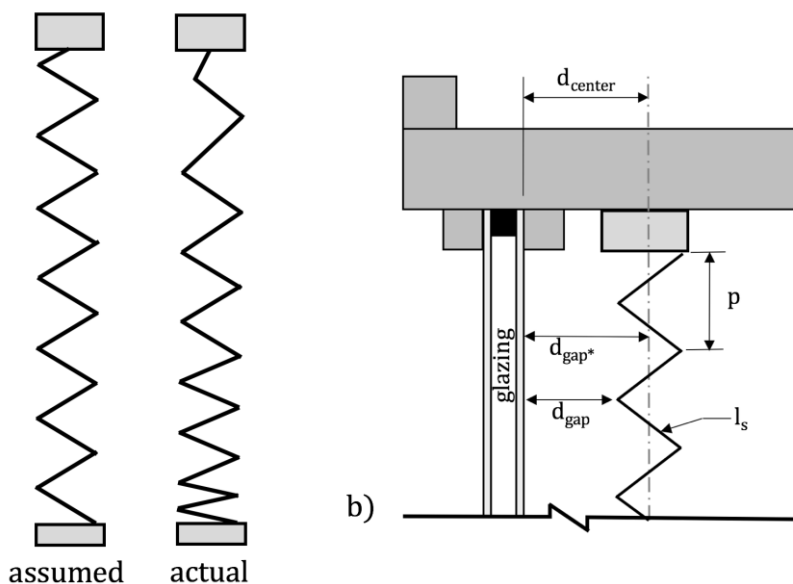
Figure 17-6. (a) End view of the assumed and actual pleated shade geometry when mounted to a window. (b) Geometry defining the distance from glazing surface to pleated shade.

Correlation between WINDOW simulation and measured heat flux for 94 measured cellular shade combinations is shown in Figure 17-7. Since no separate analysis has yet been done for pleated shades, results of heat transfer in a gap between cellular shade and glazing and room facing surface of cellular hade was used for pleated shades. Analysis is performed on the basis of heat flux in lieu of thermal transmittance (U-factor) since this property is used in WINDOW for simulation convergence. This way it is possible to perform a quantitative correlation between the measured and simulated values in an attempt to validate the model. The measured to simulated heat flux difference is 0.5 percent, with a typical spread of ±6 percent.

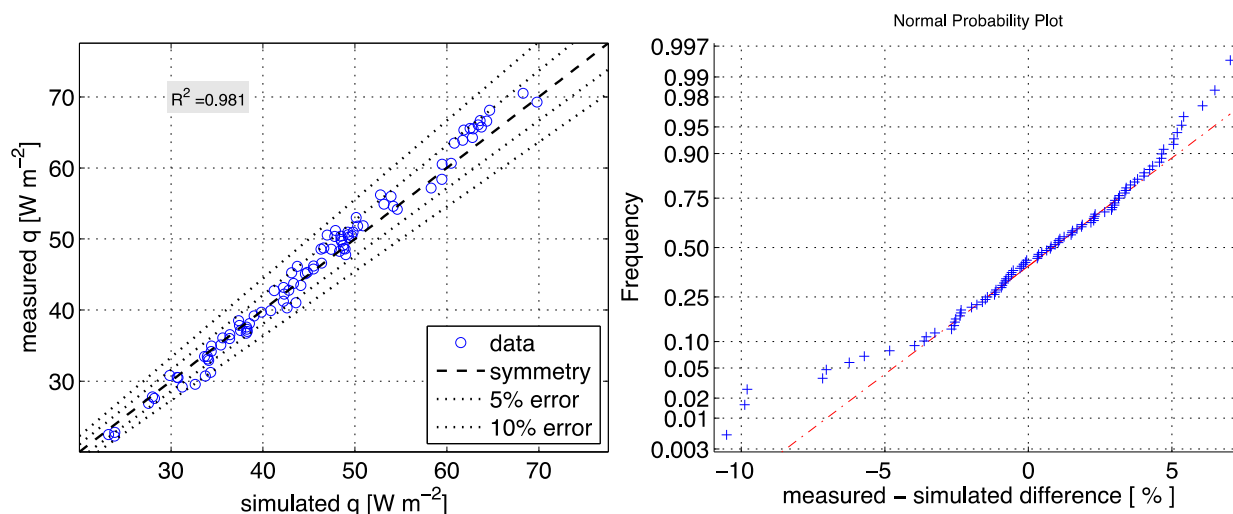*Figure 17-7. Measured to simulated heat flux comparison for 94 cellular shade configurations based on data corrected for CTS measurement error and cell shade mounting hardware.*

17.2. Optical properties implementation in WINDOW, THERM, and Radiance

Pleated shade calculations are done in several steps. First the geometry is drawn in THERM, then it is exported to Radiance format which is used in genBSDF to generate the layer properties in three wavelength bands. For each band, genBSDF is run to produce data files in the Klems coordinate system. Thermal IR properties are integrated to hemipspherical values (TIR and emissivity). Finally, visible and solar BSDFs are combined with the integrated thermal IR values to a single XML file that can be used in the multi-layer calculations of WINDOW.

17.2.1. Using THERM for drawing geometry

A drawing of the cellular shade geometry references materials in the WINDOW shade layer library for each surface of the pleated shade. The drawing contains straight line *segments*.

THERM in radiance mode require that a boundry is defined as the illuminated area (defining a single period of a periodic material). This boundry definition is passed to the –DIM parameter of the genBSDF call.

17.2.2. Exporting THERM model to .RAD format

The spectral data from the shade layer library is divided into three wavelength bands: visible, solar, and TIR. A Radiance .RAD file is created for each of the three bands. Each segment is represented in the file by the following parts

4. Two material descriptions, one for front, and one for back surface, using the trans description. E.g.

   ```
   void trans trans_segment_303

   0 0 7

   1.0    0.000000 0.000000 0.414161 0.000000 1.000000 1.000000
   ```

   The trans parameters are described in the Rendering with Radiance reference book page 325.

5. Mixfunc modifiers that make the segment invisible to rays coming from the wrong direction (i.e. rays incident on the front does not interact with the back side properties). E.g.

   ```
   void mixfunc segment_303
   ```

```
4 trans_segment_303 void if(Rdot,1,0) .

0

0
```

6. Polygons describing the space coordinates of the segment, extending it from 2D to 3D. E.g.

```
segment_303 polygon polygon_303

0 0 12

1 0.093316 -0.018937 1 0.093316 -0.017417 -1 0.093316 -0.017417 -1
0.093316 -0.018937
```

17.2.3. Running genBSDF

genBSDF is a PERL script distributed with Radiance. The input parameters used by WINDOW are

    +f +b

-r "-ad 400 –lw 0.001"	rtcontrib/rtrace parameters, ad = ambient divisions, lw = limit weight
-c 1000	Number of rays traced
-dim x0 x1 y0 y1 z0 z1	Illumination box
Solar.rad	Input geometry

The rcontrib parameters were based on experimentation with cellular shades to get reasonable runtime for 2015 desktop processors (hours rather than days)

17.2.4. Combining Visible, Solar, and Thermal IR parts

Hemispherical emissivity and TIR are obtained by integrating the BSDFs for the IR band. The Visilbe and Solar bands are kept as is and all are merged into one large XML file as described below.

The header of the file contains information about the product in the following format.

```xml
<?xml version="1.0" encoding="UTF-8"?>
<WindowElement xmlns="http://windows.lbl.gov" xmlns:xsi=
"http://www.w3.org/2001/XMLSchema-instance"
xsi:schemaLocation="http://windows.lbl.gov BSDF-v1.4.xsd">
      <WindowElementType>Layer</WindowElementType>
      <FileType>BSDF</FileType>
      <Optical>
            <Layer>
            <Material>
                  <Name>World's best fabric</Name>
                  <Manufacturer>World's best company</Manufacturer>
                  <Thickness unit="Millimeter">1</Thickness>
                  <DeviceType>Woven Shade</DeviceType>
                  <ThermalConductivity>0.15</ThermalConductivity>
                  <EmissivityFront>0.7</EmissivityFront>
                  <EmissivityBack>0.3</EmissivityBack>
                  <TIR>0.15</TIR>
                  <PermeabilityFactor>0.145</ PermeabilityFactor >
                  <Color>brown</Color>
                  <Comments></Comments>
            </Material>
```

The angle basis is defined after the initial information, the Klems coordinate system that is used in WINDOW would look like

```
<DataDefinition>
        <IncidentDataStructure>Columns</IncidentDataStructure>
                <AngleBasis>
                <AngleBasisName>LBNL/Klems Full</AngleBasisName>
                <AngleBasisBlock>
                        <Theta>0</Theta>
                        <nPhis>1</nPhis>
                        <ThetaBounds>
                                <LowerTheta>0</LowerTheta>
                                <UpperTheta>5</UpperTheta>
                        </ThetaBounds>
                </AngleBasisBlock>
                <AngleBasisBlock>
                        <Theta>10</Theta>
                        <nPhis>8</nPhis>
                        <ThetaBounds>
                                <LowerTheta>5</LowerTheta>
                                <UpperTheta>15</UpperTheta>
                        </ThetaBounds>
                </AngleBasisBlock>
                <!-- and so forth until-->
                <AngleBasisBlock>
                <Theta>82.5</Theta>
                <nPhis>12</nPhis>
                <ThetaBounds>
                        <LowerTheta>75</LowerTheta>
                        <UpperTheta>90</UpperTheta>
                </ThetaBounds>
                </AngleBasisBlock>
        </AngleBasis>
</DataDefinition>
```

After the header the same style block is repeated for each wavelength band (visible and solar) and property (reflectance/transmittance).

```
<WavelengthData>
<LayerNumber>System</LayerNumber>
<Wavelength unit="Integral">Visible</Wavelength>
<SourceSpectrum>CIE D65 standard illuminant</SourceSpectrum>
<DetectorSpectrum>CIE 1931 2deg observer Y</DetectorSpectrum>
<WavelengthDataBlock>
        <WavelengthDataDirection>Reflection Front
                                </WavelengthDataDirection>
        <ColumnAngleBasis>LBNL/Klems Full</ColumnAngleBasis>
        <RowAngleBasis>LBNL/Klems Full</RowAngleBasis>
        <ScatteringDataType>BTDF</ScatteringDataType>
        <ScatteringData>
        <!-- Data block goes here 145x145 matrix of BSDF values-->
        </ScatteringData>
</WavelengthDataBlock>
</WavelengthData>
```

This block will come back in 8 permutation with all possible combinations of three variables

- Wavelength: This can be Visible or Solar

- WavelengthDataDirection: This has two parts Reflection or Transmittance and Front or Back.

For each permutation there will be a 145 by 145 matrix with BSDF values in the data block. Each column corresponds to an incident direction and each row corresponds to the outgoing direction resulting in all specular directions being located on the main diagonal. The tail of the document only closes the blocks started in the header

```
            </Layer>
        </Optical>

    </WindowElement>
```

18. REFERENCES

1. ASHRAE. 2001. Handbook of Fundamentals, American Society of Heating, Refrigerating and Air-Conditioning Engineers, Inc. June 2001.

2. ASTM E308-17 Standard Practice for Computing the Colors of Objects by Using the CIE System, ASTM International, West Conshohocken, PA, 2017, https://doi.org/10.1520/E0308-17

3. Bernier, M. and B. Bourret. 1997. Effects of Glass Plate Curvature on the U-Factor of Sealed Insulated Glazing Units. *ASHRAE Transactions*. Vol. 103, Pt 1.

4. BS EN 673:1997: Glass in building – Determination of thermal transmittance (Uvalue) – Calculation method. European Committee for Standardization: Brussels, Belgium.

5. BS EN 13363-1:2003: Solar protection devices combined with glazing — Calculation of solar and light transmittance — Part 1: Simplified method. European Committee for Standardization: Brussels, Belgium.

6. BS EN 13363-2:2005: Solar protection devices combined with glazing — Calculation of total solar energy transmittance and light transmittance — Part 2: Detailed calculation method. European Committee for Standardization: Brussels, Belgium.

7. Collins, R.E. & Robinson, S.J. (1991). Evacuated glazing. *Solar Energy 23*(1), 27-38. http://dx.doi.org/10.1016/0038-092X(91)90060-A

8. Collins, R.E. & Fischer-Cripps, A.C. (1991). Design of Support Pillar Arrays in Flat Evacuated Windows. *Australian Journal of Physics 44*(5), 545-563.

9. Corruccini, R.J. (1959). Gaseous heat conduction at low pressures and temperatures. *Vacuum 7-8*, 19-29. http://dx.doi.org/10.1016/0042-207X(59)90766-3

10. Furler, R.A. 1991. Angular dependence of optical properties of homogeneous glasses. ASHRAE Transactions, 97 (2): 1129-1133.

11. IEA. 2000. Daylight in Buildings, A report of IEA SHC Task 21/ ECBCS Annex 29. International Energy Agency. July 2000.

12. ISO 10077-1:2006: Thermal performance of windows, doors and shutters -- Calculation of thermal transmittance -- Part 1: General. International Organization for Standardization: Geneva, Switzerland.

13. ISO 10292:1994: Glass in building -- Calculation of steady-state U values (thermal transmittance) of multiple glazing. International Organization for Standardization: Geneva, Switzerland.

14. ISO 15099:2003: Thermal performance of windows, doors and shading devices -- Detailed calculations. International Organization for Standardization: Geneva, Switzerland.

15. ISO. 2003. "ISO 15099: Thermal Performance of Windows, Doors and Shading Devices – Detailed calculations." *International Standardization Organization*. First edition. November, 2003.

16. Kaufman, J.E., editor & Christensen, J.F., associate editor. IES Lighting Handbook, 1984 Reference Volume. Illuminating Engineering Society of North America, New York, NY. 1984

17. Klems, J.H. 1994a. A New Method for Predicting the Solar Heat Gain of Complex Fenestration Systems I. Overview and Derivation of the Matrix Layer Calculation. ASHRAE Transactions V.100, Pt. 1

18. Klems, J.H. 1994b. A New Method for Predicting the Solar Heat Gain of Complex Fenestration Systems II. Detailed Description of the Matrix Layer Calculation *ASHRAE Transactions* V.100, Pt. 1

19. Klems, J.H. 2004. Detailed Equations for Connecting a 2D Blind Model with the Bidirectional Calculation, internal memo.

20. Klems, J.H. 2005. Calculating Outgoing Radiance in the 2D Venetian Blind Model, internal memo, rev.2.

21. Timoshenko, S., and S. Woinowsky-Krieger. 1959. *Theory of plates and shells*. New York: McGraw-Hill.